

***A RISK-BASED DESIGN APPROACH
TO SHIP – SHIP COLLISION***

Georgios Apostolou Mermiris, MEng

Thesis submitted to the University of Strathclyde
in fulfilment of the requirements for the award
of the degree of Doctor of Philosophy

Department of Naval Architecture and Marine Engineering
Universities of Glasgow and Strathclyde

Glasgow, April 2010

The copyright of this thesis belongs to the author under the terms of the United Kingdom Copyright Acts as qualified by University of Strathclyde Regulation 3.51. Due acknowledgement must always be made of the use of any material contained in, or derived from, this thesis.

*Pursuing a target is a time and strength consuming exercise
that is only fulfilled when the time is ripe.*

Apostolos G. Mermiris

Abstract

Every time a major marine accident occurs, society actively demands for improvement in operational safety levels. This issue is mainly addressed by national and international regulatory bodies. However, every time an accident occurs a mindless increase of standards follows with patching mentality and total disregard of the initiating causes. The existing regulatory framework for damage stability is based on the conditional probability that a collision has occurred and a compartment (or a group of adjacent compartments) is flooded, disregarding at a stroke all navigational and operational collision prevention issues, thus disincentivising any efforts to account for them. Moreover, as many collisions do not result in hull breach and flooding, collision accident analysis suffers by ignoring a large volume of valuable data.

This is indeed a serious pitfall in the newly adopted (January 2009) probabilistic regulatory framework for damage stability, considering that ship-ship collisions account for approximately 20% of all serious maritime accidents. This background provides a clear objective for this thesis, namely to develop a set of analytical tools for the explicit assessment of the probability of collision and the probability of water ingress due to collision that accounts for the operational profile of the ship and generic structural information of its side shell. The output is the collision probability and the ensuing hull breach location and size, information, which is directly utilised for ship survivability assessment and collision related flooding risk quantification. In this way, the conditional probability of the probabilistic framework for damage stability can be substituted by a more rational approach, which is solely bound by the expected level of safety. At the same time, a significant enhancement of the design process is achieved by providing a broader spectrum of choice and the freedom to explore alternative cost-efficient solutions with the much needed innovative characteristics.

Acknowledgements

I would like to express my gratitude to Prof. Dracos Vassalos for giving me the opportunity to study under his supervision for this degree. His guidance, insight and critical thinking in the intricate topics treated in this work have been invaluable.

I am also grateful to Dr. Dimitris Konovessis for the long discussions we had on several topics regarding design, safety and risk assessment either on a theoretical or practical basis. This has been a very solid input in the preparation and development of this thesis.

Dr. O. Khattab has provided the SIMX5 software for calculating manoeuvrability characteristics of ships. His support from this point of view and his encouragement in general are acknowledged and gratefully appreciated.

Mrs. Thelma Will has been very helpful with the administrative details of the preparation and submission of my thesis. I am truly thankful for her support.

Finally, I would like to thank my immediate family for talking, listening and supporting me in the course of my study. This is an achievement I would have never managed without them.

Table of contents

1	Introduction and scope of work.....	9
1.1	Introduction	9
1.2	Shipping: a high risk business	10
1.3	Regulations and design practice	12
1.4	The dual character of the project.....	15
1.5	The probability of collision event	17
1.6	The probability of water ingress due to collision	18
1.7	Thesis structure.....	19
1.8	Thesis objectives	20
2	Critical review	22
2.1	Introduction	22
2.2	Probability of a collision event.....	23
2.3	Probability of water ingress due to collision.....	33
2.4	Regulatory bodies.....	44
2.5	Chapter summary	46
3	Problem definition.....	47
3.1	Introduction	47
3.2	Philosophy of current regulatory approaches	48
3.3	Analytical models: the next phase of evolution in ship design	51
3.4	Practical safety implementation	56
3.5	Risk-based design.....	58
3.6	Probability of collision (P_c).....	63
3.7	Probability of water ingress due to collision ($P_{w/c}$)	68
3.8	Chapter summary	69

4	Probability of collision.....	71
4.1	Introduction	71
4.2	Factors affecting the collision occurrence.....	72
4.3	Entropy of information	74
4.4	Probability of collision: an alternative approach.....	81
4.5	Sensitivity analysis	87
4.6	Model calibration	89
4.7	Entropy level and point of no return	94
4.8	Chapter summary	96
5	Probability of water ingress due to collision.....	97
5.1	Introduction	97
5.2	Factors affecting the crashworthiness of ships.....	98
5.3	The geometrical link between the striking and the struck ships.....	100
5.4	Deformation of stiffened plates	107
5.5	Rupture energy	118
5.6	The Penetration Potential	123
5.7	The calculation process	124
5.8	Comparison with HARDER results	128
5.9	Chapter summary	135
6	The proposed methodology.....	137
6.1	Introduction	137
6.2	The existing regulatory framework	138
6.3	Weaknesses of the existing framework.....	139
6.4	The way forward	141
6.5	Chapter summary	145

7	Case studies	146
7.1	Introduction	146
7.2	Vessel particulars	147
7.3	Site description and scenario definition	147
7.4	Case study 1: collision of the ROPAX with the tanker	150
7.5	Case study 2: collision of the tanker with the ROPAX.....	156
7.6	Case study 3: Crashworthiness of Y-sections panel.....	161
7.7	Case study 4: Side shell configuration versus payload capacity	164
7.8	Case study 5: Comparative calculations.....	167
7.9	Chapter summary	170
8	Discussion & conclusions	172
8.1	Introduction	172
8.2	Summary of findings	173
8.3	Recommendations for future work	175
8.4	Conclusions	179
9	References	181
	Appendix A: SIMX5	207
	Appendix B: Surface representation	210
	Appendix C: Vessel drawings	228
	Appendix D: Calculation of side shell stiffness values D , D_x and D_y	233

1 Introduction and scope of work

1.1 Introduction

The subject topic is introduced in this chapter. In particular, a brief description of the problem and the motivation behind the work, followed by explanation of the dual character of the project and the approach that will be adopted is presented. The chapter concludes with the description of the project objectives and a layout of the thesis in order to provide with a concise framework of the proposed methodology.

1.2 Shipping: a high risk business

It is quite unfortunate for one to start a thesis with a discussion on accidents that a large number of people would prefer to forget. Nevertheless, these same accidents haunt us all and especially the engineering community. It is therefore very pragmatic to study and understand their nature, causes and effects, and attempt to answer some key questions concerning avoidance of the same unhappiness and misery in the future.

It is widely acknowledged that shipping is a high risk business not only because of the unpredictability of the sea environment but equally so due to human venture and ambition. This unquestionable fact is clearly demonstrated by the plethora of statistical analyses and studies performed by national and international bodies in a local or global scale. In the majority of cases, accidents are grouped as

- collision / contact
- grounding / stranding
- capsize / listing
- fire / explosion
- hull failure
- other

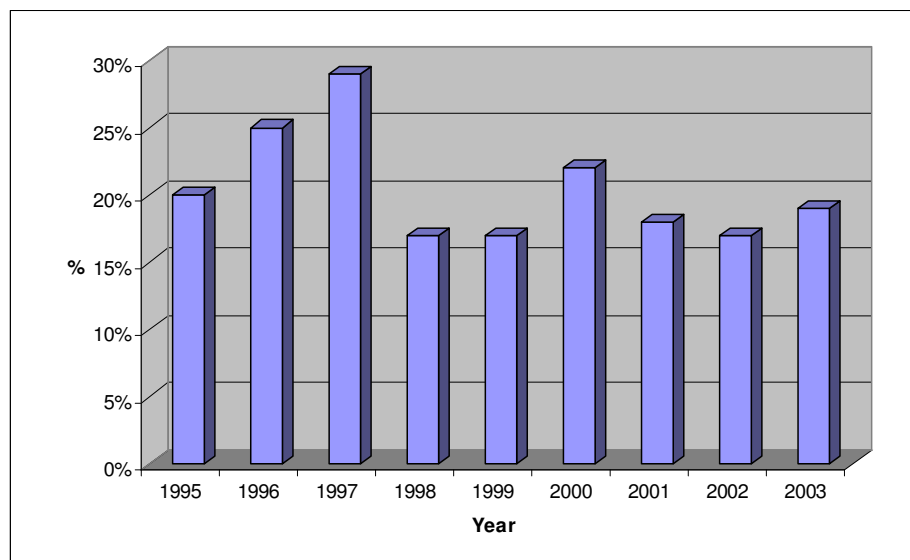
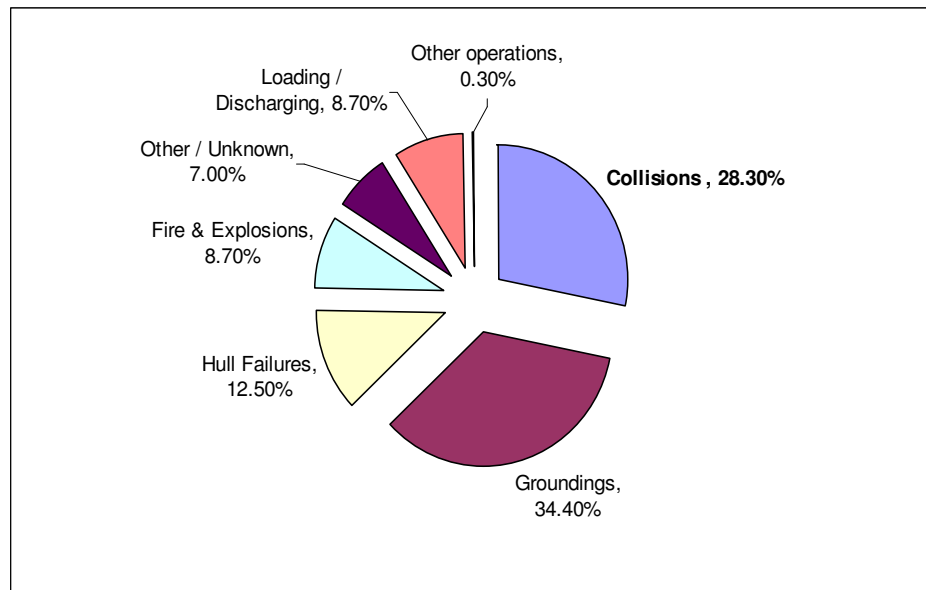
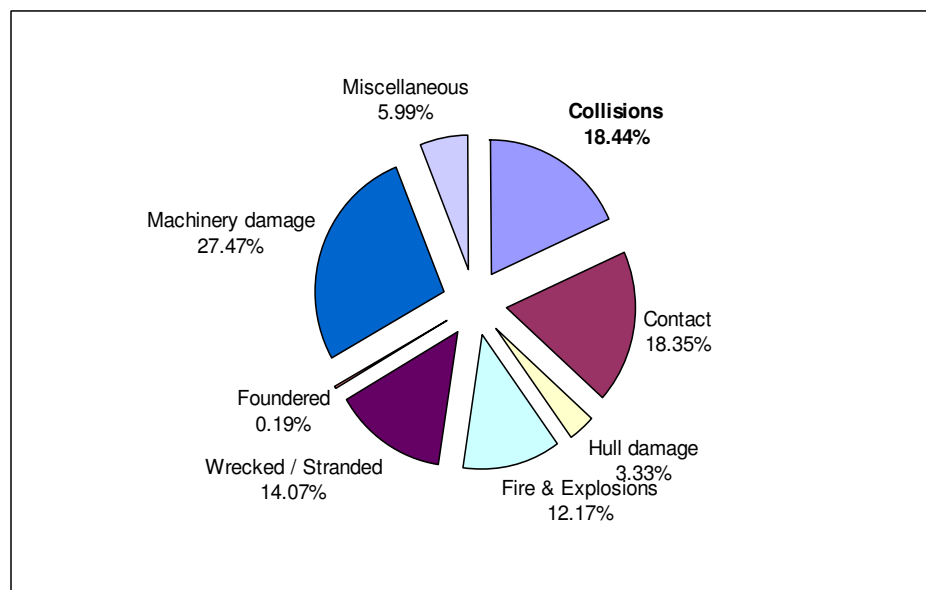


Figure 1.1: Collisions as a proportion of serious or very serious accidents according to IMO database (1995 – 2003)

This project is concerned with the particular topic of *ship – ship collisions*, which seems to correspond approximately to 20% of serious and very serious accidents on annual basis, as indicated in Figure 1.1.



(a) Oil spill incidents by cause for more than 700 tonnes of oil, 1974-2006 (www.itopf.com)



(b) Accidents involving ROPAX vessels above 1000 GRT, partially reproduced from (Konovessis et al., 2007)

Figure 1.2: Statistical data regarding collision of tanker and ROPAX vessels

More specifically, Figure 1.2 presents some statistical data regarding accidents of tanker and Ro-Ro passenger (ROPAX) ships. These two particular types of ships are exemplified because of the calamitous nature of the consequences following the occurrence of an accident involving any of them. Loss of life and environmental damage are often causing extensive societal impact, which results to political action for upgrading of the regulations for design, construction and operation of commercial ships. Some very serious collision accidents of passenger ships are summarised in Table 1.1.

Year	Vessel name	Event	Lives lost
1986	<i>SS Admiral Nahkimov</i>	Admiral Nakhimov collided with a large bulk carrier near the port of Novorossiysk in south Russia (north-east Black Sea) with 1234 people onboard.	423
1987	<i>Dona Paz</i>	Dona Paz was en route to Manila when it collided with a small oil tanker. The number of passengers on board has never been clarified and it was most probably well overloaded. After the collision, the cargo of the tanker ignited and fire spread to the Dona Paz, which sunk within a few minutes.	4375
1989	<i>Marchioness</i>	The Marchioness was a small pleasure boat that collided with a dredger in river Thames, in UK. At the time of the accident, it was carrying 132 people for a private function.	51
1991	<i>Moby Prince</i>	In April 1991, the ferry Moby Prince collided with the tanker Agip Abruzzo in Livorno harbour and it caught fire. The mayday signal transmitted by Moby Prince was not received by the Livorno port authority. The rescue party focused its efforts to Agip Abruzzo. Only one mariner was saved from the ferry	140
1992	<i>Royal Pacific</i>	The Royal Pacific was a cruise ship with over 500 passengers at the time of its collision with a Taiwanese trawler at the Malacca strait. The vessel sunk eventually.	9

Table 1.1: Some serious accidents involving collisions of passenger ships. *Dona Paz* is the most serious post war accident, (www.wikipedia.org)

1.3 Regulations and design practice

Shipping accidents have always triggered the revision of existing international rules or development of new rules in response to societal pressure for safety improvement. Every time though the pattern is the same: safeguarding human life, environmental damage and property loss are catered for by setting higher and higher standards that

new and existing ships have to comply with. Despite the broad acceptance of high standards of operation, the practical implementation is a major ongoing debate mostly due to the fact that this tactic has been progressively applied for a good part of the 20th century but accidents still happen. Under these circumstances, increasing of standards without some justifiable rationale, directly translates in very tight constraints. This, in turn, creates very infertile ground for engineering applications and has turned the creative *ship design* process into a *rule implementation*, often very expensive, exercise. All potential for innovation, and therefore evolution, has been seriously impeded.

It would be very pessimistic to believe that the situation is hopeless though. Recently, the engineering community has started to understand that it is not prescribed boundaries that provide soundness of ship operations but rather deeper and better understanding of the involved phenomena and good engineering practice that can offer the right solutions and radically alter the situation. Additionally, it is now understood (more than ever before) that solutions that can deal cost-effectively and efficiently with potential unwanted situations have to be addressed not only in the proper way but also at the right time. This time is the *early design* phase of a new ship (or marine vehicle in general), where freedom to make changes has low cost and high value for the overall project (Figure 1.3). Changes in later stages or even during the operational life have substantial impact to the services offered by the ship.

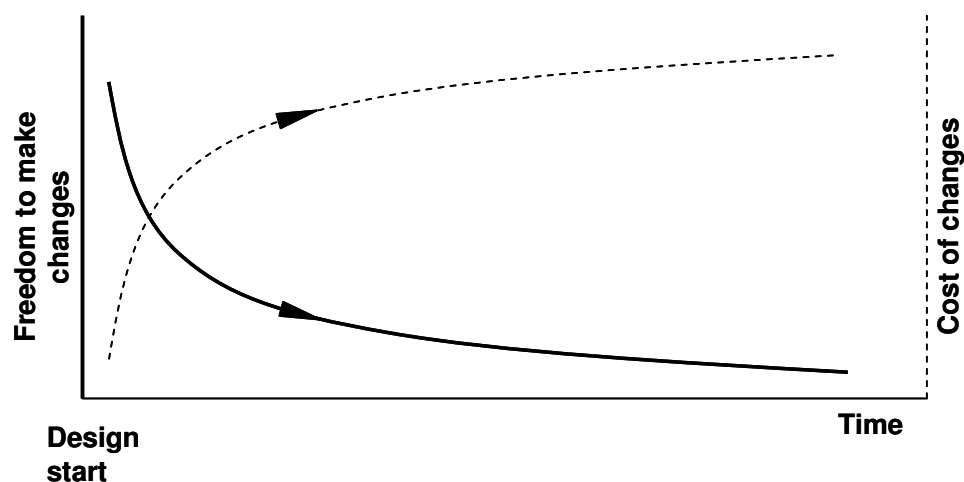


Figure 1.3: The freedom to make changes in the new design is decreasing fast with time

On the other hand, it is widely accepted that shipping operations are complicated in more ways than we would prefer to deal with. The range of approaches for addressing all the issues is very wide and with various degrees of ingenuity and complexity. Mathematical models of all aspects of operations are often followed by *experimental results* for confirmation and calibration. The time consuming character of experiments and the inadequacy of the theoretical models to capture reality together with substantial progress in computer technology has led to the development of versatile *numerical models*.

The fact that numerical modelling and numerical solutions have contributed substantially to the study of various phenomena and to the overall understanding comes at high price. That is, time-consuming development of models, processing and post-processing of results are still prohibitive attributes of this approach. However, when it comes to detailed analyses of a project, these techniques are unsurpassed but the freedom to make changes has already diminished dramatically.

Extensive development of computer applications (in terms of software and hardware) has also allowed the designers to deploy more sophisticated mathematical techniques for obtaining the best possible solution in each design case. The efficiency of searching the design space for all available solutions has increased many times over the traditional approach of relying on the ingenuity, inspiration and talent of a handful of individuals. *Multi-objective / multi-criteria optimisation algorithms* have proven an invaluable weapon in a designer's arsenal but they cannot work out miracles (at least not yet!). This is one extra reason for discarding numerical modelling in the early design phase since (in its general form) it is not compliant with design practice due to its inherent time consuming nature.

Hence, the evident gap of addressing design characteristics that are crucial for operational safety becomes very important. Considering again the complicated nature of operations and the associated incidents it is straightforward to appreciate that adequate and innovative solutions can be obtained only by addressing the situation with *first-principles analytical models*. These models will allow the designers to concentrate on all important characteristics of the new design in terms of functional requirements and performance expectations, investigate sensitive dependencies,

address challenges from an advanced point of view, make decisions with solid arguments regarding all aspects of design and operation, and comply with all safety rules at the same time. In this way, the path towards design evolution and innovation will open up (Figure 1.4).

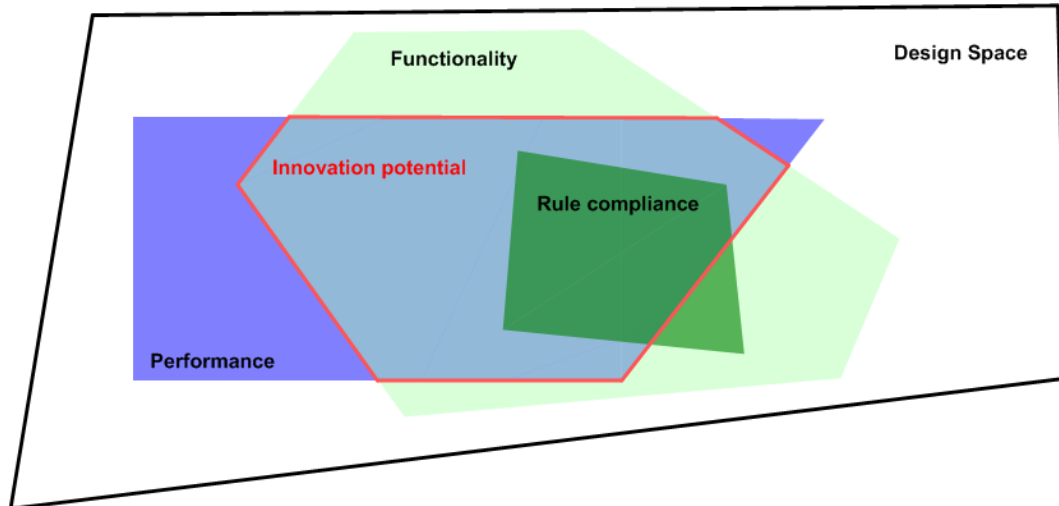


Figure 1.4: Strict rule compliance prohibits detailed search in the design space contrary to the goal-based approaches

Fully compatible with such philosophy is the *goal-based* approach (i.e. prescription of the goal rather than the means to achieve it) to regulations that International Maritime Organisation (IMO) has started considering heavily and show that further revising is still pending with very encouraging results, (Vassalos et al., 2005b).

1.4 The dual character of the project

The modern approach to ship survivability following some prescribed collision damage was first established by Prof. K. Wendel in the 60's, (Wendel, 1960), and endorsed by IMO in the mid 70's (resolution A.265 VIII). As it is described later in this thesis, this approach allows for a large number of damage case scenarios with zero survivability. Be this as it may, it is straightforward for one to realise the serious consequences that such approach could have on the development of new designs, especially so when it is a compulsory statutory requirement, which has to be fulfilled. Appreciation of this fact indicates the incentive to search for an alternative approach that addresses the fundamental requirement of a ship to stay afloat for sufficient time following the breach of its outer shell.

Such approach can naturally initiate from the simplest possible *risk* definition as the product of:

- i). the *probability* of occurrence of an unwanted event, and
- ii). its *consequences*, should it occur.

$$\text{Risk} = \text{Probability} \times \text{Consequence}$$

Breaking down the problem into its ingredients allows for more intensive study of it. In this case, the point of focus is the probability of collision occurrence and the water ingress in the hull conditioned on a collision event. More specifically, if a potentially hazardous encounter, which can lead to collision, is initiated with the probability of collision and it is expanded to the probability of water ingress and, in turn, to the survival probability, the following expression can be written (based on Bayes theorem), (Vassalos, 2004):

$$P = P_c \times P_{w/c} \times P_{f/w/c} \quad (1.1)$$

where

- P_c : the probability of collision
- $P_{w/c}$: the conditional probability of water ingress due to collision
- $P_{f/w/c}$: the conditional probability of flooding due to water ingress and due to collision.

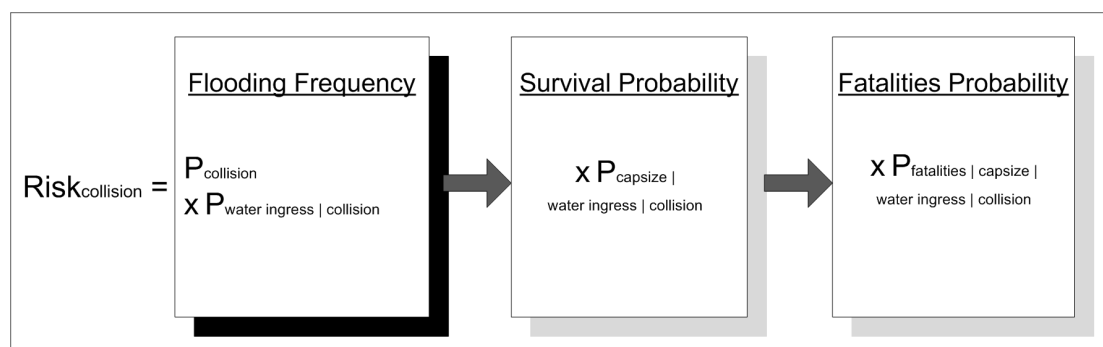


Figure 1.5: Schematic representation of the whole risk assessment process. This project focuses on the first two elements of probability.

The work presented here focuses on the first two elements of probability, (Figure 1.5). The remaining elements are addressed in separate research projects, e.g. (Zhang & Vassalos, 2007). The consequences of an accident have different forms depending on the types of vessel involved. That is, if the survivability of passenger vessels is the topic then the value of human life has to be addressed, (Skjong et al., 2005), whereas in the case of oil tankers the environmental impact and the recovery cost of spilled oil is of primary interest, (White & Molloy, 2003). Property loss is a common outcome in both cases. The difficulty here is that engineering practice alone is not enough for quantifying the consequences of an accident. Other disciplines have to contribute also (economics, social and political sciences, etc.), with highly conflicting priorities. As a result, only ranges of values can be achieved, which demand the authority of a major body (e.g. IMO) for determining, for example, the value of human life.

1.5 The probability of collision event

The very demanding operational profile of modern ships and the congested waters of straits, channels, ports and terminals naturally lead to increased risk levels regarding contact or collision between ships. The event of collision between two ships is governed by a wide range of parameters, quantitative and qualitative in nature, both with significant contribution to the frequency of occurrence of the event. For risk analysis purposes, the available semi-empirical models of (Fujii et al., 1974), (MacDuff, 1974), etc., are extensively used but they capture only part of reality due to inherent difficulties in describing soft parameters (e.g. human intervention) and their localised character.

For a more general application, the concept of “ship domain” will be used and adapted (Chapter 4). It was first established in the late 70’s and it defines a collision – free area surrounding a ship. This area can be defined as a circle or an ellipse, the dimensions of which are some multiple of ship’s overall length. If an object (either moving or stationary) penetrates this domain then a “contact” event is implied. The ship domain idea can facilitate a more concrete way of describing and quantifying the probability of collision occurrence since its size will vary according to the operational profile and the geographical area of operation of the ship. That is, its size

will be significantly reduced within channels or straits but it can extend to mathematical infinity in the open sea.

Moreover, since the collision occurrence is attributed to a series of events, which take effect in a deterministic way, they are sensitive to initial conditions (e.g. the wind speed and direction at the start of an evasive manoeuvre), and they occur recursively, the concept of *entropy of information* is introduced. In this way, improved mathematical models are developed, which can accommodate the soft issues mentioned above.

1.6 The probability of water ingress due to collision

The second focus point of this thesis addresses the probability of water ingress, i.e. breaching of the side shell of the struck ship in a collision event. It is customary to group collision events under two broad categories: the “low energy collisions” and the “high energy collisions” (even though it will be shown later that this is not entirely correct). In the first case, where no breach or very small size of breach occurs, the only consequence is related to repairing cost and, probably, the market reputation of the ship. In the second case though, ship survivability is compromised significantly. In this case, it is necessary to assess the size of the breach and its location with respect to the waterline of the struck ship.

The phenomenon is tightly connected to the absorbing capacity of impact energy of the side shell panels, i.e. their *crashworthiness* without rupturing, (Vredeveldt, 2005). The stiffeners are buckling, tripping and eventually detaching from the plating, whereas the plating itself is subjected to extreme deflection and finally rupture. Currently, assessment of this situation early in the design process is prohibitive due its complicated nature. In addition, the scantlings of the structural elements are not finalised until the basic or the detailed design stage starts due to interaction between steel weight, stability levels, compliance with regulations, maintenance and production requirements, etc.

Once the structural details are fixed, then the Finite Element (FE) technique is extensively used for predicting the response of impact loading. FE is admittedly a powerful tool for such complicated analyses and most probably the only tool

available for the demanding nature of such calculations. This however comes at a high price: proper modelling and interpretation of the results are major topics of extended discussion, which cannot be afforded in the early stages of design, where most of the fundamental characteristics of the new vessel are decided.

The alternative approach is to consider the energy content involved in such an event. That is, when the kinetic energy of the striking vessel is transferred to the struck vessel through contact, strain energy and heat are produced. The first part is directly absorbed by a restricted portion of the structure and the second is dissipated in the surrounding space (water, structure and air). The fact that the whole phenomenon is highly localised indicates the potential way in which it can be addressed. That is, the generic assessment of a stiffened panel to absorb strain energy imposed by an external (much stiffer) body, which is driven through it. The deflection (or the penetration) of the panel should be the independent variable of the accumulated strain energy. Based on these characteristics, collision events will be addressed very early in the design stage and crashworthiness will become another design objective next to seakeeping, propulsion, resistance, ultimate strength, etc. This will allow the designers to consider alternative arrangements (in space distribution and structural configuration) and improve the survivability of the new ship.

1.7 Thesis structure

Following this introductory chapter and a critical literature review, the two elements of probability outlined above (probability of collision and probability of water ingress due to collision) will be elaborated and each topic will be treated in a chapter on its own. A separate chapter will be dedicated to the consolidation of the findings into a new explicit methodology for addressing ship-ship collisions in a risk-based design context and in relation to the existing probabilistic framework for flooding, (IMO, 2006). Finally, a series of fictional case studies will demonstrate the range of applicability of the proposed ideas. The sequence of the chapters is presented in Figure 1.6.

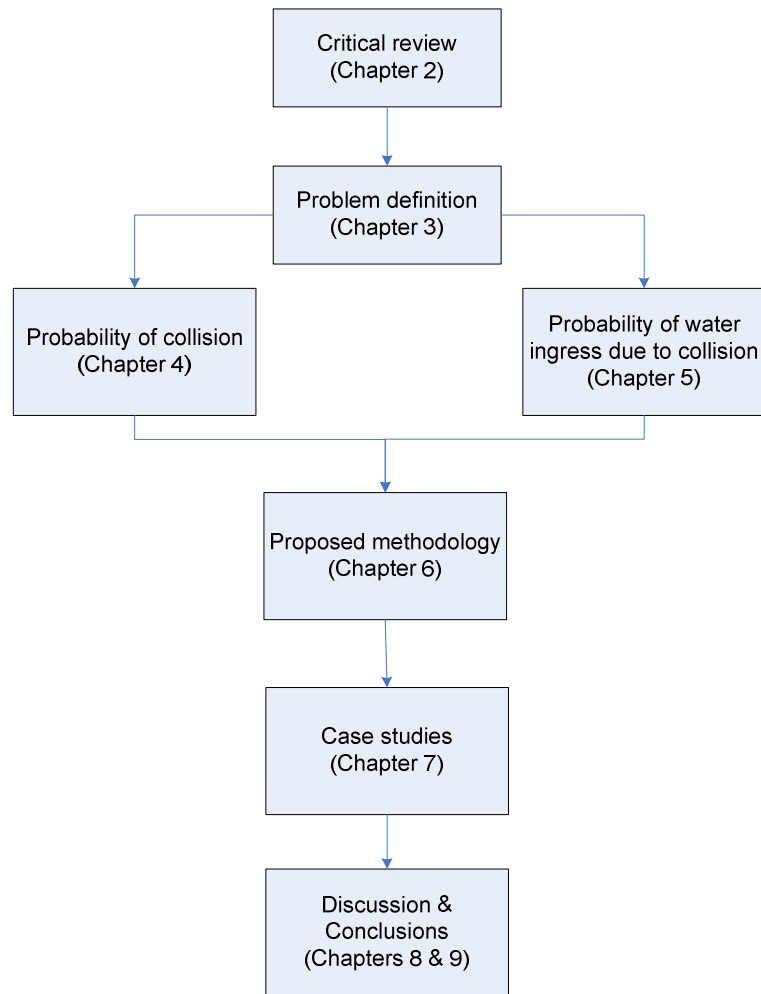


Figure 1.6: Thesis structure and chapter references

1.8 Thesis objectives

The work presented here aims to establish the missing link between crashworthiness capacity of a ship and its survivability potential in the early design stage.

This objective will be pursued along the following two strands:

1. Development of a model for the calculation of the probability of a collision event, which can take into account all the operational and design elements contributing to its occurrence.
2. Assessment of the crashworthiness potential of the side shell of a vessel in terms of size of breach and penetration.

Both models will be as generic as possible and of *analytical* nature, i.e. they will be available for the early design stage, to be used as performance measures in large scale multi-objective / multi-criteria optimisation schemes, where operational safety is a fundamental design virtue. It is not the purpose of this work to perform a risk analysis study but rather to produce the tools and the methodology for systematically incorporating risk analysis in the design process, i.e. to perform risk-based design. In this way, the main contribution of the work will be to bridge the gap between the operational profile of a ship and its survivability potential. Finally, the proposed methodology should provide input to the existing probabilistic damage stability framework of SOLAS Chapter II-1.

2 Critical review

2.1 Introduction

This chapter focuses on the critical review of existing methods and approaches established and used over the past 30 years (with some exceptions) for the study of the probability of a collision event and the probability of water ingress due to collision. The dual character of this work makes it necessary to separate the approaches into two sections, one for each topic of interest.

2.2 Probability of a collision event

Modelling the probability of a collision event for a ship entails a large number of parameters, which are not readily measurable in engineering terms. This issue makes the scholars of this topic to search for alternative techniques, which describe and assess the frequency of their occurrence more efficiently.

The very phrase *probability of collision* directs the study into stochastic approaches. By definition, these approaches allow for greater flexibility in taking into account the range of values such parameters are likely to be assigned. Based on this notion, the probability of occurrence of some event (most of the time unfavourable) is established.

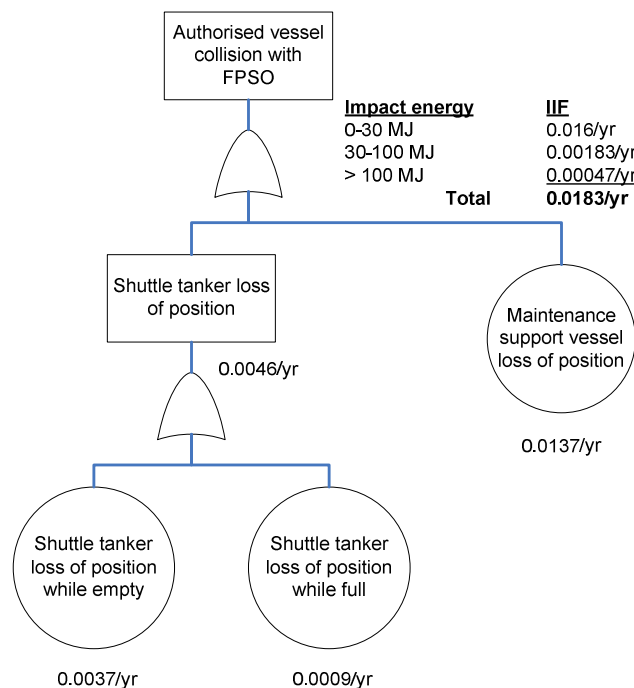


Figure 2.1: Collision probability of supply vessel with FPSO, (Husky, 2000)

It was realised quite early that a ship-ship collision happens mostly because combinations of unfavourable events occur at the same time or cascade within very short-time intervals allowing even less margin for intervention. Had each of these events happened individually, to a lesser extent or under slightly different circumstances, then the collision could be averted. Appreciation of this fact led quite

naturally into modelling of the situation with the simplest tools available. That is, *fault trees* (bottom-up) and *event trees* (top-down), (Henley & Kumamoto, 1992).

Based on the mathematical theory of probability and the experience built through the years from other fields of engineering (nuclear industry pioneered in this area), reliability theory was established and along with it the fault and event trees technique for the assessment of the probability of unwanted events in general and ship-ship collisions in particular.

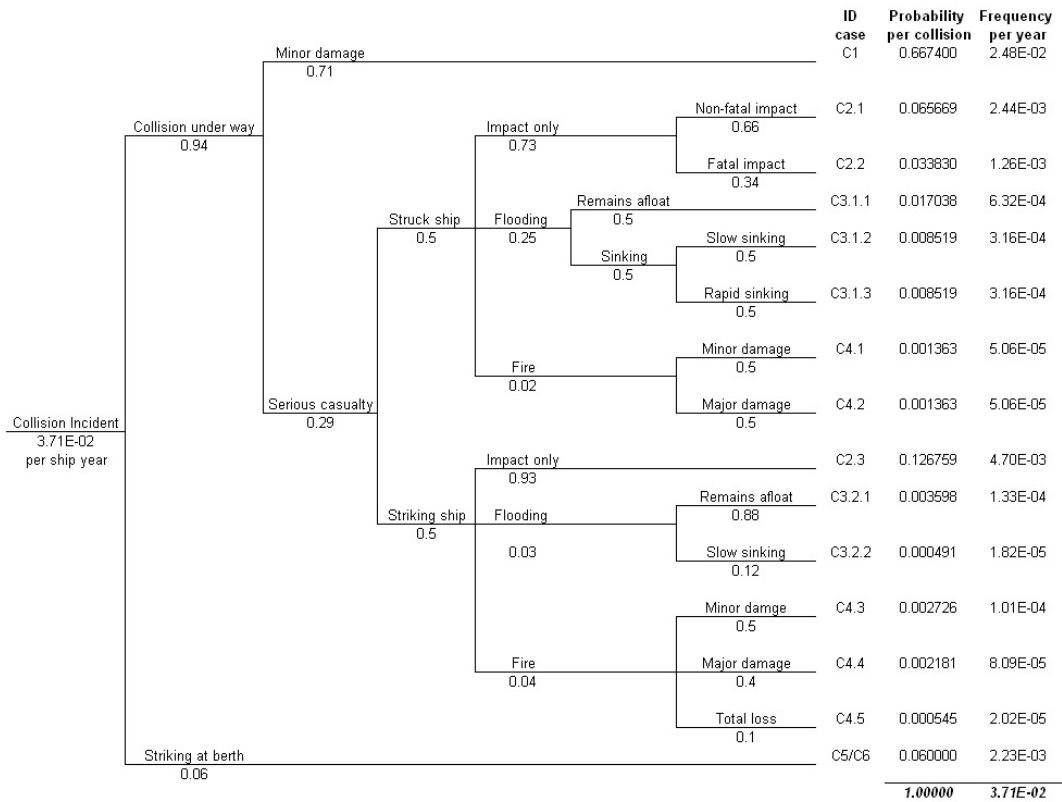


Figure 2.2: Generic event tree for collision outcomes, (Spouge, 1996)

Both techniques allow the development of models of different extent and complexity. For example in (Husky, 2000) a fault tree model is presented for predicting the collision between an FPSO and a maintenance support vessel or a shuttle tanker due to loss of position (Figure 2.1). In (DNV Technica, 1996), (Spouge, 1996) and (Konovessis et al., 2007) more sophisticated models are developed (Figure 2.2), which are used for in-depth analysis of the factors leading to such an event. Fault and

event trees are also recommended (among a gallery of tools) by US Coast Guard in the Risk-based Decision-making guidelines, (Rothblum, 2000).

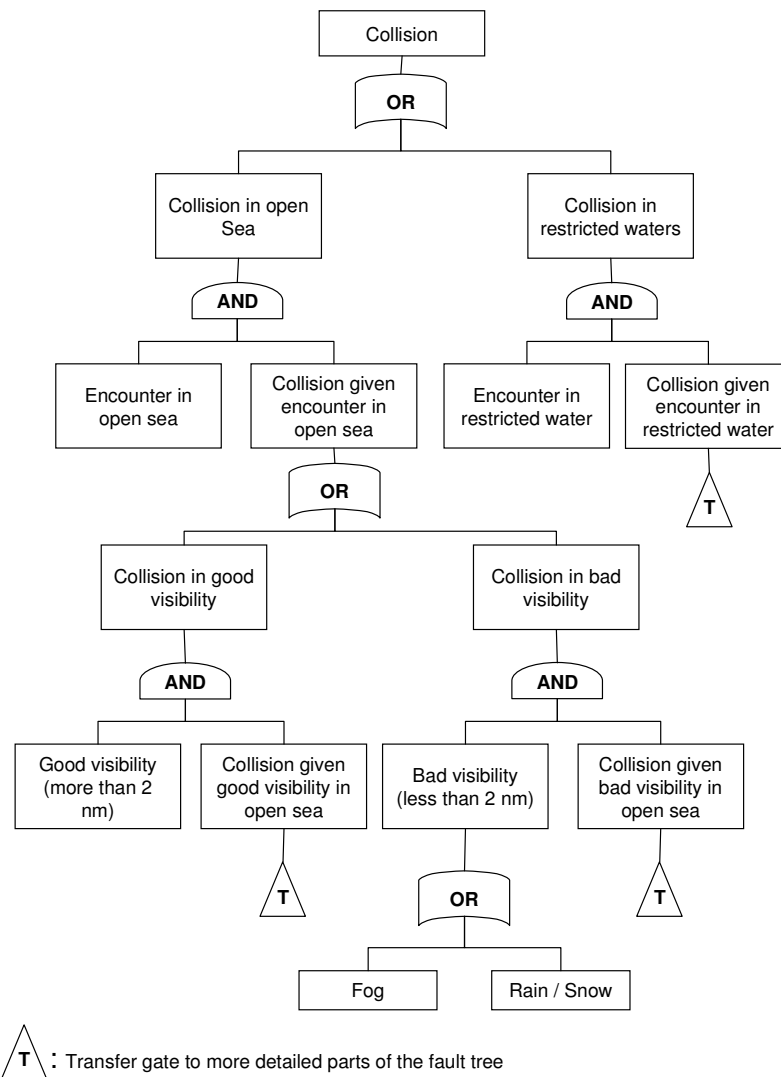


Figure 2.3: Snapshot of a fault tree for prediction of collision probability, (DNV Technica, 1996)

Study of the work presented in these publications reveals the type and quality of parameters involved, which range between a ship’s own systems, environmental effects, human factors, and combinations in various levels of interaction. Practical application of these techniques led to deeper understanding of the situations and the associated phenomena to the occurrence of highly unwanted events. As a result, the weaknesses and limitations of fault and event trees were revealed. Their *static* nature does not allow for extensive scenario consideration (different combinations of generic events that lead to the top event or interdependence of the root events, e.g.

“Fog” and “Rain / Snow” in Figure 2.3) and consequently the information they provide to a risk analysis framework has, arguably, little information content.

Contrary to these tools, *Bayesian Networks* (BN) appear to be a more robust alternative, (Jensen, 1996), (Jensen & Nielsen, 2001), etc. They are *directional* graphs that establish *cause-and-effect* relationships among the participating factors of a collision event. They are based on Bayes’ Theorem for the prediction of probability according to:

$$P(A|B) = \frac{P(B|A)P(A)}{P(B)} \quad (2.1)$$

where

- P(A), P(B): probability of occurrence of event A and B respectively
- P(A|B): conditional probability of event A due to event B

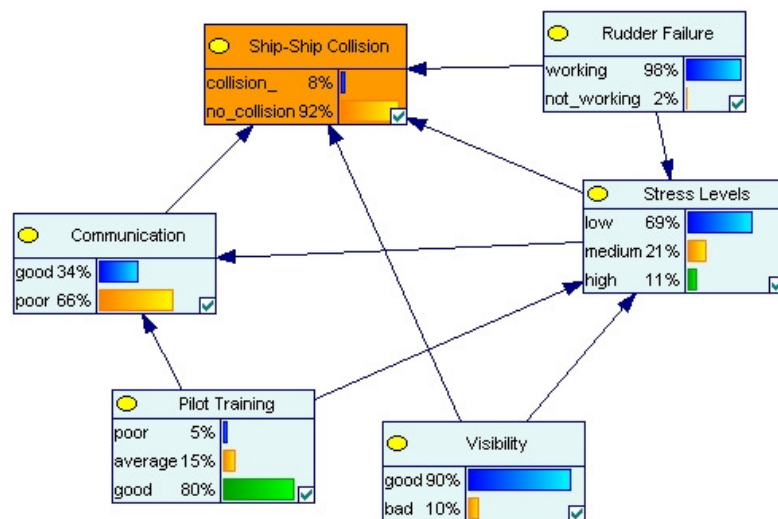


Figure 2.4: Collision occurrence due to environmental, hardware and human factors, (Mermiris et al., 2007c)

Bayes theorem essentially allows for the estimation of the probability of occurrence of a posterior event A given the observed probability of a prior event B. This property also makes BN *acyclic*. Bayes’ theorem is useful in updating a BN with a small number of nodes and states per node. When larger networks are developed, this

approach is impractical and therefore more sophisticated techniques have been developed, e.g. (Shachter, 1986).

Figure 2.4 presents an example of a BN for the occurrence of a collision event, which is governed by human element, environmental factors and hardware failure. For example, reduced visibility will increase the stress levels of the navigator. Thus, his level of experience in similar situations becomes very critical as will his control over the situation and eventually his actions and reactions in close encounters with other ships.

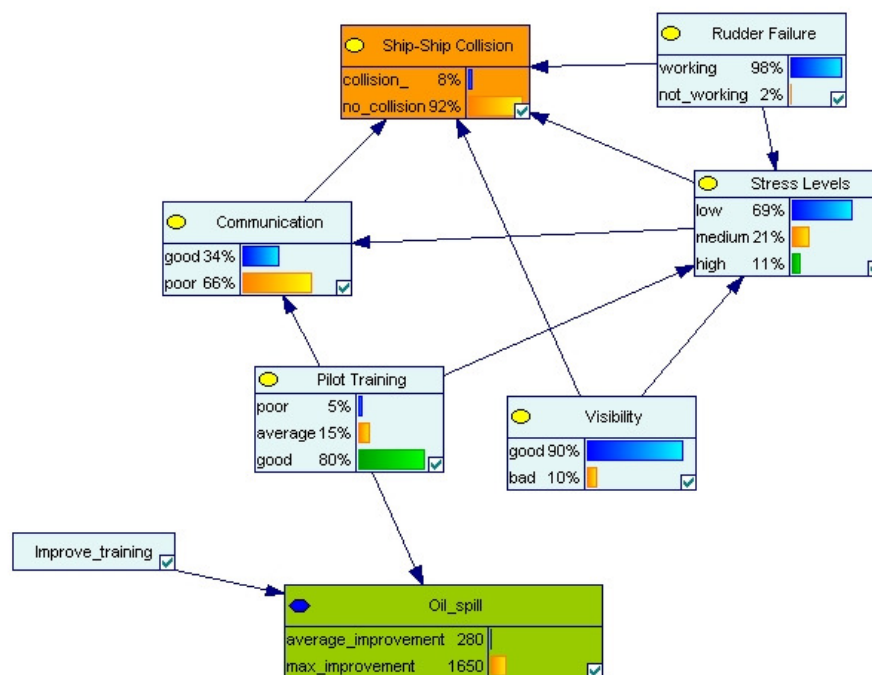


Figure 2.5: A decision node is included (“Improve_training”) with the indicative level of improvement and the associated cost for pilots in the form of utility values (“Oil_spill”), (Mermiris et al., 2007c)

BN are flexible enough to provide a dynamic framework so that a series of unwanted scenarios can be examined. The results of each scenario can be directly associated to a set of consequences expressed as *utilities*. In this case, they are called *Decision* or *Influence Graphs* and they can provide a more complete picture of a risk analysis study. For example, assuming that there is a company policy for pilot training, the decision graph of Figure 2.5 can provide some answers regarding the level of improvement that can be achieved and the associated cost. Indicative work with BN

has been presented by (Hansen, 2000), (Hansen & Simonsen, 2001), (Ravn et al., 2006) and (Datubo et al., 2006).

Human factor is the most challenging and difficult to model since the navigators make decisions (Figure 2.6), which may equally lead to disasters or prevent them from happening. W. A. O’Neil, (Secretary General of IMO) stressed in his speech in 2001 that:

“On a ship, the human element can provide a weather eye for difficulties ahead, a calm, unruffled response to situations as they develop and those indefinable qualities known as good seamanship; or it can be frail, lacking in competence, ability and concentration. People remain a basic component with all their strengths and weaknesses which can both cause a disaster or prevent it”.

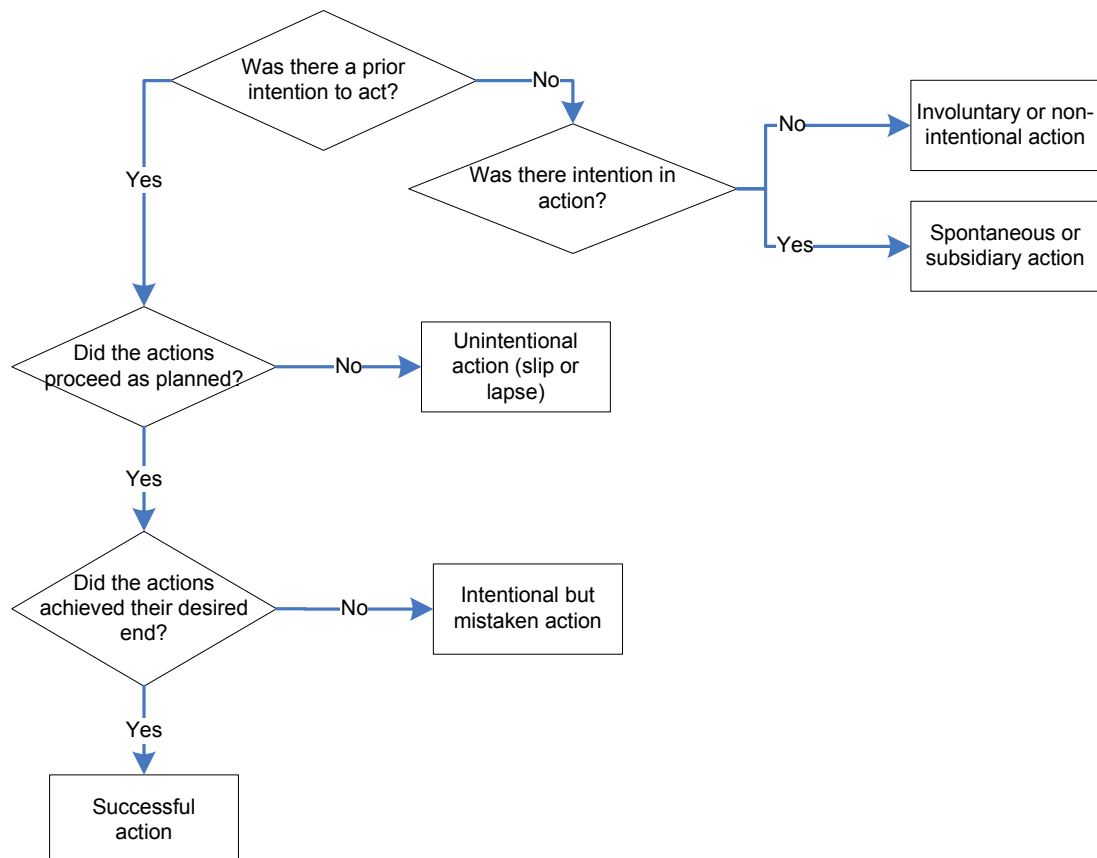


Figure 2.6: Process for distinguishing of varieties of intentional behaviour, (Reason, 1990)

Since study of the human performance and its effects on ship collisions at sea is out of the scope of this work, a few characteristic examples of the work performed in this area, like those of (Bryant, 1991), (Rothblum, 2000), (Liu & Wu, 2003), (Barker & McCafferty, 2005) and more explicitly (Amrozowicz et al., 1997), (Brown & Haugene, 1998) and (Houtman et al., 2005) can be further consulted. Accident databases can also provide useful input to such studies. A good example is the analysis presented in (ABS, 2004) with respect to human error and generic initiating hardware failures, which are developed into catastrophic events.

PSF	1 st Subcategory	2 nd Subcategory	3 rd Subcategory	...
Changes	Life Work Environment			...
Impairment	Fatigue	Sleep deprivation Circadian Rhythm Prolonged Exertion	Mental Physical	
	Well-being	Mental	Psychiatric Intellectual	
	Medical	Restrictions Side Effects		
	Drugs	Alcohol abuse Illegal / Illicit Drugs		
Training	Routine Tasks Unfamiliar Events Emergency Response			
Education	Background Principles Analytical Knowledge			
Experience	In Industry At Job / Position In Task In Environment With Equipment With Team Members			
...	...			

Table 2.1: Partial table with Performance Shaping Factors (reproduced from (Boniface & Bea, 1996)).

It is stressed in (Harrald et al., 1998) that during a risk analysis process, appreciation of human error requires deeper understanding of the personal history of the officer in charge (i.e. the officer on watch or the pilot on board). Such a situation is only possible in very detailed practical investigations. At a theoretical level, it is very difficult to classify human contribution without supporting data. For this reason, the concept of *performance shaping factors* (PSF) (Table 2.1) for describing the conditions that contribute to human error has been established in THERP (Technique for Human Error Rate Prediction from (Swain & Guttman, 1983)). Additionally, methodologies like the Generic Error Modelling System (GEMS) suggested by (Reason, 1990), where differentiation between *skill-based*, *rule-based* and

knowledge-based errors takes place, can potentially contribute more robust input to risk analyses in combination with the work of (Boniface & Bea, 1996). Despite the fact that detailed analysis of all significant issues related to the performance of navigators has been conducted, consistent quantification is still lacking and, as a result, *expert judgement* is deployed in the majority of detailed risk analyses.

Analytical formulations for the probability of collision

The following two sections are summarising the two most popular analytical approaches for assessing the probability of collision: (i) the Fujii and (ii) the Macduff models.

(i) The Fujii model

The models developed by (Fujii et al., 1974) are based on statistics of accidents occurred in Japanese waters. The main topic is the probability of collision with a fixed object: in this context, the term is used in a more general sense including stranding and contact along with the factors affecting their occurrence. Special interest is paid to the contribution of visibility level in the accident rate, which is obviously a major environmental concern for navigation in the particular area. Although this study is very generic, the developed models are largely based on interpretation of statistical data regarding the traffic density for a specific region. This approach is widely accepted in similar studies ever since but still deem the models quite specific. Inherent issues of the ship itself (e.g. its manoeuvrability capability) that can define the predicament of a hazardous situation are not considered.

The two Fujii models have the following form

For crossing / joining and leaving lanes

$$F = \frac{P_C N_1 N_2}{nHC} \left(\frac{L_1}{V_1} + \frac{L_2}{V_2} \right) \quad (2.2)$$

For head-on / overtaking encounters

$$F = \frac{P_C N_1 N_2 L}{WHC} (B_1 + B_2) \left(\frac{1}{V_1} \pm \frac{1}{V_2} \right) \quad (2.3)$$

where

- F: frequency per year of collisions involving the subject ship
- P_C: Causation probability (2.0×10⁻⁴ for medium quality personnel and management, 1.6×10⁻⁴ for high quality personnel and management)
- N₁: movements per year by subject ship
- N₂: movement per year by other ships
- n = 1 for crossing lanes; n = 2 for joining and leaving lanes
- V₁: average speed of subject ship in knots
- V₂: average of other ships in knots
- L₁: length of subject ship in metres
- L₂: average length of other ships in metres
- B₁: beam of subject ship in metres
- B₂: average beam of other ships in metres
- L: length of lane in nautical miles
- W: width of lane in nautical miles
- H: hours per year (8760)
- C: metres per nautical mile (1852)

Despite these drawbacks, Fujii models highlight three significant characteristics for the calculation of the probability of collision. These are:

- *Traffic density* (number of ships per unit area): it appears to be the most critical parameter in the models. In fact, it is claimed that the probability of collision is proportional to the square of the traffic density. This result

is not confirmed in the model developed in this work although the dependency on it is quite pronounced.

- Thorough statistical analysis of the available data confirms the correlation between accident occurrence and *low visibility* either due to darkness or environmental conditions (e.g. fog). It appears that 1 km is the threshold between high and low accident rates (approximately with a ratio of 3:1) for the geographical area considered in these studies.
- Further processing of the available data reveals the contribution of *navigator's familiarity* with local waters in accident reduction (in particular stranding). This is presented as a ratio of 15:1 for pilots / masters with long sailing experience in the particular region and others with lesser knowledge of the area (i.e. ships that do not visit these waters frequently).

Fujii models, along with models developed by other researchers, for example (Kristiansen, 2005), capture a large set of factors that can lead to a collision. However, they are based extensively on the number of ship movements in a very specific geographical area and they have various forms (not substantially different) for various situations (crossing lanes, head-on encounters, etc.). These two issues underline their basic purpose for development, which was the conduct of risk analysis. Even though this requirement follows the risk-based design methodology for incorporating risk analysis in the design process, the results are too case-specific to allow generalised conclusions and decision-making by the designer. The reasons are that the exact conditions under which a collision can occur cannot be known in advance although the vessel's operational profile is.

(ii) The Macduff model

Macduff's model, (Macduff, 1974), is based on the concept of Buffon's Needle problem, (Weisstein, 2005), from the *geometrical probability* area of mathematics. This characteristic makes this model more rigorous mathematically but implies the need to combine it with other elements of probability (systems failure, human

element, environmental conditions, etc.) to make it more robust. The probability of grounding (*grounding* can easily “translate” to *contact* or *collision*) is:

$$P = \frac{4T}{\pi C} \quad (2.4)$$

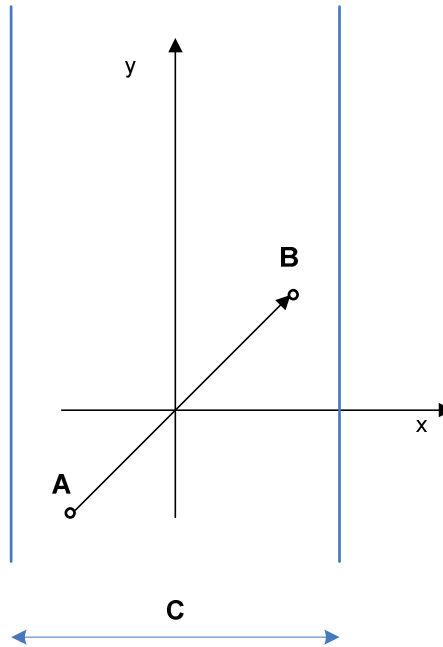


Figure 2.7: Idealised geometry for Macduff's model

The ship proceeds along a channel of width C and its crash stopping manoeuvre (straight line of length T) starts at point A and finishes at point B (Figure 2.7). Despite its straight forward character, the size of the ship, its current speed and the surrounding conditions (environment, traffic, etc.) are not included in the model, thus making it a less attractive choice in a design context.

2.3 Probability of water ingress due to collision

The second element of this research work is concerned with the crashworthiness of the side shell structure of ships. That is, the capacity of the structure to absorb impact energy following a ship-ship collision event. This property of the structure will directly define the size of breach and therefore the potential for water ingress. Obviously, the issue here is lacking the ambiguity of the probability of collision but it is still very complicated: a consistent and clear approach for *early* design assessment is still missing.

Analytical and statistical approaches

Bearing in mind the requirements for suitable formulations for design purposes, it is natural to see the first attempts to the crashworthiness assessment of the side shell structures established in an analytical fashion. The approaches vary in complexity, originality and execution, hence spreading over a broad range of fields and ideas.

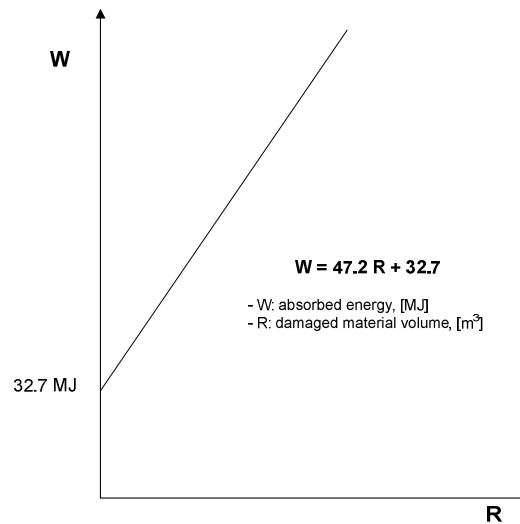


Figure 2.8: Minorsky's model as it was initially published in (Minorsky, 1959)

V. Minorsky pioneered the study of ship collisions with his simplified regression model, (Minorsky, 1959), which relates the absorbed energy of both the struck and the striking ship to the damaged volume of material (Figure 2.8). The model addresses only high energy collisions due to the fact that Minorsky was interested in collisions that would cause large penetrations and could compromise the safety of nuclear power installations. His model was further improved for low energy collisions by (Van Matter et al., 1979).

The simplified spring-mass model, with so many applications in the study of dynamical systems, is further exploited in the current context. For example, (Dias & Pereira, 2004), (Ruan & Yu, 2005) and (Gao et al., 2005) introduce some basic ideas of simple spring-mass systems and some more sophisticated Lagrangian formulations for impulsive loading.

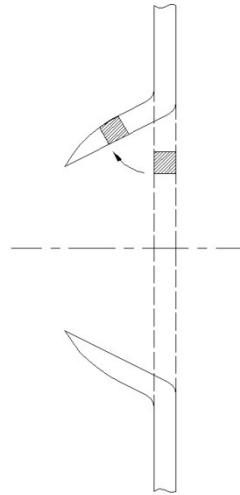


Figure 2.9: The conical crater idealised geometry in (Thomson, 1955). The fact that impact energy may be exhausted long before the plate reaches that state is not considered in the method

The physical behaviour of bodies and materials when subjected to extreme dynamic loading has often inspired further modelling. In this respect, (Thomson, 1955) quite early introduced some simplified geometry in the case of high energy collisions (reproduced in Figure 2.9) and in recent years (Wierzbicki & Driscoll, 1995), (Ohtsubo & Wang, 1996), (Paik & Wierzbicki, 1997), (Jones, 1998), (Brown & Chen, 2002) developed mathematical models based on such behaviour (as it is presented in Figure 2.10 and Figure 2.11 for example). Other models were based on the response of more complicated stiffened panels like in the cases of (McDermott et al., 1974), (Reckling, 1983) and (Paik et al., 1999a). More sophisticated approaches to geometry utilisation have been attempted by (Langhaar, 1952), (Iglesias et al., 2001) and (Quek et al., 2003) in the context of *Differential Geometry* as it is discussed later in Chapter 5 and Appendix B.

Realising the complications in the response of stiffened panels, studies were performed for understanding and describing the response of the panel elements, namely stiffeners and plates. The vast number of contributions belonging to this group is difficult to include in this review. Only the work of a few researchers can be mentioned whilst the contribution of the rest is silently acknowledged. Study of the dynamic behaviour of beams has been performed by (Jones & Shen, 1993), (Sastranegara et al., 2005), (Jones, 1995), (Lellep & Torn, 2005), (Graciano, 2003) and in the case of plates by (Wen & Jones, 1992), (Teng & Wierzbicki, 2005) and

(Wang et al. 2005). At this point it is necessary to mention the seminal work of Norman Jones in his book (Jones, 1989) for a consistent presentation of all the relevant formulations regarding plates and beams under shock and impact.

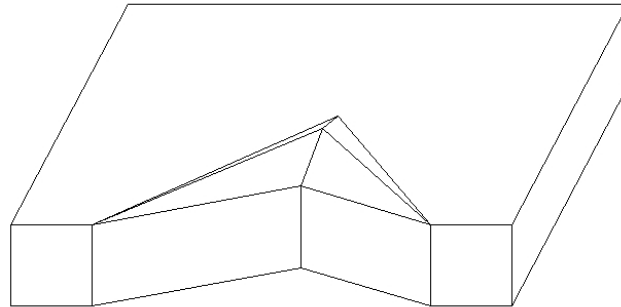


Figure 2.10: The idealised denting mode of deformation modelled in (Wierzbicki & Driscoll, 1995), (Ohtsubo & Wang, 1996) and (Zhang, 1999)

In the area of marine structures in particular, the ideas of geometrical deformation have been implemented in modelling the crushing of structural elements in (Pedersen & Zhang, 2000), (Lutzen et al., 2000) and (Ambramowicz & Simonsen, 2003). In addition, models for the physics underlining the external dynamics of collision events are well documented in (Petersen, 1982), (Simonsen, 1997), (Zhang, 1999) and (Pedersen & Zhang, 1998).

Despite the simplicity of these approaches, more sophisticated techniques, which can capture more aspects of reality and, in particular, the plastic nature in which the structure deforms can be found in (Symonds, 1968), (Chanda, 2003), (Yefimov et al., 2004) and (Micunovic, 1992). When large deflections are considered then (Berger, 1955), (Bergander et al., 1992), (Byklum & Amdhal, 2002), (Drawshi & Betten, 1992) and (Hausler et al., 2004) provide useful background and ideas. The loss of the material isotropy when it is subjected to large deflections is captured in the work of (Wang, 1970), (Morino et al., 1971a), (Morino et al., 1971b), (Vlassak et al., 2003) and (Tsakmakis, 2004). The foundations for the description of the anisotropic materials are included in (Lekhnitskii, 1968). Both of these topics are discussed further in Chapter 5.

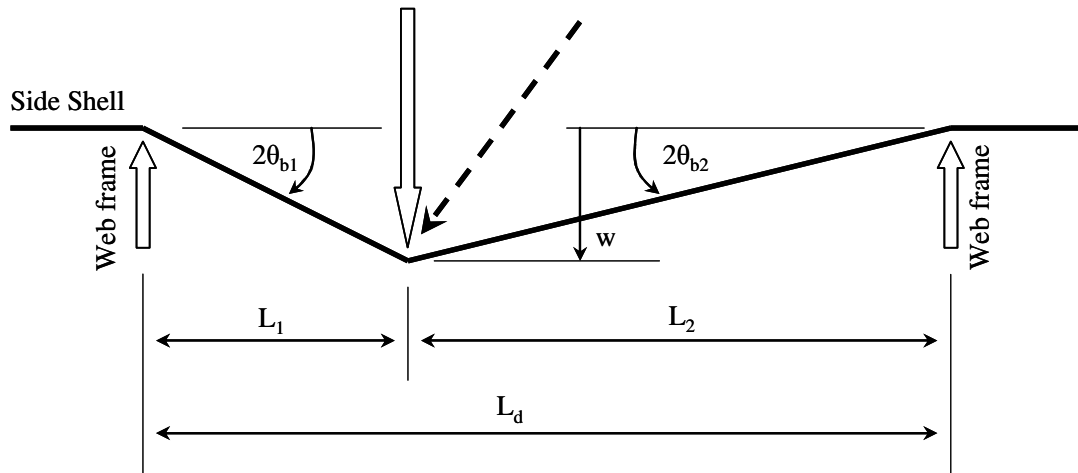


Figure 2.11: Membrane geometry, (Brown, 2002b)

Further attempts to describe the nature of rupture initiation have been modelled with *discrete dislocation models* in (Yefimov et al., 2004) or with the development of *continuous damage mechanics*, where the concept of *effective* or *actual stress* is established. That is, in cases of excessive loading of a structural element the resulting large plastic strain leads to the weakening of the material by void nucleation and growth of micro-cracks and micro-voids at grain level. In this respect, the initial cross sectional area of the material capable of carrying load is reduced (Figure 2.12). The damage imposed to the material results in a new state of stress. For the specific case of uniaxial tensile loading, the actual normal stress has the form of:

$$\sigma_{\alpha} = \frac{P}{A_0 - A} = \frac{P}{A_0(1-D)} = \frac{\sigma}{1-D} \quad (2.5)$$

σ_{α} : actual stress

σ : nominal normal stress

P: tensile load

A_0 : initial (undamaged) cross sectional area

A: damage cross sectional area

$D=A/A_0$: damage variable

Typical work has been presented in (Lemaitre, 1984), (Krajcinovic, 1984), (Lemaitre, 1985), (Kachanov, 1986), (Komori, 1999) and (Komori, 2005).

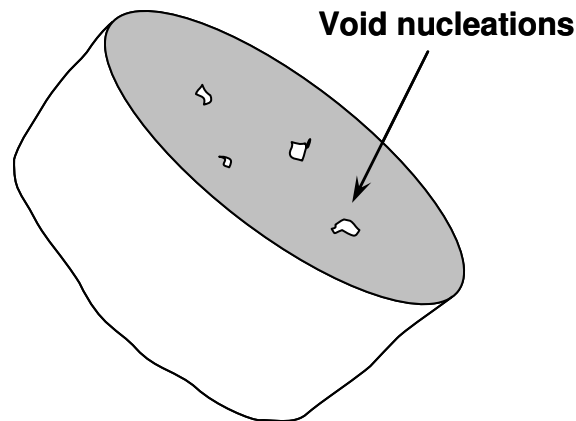


Figure 2.12: Void nucleation and micro-crack / micro-void accumulation leads to weakening of the load carrying capacity of the structure and eventually its failure, (Kachanov, 1986).

As the understanding of the complicated nature of ship-ship collision was maturing there was a migration from the traditional deterministic to a probabilistic analysis. This result signified a more general turn in the flexibility of probabilistic analysis with respect to risk assessment. Since the collision consequences can compromise the survivability of the ship and its effect on human life, property and environment, studies with this orientation appeared in the literature. Representative work in this area can be found in (Brown & Amrozowicz, 1996), (Sirkar et al, 1997), (Amrozowicz et al., 1997), (Rawson et al., 1998), (Brown & Haugene, 1998), (Brown et al., 2000), (Lutzen, 2001), (Brown et al., 2002), (Brown, 2002a), (Brown & Chen, 2002), (Wang et al., 2003) and (Brown & Sajdak, 2004).

In addition to the work of individuals or small groups of researchers, more extended projects were undertaken with important results. The HARDER project (Harmonisation of Rules and Design Rationale) belongs to this group. Its consortium was formed by 19 organisations from Europe. The project aimed at investigating the impact of existing damage stability regulations on the safety levels of existing ships and the development of alternative design solutions. Part of the delivered work is reported in (HARDER, 2001a) and (HARDER, 2001b). The DEXTREMEL project (Design for Structural Safety under Extreme Loads), (DEXTREMEL, 2001), has developed statistical analysis regarding the structural response of the shell structure in the event of collision. The topic for the CRASHCOASTER (Crashworthy Side Structures in Short Sea Shipping) project was the investigation of the safety of ships

following collisions. A series of full-scale collision experiments were devised for the needs of the project (Figure 2.13). Reports of the deliverables and the philosophy of the project can be found in (Vredeveltdt, 2001a) and (Vredeveltdt, 2001b).



Figure 2.13: Full-scale experiments from the CRASHCOASTER project
(<http://crashcoaster.rtdproject.net/>)

Finite Element analyses

Finite Element (FE) analyses prove to be the most widely used means of assessing the crashworthiness characteristics of a structure in marine accidents. The simple governing philosophy allows the development of new algorithms or refinement of existing ones. At the same time, experimental input can be used directly either for validation or calibration of the code. Furthermore, recent progress in Information Technology allows for efficient post-processing of the results: detailed visualisations and graphing facilities, which permit very detailed presentation of the way the structure as a whole or its components respond to extreme loading. These features make FE very attractive to researchers and practitioners.

Establishment of the code is, not surprisingly, based on analytical models, which for computational reasons do not perform as expected. As a result, modification of the initial analytical models leads to formulations very close to those of FE techniques. Indicative work has been presented by (Ambramowicz, 2003), (Fakuchi et al., 2006) and (Kaliszky & Logo, 2006).

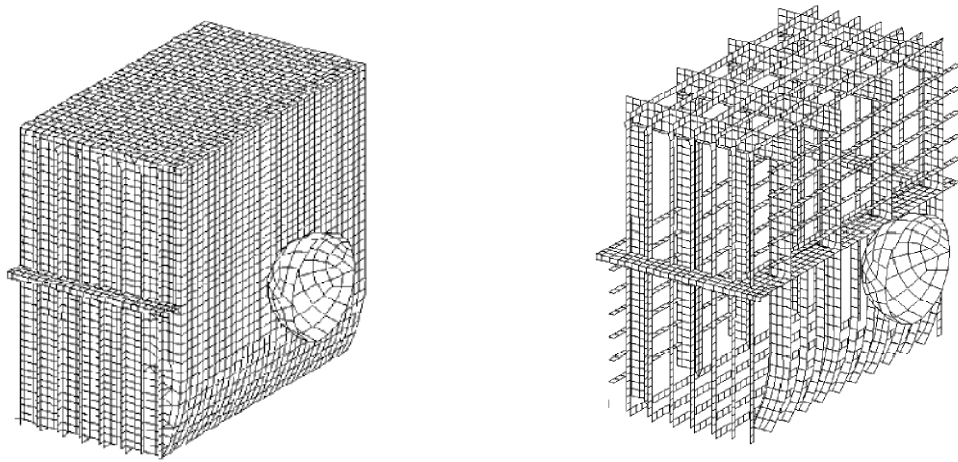


Figure 2.14: Modelling of a struck tank and its associated stiffening system, (Servis et al., 2002)

Despite the variety of approaches, it appears that a limited number of software dominate the area, that is the ANSYS / LS-DYNA and the ABAQUS / Explicit. Researchers are using these tools for studying the complicated nature of crashworthiness of a structure in different contexts and approaches. For example (Guo et al., 2003) are using LS-DYNA for different modelling strategies of panel like structures, which are subjected to perforation loading and (Leclere et al., 2004) are using ABAQUS / Explicit for implementing some void nucleation ideas in the 3D rupture simulation of elastoplastic structures.

Irrespective of the software tool deployed, obtaining the dynamic response of a structure remains one of the main topics of study with many different approaches, insights and approximations. Research is performed either in an elementary level like the study of low velocity impact on plates in (Liua et al., 2005), the interaction of plate and impactor, (Heitzer, 1996), the basic folding mechanism of plated structures, (Vafai et al., 2003) or the elastoplastic damage of two deformable bodies, (Zhu & Cescotto, 1992). In a more advanced level, stiffened panel response is the study topic of (Barik & Mukhopadhyay, 2002) and (Rigo et al., 2003).

In the area of marine vehicles there is the extra need to consider the scenario under which the structure suffers substantial deformation as it is stressed in (Servis & Samuelides, 1999). The models of Figure 2.14 and Figure 2.15 and the following publications are indicative of the work performed in this area: (Ellinas, 1995),

(Servis et al., 2002), (Lehmann & Peschmann, 2002), (Le Sourme et al., 2003), (Tornqvist, 2003), (Paik et al., 2004), (Simonsen & Tornqvist, 2004), (Wu et al., 2004) and (Ozguc et al., 2005).

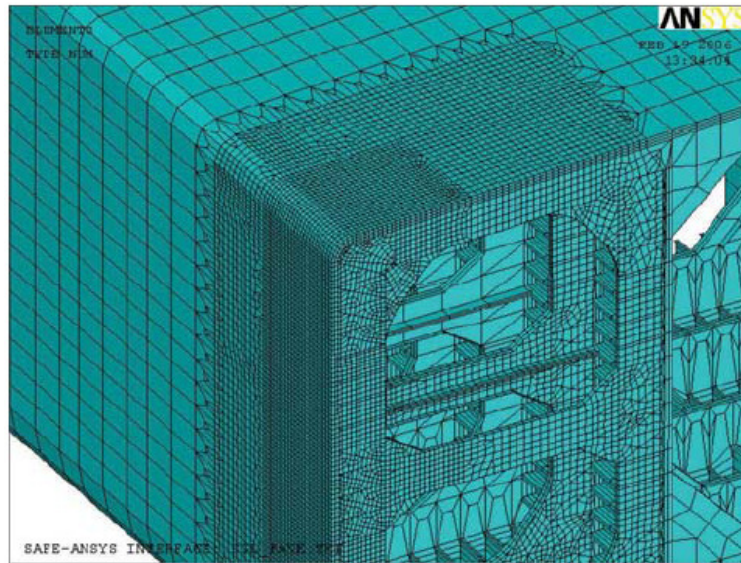


Figure 2.15: Fine meshing in areas of interest, (Zheng et al., 2007)

Simplified approaches

The deficiencies of FE analyses led some researchers in developing faster methods of estimation of side shell damage following a collision event. Effort was directed towards reducing the complexity of the model in terms of element size and number of degrees of freedom. Along these lines of thought one can find the Idealised Structural Unit Method (ISUM) as published in (Paik & Pedersen, 1996) and (Paik & Seo, 2007). The method is now implemented as ALPS/SCOL commercial code for progressive structural crashworthiness under collision and grounding (www.proteusengineering.com).

One of the outcomes of the project “Information Technology for Enhanced Safety and Efficiency in Ship Design and Operation” (ISESO, www.iseso.org) was the GRACAT software. The assessment of the structural response is made with the use of *super-elements*, which represent the variation of energy absorption of each exposed element to a collision situation. The modelling of the struck structure is composed of elements like those presented in Figure 2.16. In this way, the unstiffened span of a plate or the joint of a stiffener and a deck (T- or X- shape) are

modelled explicitly. The energy absorption is calculated for each of the identified elements and is summed up for the total of the struck surface.

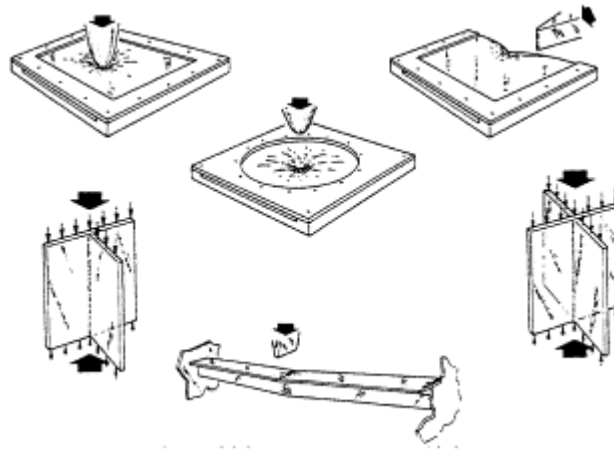


Figure 2.16: Super elements used in GRACAT, (Hansen & Simonsen, 2001)

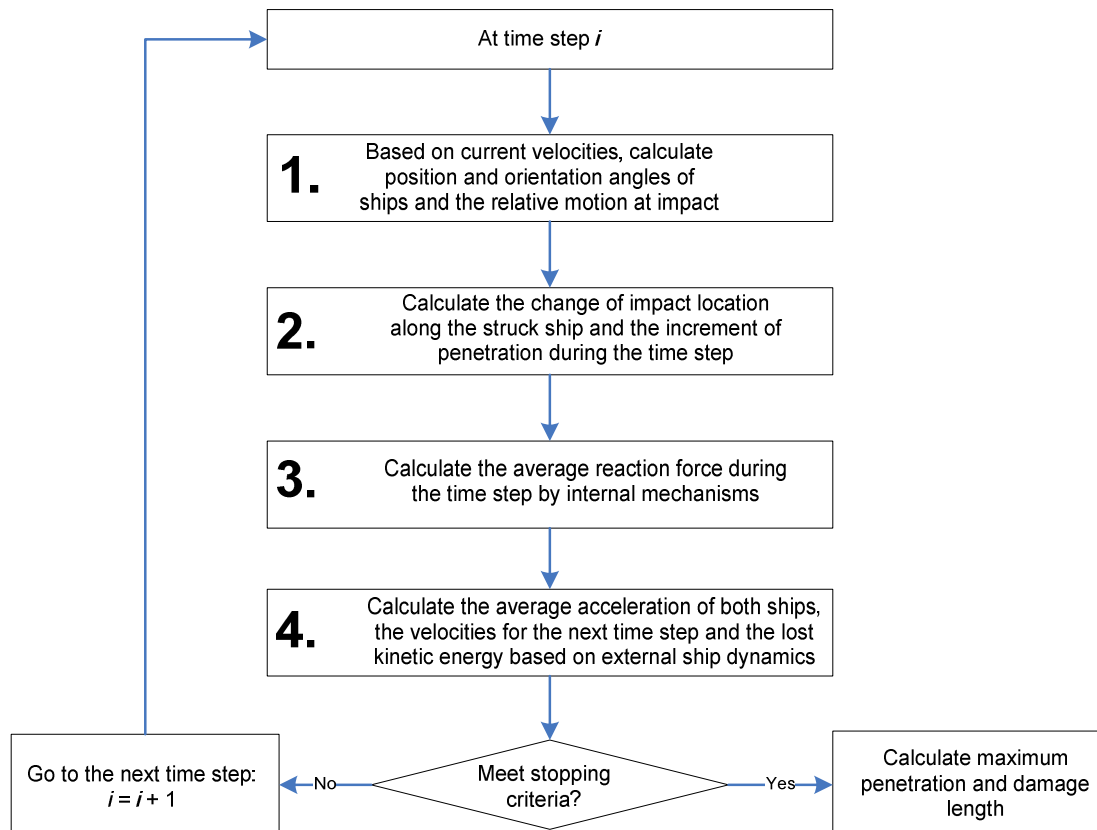


Figure 2.17: SIMCOL process reproduced from (Sajdak & Brown, 2004)

Finally, the SIMCOL software, as presented in (Brown, 2002b) and (Sajdak & Brown, 2004), is based on a more analytical formulation of idealised deformation

(Figure 2.11). The whole duration of the collision is modelled and the results are not restricted to description of the damage alone (breach size and penetration) but expand into calculation of the longitudinal extent of damage. This approach allows for more robust estimation of the consequences of a collision (e.g. in case of a tanker, the number of tanks that have been ruptured provides for a much better estimate of oil outflow). The calculation steps of the SIMCOL methodology are presented in Figure 2.17.

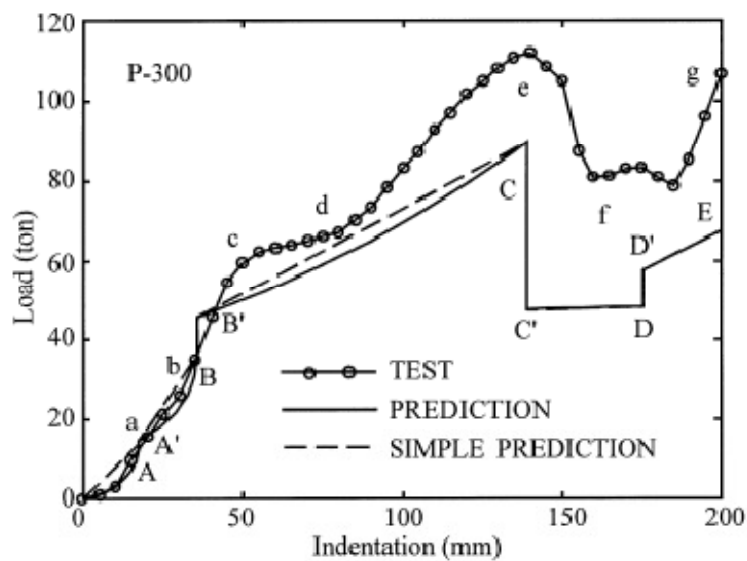
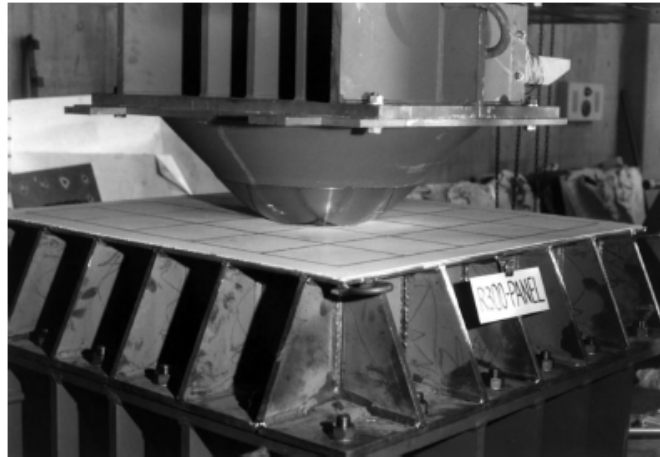


Figure 2.18: Double hull indentation experiment, (Wang et al, 2000)

Experimental studies

Irrespective of the volume of data produced by theoretical methods and the level of sophistication, experimental techniques have always occupied a special position in

the research community. There is no doubt that the theoretical predictions have to be verified or even benchmarked by experiments. Especially in the area of impact studies, where the nature of the phenomena is highly complex, experimental studies contribute to understanding and confirmation of intuitive predictions substantially (Figure 2.18). Furthermore, the controlled conditions in the laboratory can lead to the development of simplified mathematical models, which offer wide-ranging potential for application. Indicative work in this area has been performed by (Samuelides, 1984), (Zhu, 1990), (Wen & Jones, 1992), (Jones, 1994), (Ohtsubo & Wang, 1996), (Simonsen & Wierzbicki, 1997), (Simonsen & Ocakli, 1999), (Gupta & Ray, 1999), (Wang et al, 2000), (Huang et al, 2002), (Jones & Jones, 2002) and (Jones & Birch, 2006).

2.4 Regulatory bodies

The topic of dealing effectively with the damage caused by a collision event has been an issue among regulatory bodies in several countries. The nature of the regulations regarding the impact capacity of structures stresses once more the limited knowledge about the details of this phenomenon in its manifestation.

Plate rupture is usually the most common concern since water ingress can lead to catastrophic consequences compared to the structural failure of web frames for example. At the same time, it is common understanding among regulators that dealing with the detailed response of the structure is of no practical use for rule development. As a result, the criterion of the severity of a collision is always concerned with the involved energy levels. Obviously, high energy content will drive the rupture mechanism sooner than low energy content. As a result, certain energy thresholds are set as presented for example in (HSE, 2000) and (HSE, 2004). These reports from the Health and Safety Executive (www.hse.gov.uk) in the UK are concerned with the crashworthiness capacity of FPSO vessels operating in the North Sea. The limits of the study are defined by the collision of an FPSO with a supply vessel and a tanker. The threshold energy that should be absorbed by the side structure is set to 4.0 MJ.

Germanischer Lloyd, (GL, 2006), has issued probably the first non-compulsory regulations for determining the crashworthiness of the side shell of a vessel. Details of the impact scenario such as the relative draught of the struck and striking vessels (Figure 2.19), the impact speed of the striking vessel and the critical energy necessary to cause irreversible damage to the struck hull are taken into account by creating a series of alternative scenarios. The associated COLL notation is related to the critical striking speed (Table 2.2) and the capacity of the side shell to absorb energy without rupturing. In this way, the operational profile of the vessel is partially taken into consideration.

COLL Notation	Critical speed in knots
COLL1	1.0
COLL2	1.5
COLL3	2.5
COLL4	4.0
COLL5	5.5
COLL6	7.0

Table 2.2: Minimum values for the mean critical speed, (GL, 2006)

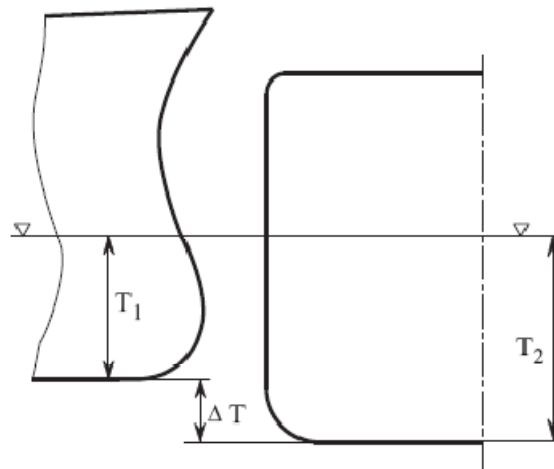


Figure 2.19: The relative draught of the striking and struck ship is considered in the calculations, (GL, 2006)

Due to high interest of the collision of supply vessels to the legs and bracing members of offshore platforms, the Standardisation Organisation in Norway (NORSOK, www.standard.no) has also issued guidelines regarding their structural strength, (NORSOK, 1999) and (NORSOK, 2004). This set of guidelines describes the external dynamics of collisions (added mass contribution in surge and sway,

supply vessel displacement and speed, etc.) along with the deformation mechanics of structural members (critical rupture strain, non-linear FE analyses, etc.). A more detailed discussion on existing regulations in the area of ship collisions can be found in (Samuelides et al., 2008).

2.5 Chapter summary

The critical review presented in this chapter provides indications of existing gaps in the methodologies, techniques and approaches available for assessment of the probability of collision and the crashworthiness of ships' sides. At the same time, study of the available material is necessary in order to gain a deeper understanding and appreciation of the complexity of the situation in each case. It is true that the two areas presented here have their very own and distinct difficulties, yet they have to be addressed in a manner that will provide consistent input to the design process when crashworthiness is considered. Further description of the difficulties introduced in this chapter will follow in Chapter 3, where elaboration on the actual problem will take place.

3 Problem definition

3.1 Introduction

The current state of regulations and a brief description of their impact on the design and performance characteristics of modern merchant shipping are presented in this chapter. Consequently, the need for establishing *analytical* models for the design process, in general, and for the collision assessment, in particular, is identified as part of the *Risk-Based Design* methodology. The concepts of *collision occurrence* and *water ingress due to collision* events are presented and discussed.

3.2 Philosophy of current regulatory approaches

As mentioned in Section 1.4, Wendel recommended for the first time the probabilistic approach for the assessment of survivability of damaged ships as an alternative to deterministic approaches, (Wendel, 1960) and (Wendel, 1968). Implementation of this method has been through a number of stages of development in IMO, spanning almost fifty years. In 1992, SOLAS part B-1 (Chapter II-1) came into force with probabilistic damage stability rules for cargo ships.

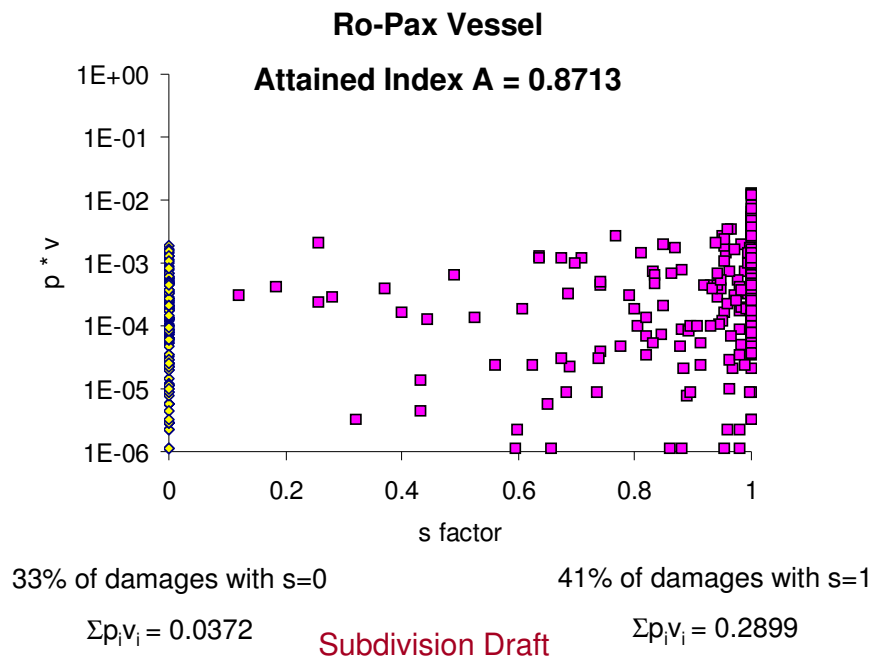


Figure 3.1: Probabilistic damage stability calculations for a ROPAX, where a third of the damages lead to zero survivability of the ship.

The distinct feature of these developments is not about the visionary ideas of Wendel but rather about the philosophy behind the rules and regulations. Every major accident in marine industry, from *Titanic* to *Estonia*, has caused major concern in society and has undoubtedly initiated improvements to regulations. The issue of providing shipping operations with adequate limits of safety has started with the first Merchant Shipping Act in 1854 in response to the foundering of the *Birkenhead* two years earlier and the loss of some 500 women and children off the coast of South Africa. A concise account of historical development of safety standards can be found in (Vassalos, 2000). The characteristic reaction of authorities to the public outcry for

safety improvement that occurred at that time seems to follow up the development of rules and regulations until today: the standards are upgraded *after* an accident happens. It seems that the approach of *curing* rather than *preventing* has always been the norm, irrespective of the context and purpose of application. The thinking has been on the mitigation side of the consequences rather than on remedying the real causes of the accident. The “patching” mentality of the regulations is presented in Figure 3.1 where despite the relatively high index A of a Ro-Ro passenger ship (i.e. relatively low collision risk) 33% of damage scenarios lead to vessel loss resulting in design changes that do little to improve its safety, (Vassalos et al., 2006b).

In engineering sciences, the central theme is about understanding of the basic mechanism of a physical phenomenon and implementation of knowledge with clearly defined and tangible objectives. Despite the fact that this route of action has repeatedly proven itself through time, still it does not attract the amount of attention it deserves among regulatory bodies of shipping industry.

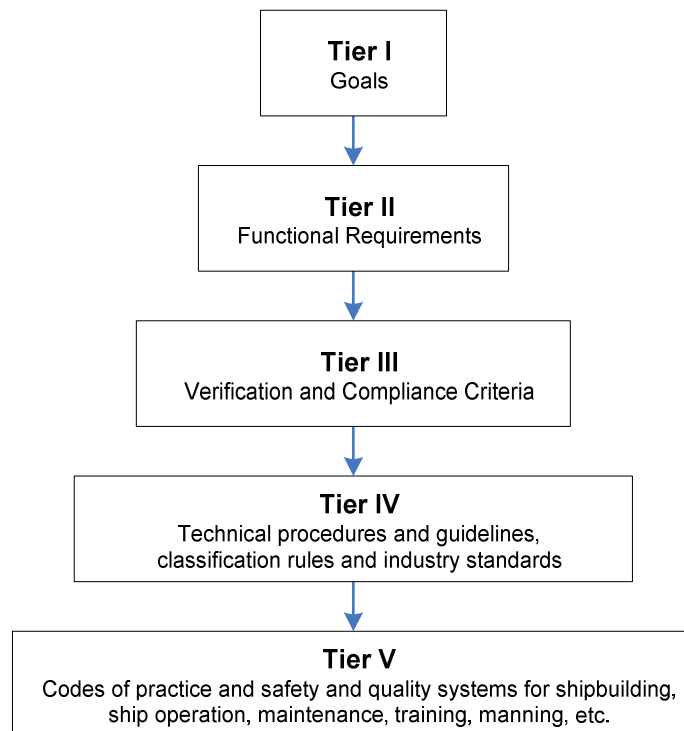


Figure 3.2: Goal-based approach in ship design and operation

The guidelines for design of marine vehicles have the rigid form of an old-fashioned doctor’s prescription for headache: a universal painkiller for all adult population.

Recently medical science has made a major break-through by mapping the human genome and associating the condition of each gene to a specific illness. In the future, doctors will be able to develop treatments based on the prediction of the susceptibility to each disease for each person in advance, and administer a tailored therapy to the needs of the particular individual before the symptoms appear.

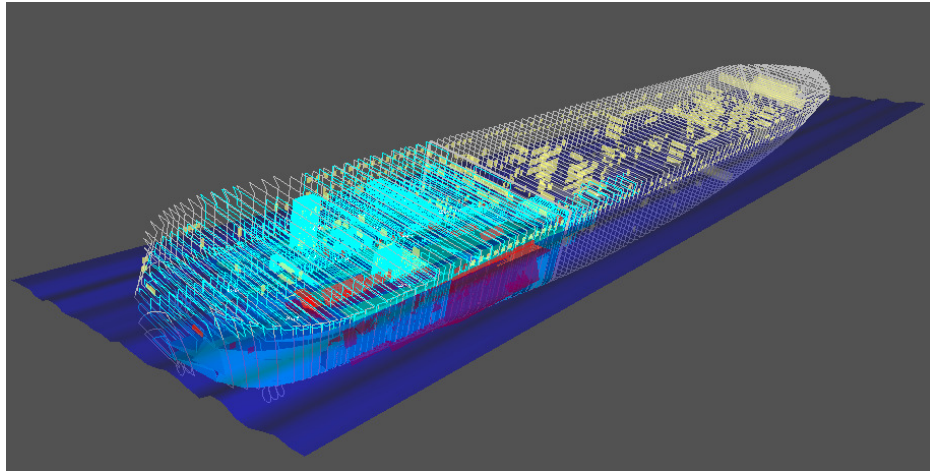


Figure 3.3: Flooding analysis model for Project Genesis comprising 717 compartments and 1,160 openings, (Vassalos, 2009)

It is probably time to have a similar break-through in maritime industry. The rules should facilitate freedom of thinking and creativity in order to allow the designers of marine vehicles to comprehend and appreciate the special nature of each design project. That is, to identify the governing parameters of the operational behaviour of each vessel and to administer the proper solutions. The *goal-based* approaches (Hoppe, 2005), largely debated in IMO recently, are probably the best vehicle to facilitate such ideas and provide the pathway to a much more promising future (Figure 3.2). This can be achieved with the development of first-principles tools (Figure 3.3) and techniques that can meaningfully describe the complicated underlying phenomena of shipping operations. Such approaches will allow better modelling of ships' operational profile during design and they will prepare the ground for development of more fit-for-purpose design solutions, which should satisfy better the service providers (owners / managers) and the service users (society) alike, in comparison to existing ones. The improved results offered by

analytical methods and the increased acceptance of probabilistic approaches by the industry over the past 20 years greatly encourage the introduction of these methods.

3.3 Analytical models: the next phase of evolution in ship design

Complexity and regulations

The complexity of the events that lead to a collision occurrence and the collision phenomenon (dynamic contact) between two ships is evident and widely accepted. The initiation of the event following a sequence of actions and the final manifestation of contact between two vessels is a function of a substantial number of parameters. To increase the complexity of the situation further, not all of the involved parameters can be quantified either because of their nature (e.g. stress levels of the navigator) or because the incident itself is so dramatic that it is simply chosen to focus all attention on the major event only, i.e. the deep deformation of the penetration. One such example is the heat produced due to friction of the striking and the struck surfaces, which alters the mechanical properties of steel and can lead to fire ignition. In the majority of collisions, both vessels are in motion and they are certainly not lacking in mass or speed (i.e. kinetic energy). It is, therefore, a major simplification to assume that all the kinetic energy of the striking vessel (including its surge added mass) is totally absorbed by the struck vessel (again considering its sway or yaw motion and the associated added mass/moment) without any dissipation in the surrounding environment (water, air and more remote areas of the structure).

Additionally, once the contact between the bow (striking ship) and the side shell (struck ship) begins, the path that the former will follow is not easy to determine. The complexity of the supporting structure of the side shell leaves almost no margin for evaluation of the amount of energy that is absorbed by each stiffener individually and of the overall affected area in total. Obviously, the more complicated the structural arrangement of the contact area is, the more the uncertainty of the calculation. Furthermore, some portion of the impact energy is absorbed by the bow of the striking vessel. The exact mechanism of the bow deformation complicates the phenomenon even further since in general the bow (stem and bulb) is one of the most heavily stiffened parts of a ship. As such, assessment of its deformation (i.e. the

proportion of the impact energy absorbed by it) becomes an even more cumbersome exercise with ambiguous results.

Existing formulations, either numerical or semi-empirical, contribute significantly to the general understanding of the phenomenon but neither can cope effectively with the involved complexity, as the deformation pattern and the energy absorption capacity of every stiffening element is extremely difficult to assess. As a result, there are special (explicit) codes of FE collision analyses (transient cases), where the constitutive equations of the structure are only approximated. On the other hand, experimental approaches can only cope with models of a limited complexity: studies are performed in unstiffened plates or stiffeners (of various cross sections), which are not attached to plates. The semi-empirical models, which are based on these results have, by definition, very limited applicability. There are very few cases where experiments have focused on panels with realistic structural configuration, (Wang et al, 2000). Yet again, the actual behaviour of a stiffened panel in the vicinity of a major structural element (a deck or a bulkhead) is totally unknown.

It seems that the only way to overcome all these difficulties is to use FE analyses with all the drawbacks this choice implies. Most importantly, designers are left without any efficient tools for early design development and performance evaluation. The time-consuming character of FEA allows only for specific scenario examination (deterministic in nature) and provides little insight for improvement (or innovation) of the structural arrangement.

Additionally, there is no clear connection to the next stage of the design development. That is, upon conclusion of this analysis (i.e. on the condition that a collision occurs), the objective is to obtain the location and size of breach. The next step is to utilise this information and calculate the damage stability of the struck vessel (depending on the case however, other issues might be more important e.g. in a nuclear ship to estimate whether any radiation leakage has occurred due to penetration). That is, calculation of the effects of water ingress in the hull, which leads to loss of stability (transversely, longitudinally or both), and results in listing and capsizing or foundering.

Currently, the first part of the calculation is prescribed by regulations for the assessment of the damage stability, conditional on the size of the damage opening. For example in (IMO, 2004) and (IMO, 2006), Regulation 8 is describing “*Special requirements concerning passenger ship stability*”. In particular, the damage extent depends on the number of passengers onboard as follows:

... where 400 or more persons are to be carried, a damage length of $0.03L_s$ but not less than 3 m is to be assumed at any position along the side shell, in conjunction with a penetration inboard of $0.1B$ but not less than 0.75 m ...

... where less than 400 persons are carried, damage length is to be assumed at any position along the shell side between transverse watertight bulkheads provided that the distance between two adjacent transverse watertight bulkheads is not less than the assumed damage length...

Constraints like those in the above extract from the IMO documents are numerous and widely acknowledged as *weaknesses* of the regulations. They have been discussed in various forums and publications through the years, for example in (Vassalos et al., 2005b), (Pawlowski, 2005), etc. with a wide range of recommendations for improvement.

The important issue is that designs have to comply with such regulations. Their admittedly complicated nature, the lack of obvious rationale and the strict conformance of the end design with them leaves small margin for creativity by the designer. Alternative solutions, which may be obtained either through insight and inspiration or more sophisticated approaches (e.g. optimisation schemes), are very early discarded, not because of their inferiority but due to their non-compliance with past design approaches on which existing regulations are based. Quite naturally, the outcome of such a process is the almost pre-determined arrangements of past designs with very little, if any, additional elements that can actively contribute towards safety improvement. The imminent result is that because of such prescribed processes and the very short-sighted practices in force, shipping accidents still occur with high toll penalties to human life, loss of property and environmental impact.

An alternative approach

Appreciation of the above facts naturally leads to the source of the uncertainty and at the same time highlights some evident answers. For example, if the number of persons onboard is to be considered as the defining parameter for the size of breach, why does it have to be 400 and not 450? Is the difference between the two limits so substantial that it requires definition of this particular border line? If the difference is so important, how it can be afforded to be flexible with the definition of the damage size for more than 400 persons and not for less?

If the number of passengers reflects the size of the vessel, which in turn reflects its operational profile and therefore the type of accidents that is likely to be involved in, the size of the vessel could be expressed as a function of the number of passengers! Analysis of the rationale behind the regulations defines the solution to the problem: it is necessary to set up high level analytical models that can capture explicitly the risk content at sea over a certain period of time as a function of a set of independent variables. Then, implementation of rules of calculus can indicate the rate of change of the function, its minima and maxima (local or global) points, any convergence or singular values, etc.

Under this prism of thought, study of accident reports of ship collisions indicate that there are only a handful of factors that can actually affect the development of a hazardous event into a real, high risk situation. In the overwhelming proportion of cases, the way to avoid such a situation is to rapidly alter course. This time, there is full agreement with regulations, (COLREG, 2003). Of course, there should be some space available in order to do so, which, once more, is related to the operational profile (area of operation, traffic conditions, speed, etc.) of the vessel, its size and manoeuvrability characteristics. Obviously, it is also necessary to take into account the intervention of the navigator (pilot, master or officer-on-watch) and his contribution to the situation.

Summarising all these, the probability of collision occurrence can actually be expressed as a function of the size of the vessel, the time interval to change its course at any given speed, the available area for manoeuvring and the human element.

Consolidation of these factors into a single function is introduced later in this chapter and in more detail in Chapter 4.

On the other hand, in the unfortunate event of collision, it is necessary to assess the crashworthiness of the vessel. This time the complexity of the phenomenon is of different nature and the model has to capture two important elements:

- The geometrical shape (sharpness) of the impacting body, which is directly related to the damage it can cause to the side of the struck vessel.
- The structural configuration of the struck area (arrangement and construction material), which defines its energy absorbing capacity.

Both these issues will be further discussed in Section 3.7 and in Chapter 5 in more detail.

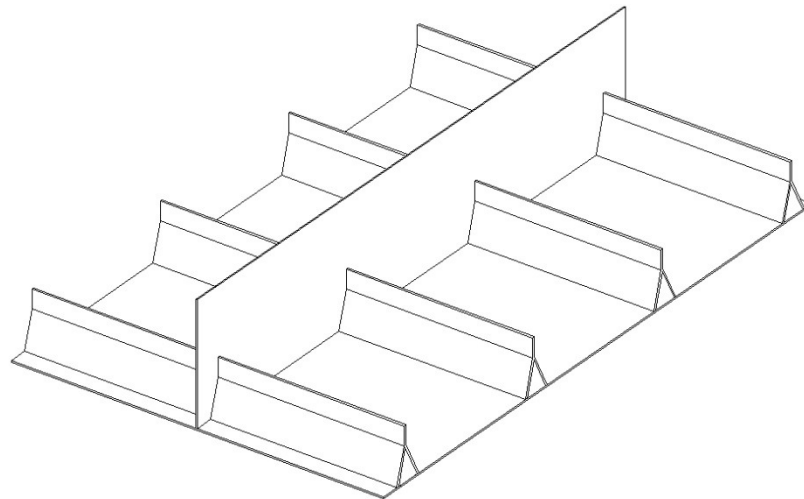


Figure 3.4: Assessment of Y-sections for side or bottom panels like those proposed in (Naar et al., 2002) is not possible with statistical analyses currently available

As mentioned earlier, collision events have substantial consequences on loss of life and property, and harmful effects on the environment. With such dramatic results, it is almost mandatory to address them as early in the design process as possible. This would directly imply that the above mentioned analytical models will constitute measures of the safety of operation of the vessel and will be addressed alongside conventional virtues of the new design (speed, seakeeping, etc.). In this way, multi-objective / multi-criteria optimisation schemes can be engaged in exploring the

design space and identify the most promising solutions. Obviously, the complexity of such a process prohibits deployment of numerical tools whilst semi-empirical models, based on statistical analyses, are limited to past designs and they do not help the search for appropriate solutions in innovative concepts. As a result, potentially more crashworthy structures like those depicted in Figure 3.4 cannot be assessed very early in the design phase. This is the case with the results presented in Figure 3.5: the analysis is based on conventional structural arrangements and as such it does not allow for assessment of alternative structural configurations, which are automatically discarded or not considered at all as design alternatives.

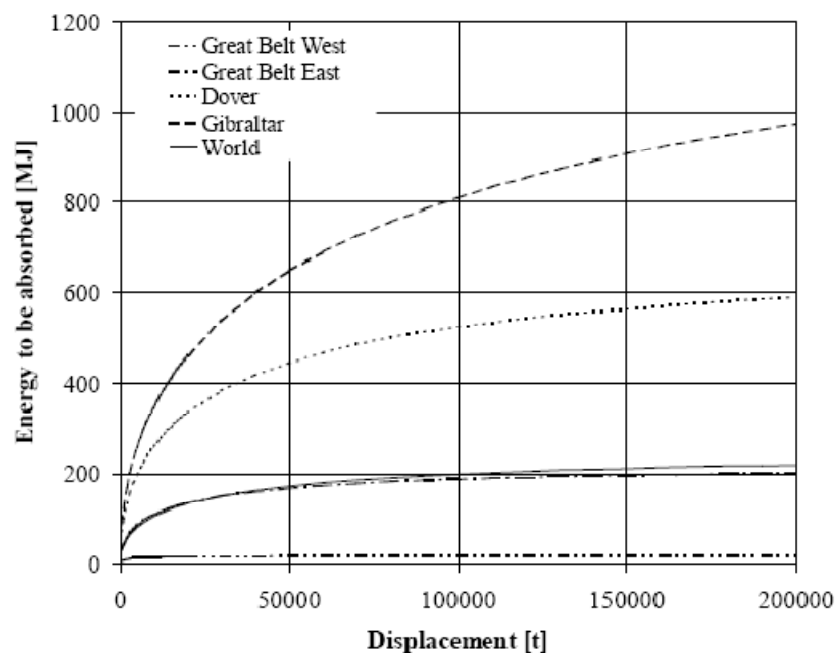


Figure 3.5: 90th percentile of energy absorption amidships versus displacement and different geographical locations, (HARDER, 2001a)

3.4 Practical safety implementation

All the above facts and ideas can also be examined from a more macroscopic perspective that addresses and verifies the reasons for the serious difficulties encountered for practical consideration of safety.

It comes as no surprise that during periods of low accident occurrence there is a general relaxation across the industry. During these periods, the continuous challenging nature of shipping operations and all the entailed risks in them tend to be

underestimated. Sooner or later this practice naturally leads to another accident and mischief. Public protest and dismay becomes nostalgic of the period of smooth operation, it focuses on the accident itself only and demands for upgrade of standards from the authorities.

Humans, by their nature, are very much attracted to the results of extended destruction and the horror it causes, and direct all their efforts towards mitigation measures against harmful situations. This tendency can probably explain why so much attention is paid by regulators for stricter standards that will prevent a certain accident from happening again in the future. But it would be fair to say that there is another, more important, underlying reason for such approach: to promote prevention it is first necessary to understand the causes and the involved mechanisms of a catastrophic event from its initiation to its conclusion. Most of the time, this is such an overwhelming task that it requires enormous effort by large dedicated groups of scientists and engineers over long periods.

In the meanwhile, business and trade still goes on and regulations should be in place in order to provide some safeguards of the shipping activities even if accidents still happen. Then, there comes a time that the need for change is admitted by everyone but no one is willing to make the first step. It seems that the property of all systems in nature to maintain the lowest possible level of energy content has its application to human mentality as well: change means upgrading to a higher energy level that requires conscious and continuous effort.

Such approach cannot couple easily with the high-risk content of the maritime business. That is, for a maritime company to nurture safety as part of its culture, which is manifested in activities ranging from design of new ships up to daily operations of existing ones, it is necessary to make the right financial investments. But in a highly competitive and uncertain market such investment can only be fruitful if the economic situation of the company is sound and healthy. In the opposite case it will create additional difficulties and eventually it will be addressed to the lowest possible level of compliance with the regulations, (Kriastiansen, 2005).

Thus, since the *need for change* is so pressing, the right vehicle should be found that can accommodate it and reliably lead it to the future. The design approach that has

been implied and progressively revealed in the discussion so far needs a fertile ground to flourish and develop. Such ground is the *risk-based design* methodology that is described next.

3.5 Risk-based design

*Design is the process of originating and developing a plan for a product*¹. In particular ship design is very much concerned with balancing a large number of objectives concerned with feasibility, performance, cost and logistics, preferences and aesthetics, etc.

The compelling need to tackle effectively a high-risk business like shipping necessitates ground-breaking techniques and approaches that can address the real risk issues at a very early design stage. This issue was briefly elaborated upon in Section 1.4 but, further to the above discussion, it becomes evident that such an approach can be most effective if applied very early in the design process, i.e. where maximum changes can be performed at minimum cost. By making safety a major performance parameter the designer (and potentially the ship owner / manager) has a unique opportunity to deal cost-effectively and efficiently with the root causes of major hazards. In fact, such an alteration in the design development has one extra advantage: there is no need to mimic past designs to their full extent just because they have proven successful. The services the new ships have to offer only remotely match those 15 or 20 years ago. For example, modern cruise liners that can accommodate more than 5000 passengers (and about 3000 crew members) have been delivered for service recently. The concentration of such an immense number of people on a single floating structure unsurprisingly requires alternative techniques, imagination and creativity and, obviously, it cannot be regulated by past experience. The fact that safety is currently considered as a design constraint (via rule implementation and compliance) facilitates a “patching” mentality rather than a remedying one thus jeopardising substantially the performance of modern marine vehicles.

¹ <http://en.wikipedia.org/wiki/Design>

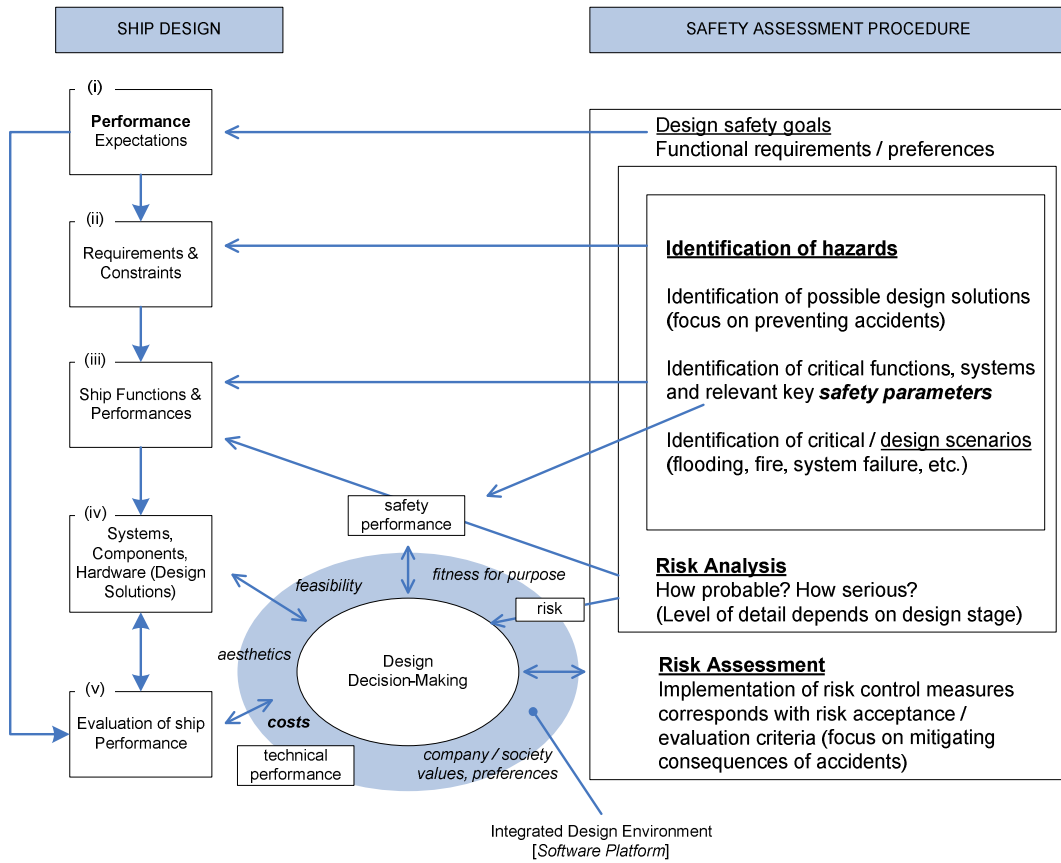


Figure 3.6: High level risk-based design, (Vassalos et al., 2006a)

Research at the Ship Stability Research Centre has focused on the development of the *Design for Safety* philosophy and the establishment of *Risk-based ship design* framework and methodology (Figure 3.6) as it is presented and advocated in (Vassalos, 2000), (Vassalos et al., 2000a), (Vassalos et al., 2000b), (Konovessis, 2001), (Oestvik, 2001), (Vassalos et al., 2003), (Vassalos et al., 2005a) and (Vassalos et al., 2006a).

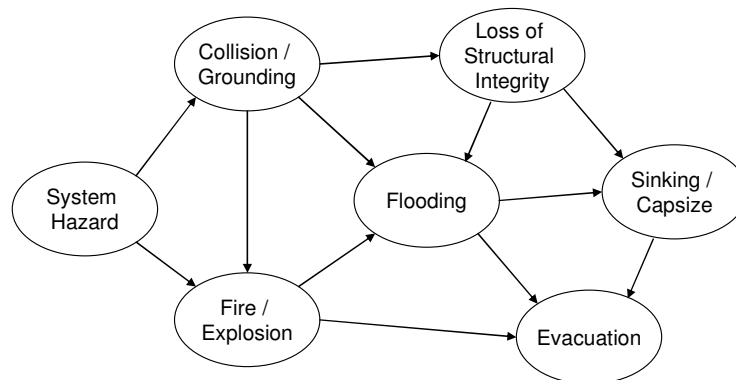


Figure 3.7: Typical sequence of scenarios, (Konovessis & Vassalos, 2003)

Risk-based ship design integrates systematically risk assessment in the design process with prevention and/or reduction of risk to life, property and the environment. Safety is expressed as another explicit design objective, alongside “conventional” design objectives (such as speed, capacity, etc).

In addressing risk-based ship design, it is important to make the following considerations, (Vassalos et al. 2006a):

- The notion of risk is usually associated with events that may result in catastrophic outcomes. Consequently there is a clear distinction from *reliability* approaches, which are heavily related to maintenance policies in finite time intervals during the life-cycle of the ship. Unfortunate events (occurring in sequence or in parallel, Figure 3.7) in ship operations have led to well-documented accidents of collision, grounding, fire, sinking, foundering, etc., in many cases with ominous results.
- Addressing safety explicitly indicates the need to measure it: in this respect, risk is considered as the *currency* of safety, which is necessary to evaluate in the design phase (especially in the early stages) where most of the fundamental characteristics of the ship are generated and easily altered.
- In risk-based design, the target is to increase the influence of good engineering practice and judgement, state-of-the-art tools and knowledge: not surprisingly these are the ingredients for innovation and, in addition, they are all parts of a Quantitative Risk Analysis (QRA), Figure 3.8.

Within this context, the essential contribution of risk-based design in the conventional ship design practice is the explicit, rational and cost-effective treatment of safety. To achieve this, the following have to be considered:

- (i) A consistent measure of safety can only be a product of proper risk analysis. That is, considering the complexity of what constitutes safety, clear focus on key safety “drivers” is necessary (major accident categories, e.g. collision) and the manner they are manifested (e.g. crashworthiness assessment). Additionally, there are various formal (post-

design) procedures for risk quantification, risk assessment and risk management in a variety of contexts like Formal Safety Assessment (FSA) for rule development, (IMO, 2002), Safety Case for specific design/operational solutions, (Kuo, 1998), etc.

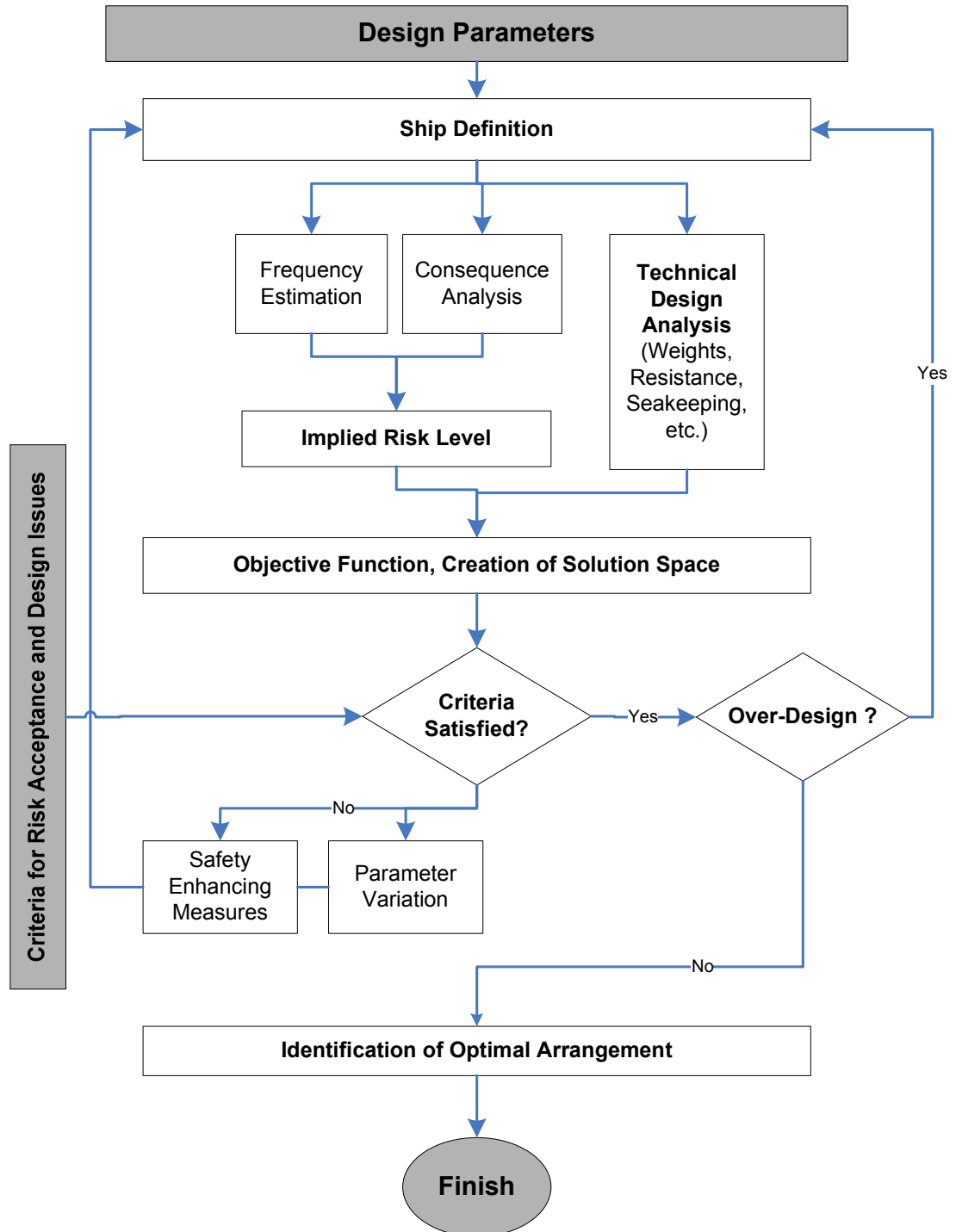


Figure 3.8: A QRA design methodology, (Konovessis & Vassalos, 2001)

- (ii) Risk analysis must be integrated into the design process to allow for trade-offs between safety and other design objectives by utilising overlaps among performance, life-cycle cost considerations and functionality. Consequently, the available amount of information for design decision making and design optimisation is significantly enriched.
- (iii) The level of necessary computations for addressing all major safety concerns and the effect of safety-related design changes on functionality and other performance can be quite substantial and requires highly sophisticated software tools, (Vassalos et al., 2004). An alternative approach is to use *analytical models* that allow trade-offs and overlaps among design objectives and access to fast and accurate *first-principles tools*. Thus, the design optimisation process becomes a typical case of a multi-objective / multi-criteria optimisation problem. A common ship design model managed within an integrated design environment (software) is required for that process to be conducted efficiently, (Majumder et al., 2005a), (Majumder et al., 2005b) and (Puisa et al., 2009).

This short description of risk-based ship design prepares the ground for the presentation of the thinking behind the analytical models for risk assessment during early stages of design.

Ever since the probabilistic damage stability was implemented in SOLAS, the collision risk was assessed as the product of probability of flooding a compartment, or group of adjacent compartments, (p-factor) and the probability of surviving a flooding of such extent (s-factor). This approach is based on three premises: (i) a collision accident has occurred, (ii) the side shell of the struck ship is breached, and (iii) the compartments under consideration are instantly flooded. These conditions are perceived as weaknesses of the existing regulatory framework as a large number of collision incidents do not lead to flooding and loss of stability of the ship. As a result, the designers are forced to impose heavy compartmentation to a new ship (which burdens substantially the construction and the operation of it) in order to comply with the rule. Consequently, the potential for any initiative (and therefore

innovation) to administer fit-for-purpose solutions according to the operational profile of the ship is taken away by the designer.

This gap of the regulation can be addressed by considering the mathematical expression of collision risk in terms of conditional probabilities. This thesis is focusing on the first two elements comprising the probability part. That is, to provide the tools for assessing the probability of collision and the probability of water ingress due to collision.

$$R = \left(\underbrace{P_c \times P_{w/c}}_{\text{focus points}} \times P_{\text{cap/w/c}} \right) \times C \quad (3.1)$$

where

- P_c : probability of collision,
- $P_{w/c}$: probability of water ingress due to collision and
- $P_{\text{cap/w/c}}$: probability of capsizing due to water ingress, due to collision.

“C” stands for the consequences further to the initiation of a collision event and it is hard to quantify due to the non-engineering elements that are attached to it. For example, the cost of human life, the environmental damage, the loss of commercial credit (the market reputation of the company), etc. All these aspects involve social, political and economical criteria. It is customary to address risk for certain categories of consequences, which effectively implies that risk is the chance of a loss. The remaining of this chapter opens the way for the development of the models for the probability of collision and the probability of water ingress due to collision.

3.6 Probability of collision (P_c)

As far as collision is concerned, a series of unwanted events (Figure 3.7) initiates with the approach and dynamic contact between two ships. Along the lines of risk-based design, such an event is associated to the probability of its occurrence, Equation (3.1), therefore, the *probability of collision between two ships in a waterway* is of interest here. Rational understanding of the situation indicates that the factors affecting, and indeed defining, the occurrence of such an event are numerous,

with various degrees of complexity and, most importantly, significant uncertainty. In every different case of a collision event, they are combined in parallel or otherwise and they create the conditions for a very hazardous situation. The critical factors affecting the collision incidences can be grouped in the following categories:

- Human element
- Hardware failure
- Environmental conditions
- Topography and traffic density

A short description of each one is included in the following paragraphs.

$$P = \lambda \exp\left(\frac{\lambda \times \text{SLI}}{t}\right)$$

where

- P: probability of human error of a given task
- λ : base error rate for the task
- SLI: The Success Likelihood Index incorporates the effect of performance shaping factors (PSF) to the calculation of P
- t: time available to conduct the task or tolerance level for magnitude of error

Values for λ are obtained from analysis of a nuclear power database as shown next:

Error category	Mean rate	Coefficient of variation
Skill based	0.0269	322.24%
Rule based	0.1160	175.81%
Knowledge based	0.1530	165.89%
Violations	0.1040	243.81%
Physical	0.0073	311.87%

SLI is calculated according to the following equation:

$$\text{SLI} = \sum_n \left[\frac{w_n \left[\Phi\left(\frac{v_n - \mu_n}{\sigma_n}\right) \left(\frac{v_n - \mu_n}{\sigma_n}\right) \right]}{\sum_n w_n} \right]$$

where

- w_n : weight assigned to each PSF
- v_n : PSF value
- Φ : normal distribution with mean μ_n and standard deviation σ_n .

Figure 3.9: Quantification of the probability of human error according to (Boniface & Bea, 1996)

Human element

Human element is perhaps the most ambiguous ingredient of all accidents at sea and has its own very special contribution in the occurrence of collision events. From an engineering point of view it is very difficult to quantify it in conventional scales of measurement and even more difficult to include and model it as part of a numerical assessment process. Nevertheless, it can affect dramatically (in a positive or negative way) the development of an event. Based on statistical evidence, approximately 80% of all accidents occurring can be attributed to human factors. What is almost impossible to measure though is the number of accidents that have been prevented due to human intervention!

Systematic effort in understanding the nature of human perception in decision-making situations (e.g. navigation) has provided insight to the factors that contribute the most to high risk events. These are no others than fatigue, lack of experience, poor training levels, increased stress, poor health, lack of communication, etc. These factors, individually or collectively, address the problem of human element in marine operations. Preventative actions are not always possible mainly due to the associated cost. Nevertheless, some steps in the right direction have been made (for example introduction of Bridge Resource Management (BRM) scheme as indicated in (IMO, 1978)).

“Hard” modelling of human behaviour is complicated mainly because of (i) lack of a consistent scale for measurement, and (ii) definition of real variables, which correspond to human virtues, is difficult to find. The work presented in (Figure 3.9) is one of the few exemptions. As a result, it is almost certain that when more concrete input is required a group of experts is involved. The so called *expert judgement* approach (for example see (Vanem & Skjong, 2006) and (Kent, 2006)) seems to be the only widely accepted way to “model” human reaction to certain events and therefore to predict what might happen under certain conditions. Depending on the study performed, members of the panel of experts are highly experienced professionals with proven records of service. In this way, their views and opinions are rarely disputed. Nevertheless, some certain degree of subjective

judgement is unavoidable and such approaches should be used only when every other means is exhausted, (Paté-Cornell & Regan, 1998).

Considering again the probabilistic character of risk-based design it is obvious that the introduction of the probability element attributed to human error fits the context very well. In this respect, studies like those presented by (Liu & Wu, 2004) can contribute towards more specific information for early design issues. The alternative way of considering human factors in design is the rather implicit way presented in Chapter 4: instead of considering directly the probabilistic response of crew to predetermined circumstances, as it is attempted with the BN presented in (Figure 2.4), certain design features of the new ship are enhanced to account for human error (e.g. reducing the size of turning circle indicates that change of course can be performed faster thus lessening the chances of collision).

Hardware failure

Hardware failure is more familiar ground for engineering analyses. Well established reliability techniques can provide (with adequate level of detail) the required information for the assessment of the functionality of all related systems that contribute to the occurrence of a collision.

At this point it is necessary to separate the failure of the main engine (e.g. black out), the propellers (e.g. of the servo mechanism of a controllable-pitch propeller), the rudders or the bow thrusters (e.g. motor failure) from the failure of navigation equipment like radars, compasses, electronic chart display (ECDIS), etc. Any failure of the first group can potentially deteriorate the steering capability of the vessel (even if it can be compensated by the remaining systems). The systems belonging to the second group are enhancing the watch keeping capability of the navigator: any failure of systems in this category can initiate a hazardous event but only because understanding and apprehension of the surrounding environment is very limited (e.g. low visibility due to thick fog or darkness). Evidently, combination of both failures can lead to very dramatic situations especially considering the effects they have on the stress levels of the navigation team. Analysis of the contribution of each group

can be quite a straightforward task, although there is the significant lack of information for commercially sensitive reasons either from the ship operators or the equipment manufacturers (contrary to what happens to offshore industry where publications like Offshore Reliability Data (OREDA)² provide such information).

Environmental conditions

Accounting for the contribution of the environment in the probability of collision is straight forward. All the required data is available in the public domain and elementary analysis or processing can be performed for generating the required information. That is, estimation of the low visibility periods and their duration, the usual directions of wind and the force of it, any tidal effects, etc. are all readily predictable.

Topography and traffic density

Rational analysis of collision accidents demonstrates clearly the effect the traffic density in relation to the geographical configuration of the sailing area. The collision occurrence in open sea is highly unlikely contrary to its occurrence in busy and confined waters, channels, straits etc. Northern Europe for example has been experiencing this high density traffic due to high development rates and increased commercial activity (Figure 3.10). As such, any models developed specifically for predicting the probability of collision should include such a parameter. From this point of view Macduff pioneered the field by explicitly considering the width of the navigation channel in his models, (Macduff, 1974) as will be discussed later.

² <http://www.sintef.no/static/tl/projects/oreda/>

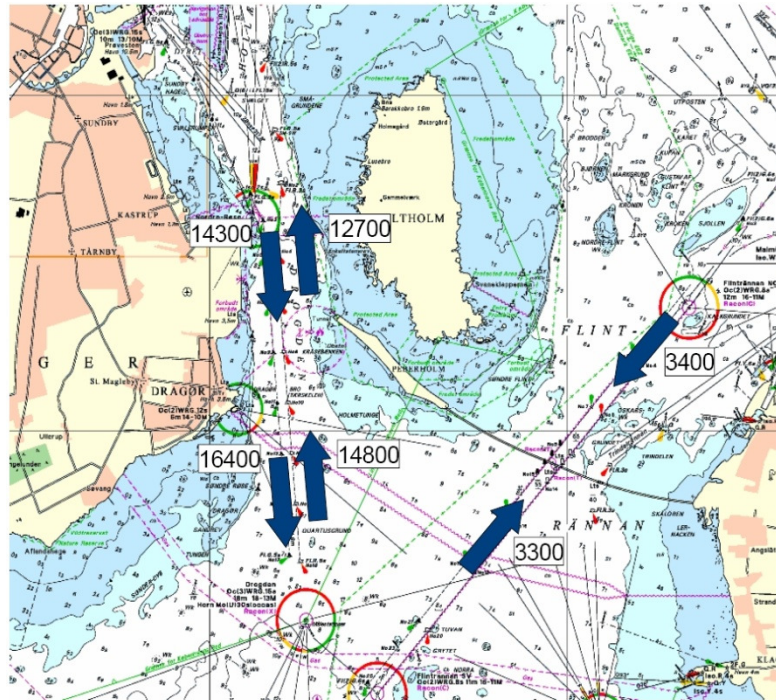


Figure 3.10: Ship movements between Flintrännen and Drogden, (Øresund, 2006)

3.7 Probability of water ingress due to collision ($P_{w/c}$)

It was stressed in Section 3.2 that the way in which damage stability is calculated is rather arbitrary. That is, a breach of certain size is assumed at a certain location according to a set of regulations (i.e. SOLAS opening). Both these factors lead to flooding and the survivability calculations follow up from there. This approach may appear suitable for analyses and studies which focus only on the stability of damaged ships but as far as design is concerned it is highly inadequate. The sole reason being the broken link from one ship function to another, i.e. from the structural integrity and the watertightness of the side shell to the stability characteristics of the vessel with one or more compartments flooded. This approach fails to incorporate fundamental hazards of the operational profile of the ship (like collision, grounding, fire, etc.) in the early design phase, like the kind of ships (size, speed, etc.) that will be encountered, the traffic density, etc. These requirements still remain an implicit characteristic of the new design rather than a series of clearly defined objectives.

As such, collision risk (along the lines of risk-based design) is addressed in a very inefficient and ad-hoc (rule-based) manner, something that appears to be not

satisfactory at all: serious marine accidents continue to occur irrespective of constant efforts to prevent them. Considering the above straightforward issues, it is clear that a robust design-oriented approach is missing.

The more thorough review of the literature (presented in Chapter 2) fully supports this argument. All the attempted ways to tackle the issue are too case-specific for ship design application (especially during its early stages). The method that will be presented in Chapter 5 is founded on two rather evident observations:

- (i) No matter what the structural configuration of the side shell of the struck ship is, it can always absorb only a limited amount of the energy made available from the striking ship. This energy packet will be dissipated locally in the *mass* of the struck structure. When the deformation exceeds a certain limit the side shell will burst in a prescribed pattern.
- (ii) The tearing pattern of the structure is associated with the geometry of the striking body, namely the shape of the bow (stem and bulbous bow) of the striking ship. This is evident throughout the literature and accident investigations. In fact, this element is so prominent in its manifestation that even before a collision occurs between two given ships it is possible, through common knowledge and intuition, to predict qualitatively the ease of the rupture and the final shape and extent of the breach.

The significance of these two issues creates a natural momentum in thinking strategies as to how to deal with the problem. On the whole, it is necessary to describe the capacity of a piece of structure (a stiffened panel of a single or double hull ship) to absorb a large amount of energy (in very short time) and to relate this energy content to the geometrical shape of the delivering body. This, in turn, will allow for the estimation of the breach size and the penetration depth. The tools to conduct such a study are described in Chapter 5 and demonstrated in Chapter 7.

3.8 Chapter summary

Lack of first-principles tools for assessing the crashworthiness of a ship as a function of its operational profile creates a gap in the design process and forces designers to resolve on prescriptive approaches for assessing its survivability levels. If such

analytical models were available they would allow the establishment of a multi-objective / multi-criteria optimisation scheme within the risk-based design context. With this design philosophy, it is essentially advocated that risk quantification is taking place alongside the conventional design process, i.e. safety becomes another design objective next to conventional design objectives for minimum resistance, maximum stability, ultimate strength, etc. In this way, creativity and innovation are greatly facilitated and at the same time the means to deal with safety cost-effectively and efficiently are presented. The chapter closes with a brief description of the parameters that will be included in the models and a rough introduction of the proposed methodology.

4 Probability of collision

4.1 Introduction

The topic of the probability of collision in a waterway is treated in this chapter. The development is based on the idea of ship domain, which is modified to account for the entropy of information as a measure of uncertainty of a hazardous situation and quantification of its irreversibility. The chapter concludes with the introduction of a new analytical model for the calculation of the probability of collision.

4.2 Factors affecting the collision occurrence

The Fujii models capture a great deal of information like the traffic density, the environmental conditions and the critical effect of the familiarity of the navigator with a particular seaway. However, publications like (MAIB, 2005), (Cahill, 2002), brief reports of National Transport Safety Board (NTSB)³, etc. reveal additional sources of error, miscalculations, over-confidence, lack of communication and other unforeseen circumstances that have contributed to accidents.

All the available material of past investigations assists in better understanding of the very special character of collision events. It becomes evident that accidents never occur from one moment to the next (even a thunder strike requires the right conditions) and the sequence of events leading to a collision is definitely not random (at least in their vast majority). Events occur one after the other, in sequence or in parallel. There is always a succession of events that leads to the final occurrence of the accident given some certain setup (e.g. a narrow passage, early morning hours, reduced visibility due to dense fog) or scenario. Once everything is orchestrated properly, then there is always a critical *point of no return*. Accident investigators seem to underline this point in every chance they have: whatever corrective action follows that point is futile and the final result is totally irreversible.

Surprisingly, this very critical time interval appears to be measured in the range of 1 or 2 minutes! This fact is stressed in a number of cases in (Cahill, 2002), where analyses of past accidents investigations take place and comments from the litigation background of each case are included. This fact justifies (once more) the challenging nature of these accidents and it further provides a better feeling of the marginally available time to the navigators to make a decision and to correct it, if it proved wrong.

It is mostly appealing that trivial practices in navigation of commercial ships appear to be quite “safe” in the majority of times, but under the “right” conditions they

³ <http://www.nts.gov/publictn/2001/MAB0104.htm>

prove extremely inadequate. For example, release of the watch officer by the captain for a tea break, which results in having to be alone on the bridge with the helmsman and instead of keeping his attention on the surrounding traffic he checks whether information has been registered correctly in the log book, is ordinary practice, (Cahill, 2002). This is true not only for the crew but also for the pilots that often go onboard ships and assume full responsibility for the manoeuvring of the ship. There are times that even these highly accredited professionals slip in their judgement because of rather trivial details, overconfidence or poor briefing by the master about the ship's condition prior to taking over their duties. Again, in a hazardous situation, the threshold point of no return is valid for the pilot as well and any following action is hopeless.

Finally, what is the most intriguing aspect of ship-ship collisions is that no matter how much analysis, study and publication of results takes place they always seem to repeat themselves for a very specific set of initial conditions. The recursive character of collision occurrences indicates that the modelling philosophy followed so far is not adequate as it does not capture reality accurately. As far as the human element is concern, it appears to be a great deal of variability in the way navigation officers react in similar situations as the uncertainty in various circumstances is perceived differently: this fact is captured in the studies related to human error, (Reason, 1990), but it is not utilised in practice. However, crew performance is not the only aspect that should be taken under consideration: rapid changes in environmental conditions, systems reliability, traffic patterns, geographical restrictions, etc., are the ingredients of the conditions that lead to a collision. Collectively, the contribution of each of them is only intuitively understood (or implicitly described with BN) as there is no explicit way to capture it. For that reason, a more elaborate view at the uncertainty entailed in various circumstances is necessary under the prism of information theory and entropy, a key measure of disorder and, therefore, the unpredictability of a system, (Moon, 1992), with unwanted outcomes.

4.3 Entropy of information

Since every collision event is affected and dependent upon a number of parameters, a mechanism that can quantify this link and take it into account for estimating the probability of collision is needed.

Each of the governing factors of the end result (tidal currents, visibility levels, presence of third ships in the vicinity of navigation, etc.) has a probability element attached to it and some explicit meaning. That is, each of these factors occurs in some certain pattern through time that is interpreted by the navigator in various ways. For example, assuming navigation around the west coast of Shetland Islands, wind speed exceeds 5 m/s (Beaufort scale 3) in approximately 85% of the cases⁴. It would be no surprise to the navigator to measure wind speeds of 5 m/s or higher and take this fact into account during his shift. On the other hand, a calm windless day would certainly be welcomed and discussed over lunch and probably dinner. This example indicates that trivial situations in life have little to add to general knowledge level, i.e. they offer little *information*. In contrast, events that do not occur as expected (or according to a forecasted way) appear to be quite surprising (whether they are a good or a bad surprise is a different issue altogether). Considering this situation, it is easy to conclude that probability and information seem to be inversely proportional to each other: high probability implies low information content and vice versa.

Assuming that an event has only one outcome (deterministic), then its information content is predetermined and equal to zero (i.e. minimum). If the event under consideration has two equally possible outcomes, then the final result will be either of the two. In this case, the information is not very much either, but it is certainly more than in the first case.

If the number of possible states of the event is increased further, then information about the final outcome becomes more and more important. The link between the

⁴ Atlas of the Oceans: Wind and Wave Climate on CD-ROM, version 1.0, © 1996

number of states (N) and the information content (I) could be approximated by a simple proportional relation of the form:

$$N \propto I \quad (4.1)$$

Considering again the complicated nature of the systems that are modelled here and the even more complicated situations they are involved in, it is necessary to think how the information content in each case will support the related calculations. That is, in real situations the sound operation of a system is comprised by the reliable operation of a number of sub-systems. For example, propulsion and navigation systems cannot be treated individually in a study of navigational risks. Both have a discrete number of operational states and different probability distributions of nominal operation among these states. As a result, the information content of the overall system, should possess two distinct qualities:

- (i) the total amount of information should be equal to the sum of the individual information elements, and
- (ii) the number of states of the overall system should relate to the number of states of the individual systems.

Considering the example of Figure 4.1, system X has 2 states (X_1 and X_2) and system Y has 3 states, (Y_1 , Y_2 and Y_3). The overall system XY has 6 states, i.e. the possible combinations of X and Y: (X_1, Y_1), (X_2, Y_1), (X_1, Y_2), (X_2, Y_2), etc. Implementation of Equation (4.1), i.e. equating number of states with information, the overall system should have 5 states, which is obviously not correct.

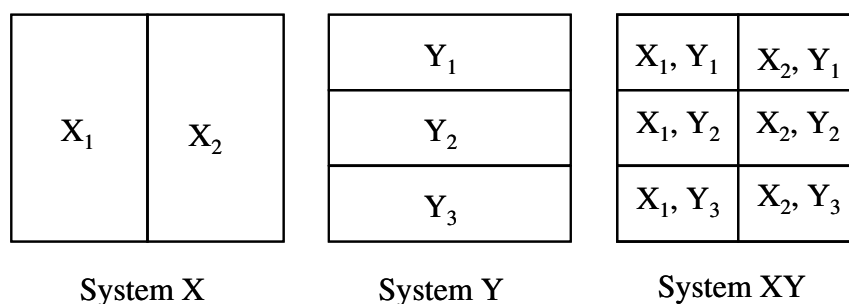


Figure 4.1: State combination of systems X and Y into system XY, (Williams, 1997)

An alternative expression can have the form of an exponential function of constant base:

$$y(x) = a c^{bx} \quad (4.2)$$

c is the constant base and can be equal to 2, 10 or e (the base of natural logarithms). Parameters “ a ” and “ b ” are also constants (alternative cases are not considered here). The equation denotes exponential increment if $bx > 0$ and decay in the opposite case. The new formulation has the form of:

$$N \propto \text{base}^I \quad (4.3)$$

This time, combination of events X and Y into XY can satisfy requirements (i) and (ii). This can be proved algebraically as follows:

$$\left. \begin{array}{l} N_X \propto \text{base}^{I_X} \\ N_Y \propto \text{base}^{I_Y} \end{array} \right\} \Rightarrow N_X N_Y \propto \text{base}^{(I_X + I_Y)} \quad (4.4)$$

By taking the logarithms of both sides and introducing a constant of proportionality c_2 , the following expression is obtained:

$$\begin{aligned} \log(N) = c_2 (I_X + I_Y) \log(\text{base}) \quad \text{or} \quad I = I_X + I_Y = \frac{\log(N)}{c_2 \log(\text{base})} \\ \text{or} \quad I = c \log(N) \end{aligned} \quad (4.5)$$

since $c = \frac{1}{c_2 \log(\text{base})}$ is always constant.

Considering again that the system under examination has a finite number of states (for the sake of engineering analysis), then if each state has equal chances to be the final outcome, the probability will be equal to the inverse of the number of states: $P = 1/N$. Substituting in Equation (4.5) and assigning $c = 1.0$ (the simplest case), an expression, which quantifies information with respect to probability can be obtained:

$$I = c \log_2 \left(\frac{1}{P} \right) = -c \log_2 (P) \quad (4.6)$$

Base 2 is most frequently used and it is introduced here for consistency with the supporting theory on these concepts. Further details on the topic can be found in the

introductory text of (Smith, 2007) and the more elaborate presentation in (Williams, 1997).

Going back to the example of navigating in the vicinity of Shetland Islands, the difference between the cases of wind speed over 5 m/s and below, is the amount of information contained each time. This fact reflects the choices that could be made during the operation of the vessel (watch-keeping duties) or the qualities appointed (and controlled) by the designer (during the early design stage, e.g. choice between one or two rudders). The information content of such an event can be represented as follows:

$$I = \log_2 \left(\frac{1}{0.85} \right) = 0.234 \text{ bits}$$

“bits” is the unit of information used more often but most of the times is discarded⁵. In the case of the calm day, the contained information will be:

$$I = \log_2 \left(\frac{1}{0.15} \right) = 2.737 \text{ bits}$$

The result duly justifies the surprise of the officer-on-watch, i.e. the larger amount of information contained in the particular good-weather case.

An extension of this idea is to consider the probabilities of the rest of the parameters that affect the decision-making of the crew further. In this case, it is necessary to take into account the contribution of each bit of available information by calculating their weighted average at any given time frame. This would result in an expression for the *entropy* contained in the system:

$$H = \sum_{i=1}^N P_i \log_2 \left(\frac{1}{P_i} \right) \quad (4.7)$$

where, N is the number of states of the event.

⁵ “bits” is a short name for “binary digits”. Its routes can be found in description of events with two equally possible states and the usage of binary state (i.e. 0 or 1) of transistor switches in computer technology. It is further associated with the base of 2 used in the logarithmic formulation irrespective of the number states a system may have.

The term *entropy* was assigned by Shannon, (Shannon, 1948), an electrical engineer who worked for the Bell Telephone Laboratories in the middle of the past century and who effectively developed and established the branch of applied mathematics that today we call *Information Theory*, (Applebaum, 1996).

High entropy	Low entropy	Remark / Example application
Disorder, disorganisation, thorough mix-up	Order, high degree of organisation	The presence of a Vessel Traffic System (VTS) in the area of navigation is of catalytic importance for the traffic management.
Great uncertainty	Near certainty, high reliability	Information about wind gusts, when close quarter manoeuvring is required, is highly important for averting collisions in channels and straits.
Unpredictability	Accurate forecast	Unexpected congestion due to alteration in loading / unloading schedule can increase the traffic density and the stress levels of the navigator.
Freedom of choice of alternatives	Few alternatives available	The wider the navigation channel is, the more freedom the navigator has to apply an emergency manoeuvre without the risk of averting one accident and causing another.
Large diversity	Small diversity	The small variation in size and speed of the vessels sailing in the surrounding area create a sense of familiarity to the bridge officers as their response can be anticipated to a large extent. This is hardly the case when wider variety of ships is operating in the vicinity.
Great surprise	Little or no surprise	The familiarity of the navigator with the area of operation and specific traffic and environmental characteristics is a source of lesser amount of unexpected encounters with other ships, geography, weather, etc.
Much information available to assess the situation	Scarce information available to assess the situation	Good communication with surrounding traffic and the harbour master can lessen the chances for unpredictable situations.
High data accuracy	Low data accuracy	Topology maps, bathymetry data, Automatic Identification System (AIS), GPS data, etc. all contribute towards a robust picture of the operational conditions and the surrounding traffic and allow the crew to identify potentially hazardous situations in close encounters.

Table 4.1: The different meanings of entropy (modified and adapted for the purposes of this research from (Williams, 1997))

Entropy is not a new concept in the engineering community. Ever since it was first established by R. J. E. Clausius, it has been closely related to the disorder or the uncertainty in a system, and its quantification. There is a wealth of literature on the concept of entropy and its applications have been extended beyond thermodynamics and engineering into everyday life, as it is discussed in (Cengel & Boles, 2005).

In the current context it is adopted with a variety of interpretations, all of which rotate around the same general idea: the less is known of (or exercise control on) the development of a potentially hazardous situation, the higher its entropy content is.

Sailing in a foggy day and in a narrow channel can be the source of large frustration and stress to the navigator. If a pilot is on board the ship, his intimate knowledge of the area and the takeover of responsibility can relieve some of the tension from the crew. An unexpected damage to one of the systems (e.g. the radar) will increase the anxiety levels of everyone on the bridge. The more crucial the damage is the more tension is added and more biased (stressed) will be any decision taken in case of an emergency (e.g. evasive manoeuvre). Contrary to this, sailing in open sea with good visibility in all directions allows for a more unbiased decision if a similar damage occurred. This time, the officer on watch has more time to assess the criticality of a situation (e.g. a failure in the hydraulic system of the rudder), confer with the master and together plan their next action. In this case, the initial surprise of the damage can be surpassed by sending someone to visually check where the damage has occurred and how serious it is. In all similar situations it seems that the defining factor is the available time to make a decision based on the quality of the data provided by the decision-support systems installed on the bridge. In the context of the ship-ship collision events the above suggestions can be interpreted in a multitude of ways as exemplified in Table 4.1.

Entropy in risk-based design

Entropy is introduced in the risk-based design methodology as a structured way to consolidate quantitative and qualitative (e.g. training levels of deck officer) information simultaneously with the sole purpose of arriving at more rational

conclusions. As a result, the initial definition of entropy of one event (with N states) affecting the situation, can be expanded to multiple events (M events) to reflect the reality that a collision is very tightly connected to a series of events, the sequential or parallel occurrence of which leads to the final result:

$$H = \sum_{j=1}^M \sum_{i=1}^{N_j} P_{ij} \log_2 \left(\frac{1}{P_{ij}} \right) \quad (4.8)$$

Where:

i : counter for the number of states of each event

j : counter for the number of events

M : number of events

N_j : number of states of event j

The higher the value of entropy, the more imminent the collision occurrence is. In this respect, the idea of the *point of no return* can be supported since the contribution of each of the events participating in the development of a particular incident can be quantified and measured (irrespective of its nature, i.e. qualitative or quantitative) in selected time intervals. As consecutive events take place (possibly new ones are introduced on the way), estimation of the entropy of the situation can quantify its seriousness and provide better decision-support to the navigator or port authorities when certain thresholds are exceeded. More discussion on the contribution of entropy of information to the probability of collision will follow in Section 4.7.

In the risk-based design context the entropy of information complements the analytical calculation of the probability of collision by taking into consideration a variety of causal factors that constantly threaten safe navigation and can lead to collision. In particular, consideration of elements like those presented in Table 4.2 can be taken into account by aggregating suitably their probabilities into the entropy of the system, Equation (4.8), in certain time intervals. That is, environmental conditions (wind, wave, current, visibility, etc.), systems functionality (propulsion, steering, navigation, etc.), and human element.

Despite the lack of threshold values for the entropy of information, the apparent novelty of the concept is rather appealing since it allows for a broad range of critical information to be consolidated into a single number.

Causal factor group	Causal factor
External factors	External conditions influencing navigation and auxiliary equipment
	Less than adequate markers and buoys
	Reduced visibility
	External influences like channel and shallow water effects
Technical failure	Failure in ship's technical systems
	Serviceability of navigational aids
	Remote control of steering and propulsion
	Failure in communication equipment
Navigation factors	Bridge design and arrangement
	Error / deficiency in charts or publications
	Bridge manning and organisation
	Internal communication failure
	Inadequate knowledge and experience
Navigation error	Failure due to navigation and manoeuvring
	Wrong use of the information from buoys and markers
	Failure in operation of equipment
	Wrong appreciation of traffic information
Non-compliance	Inadequate coverage of watch
	Special human factors
Other ships	Fault or deficiency of other ship
	Navigational error of other ship

Table 4.2: Causal factors for Norwegian waters grounding accidents, partially reproduced from (Kriastansen, 2005)

4.4 Probability of collision: an alternative approach

Ship domain

The idea of *ship domain* is not new in the literature. It was introduced in the late 70's, (Goodwin, 1979), and has been treated by authors in different contexts and studies, e.g. (Hansen et al., 2004), (Filipowicz, 2004), (Kao et al., 2007). The ship domain was initially defined as the collision-free area surrounding a ship: any object (stationary or not) that enters this area causes a collision (Figure 4.2).

In this work, a variation of this idea will be developed further. The size of the ship domain depends on a number of parameters related to the design of the ship itself as well as its operational profile. In particular, its manoeuvrability characteristics appear to be very important in this case. Of course, the size of the ship in terms of its length provides an indication of this virtue but also a relative measure of the space it occupies in a seaway. Operational characteristics are related mainly to the traffic

density in the area (in terms of ships per unit area or passages per unit time), which is a function of the channel width where the vessel navigates. The relative position of the ship is provided by the allowable speed for the particular waterway and depends on rules and regulations issued by national or international authorities. In any case, (COLREG, 2003) defines the rules of navigation for collision avoidance, yet the human intervention makes the situation unpredictable. For example, pilots with long experience in navigation in narrow passages tend to underestimate close-quarters situations and as a result a large number of accidents occur in restricted waters, (Cahill, 2002).

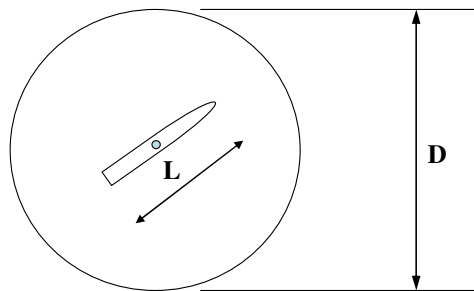


Figure 4.2: Ship domain in the form of a circular disk

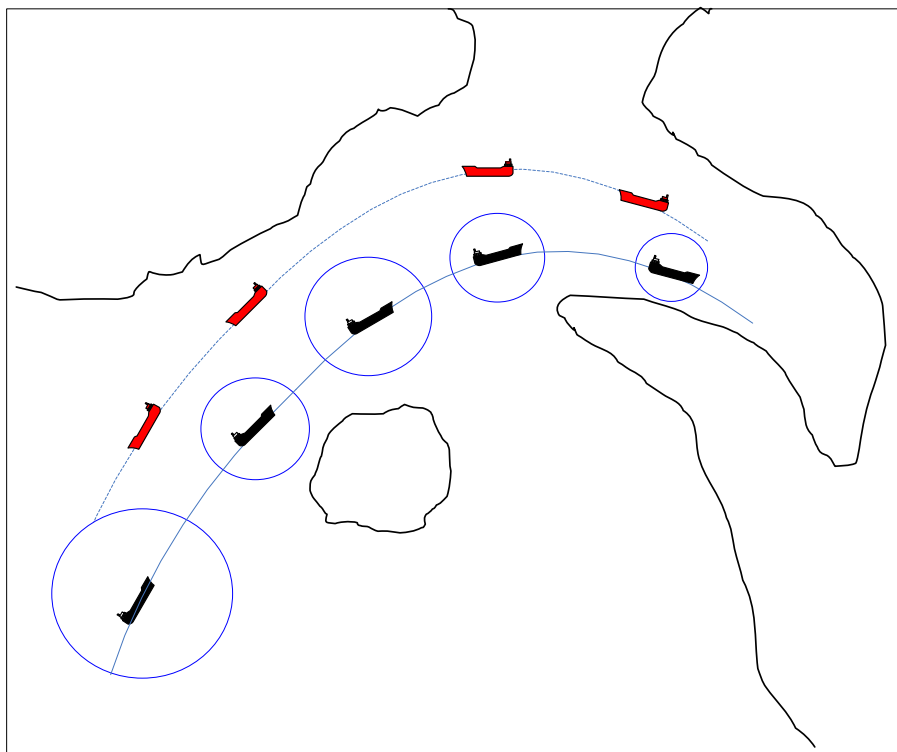


Figure 4.3: Variation of ship domain size for an arbitrary geographical area by considering the channel width and two lanes in every step of the approach

The simplest form a ship domain can have is that of a circular disk with its centre at the waterline amidships (Figure 4.2). As the operational characteristics change (channel width, proximity to other ships in the vicinity, etc.) the size of the ship domain also changes (Figure 4.3). The dynamic behaviour of the domain is necessary since it captures reality in a more efficient way rather than assuming it is constant, (Ravn et al., 2006). This effectively means that the available time for evasive manoeuvres varies along the path of a vessel.

With this in mind, the initial definition of the ship domain is modified as follows: the diameter of the domain disk should be some multiple of the ship's length and if it becomes equal to or less than the ship length then a collision occurrence is assumed. During the design stage, where the operational profile of a vessel should be heavily taken into consideration, assessment of the ship domain for various waterways and traffic conditions can be directly associated to the calculation of collision probability for these areas.

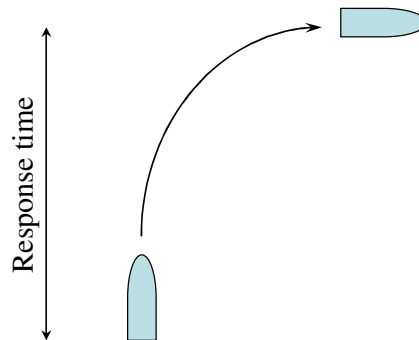


Figure 4.4: Course alteration is probably the only immediate action the navigator can take to avert a collision, (Ravn et al., 2006)

The new model

Considering the basic ideas underlining the ship domain, its size can be expressed as a function of a series of parameters related to generic design characteristics and the operational profile of a ship.

A main feature that contributes to the definition of the domain size is the time necessary for the vessel to advance at 90 degrees (Figure 4.4), contrary to the distance that is needed to perform such a manoeuvre, as it is advocated by (Ravn et al., 2006). This feature reflects a multitude of design parameters and at the same time

it occupies a central position in the development of a close proximity situation or an erroneous action that is made by the pilot or the navigation officer. That is, how fast the ship will respond to the command for an evasive manoeuvre (i.e. rudder hard to starboard as is often the case) in order to avoid collision with a near-by ship. This concept closely follows the idea described earlier concerning the limited available time that can increase the severity of a situation with an unwanted outcome. From a risk-based design point of view, this quality requires minimisation at an early design stage by improving the manoeuvrability of the vessel.



Figure 4.5: Dense traffic in the Kiel Canal (www.kiel-canal.org)



Figure 4.6: Typical traffic in Houston Ship Channel (www.uscg.mil/vtshouston/images/morgansptpassing.jpg)

The other representative design feature of the ship is its length which in this case reflects the size of the vessel in a seaway. Both the response time and the length of

the vessel are reciprocal to the size of the domain: the smaller their value is, the larger the diameter of the domain will be.

From an operational point of view the speed of the vessel is also of critical importance. Its value reflects the conditions (traffic density, visibility, time schedule, etc.) under which the vessel sails and its variation depends on the topology of the navigational area. Passage through straits and narrow channels (Figure 4.5 and Figure 4.6) require very careful speed control in order to allow as much time as possible for corrective action in case of an emergency, bearing in mind the reduced manoeuvring capability at low speed. Traffic density in such passages can impose further restrictions to the speed range. Quite naturally, speed and traffic density are inversely proportional to the domain size as well.

The final element that defines the operational limits of the ship is the size of the channel in terms of its transverse width, which in turn affects the traffic density in the area. Additionally, any regulatory measures from local port authorities are further governed by this geographical restriction (like in the case of Vessel Traffic System – VTS). The channel width varies proportionally to the domain size. The final element that is mutually linked to the deterioration of the manoeuvrability of a ship and the geographical features of a waterway is the water depth. This issue is not addressed here and it is assumed that the waterways under consideration have sufficient depth to alleviate such effects.

Parameter	Description	Dimension
L	Waterline length of the ship	m
R	Response time for changing direction by 90°	s
V	Speed of the vessel	m/s
C	Channel width	m
ρ	Traffic density (number of vessels per unit area)	m ⁻²
D	Ship domain diameter	m

Table 4.3: The parameters considered in the new model (SI units)

The five parameters described above are summarised in Table 4.3. In its simplest form, the diameter of the ship domain can be expressed as:

$$D \propto \frac{C}{V \times L \times R \times \rho} \quad (4.9)$$

Equation (4.9) is just a representation of the parameters involved in the calculation of the diameter of ship domain rather than a functional expression of it. Care should be taken as to the variables selected for this model: not all of them are totally independent from each other. There are two issues of concern:

- (i) the relation of the response time (R) to the speed of the vessel (V) when an evasive manoeuvre starts, and
- (ii) the relation between the traffic density (d) and the channel width (C).

The first point can be demonstrated easily by use of SIMX5 or other similar tools as presented in Appendix A. As this feature is related to the manoeuvring performance of the ship it falls outside the scope of this thesis. Direct input of SIMX 5 results are used in Chapter 7 for various speeds and for the tanker and the ROPAX vessels in the example cases.

In order to address the latter point it is necessary to combine information of the geography of the passage and the number of ships navigating this passage. According to (Kriastiansen, 2005) the number of ships per unit area can be expressed as:

$$\rho = \frac{N}{V \times C} \quad (4.10)$$

Where:

N: number of ship passages per unit time (e.g. annually)

V': speed of surrounding traffic

C: channel width

The ship domain diameter can then be obtained by adding the effect of entropy of information. The final equation has the form of:

$$D = \frac{C}{V \times L \times R \times \rho} \times 10^{-H} \quad \text{or} \quad D = \frac{V \times C^2}{V \times L \times R \times N} \times 10^{-H} \quad (4.11)$$

A scale factor can be further added in Equation (4.11) to account for more case-specific applications but for the time being it is assumed equal to 1.0. The probabilistic nature of the domain diameter, which defines whether or not a collision occurs, is determined through Monte Carlo (MC) simulation, (Vose, 2000), of the

channel width (C), the speed of the vessel (V), the annual number of passages (N) and the speed of surrounding traffic (V'). The probability of collision per unit time (e.g. on a yearly basis) can be obtained by identifying the number of times the domain diameter is smaller or equal to the vessel length divided by the total number of samples of the MC sampling process (typically 10,000 samples). Inversion of the probability of collision will provide the return period between two consecutive collision events.

This form of calculation of collision probability implies that the ship is in sailing mode, i.e. it is not in anchorage or by the dock side. Furthermore, implementation of the model in a deterministic manner indicates only whether collision occurs or not, i.e. whether the domain diameter is smaller or greater than the ship length, respectively, at a certain time instance. Finally, it should be stressed that this model can only be used for the calculation of the probability of collision with other ships. It cannot be deployed in calculations for the probability of grounding or collision with stationary objects since the element of speed of surrounding traffic (V') and the traffic density (ρ) become meaningless. In cases like this alternative models can be used, e.g. (Kristiansen, 2005).

4.5 Sensitivity analysis

In order to assess the sensitivity of the proposed model with respect to the involved parameters of Equation (4.11), MC sampling will be performed for each one of them. Each parameter in turn will be sampled and the mean and standard deviation of the ship domain diameter will be obtained. Comparison of these two quantities will provide the measure of the variation of the domain diameter. The MC scheme will be performed for 10,000 samples. The ranges of the parameters in the calculation are presented in Table 4.4. All sampling is based on the Normal distribution.

Table 4.5 summarises the mean and standard deviation values for the diameter of the ship domain when each parameter is changed and the rest remain constant. The bar chart of Figure 4.7 stresses the sensitivity of the model with respect to the value of entropy. It should be mentioned that the ship speed has zero standard deviation as it

is simplified from Equation (4.11). This is due to the assumption that the speed of the surrounding traffic is the same as the ship speed.

Parameter	Constant value	Parameter variation	
		Mean	Standard deviation
Channel width	15 nm	15 nm	5nm
Ship length	200 m	200 m	25 m
Ship response time	300 s	300 s	60 s
Ship speed	15 kn	15 kn	4 kn
Entropy	4.0	4.0	0.5
Traffic density	150,000 passages / year	150,000 passages / year	25,000 passages / year

Table 4.4: The parameters involved in Equation (4.9) and their values

Examined parameter	Domain diameter variation	
	Mean	Standard Deviation
Channel width (C)	304.68	189.9
Ship length (L)	274.95	36.08
Ship response time (R)	282.84	65.4
Ship speed (V)	270.6	0
Entropy (H)	488.48	643.63
Traffic density (N)	280.37	52.74

Table 4.5: The effect of entropy on the ship domain diameter is very pronounced

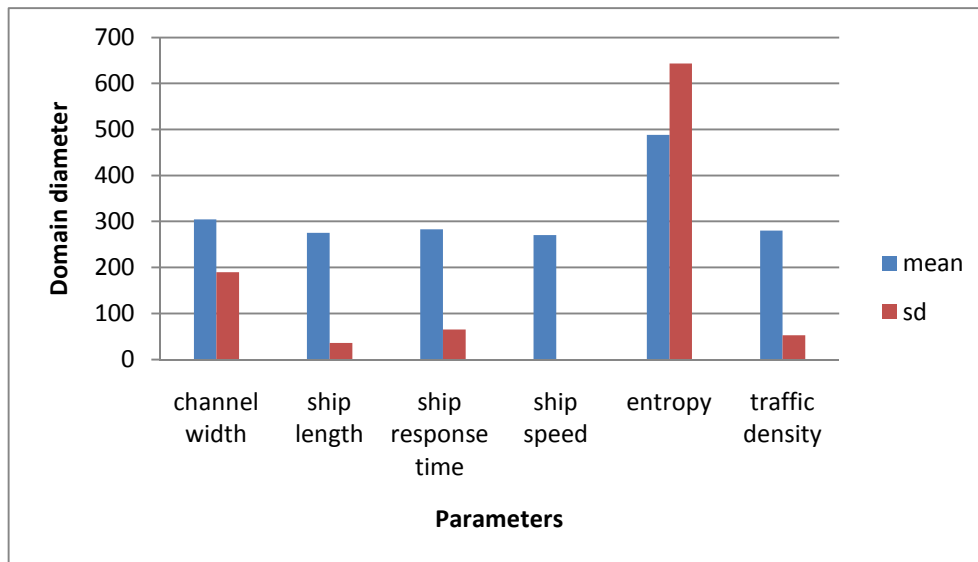


Figure 4.7: The magnitude of entropy has the greatest effect on the domain diameter

4.6 Model calibration

Considering that the model presented in Equation (4.11) is largely based on the operational profile of the ship under consideration it is necessary to compare its results with existing studies and data. This will be pursued in two modes: (i) the ship operates in relatively open water at its operational speed, and (ii) the ship operates in confined waters. In both cases the average number of ship movements in the surrounding area is 50,000 per year.

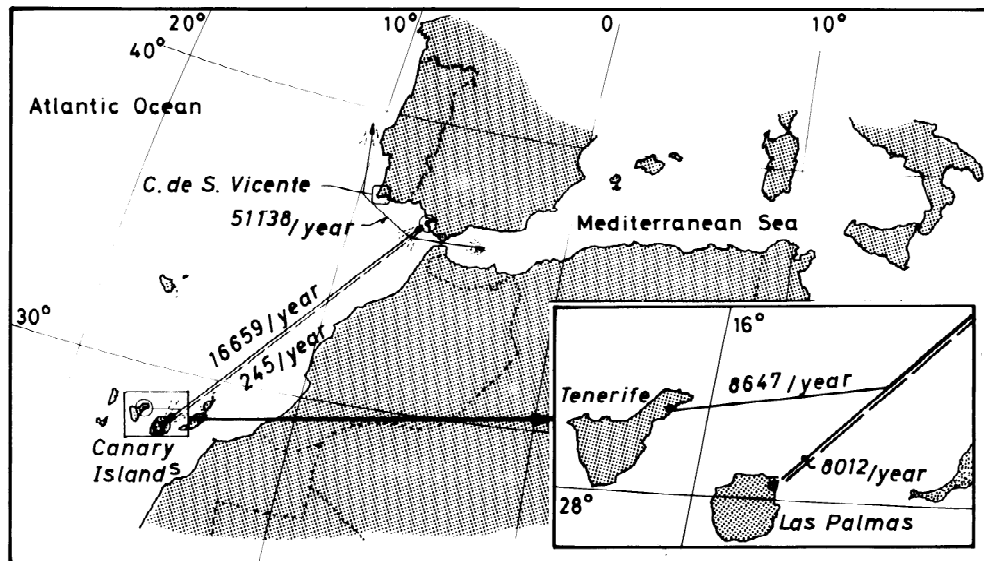


Figure 4.8: The geographical area of operation of *MS Dextra*, (DEXTREMEL, 2001)

(i) Case 1: open waters

The input information for this case originates from (Pedersen & Zhang, 1999). The analysis is performed for the ROPAX *MS Dextra* and it was conducted in the course of the DEXTREMEL project, (DEXTREMEL, 2001). The geographical area of operation and the particulars of the ship are presented in Figure 4.8 and in Table 4.6 respectively.

Dimension	Value
Lpp	173.0 m
B	26.0 m
T	6.5 m
V	28.0 kn
Δ	16,800 tonne
DWT	4,500 tonne

Table 4.6: Particulars of *MS Dextra*, (DEXTREMEL, 2001)

Causation factor for loss of navigational control per passage, (Kristiansen, 2005)	
$2 \times 10^{-4} \log_2 \left(\frac{1}{2 \times 10^{-4}} \right) + (1 - 2 \times 10^{-4}) \log_2 \left(\frac{1}{1 - 2 \times 10^{-4}} \right) =$	2.75×10^{-3}
Causation factor for human error per passage, (Liu & Wu, 2004)	
$0.0168 \log_2 \left(\frac{1}{0.0168} \right) + 0.983 \log_2 \left(\frac{1}{0.983} \right) =$	0.123
Wind direction bearing 280°	
$0.833 \log_2 \left(\frac{1}{0.833} \right) + 0.167 \log_2 \left(\frac{1}{0.167} \right) =$	0.651
Wind speed less than 11m/s	
$0.10 \log_2 \left(\frac{1}{0.10} \right) + 0.90 \log_2 \left(\frac{1}{0.90} \right) =$	2.656
Wave height less than 1.5m	
$0.50 \log_2 \left(\frac{1}{0.50} \right) + 0.50 \log_2 \left(\frac{1}{0.50} \right) =$	1
Thick fog	
$0.005 \log_2 \left(\frac{1}{0.005} \right) + 0.995 \log_2 \left(\frac{1}{0.995} \right) =$	0.045
<i>Total</i>	<i>4.478</i>

Table 4.7: Calculation of the entropy of information for the open waters case

According to the study presented in (Pedersen & Zhang, 1999), the annual probability of MS Dextra to participate in a collision event was estimated at 0.042 or once every 24 years. The MC simulation on the variables of Equation (4.11) according to the available data indicated that the probability of collision obtained should be multiplied by a factor of approximately 100 for agreement with the DEXTREMEL results. The calculation of the entropy and the mean and standard deviation of the variables used in this case are presented in Table 4.7 and Table 4.8 respectively.

Variable	(Probability density function, mean, standard deviation)
Speed of subject ship in knots	Normal distribution, 25 kn, 7 kn
Speed of surrounding traffic in knots	Normal distribution, 14 kn, 7 kn
Number of ship passages per year	Normal distribution, 65000, 1000
Channel width in nautical miles	Normal distribution, 15 nm, 5 nm

Table 4.8: Details of the sampled variables according to data provided in (Pedersen & Zhang, 1999)

(ii) Case 2: confined waters

The second comparative study draws information and results from (Øresund, 2006). The area of analysis is focused in the sound between Denmark and Sweden (Figure 4.9). Based on recorded accident data for the years between 1997 and 2005, the statistical frequencies are presented in Table 4.9.

Accident type	Number of accidents	Number of years	Frequency per year
Grounding	92	9	10.2
Collision	28	9	3.1
Ship-obstacle collision	12	9	1.3
Miscellaneous	7	9	0.8
<i>Total</i>	<i>139</i>		<i>16.7</i>

Table 4.9: Summary of historical data analysis as presented in (Øresund, 2006)

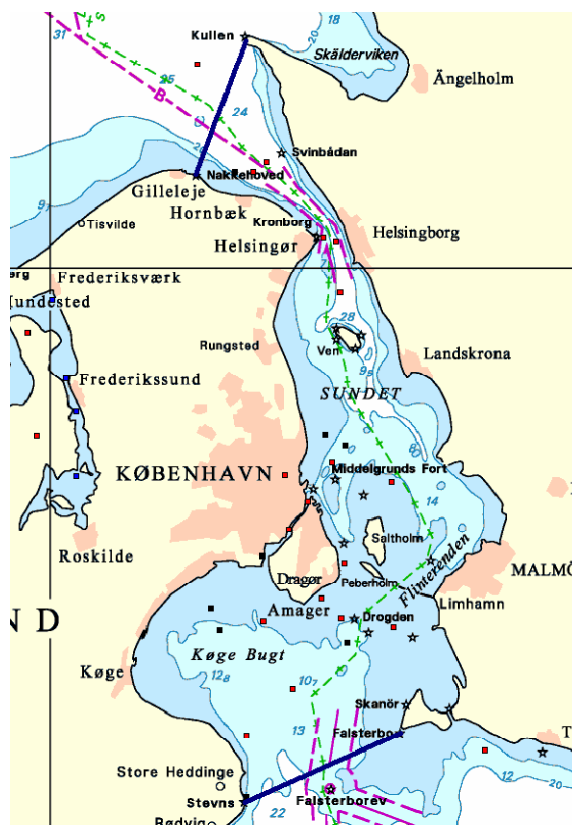


Figure 4.9: Analysis area between Denmark and Sweden

This time the subject vessel was assumed to be the ROPAX, the particulars of which are presented in Chapter 7. The calculation of entropy of information and the necessary statistical information for the MC simulation are presented in Table 4.10 and Table 4.11, respectively. It should be stressed that the speed of the subject ship and the surrounding traffic are significantly reduced to reflect the restricted area for evasive manoeuvres in the case of emergency. Furthermore, owing to detailed historical data, the vessel movements in the area have a very small standard deviation. This time the resulting probability of collision should be multiplied by a factor of approximately 0.225 to achieve agreement between the two results.

Causation factor for loss of navigational control per passage, (Kristiansen, 2005)	
$2 \times 10^{-4} \log_2 \left(\frac{1}{2 \times 10^{-4}} \right) + (1 - 2 \times 10^{-4}) \log_2 \left(\frac{1}{1 - 2 \times 10^{-4}} \right) =$	2.75×10^{-3}
Causation factor for human error per passage, (Liu & Wu, 2004)	
$0.0168 \log_2 \left(\frac{1}{0.0168} \right) + 0.983 \log_2 \left(\frac{1}{0.983} \right) =$	0.123
Wind direction bearing 270°	
$0.99 \log_2 \left(\frac{1}{0.99} \right) + 0.01 \log_2 \left(\frac{1}{0.01} \right) =$	0.081
Wind speed less than 10m/s	
$0.40 \log_2 \left(\frac{1}{0.40} \right) + 0.60 \log_2 \left(\frac{1}{0.60} \right) =$	0.971
Wave height less than 1.4m	
$0.40 \log_2 \left(\frac{1}{0.40} \right) + 0.60 \log_2 \left(\frac{1}{0.60} \right) =$	0.971
Thick fog	
$0.03 \log_2 \left(\frac{1}{0.03} \right) + 0.97 \log_2 \left(\frac{1}{0.97} \right) =$	0.194
<i>Total</i>	<i>2.343</i>

Table 4.10: Calculation of the entropy of information for the confined waters case

Variable	(Probability density function, mean, standard deviation)
Speed of subject ship in knots	Normal distribution, 10 kn, 5 kn
Speed of surrounding traffic in knots	Normal distribution, 10 kn, 8 kn
Number of ship passages per year	Normal distribution, 40000, 1000
Channel width in nautical miles	Normal distribution, 3 nm, 1 nm

Table 4.11: Details of the sampled variables according to data provided in (Øresund, 2006)

Discussion

Based on the comparison of the results obtained with the proposed model and the two case studies referenced above, the following conclusions can be drawn regarding the validity of Equation (4.11):

- The comparison with the two studies is implicitly based on their accuracy. That is, the end results of these projects, which are based on a set of assumptions and available information, are as accurate as they could be at the time they were conducted. However, it should be stressed that the work presented in (Øresund, 2006) was primarily based on analysis of historical data contrary to the study of (Pedersen & Zhang, 1999), which was the result of a research project and therefore entailed more thorough processing of the available information.
- Considering that in the case of *MS Dextra* agreement of results can be achieved with a coefficient of 100 whereas in the case of navigation between Denmark and Sweden the coefficient should be only 0.225 indicates that the proposed model is more applicable in restricted waters and when navigation is conducted very close to shore. This result is very encouraging for further development considering that the majority of ship-ship collisions occurs close to the coast line (Figure 4.10).

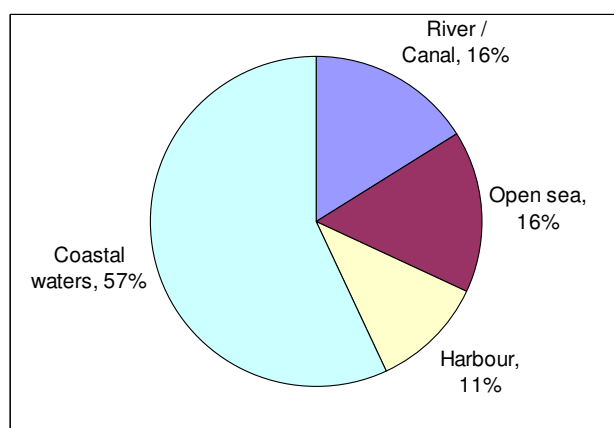


Figure 4.10: Locations of collision, (Samuelides et al., 2008)

- The large variation between the two cases is directly attributed to the non-linear dependence of the domain diameter on the value of entropy as it was discussed earlier in Section 4.5 (Figure 4.11).

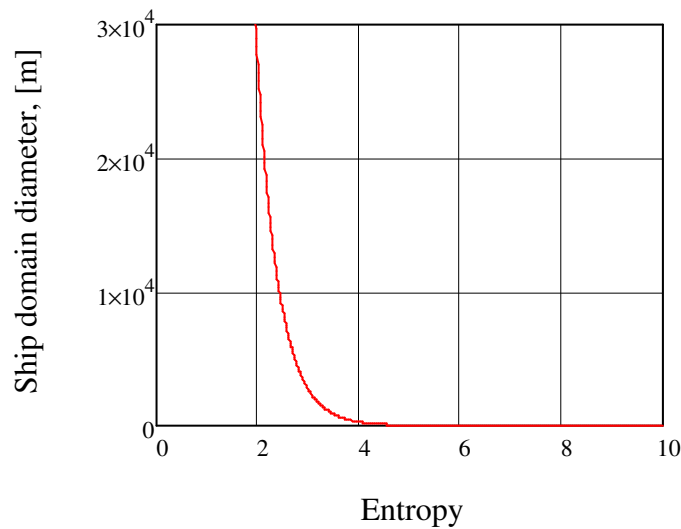


Figure 4.11: Small variations of entropy can affect the size of the domain diameter substantially

- In these two case studies, entropy is comprised by information concerning systems failure, human error, wind speed and direction, wave height and visibility levels. It should be stressed that different geographical locations will require consideration of additional pieces of information, e.g. wind gusts, currents, etc. Such “locality” is very important as the circumstances leading to collision can be drastically altered. As a result, reproduction of existing case studies or application to new ones is necessary in order to identify the entropy contributors in every case and establish the universal application of the proposed model, without the need to resolve to tailored models for specific areas and circumstances.

4.7 Entropy level and point of no return

Earlier in this thesis it was discussed how very short time intervals can often have a definitive role in the development of a collision event and that when a point of no return was reached then the collision was unavoidable. In this context the concept of entropy of information is deployed in the course of obtaining the probability of collision for a given waterway and operational profile of a ship. Even though the

acceptable limits of entropy are not defined, the analysis presented in the following indicates the limiting values of entropy above which a collision event will definitely occur, i.e. the domain diameter will become less or equal to the ship length.

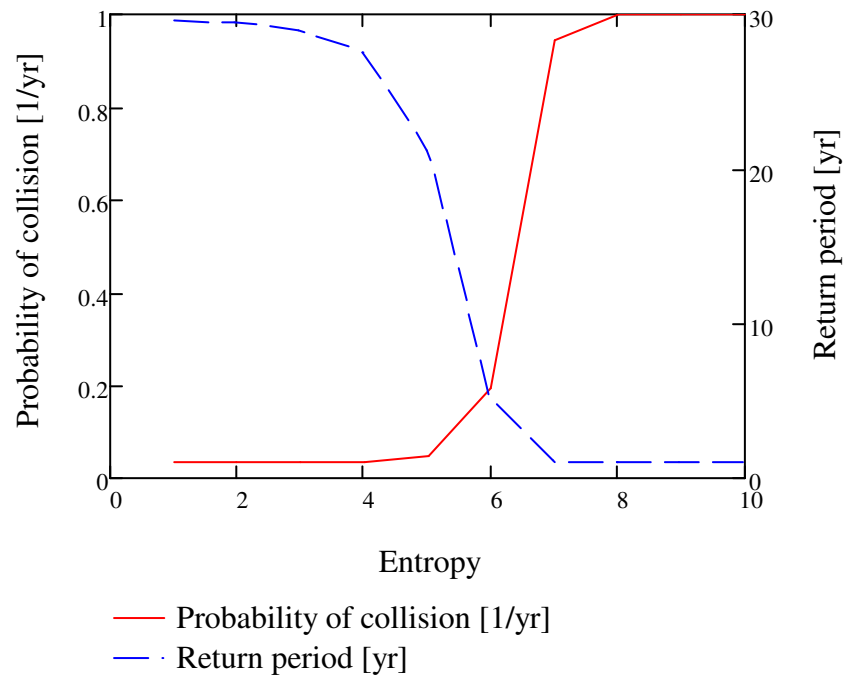


Figure 4.12: Entropy variation for the case of open waters navigation

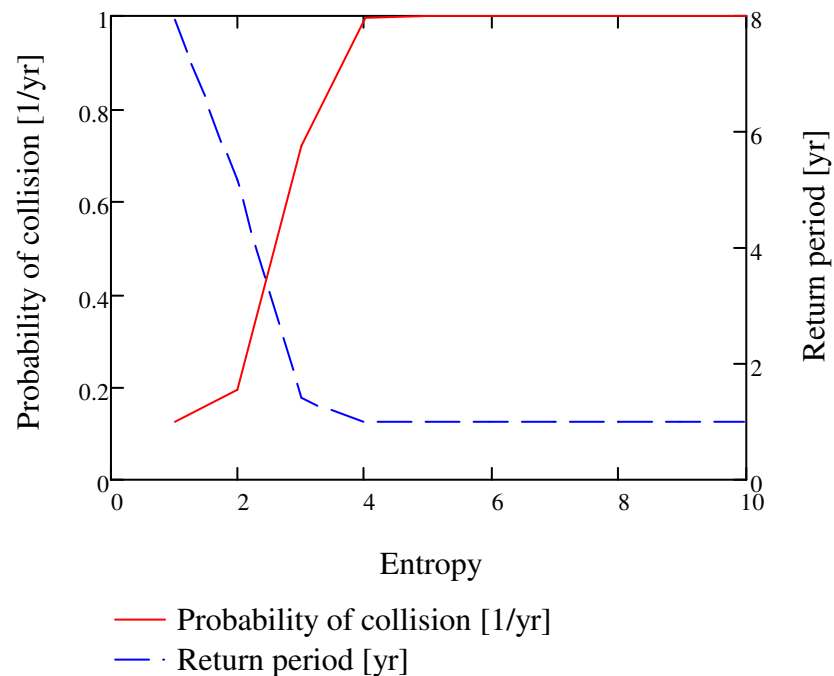


Figure 4.13: Entropy variation for the case of confined waters navigation

As before the results are presented for the case of open waters and confined waters navigation, respectively, for comparison between different entropy levels. In both cases the data are used as described above and only entropy is allowed to take real and positive values. The results are presented in Figure 4.12 and Figure 4.13 for each case.

It becomes immediately apparent that in the open waters case a collision event is predicted with probability equal to 1.0 for values of entropy approximately equal to 4.0. In the second case, however, the entropy levels for a similar situation will have to be doubled. The fact that space availability (i.e. open sea) allows more flexibility for manoeuvring and, in the case of any damage to the equipment, bad weather, etc., longer decision-making times, are reflected in the proposed model. Additionally, the choice of entropy of information as a viable means for capturing quantitative and qualitative information in different circumstances, which define the safety of navigation, is well justified.

4.8 Chapter summary

In conclusion, this chapter elaborates on the development of a new analytical model for the calculation of the probability of a ship-ship collision in a seaway. The model is founded on the idea of ship domain, it is very generic in its nature and it combines design and operational parameters. Additionally, the concept of entropy of information is presented in the context of risk-based design to account for the effect of *soft*, not easily quantifiable, elements and to allow the consideration of a range of operational scenarios and the prediction of their outcomes in a consistent and holistic manner. As a result, it can be used for risk analysis as performance measure of the probability of collision during early design. Its potential weak point may be identified in the need for threshold values for certain geographical locations, as the examples presented in Section 4.6 are not adequate for drawing conclusions for its range of application. In any case, it is flexible enough for more universal application and definition of a minimum threshold for the entropy of a situation. Demonstration of the model application is performed in the case studies of Chapter 7.

5 Probability of water ingress due to collision

5.1 Introduction

This chapter elaborates on the crashworthiness characteristics of the side shell of a ship. The thinking and arguments behind the developed models are presented. In the final section, an algorithm for calculating the probability of flooding due to collision is proposed. The input to the routine combine elements from both the struck and the striking ships and the output is the breach size and the magnitude of penetration either in a probabilistic or deterministic mode.

5.2 Factors affecting the crashworthiness of ships

At an early design stage, the crashworthiness of a ship can be defined by its structural configuration whilst accounting for the properties of the striking ship. That is, on the available kinetic energy prior to impact (striking ship displacement and speed) and the striking bow geometry and rigidity. The former issue is evident and all the necessary information for establishing these parameters can be derived by the operational profile of the ship in terms of the surrounding traffic (i.e. the size and the speed of other vessels). In this way, the range of available kinetic energy can be defined. Statistical analyses performed in various studies, e.g. (HARDER, 2001a), can greatly assist towards this direction.

The issue of the geometrical configuration of the striking bow complements, and most of the times, enhances the expectation of rupture of the side shell. It is true that the sharper the contact edge of the striking body is, the easier the panels of the side shell will rupture (i.e. with less expenditure of kinetic energy). This rational expectation is not only confirmed by intuition but also by the majority of the numerical and experimental approximations to the topic.

Explicit consideration of the sharpness of the impacting body in the models will enable the designer to examine a broader variety of geometrical bow configurations that in conjunction with the available kinetic energy can compromise the watertightness of the new ship. In this way, it becomes possible to assess a wider and more representative range of collision scenarios, which will allow the designer to gauge the operational risks of the vessel in greater detail. This momentum of thinking naturally creates the incentive for more thorough search of the design space and leads to the generation of more fit-for-purpose structural design solutions and arrangements.

A further issue that defines the sharpness of the striking bow is the angle of collision. Traditionally, the majority of studies addressing collision accidents and crashworthiness assessment are conducted on the premise that the collision event occurs at right angles between the struck and the striking ship. This fundamental assumption has merit from a theoretical point of view as it considers the worst

possible scenario and simplifies modelling. However, this does not represent reality as most of the times a collision occurs as a result of some failed manoeuvre to avert the accident and therefore hardly ever at 90° with respect to the struck ship (the accident presented in Figure 5.1 is one of the few exemptions). Based on this argument it becomes evident that the sharpness of the striking bow will change in oblique angle collisions and therefore the deformation of the struck panel will develop in a different manner.



Figure 5.1: The bow of the significantly larger striking ship is driven substantially into the side of the struck vessel (http://www.cargolaw.com/2003nightmare_t-bone.html)

The remaining factors, which can affect the development of a collision event, are related to the inertia of the two vessels and in particular their hydrodynamic added mass before and after the contact. The added mass of the striking vessel during its forward motion slightly increases its real displacement. Similarly, the struck vessel will experience some more substantial increase of added mass/moment in sway/yaw motions, respectively, following a collision event. The increase of the involved displacements highlights the fact that the dynamic response of the struck vessel will no longer be the same, i.e. a larger portion of the provided kinetic energy will be dissipated as it will be demonstrated next (Figure 5.7). This argument stands even if a quasi-static approach is followed as it would be the case for early design.

5.3 The geometrical link between the striking and the struck ships

Past accidents reports and the published work of numerous researchers on the topic of ship-ship collision are instructive in various ways. Once a collision initiates it is impossible to stop it: it will only terminate when the available kinetic energy is exhausted.



Figure 5.2: The highly localised character of collision is demonstrated in this picture. The imprint of the striking vessel (right) is clearly seen, (BMT, 2005)

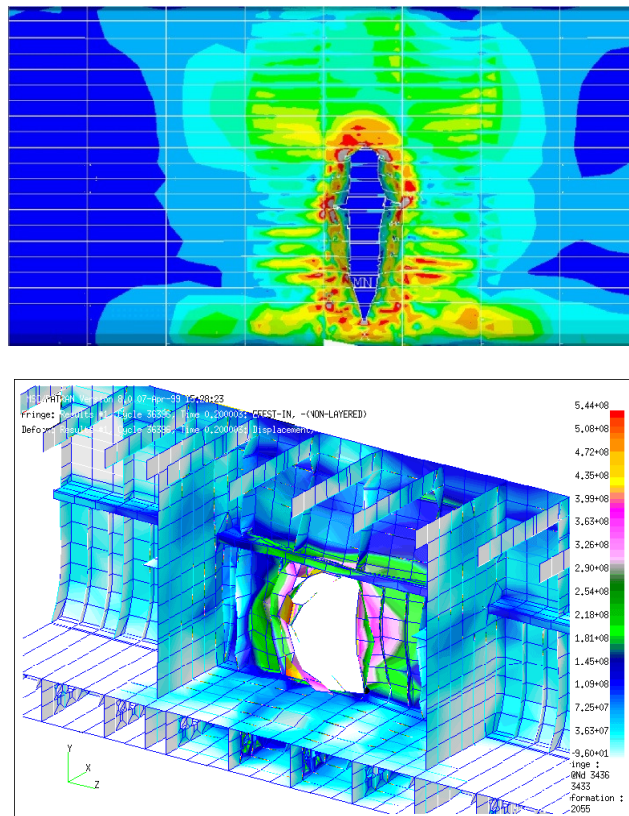


Figure 5.3: FE analysis of the indentation of bulbous bows of different geometry, (Servis & Samouelides, 1999)

If the two vessels are of similar size then the damage will be restricted to the contact area of the struck vessel. In the opposite case, the collision damage can be quite extensive and can lead up to the collapse of the hull girder. The dividing line between the two alternatives is difficult to define as it is not only the relative size of the two ships that matters but also the ambiguity associated with the hydrodynamic characteristics of the struck ship, namely its added mass in sway. More discussion will follow in the next section.

Further to this fact, the imprint of the striking vessel to the side of the struck ship is very obvious and it is confirmed either from accident investigations (Figure 5.2), FE analyses (Figure 5.3), experimental studies or combinations of these.

The link of the side structure deformation and the striking body geometry is the *principle radii of curvature* of the latter, which provides a measure of its sharpness. The radii of curvature of a three-dimensional surface can be obtained by its parametric definition:

$$x = x(p,t), \quad y = y(p,t), \quad z = z(p,t) \quad (5.1)$$

where x , y and z are real, continuous and differentiable functions (the second derivative with respect to either of the two parameters should exist) defined in a right-handed coordinate system; p and t are the two parameters (independent real variables), which take values within certain closed intervals. In this thesis, there is additional interest in the extent of deformation of the structure and, in particular, in the necessary deflection to cause rupture of the struck panel. Based on this requirement, the above set of functions is modified to include the indentation w_0 :

$$x = x(p,t,w_0), \quad y = y(p,t,w_0), \quad z = z(p,t,w_0) \quad (5.2)$$

Following this definition, calculation of the 1st and 2nd *fundamental forms* of a surface takes place, which eventually leads to the calculation of its radii of curvature. This information is used as direct input to the definition of the parametric surface of the side shell. For the current stage of development there are three surfaces modelled and used to represent solid striking bodies. That is, a sphere, an elliptic paraboloid and a Bezier surface. The first two surfaces are simple to define and are used in the majority of experimental studies. On the other hand, description of the striking bow

with Bezier surfaces allows more rational representation of the actual size of damage compared to the regulations prescribed by SOLAS (Figure 5.4), where the damage size is a function of the length and the breadth of the struck ship. More discussion on this issue will follow in Chapter 6.

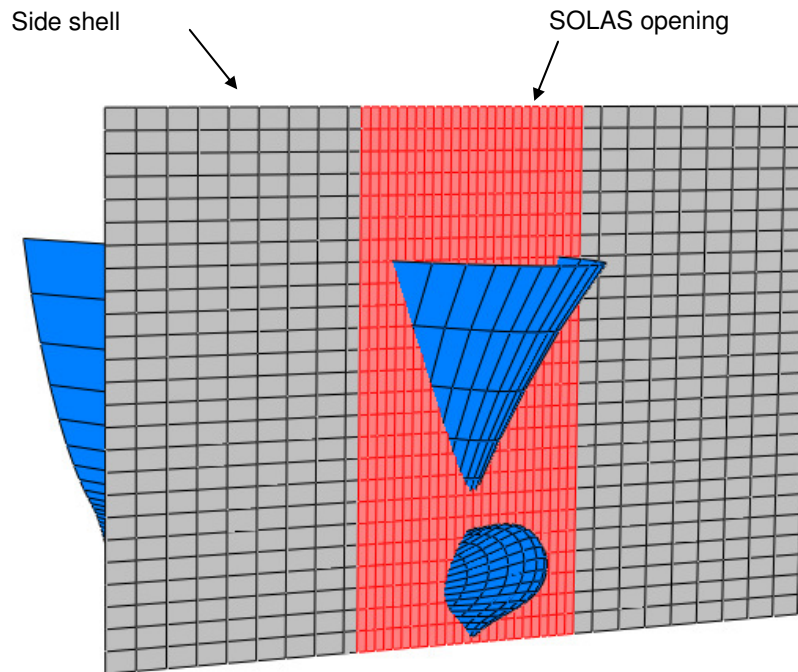


Figure 5.4: Schematic comparison of the SOLAS opening and the actual breach size following collision and penetration. The level of overestimation of the situation is obvious.

The struck surface deformation is modelled with the *Witch of Agnesi* function which allows for explicit consideration of deflection w_0 as a function of radii of curvature of the striking body. All the relevant material is presented in Appendix B and more thorough presentation of the related concepts of differential geometry can be found in (Struik, 1988).

One basic assumption that is made here is that the bow of the striking ship is not deforming at all. In reality the amount of deformation of the bow structure is not easy to be assessed due to the high degree of stiffening and its highly irregular geometry. Accident investigation has demonstrated a large variation of bow deformation which is also a function of the crashworthiness capacity of the struck panel. As a result modelling the amount of impact energy that can be absorbed by the bow would add more ambiguity in an already complicated situation. The assumption of a rigid bow,

which absorbs no impact energy, can help alleviate this problem whilst offering predictions on the conservative side that would serve safety considerations well. At the same time, it is implied that the radii of curvature of a rigid bow remain constant during the deformation of the struck panel. The only element that is taken into consideration is the friction generated with the side shell of the struck ship during indentation and penetration.

Analytical presentation of the striking bow geometry can be directly included in early design studies in the form of parametric models and in combination with the statistical data of bow configurations presented in (Zhang, 1999). However, this information cannot provide any measure of sharpness of the striking bow other than a general description of the most widely used bow arrangements in practice. In cases where more detailed description of the energy absorbed by the striking bow is of interest, approaches like the one proposed in (Pedersen et al., 1993) and (Endo et al., 2004) can prove very useful.

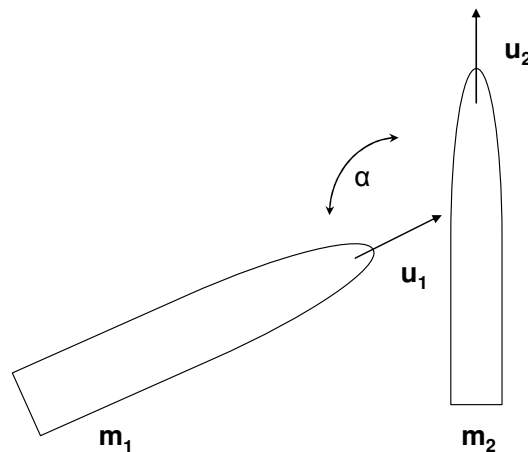


Figure 5.5: The general case between a striking and struck ship

Effect of relative size of struck-striking ships

The effect of the relative size of the struck and striking vessels in the development of a collision can be demonstrated by utilising the formulation introduced in (Petersen, 1982). Considering the general case of two ships whose paths are crossing as depicted in Figure 5.5 and assuming that (i) the struck ship will not rotate after the strike, (ii) both ships will remain in contact after the collision, and (iii) there is no

hydrodynamic damping in the system, application of the conservation of momentum of the two ships will lead to the following expression:

$$m_1 u_1 \sin(a) = [m_1 + (1 + C_a) m_2] u \quad (5.3)$$

where m_1 and m_2 are the displacement of the striking and struck ship respectively, u_1 is the speed of the striking ship, u is the common speed of the two vessels following the collision and C_a is the added mass of the struck ship in sway. According to (Matora, 1960), the added mass coefficient for the forward motion of the striking ship is 0.02-0.07 and it will be ignored. The loss of kinetic energy after the collision can be expressed as:

$$\Delta E_k = \frac{1}{2} m_1 (u_1 \sin(a))^2 - \frac{1}{2} [m_1 + (1 + C_a) m_2] u^2 \quad (5.4)$$

By eliminating the common speed component u and re-arranging, the loss of kinetic energy can be expressed as:

$$\Delta E_k = \frac{1}{2} \frac{m_1 (1 + C_a) m_2}{m_1 + (1 + C_a) m_2} (u_1 \sin(a))^2 \quad (5.5)$$

The value of the added mass coefficient in sway is varying in the literature. The experiments conducted by (Matora et al., 1971) have showed values of 0.4 to 1.3. Minorsky has suggested the value of 0.4 for collisions of short duration and (Zhang, 1999) is using the value of 0.85.

By setting the mass ratio equal to the ratio of the displacement of the striking ship over the displacement of the struck ship, i.e. m_1/m_2 and assuming the displacement of the striking ship is $m_1 = 100,000$ tonnes, its speed $u_1 = 10$ knots and the striking angle equal to 90° , then the percentage reduction of the kinetic energy for added mass coefficients equal to 0.4, 0.85 and 1.3 is presented in Figure 5.6.

The effect of the added mass coefficient on the loss of kinetic energy is moderate. For example, 50% loss of kinetic energy of a striking ship of displacement m_1 , which is moving with speed u_1 , will occur at mass ratios of 1.415, 1.865 and 2.313 (with proportions $1.0 \div 1.24 \div 1.39$) for 0.40, 0.85 and 1.30 added mass coefficients respectively. For 75% energy loss the mass ratios are 0.477, 0.634 and 0.787 with the

same proportions as above. For 25% energy loss the mass ratios are 4.211, 5.553 and 6.904. As before the proportions are constant which demonstrates that the three curves of Figure 5.6 are offset from each other.

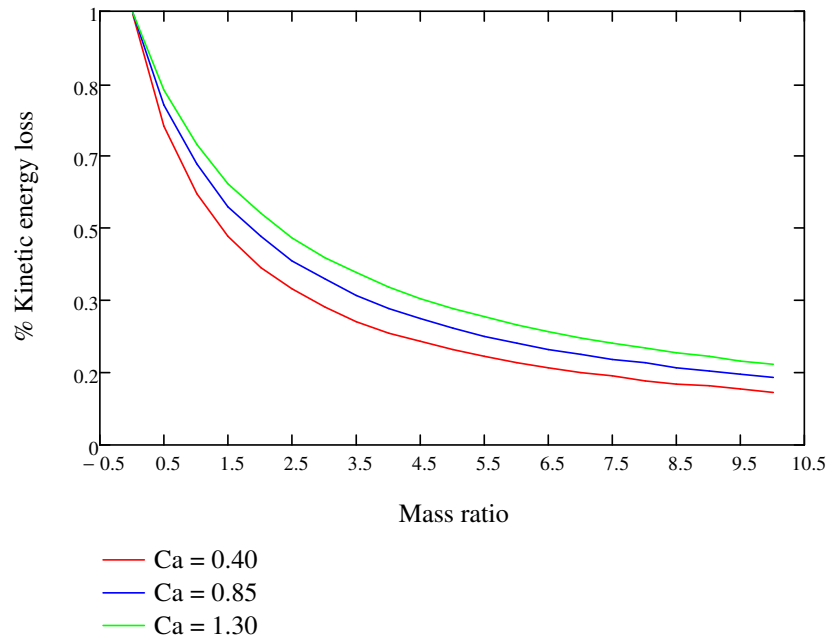


Figure 5.6: Comparative loss of kinetic energy for various added mass coefficients

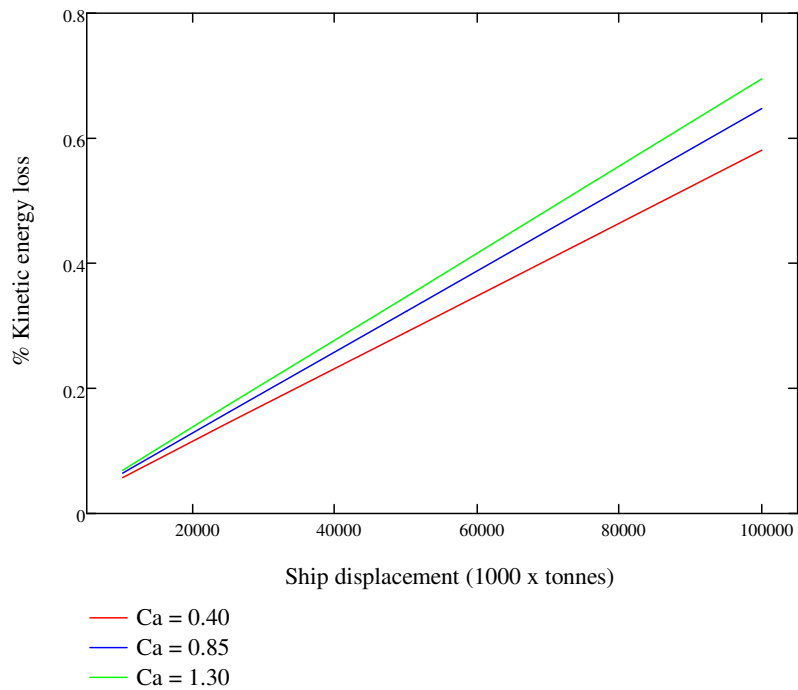


Figure 5.7: The kinetic energy loss is linearly proportional to the displacement of the striking ship when the mass ratio is equal to 1.0

As the mass ratio increases, i.e. decrease of m_2 , gradually more kinetic energy is available to create damage to the side shell panels of the struck ship with limiting value 0.0% loss of energy, where all curves become asymptotic to the horizontal axis. For values of the mass ratio between 0.0 and 1.0, i.e. when $m_2 > m_1$, the same trend is observed. For very small displacement of the striking ship, the loss of the initial kinetic energy is almost complete as expected.

A point worth mentioning is the special case where the displacement of the struck and the striking ships are similar, i.e. mass ratio is approximately equal to 1.0. In this case a large amount of energy is still lost as it is demonstrated in Figure 5.7.

In conclusion of the above discussion, the effect of the relative size of the two ships involved in a collision event will be taken into consideration. Given the graphs presented in Figure 5.6 and Figure 5.7, the added mass coefficient of the struck ship in sway will be set equal to 0.85.

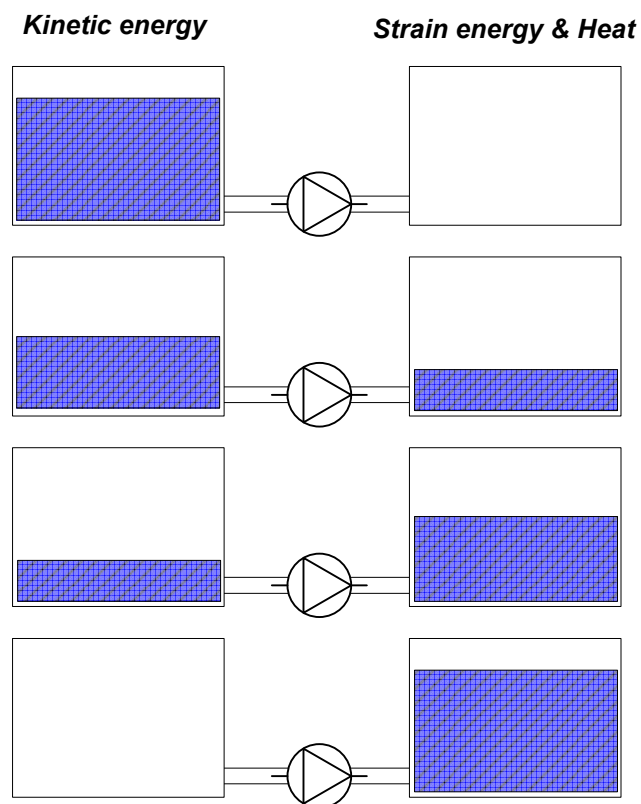


Figure 5.8: A simple analogy for the energy transfer between the striking and the struck ship in various random phases. The total energy of the system remains constant.

5.4 Deformation of stiffened plates

The side shell panels of the struck ship are deforming under the provision of a certain amount of energy from the striking ship. The proposed approach is founded on the idea that the total available energy in the system *struck ship – water – striking ship* remains constant. That is, the available kinetic energy is *quasi-statically* conveyed via contact to the side panels and transforms into strain energy and heat. A direct analogy of the process is depicted in Figure 5.8, where the available energy contained in the left tank is flowing to the right through the connecting pipe and the regulating mechanism in the middle. The nature of this mechanism depends on factors (e.g. the relative position of the two tanks) that are not important here. The flow rate depends on the outlet diameter of the tank on the left, which corresponds to the sharpness of the impacting bow, and the inlet diameter of the tank on the right, which corresponds to the rate of energy that a stiffening configuration can absorb. It is important to stress that:

- (i) The capacity of both tanks is the same: all the available kinetic energy will be eventually transformed in strain energy and heat (irrespective of the extent of the plastic deformation and penetration that will take place in the process);
- (ii) The phenomenon starts with the tank on the right totally dry, and when it ends, the tank on the left is empty.

Despite the universal application of energy conservation, very little can be said about the heat dissipation in the structure and the water surrounding the contact point so this issue will be ignored.

The alternative way to the quasi-static approach would be to consider the dynamic response of a stiffened panel but in this case the duration of the collision phenomenon (from the point of first contact up to the deformation or end of penetration where all the available energy would be exhausted) is creating one extra uncertainty parameter. In various publications, e.g. (Jones, 1979), it is advocated that a collision event has a dynamic character if the duration of contact is shorter than the natural period of the struck body in elastic vibration, whereas, in the opposite case a static analysis can be used with satisfactory results. Therefore, although dynamic

analysis can provide a more realistic approximation to the extent of deformation, it would require one extra complicated calculation (i.e. the estimation of the natural period of the struck panel at an agreed mode of vibration) and one extra assumption (i.e. the duration of impact, which should be lower than the natural period). The computational effort of the former case will add to an already pressed time schedule (since the early design stage has to be completed very fast) whilst the latter is adding more ambiguity to the results and the design decision-making process. For these reasons, the quasi-static approach was favoured in this thesis.

Unstiffened plate

The strain energy accumulated in a piece of plating (of length L and width B) if a bluff indenter is pushed through it has the form of:

$$V_U(w_0) = \frac{1}{2} D \int_0^L \int_0^B \left[\left(\frac{\partial^2 w}{\partial x^2} + \frac{\partial^2 w}{\partial y^2} \right)^2 - 2(1-\nu) \left(\frac{\partial^2 w}{\partial x^2} \frac{\partial^2 w}{\partial y^2} - \left(\frac{\partial^2 w}{\partial x \partial y} \right)^2 \right) \right] dy dx \quad (5.6)$$

The real function w (continuous and differentiable in the x and y directions along the length and width of the plate, respectively) describes the deformation of the plate in relation to the geometry of the indenter. This approach allows for establishing a link between the striking and the struck body as described in Section 5.3: the strain energy accumulated in the struck plate is expressed as an explicit function of the indentation w_0 and provides the potential to quantify the different levels of deformation of the plating.

Assuming that E is the Young's modulus, t the thickness of the plate and ν the Poisson's ratio of the material, the flexural rigidity of the plate is:

$$D = \frac{Et^3}{12(1-\nu)} \quad (5.7)$$

Stiffened plate

The stiffener effect is modelled by varying the plate rigidity in the two directions of the stiffening, as it is described in (Timoshenko & Woinowski-Kreiger, 1964) and (Lekhnitskii, 1968):

$$V_s(w_0) = \frac{1}{2} \int_0^L \int_0^B \left[D_x \left(\frac{\partial^2 w}{\partial x^2} \right)^2 + D_y \left(\frac{\partial^2 w}{\partial y^2} \right)^2 + 2D_1 \frac{\partial^2 w}{\partial x^2} \frac{\partial^2 w}{\partial y^2} + 4D_{xy} \left(\frac{\partial^2 w}{\partial x \partial y} \right)^2 \right] dy dx \quad (5.8)$$

where D_x , D_y are the plate rigidities along x and y -directions respectively (Figure 5.9) and D_{xy} accounts for the shear rigidity. In this context, the involved rigidities are expressed as follows:

$$\begin{aligned} D_x &= \frac{Et^3}{12(1-\nu^2)} + \frac{E_x I_x}{a} \\ D_y &= \frac{Et^3}{12(1-\nu^2)} + \frac{E_y I_y}{b} \\ D_{xy} &= \frac{Gt^3}{12} \\ D_1 &= D - 2D_{xy} \end{aligned} \quad (5.9)$$

where

- E_x and E_y are the Young's moduli for the materials of the stiffeners (in the general case)
- G is the shear modulus of rigidity
- a and b are the stiffener spacing along y and x -axis respectively
- I_x and I_y are the second moments of area of a stiffener along the neutral axis of the plate.

In order to take into account other structural members in the vicinity of contact, like decks and bulkheads, which contribute substantially to the crashworthiness capacity

of the side shell of the struck vessel, D_x and D_y can be modified for the general case as follows:

$$\begin{aligned} D_x &= \frac{Et^3}{12(1-\nu^2)} + \sum_i \frac{E_x^i I_x^i}{a^i} \\ D_y &= \frac{Et^3}{12(1-\nu^2)} + \sum_j \frac{E_y^j I_y^j}{b^j} \end{aligned} \quad (5.10)$$

where

a^i and b^j are some characteristic lengths of the structure (bulkhead interval, double hull span, etc.).

Detailed description of the calculations concerning the two ships considered in the case studies (Chapter 7) is presented in Appendix E.

Finally, it is assumed that the struck panel is in *as-built* condition: all the welding joints are perfect and its surface is well coated and maintained. Since there is no available sensitivity study as to how the presence of these defects would reduce its crashworthiness capacity, a comprehensive investigation should be performed in future studies (Chapter 8).

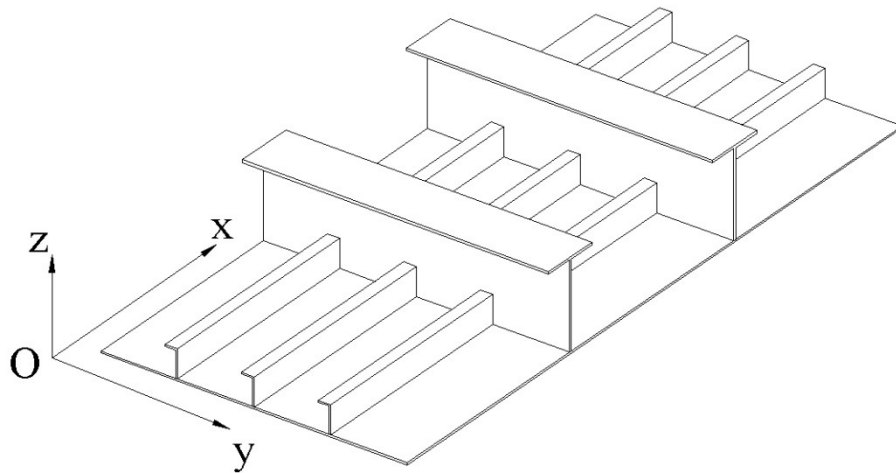


Figure 5.9: Sketch of a classic stiffened panel and the orientation of the Cartesian coordinate system; loading of the panel is performed along the positive z-direction

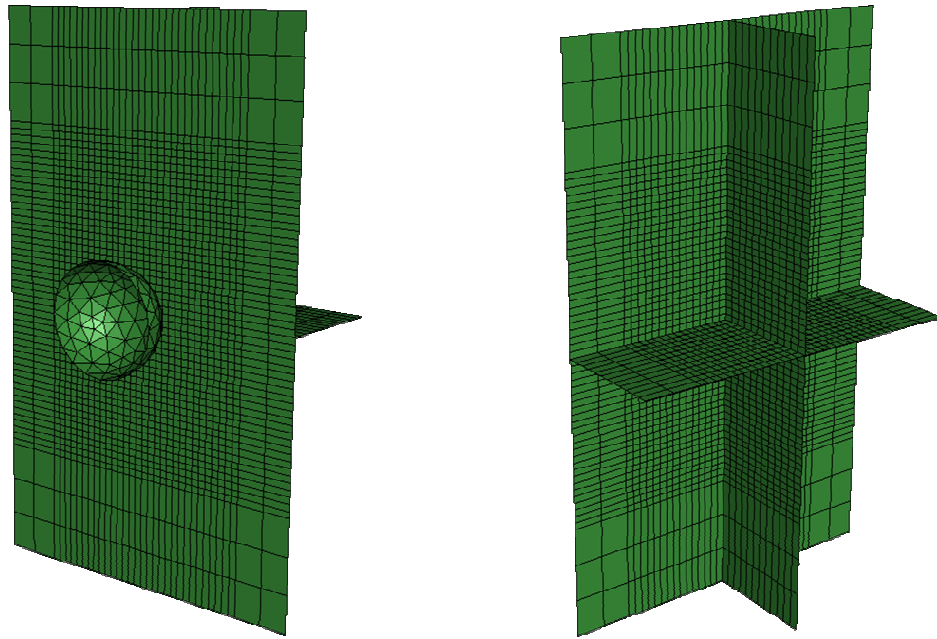


Figure 5.10: A simplified FE model for the demonstration of the effect of substantial stiffening provided by decks and bulkheads

Contribution of decks and bulkheads

The contribution of a deck or bulkhead in the response of the stiffened panel under extreme loading cannot be captured accurately. The fact that a stiffening element of much larger dimensions and extent of supports than the longitudinal and transverse local stiffeners participates in the deformation can create much stiffer response, the effect of which is assessed only subjectively in the literature, (Zheng et al., 2007).

Simplified FE models (ABAQUS 6.6) can readily demonstrate such effect. A sphere of 1.0 m diameter, weighing 130 tonnes is moving with 5.0 m/s. The dimensions of the plate are 5×3 metres. There are three cases examined: (i) the unstiffened plate, (ii) the plate supported only by a deck with span of 1.0 m, and (iii) the plate supported by a bulkhead and a deck of 1.0 m span (Figure 5.10). The plate, the deck and the bulkhead have 15 mm thickness. Figure 5.11 presents the percentage increase of stiffening of the panel in terms of kinetic energy dissipation following the contact event.

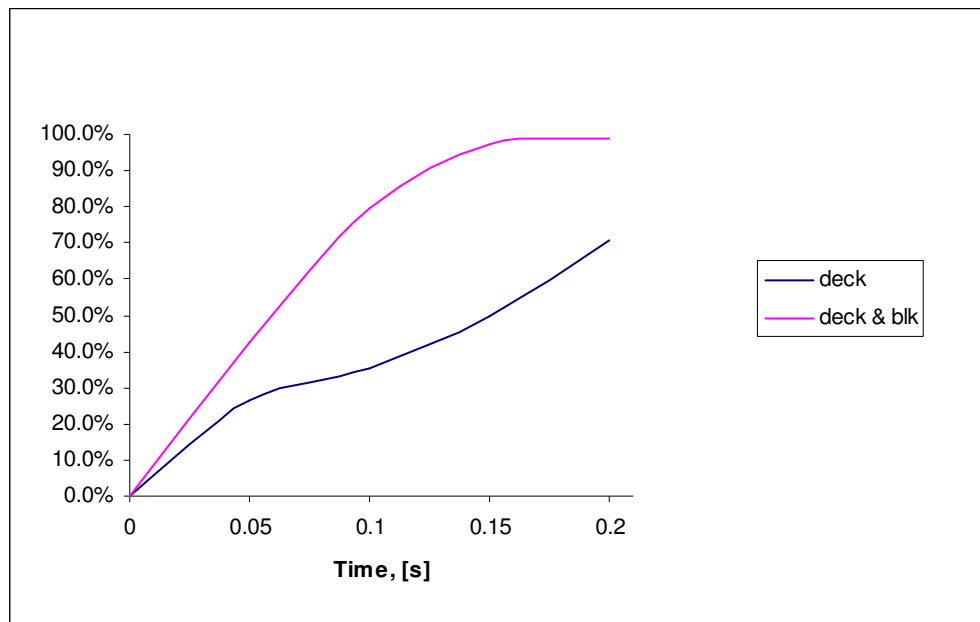


Figure 5.11: Percentage of kinetic energy loss in the vicinity of major structural elements like decks and bulkheads

As will be demonstrated in the case studies of Chapter 7, consideration of this effect is only important for ships with high level of subdivision. In the case of the tanker vessel, the contribution of transverse bulkheads is totally ignored due to the large span of uniform double hull stiffened panels. The areas of immediate effect of bulkheads are restricted in relation to the exposed area of the vessel, thus the probability of accepting a strike there is very small.

However, the case of the ROPAX vessel is approached in a different manner due to the uniformity of the structural arrangement up to bulkhead deck (13.50 m above base line). The effective plating of decks and bulkheads is considered to be twice the web height of stiffened frames in the particular area. This choice is justified by the FE model presented in Figure 5.12 and the graph of Figure 5.13. The configuration of the FE model is the same as previously but without the bulkhead. The simulations were repeated for four different deck spans and indicate that the deck plating with span more than 0.5 m has small effect in kinetic energy absorption.

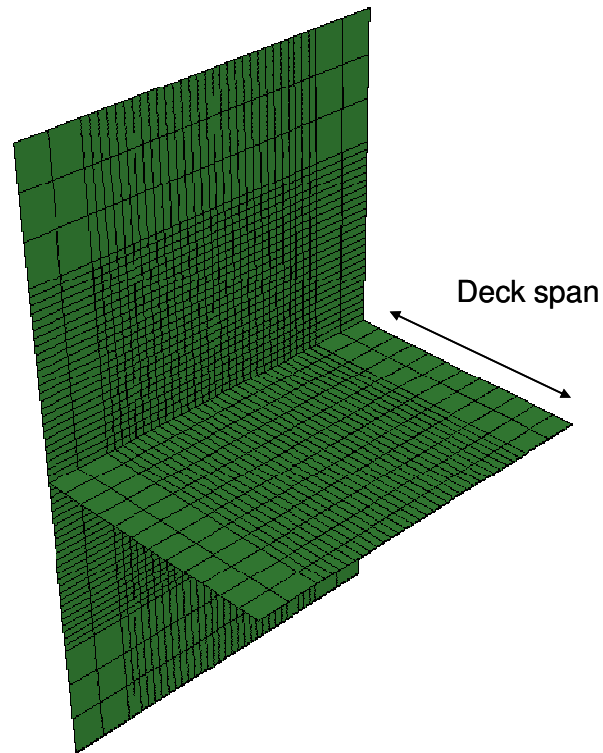


Figure 5.12: A simplified FE model to demonstrate the effect of various spans of deck in the stiffening capacity of the plating

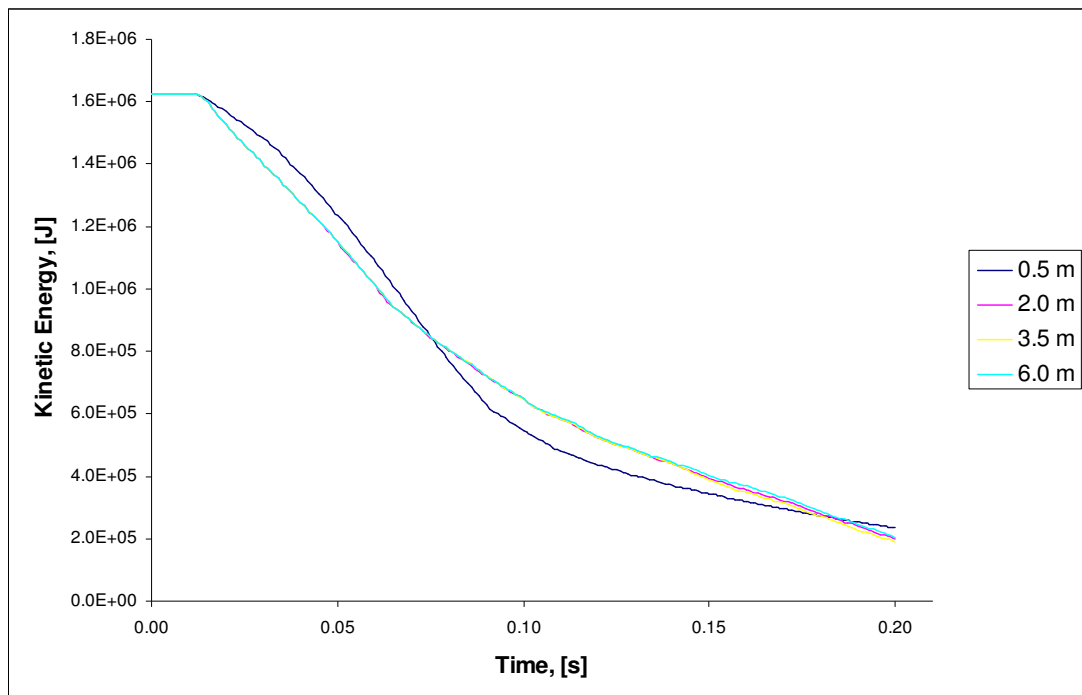


Figure 5.13: Kinetic energy loss for various deck spans

Large deflections

The ideas discussed earlier for the deformation function w of the struck panel are repeated here for functions u and v . The purpose is to capture the deformation of the panel along its initially straight edges. Both functions have to be real, continuous and differentiable within closed intervals. Additionally, they should include indentation of the plate as an independent variable and they should be *tuned* by the stiffness of the panel in their respective direction. The general form of the deformation functions u , v and w included is:

$$\begin{aligned} u(x, y, w_0) &= (D_x)^c \frac{w_0}{\left(1 + \left(\frac{x}{r_1}\right)^2\right)}, & v(x, y, w_0) &= (D_y)^c \frac{w_0}{\left(1 + \left(\frac{y}{r_2}\right)^2\right)} \\ w(x, y, w_0) &= \left(\frac{D_x + D_y}{2}\right)^c \frac{w_0}{\left(1 + \left(\frac{x}{r_1}\right)^2 + \left(\frac{y}{r_2}\right)^2\right)} \end{aligned} \quad (5.11)$$

where

- r_1 and r_2 are the principle radii of curvature of the striking surface
- c is the deflection exponent (see Section 5.8)

The different level of stiffening along the x and y -directions is considered in the function w by taking into account the proportional contribution of D_x and D_y rigidities.

Considering the geometry for large deflections described in Figure 5.14, the strain ϵ_x of the plate element dx can be approximated as follows.

$$\epsilon_x = \frac{u + \frac{\partial u}{\partial x} dx - u}{dx} + \frac{\sqrt{(dx)^2 + \left(\frac{\partial w}{\partial x} dx\right)^2} - dx}{dx} = \frac{\partial u}{\partial x} + \left[\sqrt{1 + \left(\frac{\partial w}{\partial x}\right)^2} - 1 \right] = \frac{\partial u}{\partial x} + \frac{1}{2} \left(\frac{\partial w}{\partial x}\right)^2 \quad (5.12)$$

The same idea applies for ϵ_y and γ_{xy} , as summarised in the following:

$$\begin{aligned}\epsilon_x &= \frac{\partial u}{\partial x} + \frac{1}{2} \left(\frac{\partial w}{\partial x} \right)^2 \\ \epsilon_y &= \frac{\partial v}{\partial y} + \frac{1}{2} \left(\frac{\partial w}{\partial y} \right)^2 \\ \gamma_{xy} &= \frac{\partial u}{\partial y} + \frac{\partial v}{\partial x} + \frac{\partial w}{\partial x} \frac{\partial w}{\partial y}\end{aligned}\quad (5.13)$$

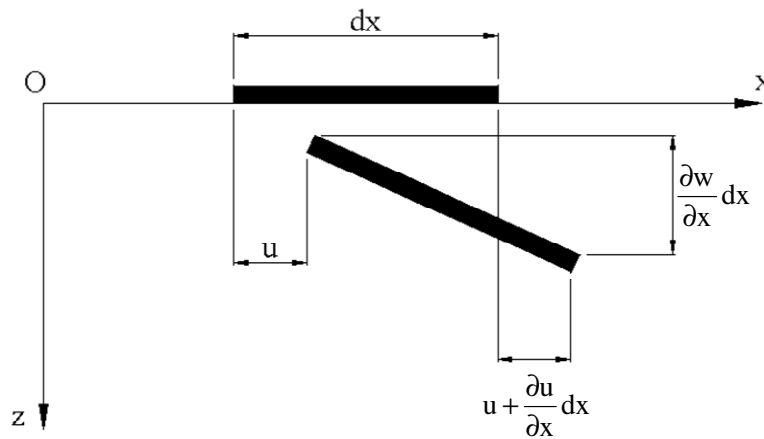


Figure 5.14: Large deflections of a plate element, (Timoshenko & Woinowski-Kreiger, 1964)

Membrane forces

Because of the large deformations experienced by the stiffened panel (before plate tearing), the character of the plating is changing and it starts to behave like a membrane, (Hartog, 1952). The accumulated strain energy due to action of the membrane forces is expressed as:

$$V_{\text{mem}}(w_0) = \frac{1}{2} \int_0^L \int_0^B [N_x \epsilon_x + N_y \epsilon_y + N_{xy} \gamma_{xy}] dy dx \quad (5.14)$$

N_x , N_y and N_{xy} are forces per unit length of the plate edge and ϵ_x , ϵ_y and γ_{xy} are the corresponding strains.

Estimation of the membrane forces is performed by considering the Airy stress function definition as it is discussed in (Timoshenko & Woinowski-Kreiger, 1964) and (Fung, 1965). A simplification of this process is proposed in (Hughes, 1995). That is, assuming that the membrane forces are constant along the faces of a plate

element, then by modification of the Hooke's law for normal stress the following expression can be obtained:

$$\begin{aligned}
 N_x(w_0) &= \frac{Et}{2B} \int_0^B \epsilon_y dy \\
 N_y(w_0) &= \frac{Et}{2L} \int_0^L \epsilon_x dx \\
 N_{xy}(w_0) &= \frac{Gt}{\sqrt{L^2 + B^2}} \int_0^L \int_0^B \frac{\partial w}{\partial x} \frac{\partial w}{\partial y} dy dx
 \end{aligned} \tag{5.15}$$

As before, L and B are the length and breadth of the struck panel, respectively, and t is the plating thickness. Because of the nature of the rupture criterion that will be introduced in Section 5.5, the effective plating thickness (accounting for longitudinal and transverse stiffeners) is used in these calculations as it is documented by various authors like (Paik & Wierzbicki, 1997), (Sajdak & Brown, 2004), etc.

Total strain energy

The overall strain energy will be expressed as the combination of Equations (5.8) and (5.14). The important feature of this formulation is the fact that the membrane energy dominates in magnitude over the bending strain energy of the panel in large deflections. This is not a surprising result and it is well covered in the literature since the plate is always the first element that completely fails under extreme loading. In the proposed approach this feature is of additional interest since it signifies the deflection beyond which the watertight integrity of the structure is compromised. For this reason both components of energy are retained in the formulations to account for collision events where the struck panel deforms without rupturing or where rupturing and deep penetration occurs.

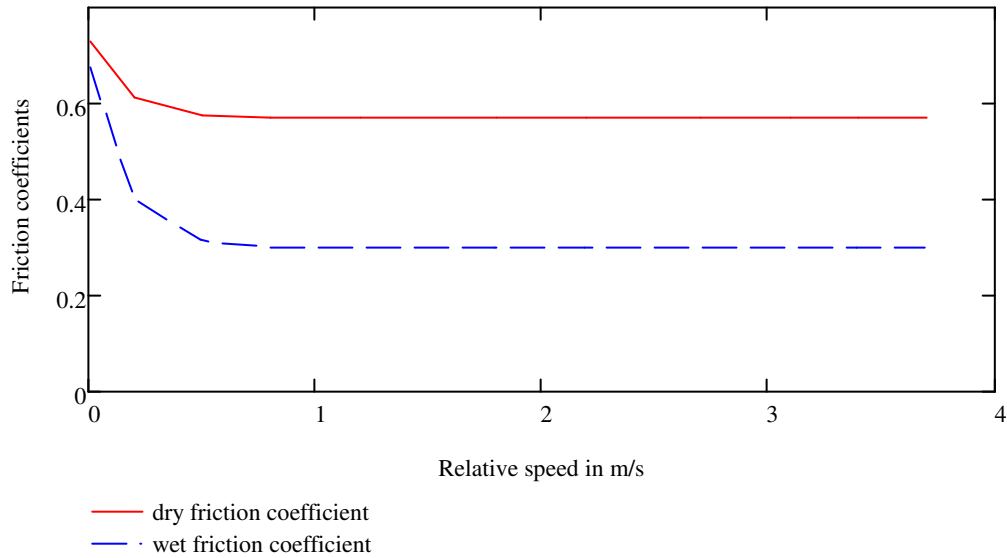


Figure 5.15: Comparison of wet and dry friction coefficients as a function of relative speed between the two bodies in contact

Friction considerations

A final point regarding inelastic deformation and rupture of the side shell is the friction between the struck and striking bodies. This highly ambiguous quantity has not received adequate attention in the literature related to ship-ship collisions and explicit formulations are very rare. In the theoretical manual of LS-DYNA Coulomb friction coefficient is expressed as:

$$\mu_c = \mu_d + (\mu_s - \mu_d) \exp(-c|v|) \quad (5.16)$$

where

- μ_c : Coulomb friction coefficient
- μ_d : dynamic friction coefficient
- μ_s : static friction coefficient
- c : exponential decay constant
- v : relative velocity between colliding bodies

In (Hallquist, 1998) it is recommended to use $\mu_d = 0.57$ and $\mu_s = 0.74$ for dry friction of mild steel on mild steel. The exponential decay coefficient is taken equal to 7.0. Moreover, in (Sajdak & Brown, 2004) it is mentioned that the average values from

the literature for wet friction are $\mu_d = 0.30$ and $\mu_s = 0.70$. The graph in Figure 5.15 presents the difference in estimation of friction coefficient as a function of relative speed when either set of values is used. It becomes immediately obvious that only for small values of relative speed the variation of friction coefficients becomes important.

This issue has been discussed further in (Simonsen & Wierzbicki, 1997), (Pedersen & Zhang, 1998) and in (Cox et al., 2005) as a dominant feature of dynamic fracture, yet it remains one of the least understood aspects of material behaviour. Estimation of the part of the kinetic energy that is transformed into heat can be obtained by crossing in the area of irreversible thermodynamics, (Chaboche, 2003). In this study, friction is modelled as a reduction factor of the available kinetic energy. The values for dry and wet friction are 0.30 and 0.57, respectively.

5.5 Rupture energy

Existing approaches

The most ambiguous parameter that defines the crashworthiness of the side shell structure is the size of deflection before rupture when it is expressed as a function of its stiffening configuration and the geometry of the striking body. The current approach in FE analyses is to take into account the rupture strain of the fabrication material of the struck panel. This information is usually obtained from simplified laboratory experiments of steel specimens subjected to tensile loading.

Even though this approach has scientific reasoning, the well-controlled variables of the loading of a cylindrical specimen have little correlation with the actual loading of a stiffened panel and even less with the response of the panel under collision loading. As a result the failure strain parameter used in FE analyses is open to interpretation and wide variation (Figure 5.16) and it is usually considered in conjunction with the size of the elements used in each study. This approach is very subjective and it is based on the availability of experimental data for the calibration of FE models. In (Zhang et al., 2004) it is stressed that FE results can be misleading if the wrong failure strain is used.

Quite evidently, one extra dimension of uncertainty is created, which results in the very narrow band of application of each study. Explicit selection of rupture strain and element size (in addition to a wide range of other parameters) is inherent in FE analyses or other simplified methods. This fact, in combination with the detailed structural description and the large number of elements, which increases the computational time substantially, are required for meaningful results but make the method prohibitive for application in a risk-based design context.

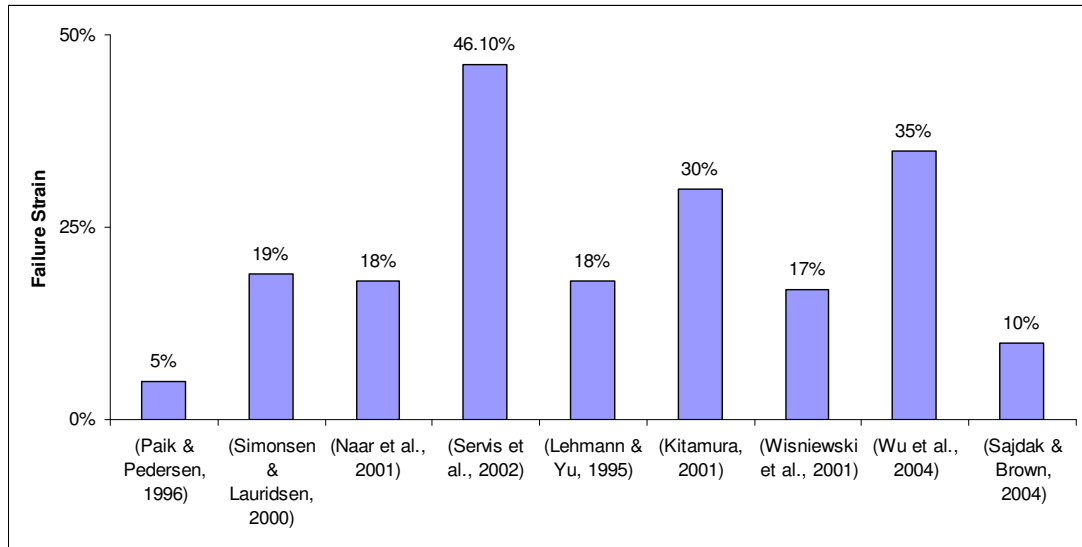


Figure 5.16: Failure strain variation in various FE studies

The effect of rupture strain on the failure pattern of a piece of plating can be demonstrated with the FE model used in the above discussion (Figure 5.10) but without any stiffening: this time the objective is to demonstrate the comparative response of the plating for failure strains of 0.1, 0.2 and 0.3. The kinetic energy absorption for the three cases is presented in Figure 5.17. The variation in response is becoming immediately obvious for strain of 0.1 compared to the other two values. When the failure strain is set to 0.3, the plate becomes very stiff and the striking sphere starts to bounce in the opposite direction. Quite evidently, no plate rupture is observed for failure strains of 0.2 and 0.3. It should be stressed, however, that the size of the elements is retained the same for all three simulations. The significance of this factor is out of the scope of this study and it is not investigated further. More detailed discussion can be found in (Sajdak & Brown, 2004).

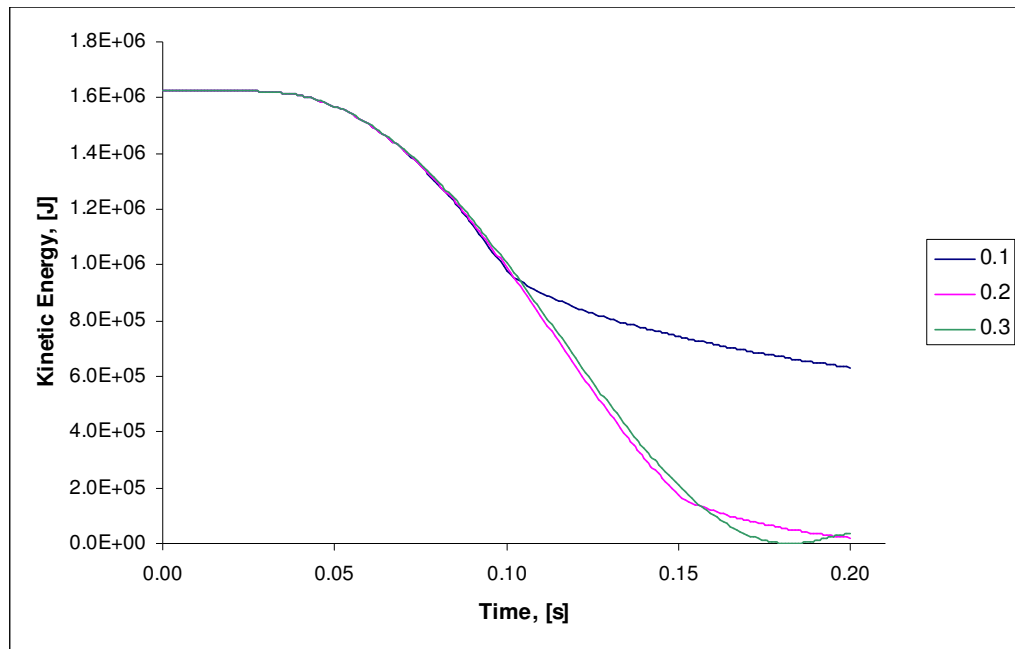


Figure 5.17: Kinetic energy dissipation for deferring failure strains

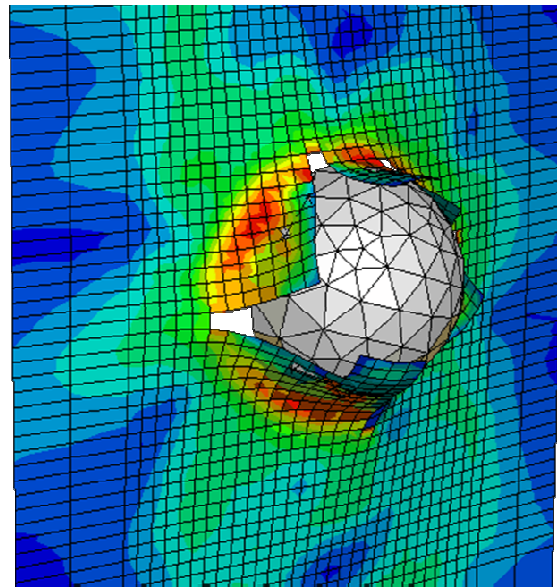


Figure 5.18: Plate rupture for 0.1 failure strain

In contrast to FE modelling and analyses, there are very few experimental results regarding stiffened plates under extreme loading applied in low speeds (otherwise ballistic behaviour should be considered, which falls outside the scope of the current work) in relation to the data available for beams or plain plates. The reasoning behind such a gap can be attributed collectively to the very complicated nature in

which a stiffened panel deforms, buckles and collapses. Inadequate theoretical formulation for such extreme response indicates that experimental approaches are lacking consistency in their execution as the important parameters are overlooked or are not highlighted adequately. As a result, the information acquired during experiments cannot be utilised in practical applications and design. That is, either the tests are too simplified or major characteristics that affect the response of the panel are not examined in depth. For example in (Wang et al, 2000) only the size of the indenter and the location of initial contact are systematically varied (e.g. on the crossing of two stiffeners or between two successive stiffeners). It would be extremely fruitful to repeat these experiments for a series of panels of different scantlings and structural arrangements and therefore associate the rupture deformation to a series of external (e.g. speed) and internal parameters (scantlings, material, etc.) simultaneously.

All these difficulties indicate clearly the need for analytical models for the early design process, which are founded on the global response of the side shell panel rather than on the response of its individual components. Assessment of the total strain energy content of a panel before and after rupture facilitates the calculation of the breach size and the penetration depth of the struck vessel. Nevertheless, the critical rupture energy is still largely unknown, which needs further exploration with support from materials science in combination with high level mathematical modelling and experimental verification.

Rupture criterion

The work performed in (Jones & Birch, 2006) is a good vantage point for addressing this issue in the current context of crashworthiness assessment. The rupture energy is provided as a non-dimensional parameter Ω which combines the material properties and geometrical configuration of the panel, the available kinetic energy and the geometry of the indenter.

$$\Omega = \frac{0.5GV^2}{\sigma_y t^3} = \frac{\pi d}{2 t} + 2 \left(\frac{d}{t} \right)^{1.53} \left(\frac{S}{d} \right)^{0.21} \quad (5.17)$$

Where,

- Ω : dimensionless perforation energy
- G : mass of the impacting body (i.e. the displacement of the striking ship)
- V : the striking speed
- σ_y : the yield stress of the plating
- t : the thickness of the plating
- d : diameter of the striking body
- S : span of the panel

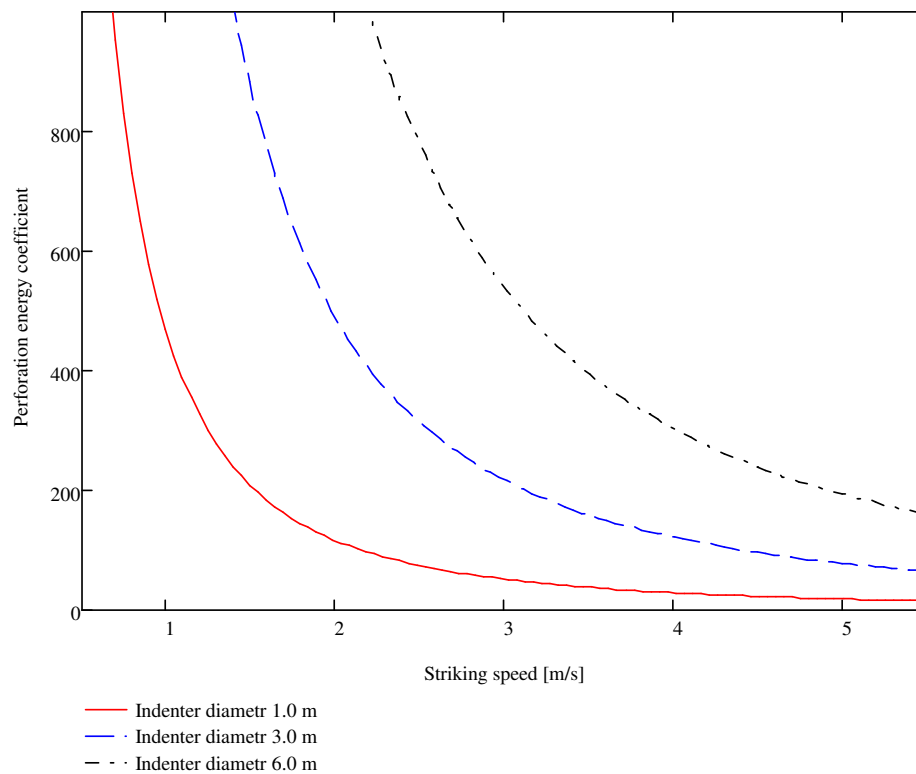


Figure 5.19: Perforation coefficient according to the model suggested by (Jones & Birch, 2006)

The derivation of this equation is based on a series of experiments with clamped circular plates (2 to 8 mm thick) and blunt striking bodies at maximum speed of 13 m/s. Careful consideration of these factors demonstrates the shortcomings of Equation (5.17) and at the same time opens the way for more detailed experimental investigation. For example, stiffening, scaling issues and energy loss due to friction

are not included in the model. Despite these shortcomings, the model is deployed in the current analysis since it incorporates consistently geometrical information for the striking body (i.e. the sharper it is, the easier the panel will rupture) and its kinetic energy. Both of these aspects play a protagonist role in this research but it should be appreciated that further investigation on this topic is needed.

Figure 5.19 presents a numerical calculation of the perforation coefficient for a square plate of mild steel ($\sigma_y = 235$ MPa) with dimensions $4 \text{ m} \times 4 \text{ m}$ and thickness of 10 mm that is hit by a 3.5 tonne spherical body as a function of speed. The pronounced dependency of rupture energy on the striking body geometry and speed fully confirms the expectation that a sharper object possessing the same energy as a bluffer one will cause different extent of damage. This is the reason why the terms “high energy collision” and “low energy collision” can be very misleading. Without knowledge of the geometry of the striking body it is impossible to establish a picture of the expected damage.

5.6 The Penetration Potential

In order to establish a proper design criterion, which will indicate the crashworthiness capability of the side structure of a ship as a function of its operational profile, the concept of *Penetration Potential* is described here. The idea has been also introduced in (Mermiris & Vassalos, 2007a) and (Mermiris et al., 2007b).

If the ratio of the rupture energy (W_r) of the stiffened panel and the available kinetic energy (E_k) of the striking body is considered (taking into account the added mass and the friction), an index of the crashworthiness capacity of a stiffened panel can be established.

$$P_p = \frac{W_r}{E_k} \quad (5.18)$$

P_p is a positive real number and has a critical value of 1.0. That is,

- $0 < P_P < 1$: As long as the value of P_P is within this range, rupture will occur with various severance levels. As its value approaches zero, the available kinetic energy dominates and the panel ruptures easily.
- $P_P \geq 1$: In the opposite case, as P_P approaches 1.0, the panel can absorb a large portion of the available energy and the consequences further to the impact are minimised. For any value of P_P equal to or greater than 1.0 the panel can sustain the impact and suffer deformation only without compromising its watertightness.

The concept of the penetration potential is tightly connected to the seaways in which the ship will be chartered. In this way, the type and size of the vessels that it will encounter compose a rather definitive picture of its operational life. Similar to the variation of ship domain (Figure 4.3), which provides information for the *active* role of the ship in a waterway, the penetration potential establishes its *passive* character in case of collision and allows for the crashworthiness assessment (water ingress, cargo outflow, damage to internal machinery due to high penetration, etc.) of the side shell plating of various areas and compartments.

5.7 The calculation process

Application of the above models is included in a calculation process with well defined and explicit steps. There are two modes of calculation: (i) in *deterministic* mode the calculations are performed for a single collision scenario of a striking ship at certain speed and angle (Figure 5.20); (ii) in a *probabilistic* mode Monte Carlo (MC) simulation, (Vose, 2000), is performed for a selected number of parameters (Figure 5.21). A FORTRAN program (Crashworthiness Assessment for Early Design – *CRASED*) was developed for this purpose, the main steps of which are summarised in the following lines.

1. Analysis of the striking body surface and estimation of the principle radii of curvature. For any striking surface that is selected (sphere, elliptic paraboloid or Bezier surface) MC sampling of the main parameters can be performed.
2. Definition of the struck body geometry as an initially flat surface which progressively deforms according to the principle radii of curvature of the

striking body. The objective is to achieve a geometrical conformance between the two bodies and therefore capture critical characteristics of one body which define largely the development of the collision phenomenon (e.g. the sharpness of the indenter). The outcome of this step is the calculation of the deflection of the struck surface.

3. Calculation of the available kinetic energy (E_k) before the impact reduced to account for size and added mass effects. That is, estimation of the displacement of the striking vessel and its speed according to the operational profile of the vessel. Sampling for MC simulation is performed at this stage if a probabilistic approach is followed. All the heat losses are accounted for by multiplying E_k by a friction coefficient.
4. Establishment of the rupture energy (W_r) of the stiffened panel. The existing models capture all the relevant parameters involved in the phenomenon up to certain extend: the type and amount of stiffening of the plate cannot be readily expressed. As a result, for the current stage of development the *equivalent* plate thickness is used.
5. Comparison of the kinetic energy and the rupture energy of the panel reveal whether rupture of the plating will occur.
6. In case of breaching, calculation of breach size and penetration takes place. In the opposite case, calculation of denting of the struck panel follows. At this stage, scantlings and structural configuration are explicitly introduced in the process by calculating plate rigidities D , D_x , D_y and D_{xy} , as it is discussed in Section 5.4.
7. The calculation of the penetration potential provides a more general idea about the crashworthiness capacity of side shell for the selected operational profile. As expected, the value of P_p is only meaningful if the probabilistic mode of calculation is followed.

Calculation in a probabilistic mode allows for deeper appreciation of the response of the structure since it requires assessment in the most probable conditions that may be encountered. After all, the extreme loading explicitly considered in the majority of

studies may never occur, so there is no reason to over-design (i.e. design for the worst possible scenario) with this effect in mind. It is much more cost-effective and rational to consider only the most probable loading and if design constraints (weight, cost, etc.) allow it, then it is possible to expand further and cover a wider range of loadings and vulnerability scenarios.

Information about the operational profile of the new vessel will provide data regarding the type and size of the ships that will be encountered. In addition, it will highlight all the geographical restrictions which, in turn, imply speed limitations in various traffic routes. The clear picture that will be drawn in this way will improve the perception of collision risks in one or more waterways.

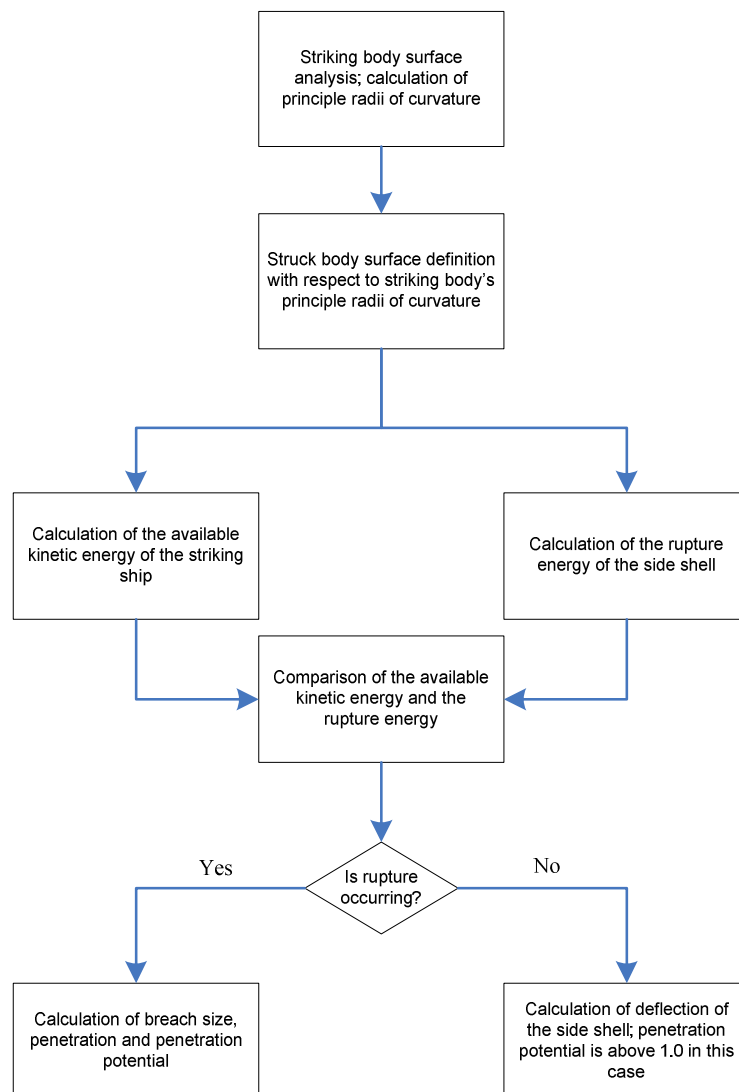


Figure 5.20: Deterministic algorithm of the process

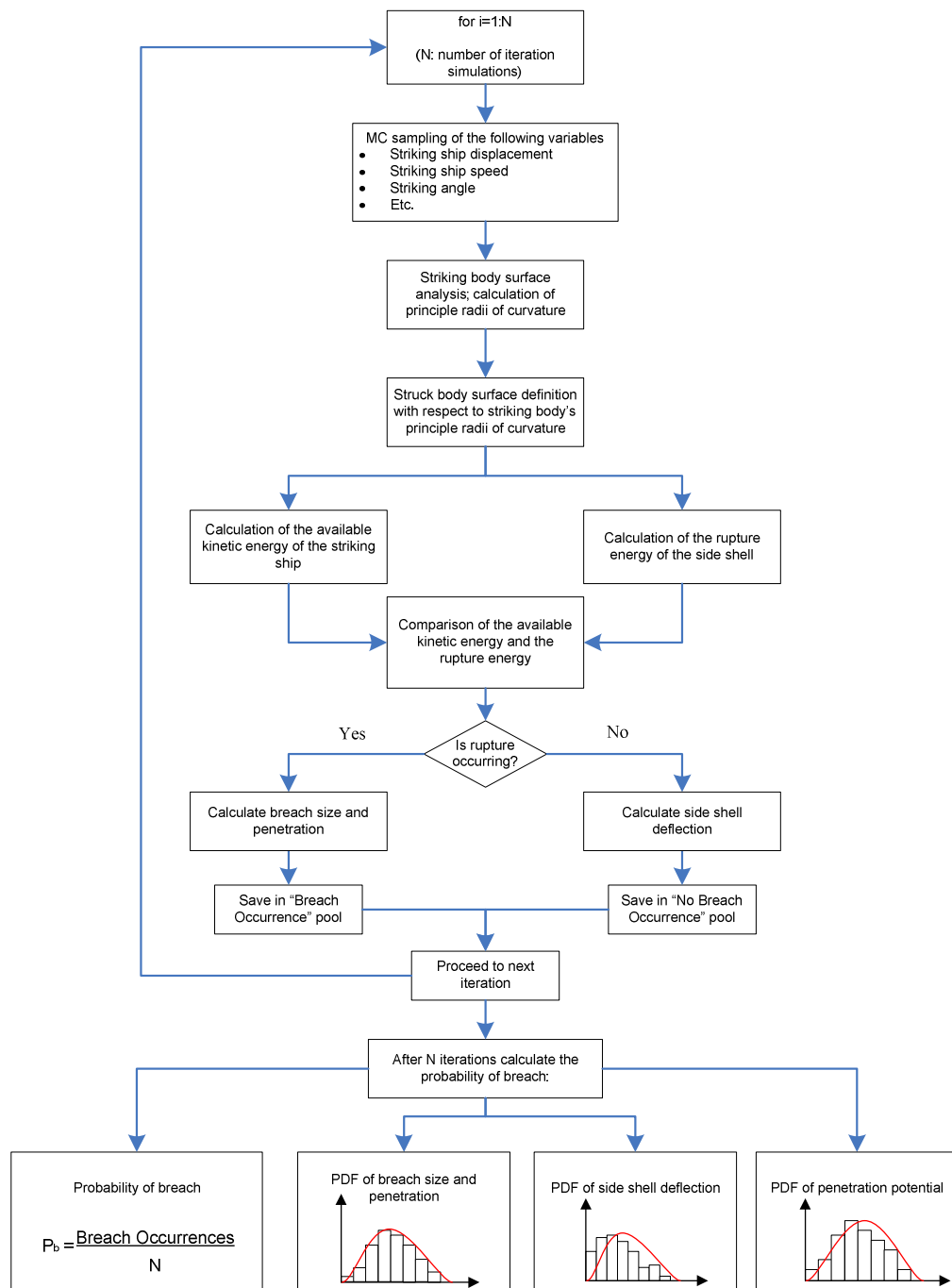


Figure 5.21: The probabilistic character of the process has generated substantially more input data for the design process

The following list provides some ideas regarding the way that some definitive parameters of the collision event can be consistently modelled in order to produce the required input for design definition and therefore to facilitate rational solutions:

- Displacement, speed and angle of striking ships according to expected traffic data and geographical restrictions;
- Geometrical information and variation of the stem and bulbous bow (based on existing statistical studies);
- Operational draught of own ship;
- etc.

In this way, the size of breach in a collision event is no longer expressed as a single number of certain square meters but as a *probability density function*, which provides information about the expected breach size and its variation according to the trading route of the ship. With this information available, the designer can proceed to the next stage and calculate the damage stability and survivability of the ship. If the results are not satisfactory alteration of stability characteristics and / or structural re-assessment of the side shell can follow. This exercise may include simple increase in scantlings or selection of alternative structural arrangements like the one presented in Figure 3.4. In any case, the tool for a more rational multi-objective / multi-criteria optimisation process is now available and can be used alongside other analytical (parametric) tools in a risk-based ship design process.

5.8 Comparison with HARDER results

In the course of the HARDER project, the crashworthiness assessment was based on the extensive survey of past accident data. Under the consideration that the damage extent following a ship-ship collision can be defined by the length, the height and the penetration of the damage opening, the consortium analysed the available data and presented it in statistical format. Figure 5.22 to Figure 5.24 present the available information along with the normal distribution fit currently used where appropriate. The damage length and the damage penetration are non-dimensionalised with the length and the breadth of the struck ship respectively.

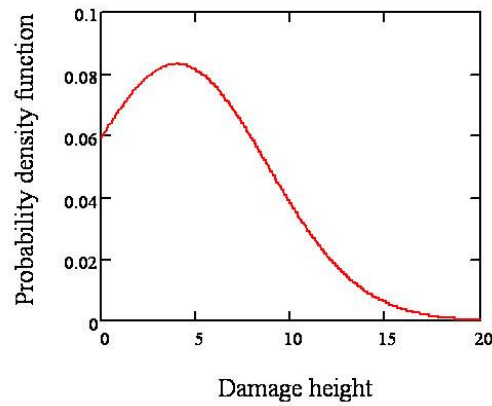


Figure 5.22: Probability density function for the vertical extent of damage with $\mu = 4.0\text{m}$ and $\sigma = 4.8\text{m}$, (Herbert Engineering, 2001)

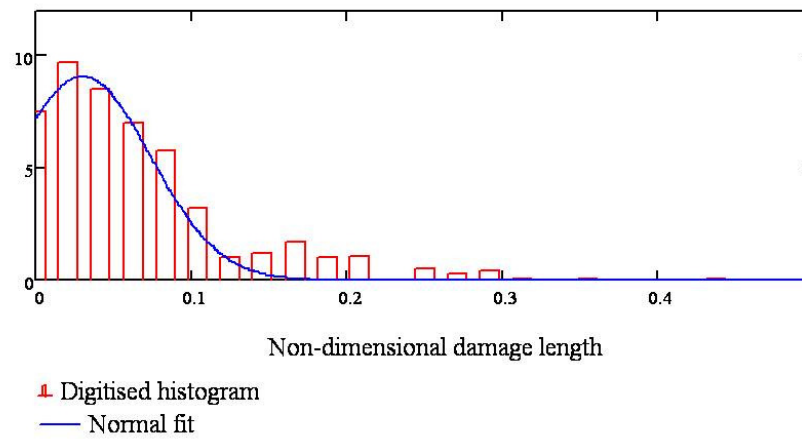


Figure 5.23: The non-dimensional damage length and the normal distribution fit with $\mu = 0.03$ and $\sigma = 0.0044$, (HARDER, 2001b)

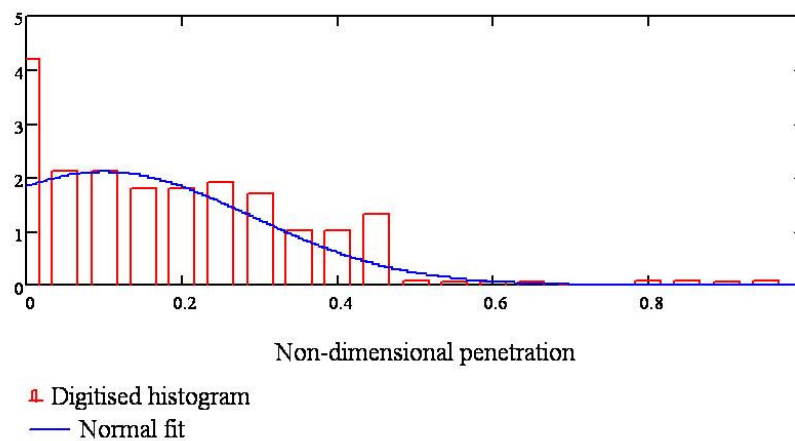


Figure 5.24: The non-dimensional damage penetration and the normal distribution fit with $\mu = 0.1$ and $\sigma = 0.19$, (HARDER, 2001b)

In order to compare the results obtained using the CRASED program with the statistical data from the HARDER project a MC simulation is conducted taking into consideration the three probability density functions discussed above. The objective is to express the damage length and height as a function of penetration. Following this, three ship-ship collision simulations were conducted with CRASED: (i) a ROPAX striking a ROPAX, (ii) a ROPAX striking a tanker, and (iii) a tanker striking a tanker. The main particulars of both ships are presented in Table 7.1. The MC simulation in CRASED is based on variation of striking speed and angle only (Table 5.1). The results of both MC processes are superimposed for comparison and presented in Figure 5.25, Figure 5.26 and Figure 5.27.

Monte Carlo parameters		Simulation 1: ROPAX on ROPAX	Simulation 2: ROPAX on tanker	Simulation 3: tanker on tanker
Striking speed	Mean value	15.0	28.0	14.0
	Standard deviation	5.0	5.0	5.0
Striking angle	Mean value	20.0	20.0	20.0
	Standard deviation	5.0	5.0	5.0

Table 5.1: The MC data for the three simulations with CRASED

It becomes apparent that as far as the study of ROPAX ships is concern, the obtained results with CRASED compare favourably with the statistical data obtained in HARDER. The study of tanker ships on the other hand presents serious disagreement with existing accident data. Such a result fully justifies the arguments made in previous chapters that drawing conclusions on dramatic events like ship-ship collisions based on past experience is an inherently inadequate approach. In the case where the database has limited or no information concerning the specific ship type and its general operational profile the results will be seriously impeded, and they will not reflect reality appropriately.

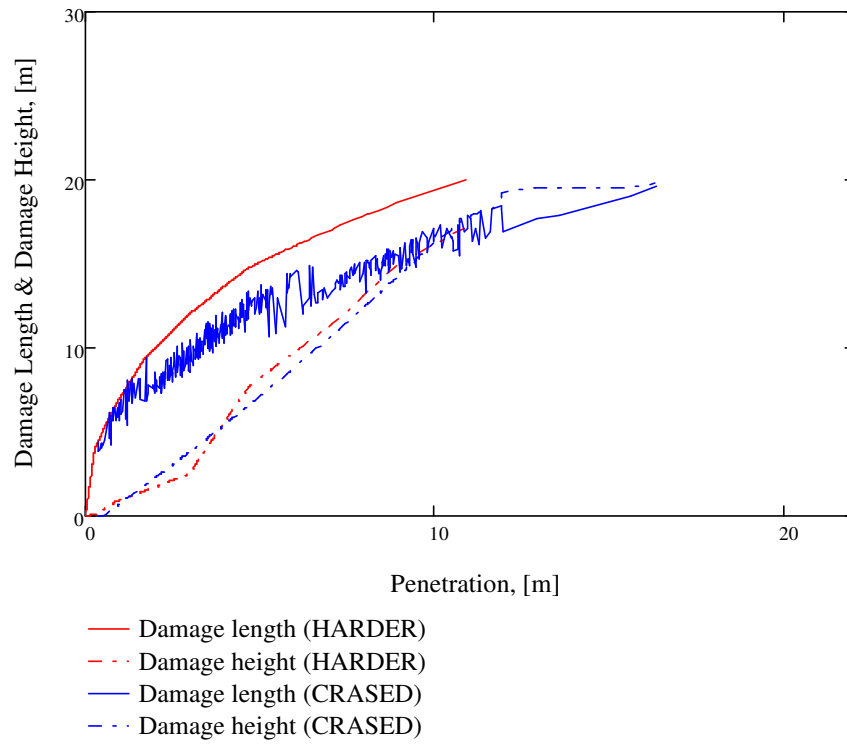


Figure 5.25: ROPAX on ROPAX (Simulation 1)

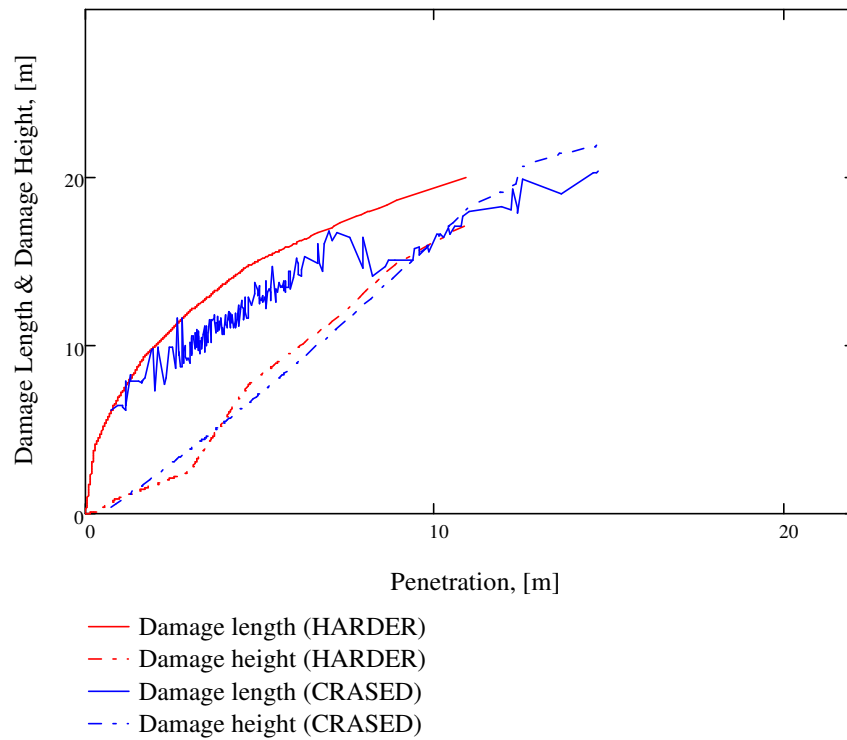


Figure 5.26: ROPAX on tanker (Simulation 2)

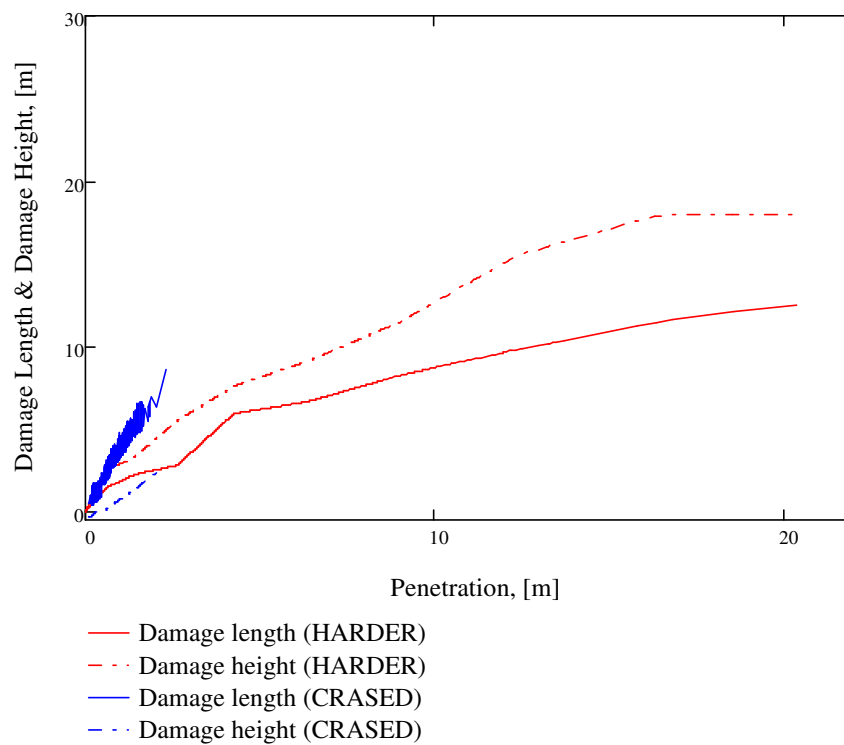


Figure 5.27: Tanker on tanker (Simulation 3)

Finally, it should be mentioned that HARDER curves of Figure 5.27 are not the same with the first two simulations due to different bow geometry of the tanker.

Sensitivity of the results

From a modelling point of view, the value of the exponent c , Equation (5.11), included in the functions u , v and w expressing the deformation of the struck panels plays an important role as to how susceptible these panels are to a striking incident. In order to investigate this effect further, a series of simulations are conducted for the case where a ROPAX collides with ROPAX. The reason for this choice is associated with the above discussion concerning initial agreement with the preliminary comparison of the CRASED results with those produced in the HARDER project. In the analysis, the values of the exponent vary between -0.10 and -0.01 . Indicative graphs for $c = -0.02$ and $c = -0.07$ are presented in Figure 5.28 and Figure 5.29 respectively.

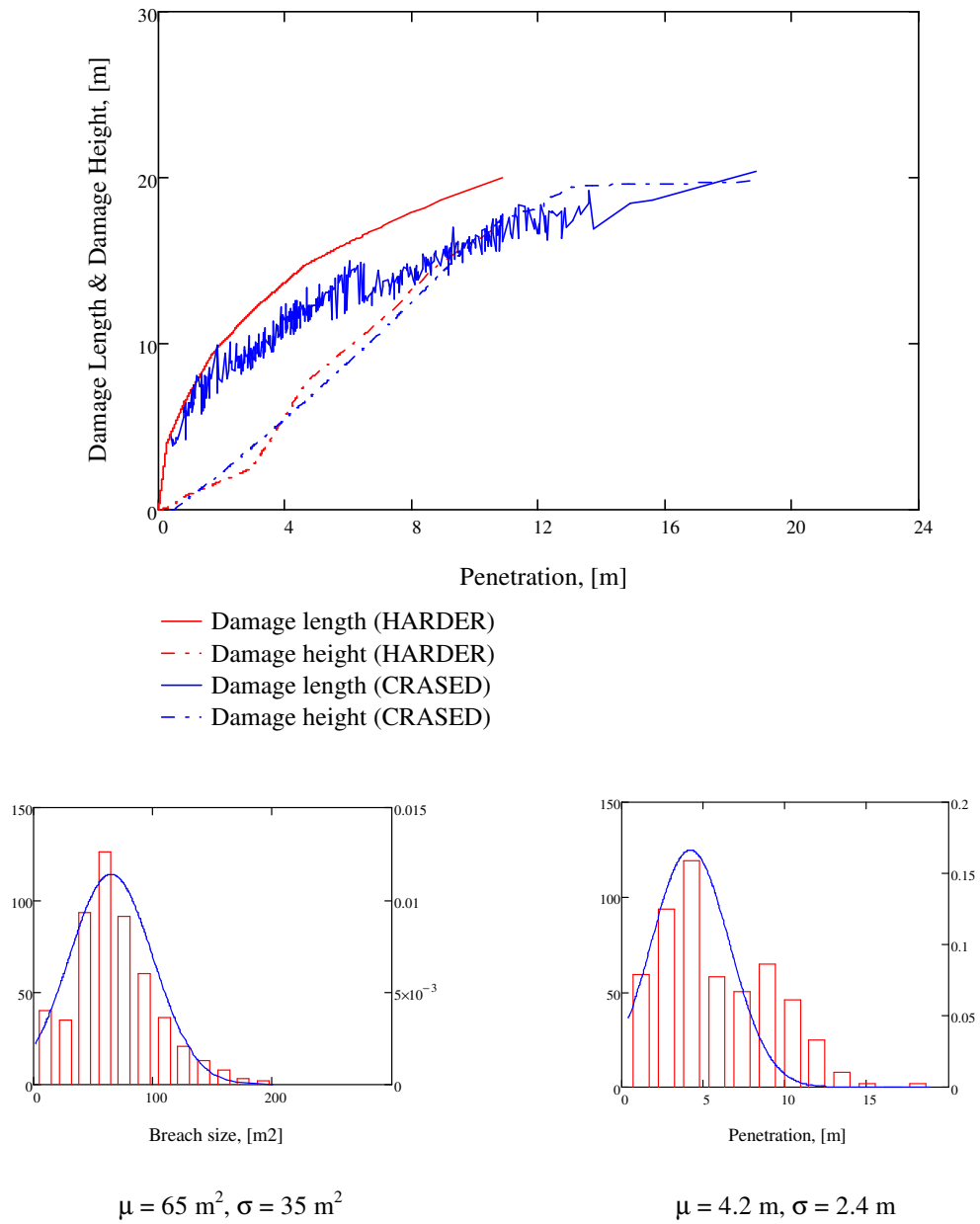


Figure 5.28: Simulated results for $c = -0.02$

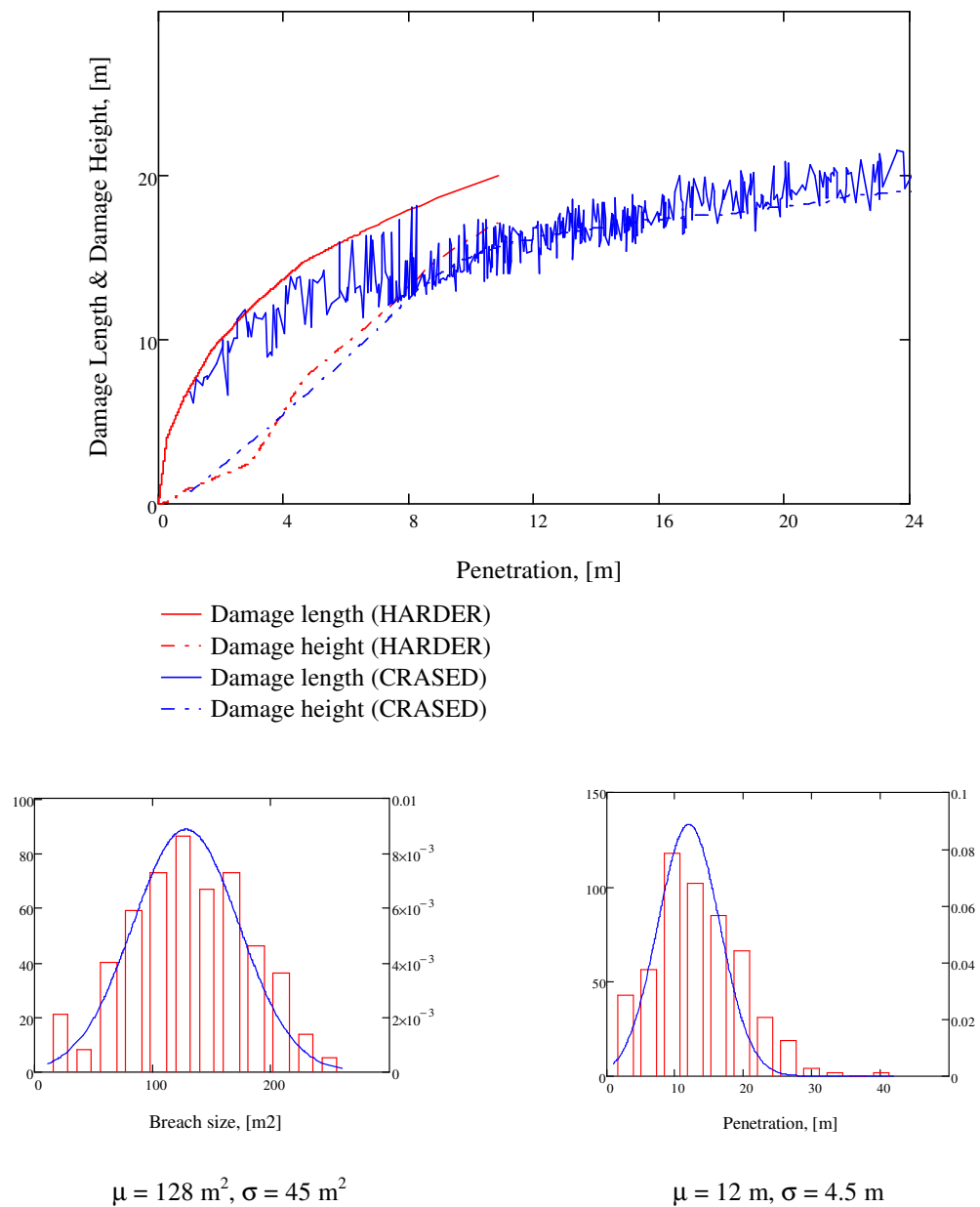


Figure 5.29: Simulation results for $c = -0.07$

The more negative the value of the exponent c is the “softer” the response (deformation and penetration) of the side shell is. This is demonstrated by the probability density functions for the breach area and the penetration in the two cases. In order to establish a more appropriate value for the exponent c , a sensitivity analysis was conducted. Systematic variation of c value indicated that as its value decreases, the probability of water ingress converges to the value of 0.526, (Figure 5.30).

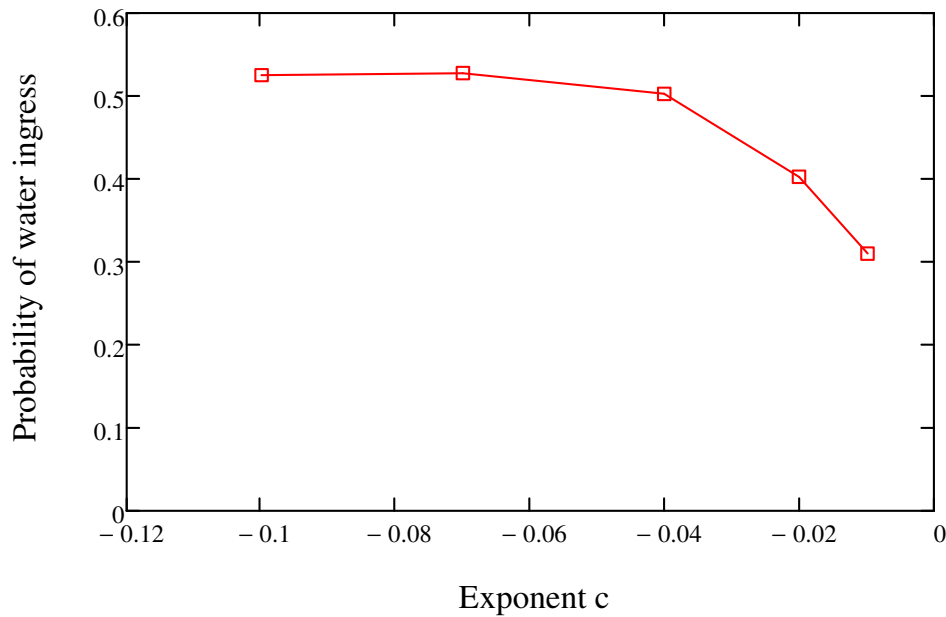


Figure 5.30: The probability of water ingress is converging to 0.526 as the value of the exponent c becomes more negative.

As mentioned earlier, the most critical parameter in the recreation or simulation of a ship-ship collision event is the identification of the rupture strain of a stiffened panel under extreme loading. Lack of this information highlights another important issue: even if statistical results like those obtained in the HARDER project are available, the exact nature of the collision development is still unknown. Statistical information of past accidents can only be used for general guidance and tendency identification in a risk-based design or general risk analysis context.

5.9 Chapter summary

The topic of probability of water ingress due to collision is developed in this chapter. This property of the ship is directly associated with the structural configuration of the side shell. However, study of accident reports can clearly indicate that damage caused to the side shell is also a function of the bow geometry of the striking vessel. These two qualities are blended together through the expression of the principle radii of curvature of the striking body and the conformance of the deformation of the struck stiffened panel. An algorithm for the calculation of the deformation or the

breach size is presented, which can be easily modified to account for a probability distribution of the breach size and, when necessary, the penetration. The algorithm is implemented in program CRASED and it is validated with the statistical results obtained in the course of the HARDER project. The algorithm is based on the notion of deformation of the side panels rather than their rupture strain due to the large uncertainty associated with this quantity. More research is needed towards this direction in order to obtain more meaningful and consistent results when FEA or simplified approaches are deployed for crashworthiness assessment. The proposed model can be deployed in multi-objective / multi-criteria optimisation routines (alongside other parametric tools), which can improve the exploration of the design space and facilitate creativity and innovation.

6 The proposed methodology

6.1 Introduction

Following the introduction of the models for the prediction of the probability of collision and the probability of water ingress due to collision, this chapter in consolidates the findings in a new methodology for the rational calculation of the pre-requisite conditions for the assessment of the survivability of a ship following a collision event. Moreover, the contribution of the methodology will be highlighted with a succinct presentation and discussion of various weaknesses of the existing regulatory framework.

6.2 The existing regulatory framework

The assessment of the risk level following a ship-ship collision event is presently performed according to Wendel's probabilistic approach, (Wendel, 1960), which is practically implemented with the attained index of subdivision A:

$$A = \sum_{j=1}^J \sum_{i=1}^I w_j p_i s_i \quad (6.1)$$

Where

j: the counter for loading conditions

i: the counter for damaged compartments or groups of adjacent compartments

J: the number of loading conditions under consideration

I: the number of damaged cases under consideration for each loading condition; each damage case is comprised of a single compartment or a group of adjacent compartments in combinations of two, three, etc.

w_j: probability mass function of the loading conditions

p_i: probability mass function of flooding extent of a compartment or group of compartments for loading condition j; the sum of all probabilities should be equal to 1.0

s_i: the average probability of surviving the flooding of a compartment (or group of compartments), for loading condition j.

Index A is the expected value of the probability of survival (weighted average), E(s), of all damage cases for a ship. As long as the value of index A is greater than a prescribed threshold value (index R), the safety level of the ship is considered satisfactory, (IMO, 2004), at least from a regulatory point of view.

In the context of this project, the point of interest is the calculation of the p-factor, which, as explained above, in the current probabilistic regulatory framework it is obtained by examining all possible combinations of flooding extents as derived from distributions of statistical damages. This approach implies that a compartment or a

group of adjacent compartments has been hit during a collision event and that the side shell structure is totally removed (i.e. it has not sustained the collision) thus allowing the compartment to be instantly flooded.

6.3 Weaknesses of the existing framework

The philosophy of the current regulatory framework appears to be quite attractive (primarily because it is founded on probability theory) and special (as few precedent frameworks, if any, have ever adopted a similar approach). However, the framework is based on statistical analysis of a large number of accidents and related scenarios, and entails the assumption that a collision has occurred and a compartment is flooded. In this way, the prescribed assessment becomes a vulnerability analysis and its emphasis is redirected on the mitigation of a series of unwanted events (worst case scenarios) rather than on the assessment of the most probable scenario and its prevention. Closer consideration of the provisions of the framework will reveal that it suffers from determinism and inconsistency, as it is explained next:

- (i) The calculation of the p-factor is conditional on the probability of collision occurrence. That is, according to Equation (3.1), $P_c = 1.0$. However, even in the most congested waters collisions do not occur as often as expected. Modern communication means and information technology developments in combination with improved training of the navigation officers contribute significantly towards the reduction of collision accidents.
- (ii) The calculation of the p-factor is also conditional on the probability of water ingress, i.e. the outer shell breach and the penetration are of sufficient size to cause large scale flooding of one or more compartments instantly. Once more, the extreme case of $P_{w/c} = 1.0$ is considered. The fact that a collision occurs does not mean that the watertightness of the hull is lost. This can be attributed to a series of factors ranging between the manoeuvres of the involved ships the final moments before contact (i.e. variation of striking angle which can drastically alter the pattern of the indentation and tearing of plating), the loss of momentum of the

striking ship and the internal arrangement of the struck ship (e.g. with double-hull tankers the penetration in relation to the double-hull span should be considered before any conclusions about the severity of the situation are made). In numerous cases, a collision occurs but the overall damage is restricted to an extensive dent and paint removal. For the same reasons, even if the side shell is breached the size of the opening varies substantially and the creation of a breach of sufficient size that will lead to complete flooding of a compartment in very small time is very rare.

- (iii) The calculation of the p-factor is solely based on the geometry of the watertight subdivision of the struck ship. That is, (a) location of its transverse bulkheads, (b) number of longitudinal bulkheads, and (c) their offset from the outer shell, which represents a potential boundary of penetration and flooding extent. The structural characteristics of the side panel of each compartment (scantlings, stiffeners, presence of bulkheads or decks in the vicinity of collision, etc.), or group of compartments, are totally disregarded. The calculation process is based on past accident statistics and because the physical properties of the struck ship are ignored, the p-factor loses its probability content and becomes a weighting factor for the probability of survival (s-factor).
- (iv) The operational profile of the struck ship is of paramount importance for the calculation of the probability of collision and the probability of water ingress due to collision. In the first case, information for traffic density will indicate the level of congestion of a seaway and in the second case it will offer an estimation of the available kinetic energy and bow geometries that can compromise the side shell. In this way, two different ships (in terms of size and type), which operate in different geographical areas, will evidently experience different collision risk levels. Currently, the calculation of p-factor ignores the operational profile of a ship. This means that as long as the two ships have the same subdivision, their p-factor will remain the same.

Based on the above discussion, the level of assumptions in the calculation of the p-factor (one of the two basic ingredients of index A) renders the value of A questionable. More importantly though, index R is derived on the basis of a sufficient number of A-values of ships that have survived the elements over their life-cycle and represents an acceptable level of safety standard (HARDER, 2003). But if R is based on the values of A, and A carries a substantial level of uncertainty, then the value of R is also uncertain and hence difficult to quantify!

Very little can be said following this conclusion except that the inconsistency of a regulatory framework with probabilistic origin and deterministic implementation (i.e. totally focusing on risk mitigation resulting from collision damages) naturally raises the question whether the real potential for the benefit of industry and the society at large is harvested. As such, unnecessary constraints are imposed on new ships (e.g. the definition of a large number of compartments, which increases production and operational cost due to extensive maintenance considerations) and new innovative features are excluded from the outset. In this way, ship design turns from a creative exercise into rule application in the regime of an infertile and mitigation-oriented regulatory framework.

6.4 The way forward

The various pitfalls in the calculation of index A and their impact on the level of operational ship safety are addressed with the methodology proposed in this thesis, which appoints a truly probabilistic character to the calculation of the p-factor.

Traditionally, the marine environment (in terms of wind, waves, etc.) in which a new ship would operate largely defined its design characteristics associated to hydrodynamic and structural performance. Concurrently to the imposed loading of the hull girder, the operational environment (in terms of geographical restrictions, congestion levels, information about the size, speed and direction of the surrounding traffic, etc.) can also provide information which until recently was of secondary or no importance during design. With this information readily available, the calculation of the p-factor can be rationalised, instead of being a weighting factor, as follows:

- (i) By the model presented in Ch. 4, the probability of collision (P_c) can be obtained according to a set of:
- operational parameters – channel width, traffic density and speed;
 - design parameters – ship length and time to advance to 90°;
 - entropy level of environmental conditions and human factors.

Probabilistic framework, (IMO, 2009)		New methodology
P_c - Probability of collision		
Input	N/A	<ul style="list-style-type: none"> ○ C: channel width ○ L: length of ship ○ V: speed of ship ○ R: response time ○ d: traffic density ○ H: entropy
Output	$P_c = 1.0$	$P_c = f(C, L, V, R, d, H)$ $0 \leq P_c \leq 1$
$P_{w/c}$ – Probability of water ingress due to collision		
Input	<ul style="list-style-type: none"> ○ L_s : subdivision length of ship ○ x_1: distance from the aft terminal of L_s to the aft end of the zone in question ○ x_2: distance from the aft terminal of L_s to the fore end of the zone in question ○ b: position of longitudinal bulkhead offset from outer shell 	<ul style="list-style-type: none"> ○ Information on surrounding traffic in terms of displacement, speed, draught and bow geometry ○ Radii of curvature of the bow geometry ○ Definition of zones under consideration (the grouping is not performed necessarily according to watertight compartments) ○ Stiffness values of the orthotropic side shell (D_x, D_y, D) for every zone ○ Rupture criterion for each stiffened panel ○ Friction coefficient (dry and wet) ○ Added mass coefficient in surge (striking ship) and sway (struck ship)
Output	<ul style="list-style-type: none"> ○ 1-compartment damage $p_i = p(x_1, x_2) [r(x_1, x_2, b_k) - r(x_1, x_2, b_{k-1})]$ ○ 2-compartment damage $p_i = p(x_1, x_{2j+1}) [r(x_1, x_{2j+1}, b_k) - r(x_1, x_{2j+1}, b_{k-1})]$ $- p(x_1, x_2) [r(x_1, x_2, b_k) - r(x_1, x_2, b_{k-1})]$ $- p(x_{1j+1}, x_{2j+1}) [r(x_{1j+1}, x_{2j+1}, b_k) - r(x_{1j+1}, x_{2j+1}, b_{k-1})]$ ○ 3 or more-compartment damage $p_i = p(x_1, x_{2j+n-1}) [r(x_1, x_{2j+n-1}, b_k) - r(x_1, x_{2j+n-1}, b_{k-1})]$ $- p(x_1, x_{2j+n-2}) [r(x_1, x_{2j+n-2}, b_k) - r(x_1, x_{2j+n-2}, b_{k-1})]$ $- p(x_{1j+1}, x_{2j+n-1}) [r(x_{1j+1}, x_{2j+n-1}, b_k) - r(x_{1j+1}, x_{2j+n-1}, b_{k-1})]$ 	<ul style="list-style-type: none"> ○ Probability density function for breach size per zone ○ Probability density function for penetration per zone ○ $0 \leq P_{w/c} \leq 1$

Table 6.1: Process comparison for the calculation of the p-factor

The design parameters are constant but the operational parameters can be expressed in a probabilistic manner. MC simulation will provide a sufficient number of ship domain diameters for a particular route, which in comparison to the ship length will deduce the probability of collision occurrence.

- (ii) By the model presented in Ch. 5, the probability of water ingress due to collision ($P_{w/c}$) can be obtained according to the displacement, speed and shape of the bow geometry of the striking ship, and the structural configuration (side shell scantlings and compartment location) and the displacement of the struck ship. The calculations between the striking bow and the indentation of the side shell are based on the radii of curvature of the former and the conformance of the latter. In this way, a sharp bow (small radii of curvature in one direction) with the same kinetic energy will breach the struck panels much easier than a bluff one and will penetrate deeper in the struck ship causing more extensive flooding. The output of the calculation is the breach size, the location of the damage and the penetration of the striking bow.

Putting the two elements of probability together (for a particular waterway or a set of routes) will provide a rational picture of the flooding probability and its extent due to collision and will highlight potential deficiencies (in structural arrangement and watertight subdivision) that need to be addressed at design level. In this way, the operational profile of a new ship and its physical properties are mutually contributing to the derivation of the ship-ship collision risk levels (Table 6.1). The proposed methodology not only provides an alternative approach to the existing regulations but also supports other strands of research and development, regulations, and design as it is explained next.

Survivability assessment

Currently, the capsize risk assessment is conducted in a rather fragmented way. That is, the probability of collision by a ship with a given operational profile is replaced by the estimation of collision frequency per ship-year for the ship type in question

followed by the calculation of consequences, (Vassalos, 2009). The former element is based on worldwide statistics and the number of ships exposed to collision events. Naturally, the assumption is related to the generalisation of the estimation of the probability of collision from global data to a certain geographical area. In the latter case, the hypothetical collision event has created a damage the size of which is obtained from statistical analyses conducted in (HARDER, 2001b).

Safe-return-to-port

The idea of the safe-return-to-port has recently been introduced by IMO (SLF 47, 2003): following a flooding (and/or fire) incident a passenger ship should be able to stay afloat and return by its own means to safe haven. The underlying philosophy of this approach is zero tolerance to loss of life, (Vassalos, 2007), and it can be achieved only if the ship can retain its floatability and stability, and its major onboard systems functional (power generation, power distribution, etc.). With the tools developed earlier, the crashworthiness of the side shell panels of the compartments containing critical systems can be readily assessed (i.e. their penetration potential should be greater or equal to 1.0) in early design stage and alternative arrangements or stiffening options can be examined.

Risk-based design and optimisation

Finally, the tools for the calculation of P_c and $P_{w/c}$ can be integrated in the risk-based design process and they can be readily deployed in multi objective / multi-criteria optimisation schemes, (Puisa et al., 2009). In this way, alongside the rest of the objective functions of the optimisation scheme (adequate stability, minimum resistance, etc.) the objective functions related to ship-ship collision risk can be formulated as follows:

- Minimisation of the probability of collision will be achieved when the ship domain diameter is greater than the ship length.

-
- Minimisation of the probability of water ingress due to collision will be achieved when the penetration potential is greater than or equal to 1.0.

6.5 Chapter summary

Following the presentation of the models for the probability of collision and the probability of water ingress due to collision, this chapter is used as the ground for consolidating the proposed methodology and for highlighting the contribution made in the field. The need for such contribution is explained over discussion on the pitfalls for the calculation of the p-factor in the existing regulatory framework (SOLAS II-1). The chapter closes with a short discussion on various applications of the proposed method.

7 Case studies

7.1 Introduction

The focus of this chapter is to demonstrate the applicability of the proposed methodology comprising the probability of collision and the probability of water ingress due to collision. For this purpose a ROPAX and a double-hull tanker will be used for two case studies in the Dover Strait. One additional case study will be presented for the assessment of a stiffened panel with Y-shaped stiffeners and another one will focus on a design application for cost minimisation. The final case study is a comparison between the proposed methodology and the calculation of (i) the p-factor as it performed in the SOLAS 2009 and (ii) the current risk analysis of flooding accidents.

7.2 Vessel particulars

The particulars of both vessels are summarised in Table 7.1. Additionally, midship sections and profile plans are included in Appendix C.

ROPAX		Tanker	
LOA	168.00 m	LOA	213.00 m
Lpp	155.00 m	Lpp	205.00 m
B	24.00 m	B	37.00 m
T	5.80 m	T	12.80 m
D	16.50 m	D	19.00 m
V	19 kn	V	15.00 knots
Δ	16,500 tonne	Δ	78,000 tonne
No of passengers:	2,000	Crew	28
No of vehicles / lane metres	550 / 750	No of propellers	1
No of propellers	2	Type of propellers	CPP
Type of propellers	CPP	Propeller diameter	6.65 m
Propeller diameter	5.00 m	Main engine	12,250 kW
Main engines	4 × 5,350 kW	No of rudders	1
No of rudders	2	Lateral windage area	1,640 m ²
Lateral windage area	4,145 m ²	Transverse windage area	645 m ²
Transverse windage area	560 m ²	Double hull span	2.10 m

Table 7.1: Vessels' particulars

7.3 Site description and scenario definition

Implementation of the approach described in the previous chapters is performed for the Dover Strait, one of the busiest passages in Europe and probably the world. It is estimated that 120 vessels are transiting in the North-East lane and 175 in the SW totalling approximately 300 vessels per day. Additionally, there are about 120 daily ferry crossings between France and United Kingdom, (Squire, 2003). This creates a very dynamic environment where collision avoidance is a major concern of crews, operators and port authorities.

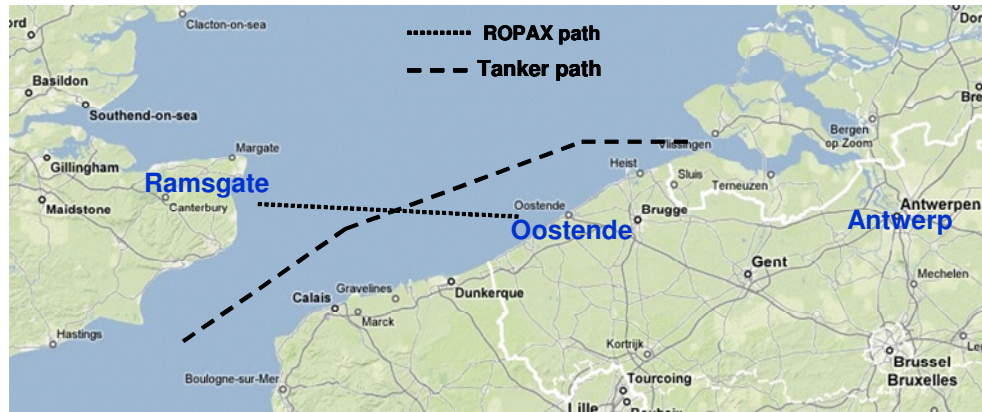


Figure 7.1: Geographical location for the case studies

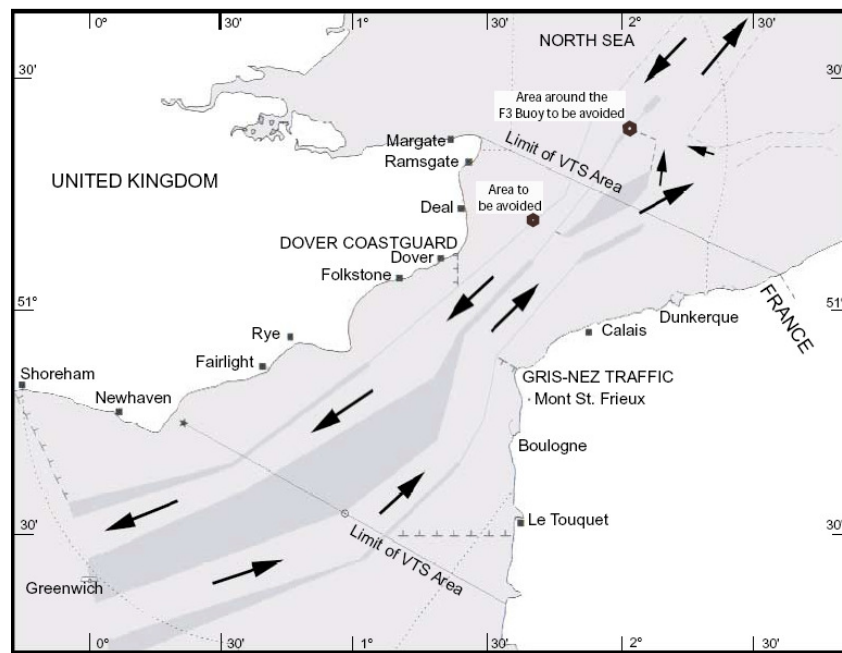


Figure 7.2: North-East and South-West lanes in the Dover Strait VTS area
<http://www.worldvtsguide.org/MenuPages/UKMenu/DoverStrait.html>

In this particular study, the ROPAX vessel crosses from Ramsgate to Oostende and the tanker vessel is following the NE lane of the Vessel Traffic System (VTS) in the area (Figure 7.1 and Figure 7.2) with destination the Antwerp terminal. The ferry travel duration is 4 hours and the distance approximately 56 nautical miles, which corresponds to an average speed for the ROPAX vessel of 14 knots. The travelling speed of the tanker is not exceeding 12 knots, which will allow it to travel relatively fast and with acceptable levels of safety.

The environmental conditions in the area in terms of wind speed, wind direction and wave height are presented in Figure 7.3 and Figure 7.4. The visibility levels are good in general with approximate 2-3% of thick fog occurrence on an annual basis (Figure 7.5).

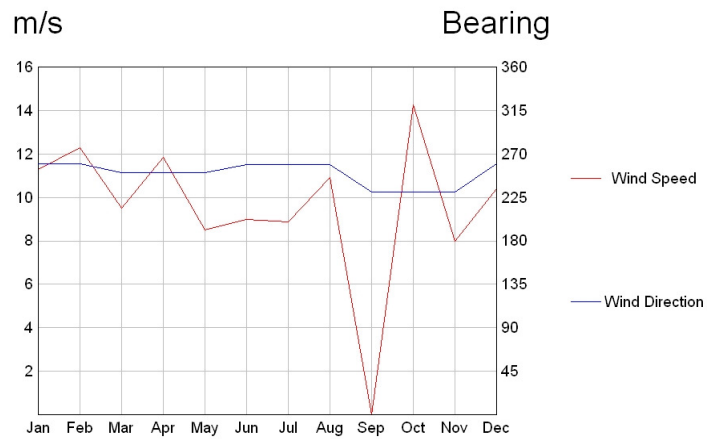


Figure 7.3: Wind speed and direction

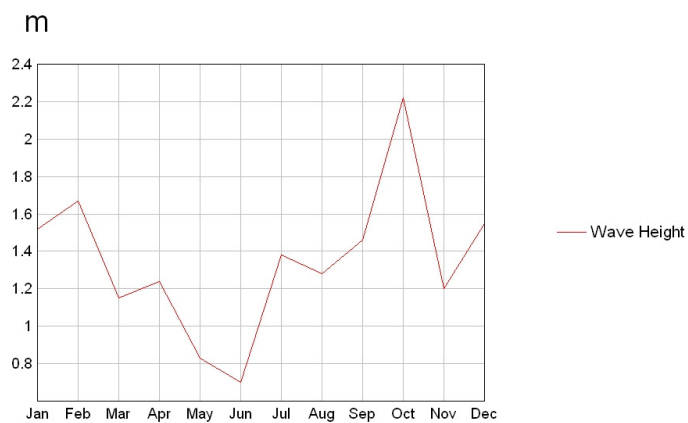


Figure 7.4: Significant wave height⁶

⁶ Data in Figure 7.3 and Figure 7.4 were produced with "Atlas of the Oceans: Wind and Wave Climate on CD-ROM", Version 1.0, Elsevier Science Ltd, 1996

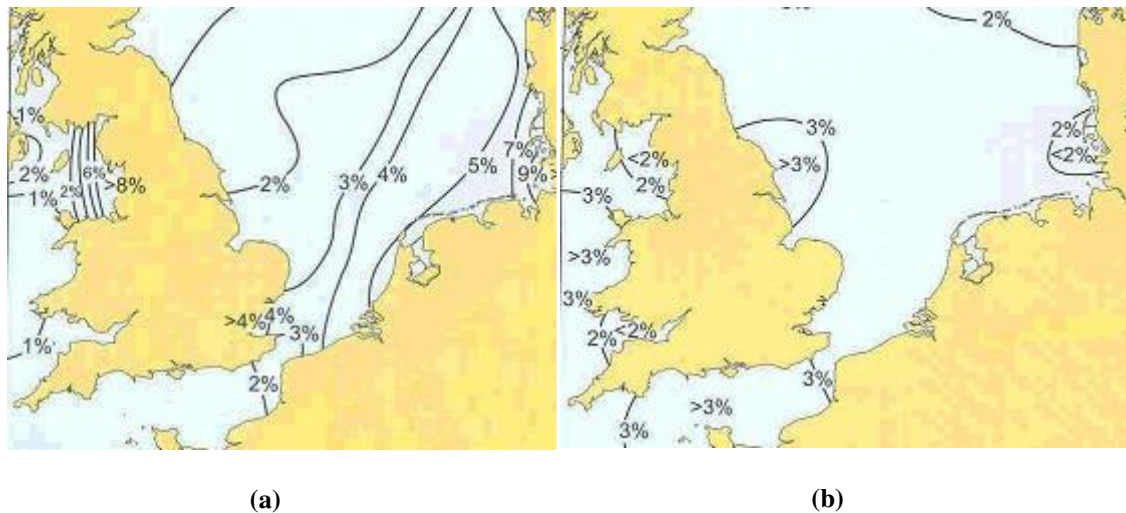


Figure 7.5: Thick fog levels in the Dover area during (a) January and (b) July (<http://www.franksingleton.clara.net/fog.html>)

7.4 Case study 1: collision of the ROPAX with the tanker

In this case, the struck vessel is the tanker. The factors affecting its probability of collision and the probability of oil outflow due to collision are described next.

Wind direction	
Bearing 225 °	0.833
Other bearing	0.167

Wind speed	
14.0 m/s	0.0835
10.0 m/s	0.833
0.00 m/s	0.0835

Wave height	
More than 1.4 m	0.583
Lower than 1.4 m	0.417

Thick fog	
Occurrence	0.03
No occurrence	0.97

Table 7.2: The elements of probability considered in the case study

Probability of tanker collision

The probability of collision estimation is based on Equation (4.11) and the MC simulation scheme described in Chapter 4.

For the calculation of entropy, there are four environmental parameters considered: wind speed, wind direction, wave height and visibility. The definitive contribution of these events to the occurrence of collision has been described in detail in Chapter 4. Table 7.2 is depicting the states and the associated probability for each state for these

four events. Additionally, the causation factor for loss of ship control is considered equal to 2×10^{-4} , (Kristiansen, 2005), and the human error probability equal to 0.0202, (Liu & Wu, 2004). Calculation of the entropy of information provided in this way is performed in Table 7.3.

Causation factor for loss of ship control		
$2 \times 10^{-4} \log_2 \left(\frac{1}{2 \times 10^{-4}} \right) + (1 - 2 \times 10^{-4}) \log_2 \left(\frac{1}{1 - 2 \times 10^{-4}} \right) =$		2.746×10^{-3}
Human error		
$0.0202 \log_2 \left(\frac{1}{0.0202} \right) + 0.98 \log_2 \left(\frac{1}{0.98} \right) =$		0.143
Wind direction		
$0.167 \log_2 \left(\frac{1}{0.167} \right) + 0.833 \log_2 \left(\frac{1}{0.833} \right) =$		0.651
Wind speed		
$0.0835 \log_2 \left(\frac{1}{0.0835} \right) + 0.833 \log_2 \left(\frac{1}{0.833} \right) + 0.0835 \log_2 \left(\frac{1}{0.08355} \right) =$		0.818
Wave height		
$0.417 \log_2 \left(\frac{1}{0.417} \right) + 0.583 \log_2 \left(\frac{1}{0.583} \right) =$		0.980
Thick fog		
$0.03 \log_2 \left(\frac{1}{0.03} \right) + 0.97 \log_2 \left(\frac{1}{0.97} \right) =$		0.194
		<i>Total</i>
		2.787

Table 7.3: Calculation of the entropy of information of environmental conditions

For the calculation of the probability of collision, the parameters that will be addressed with MC simulation are presented in Table 7.4.

Parameter	Mean value	Standard deviation
Speed of tanker	12 knots	2 knots
Speed of surrounding traffic	14 knots	7 knots
Annual number of ship passages	109,500	10,000
Channel width	5 nm	0.5 nm

Table 7.4: The parameter details for the MC simulation scheme

The time it takes the tanker to advance at 90° for various speeds is calculated according to the following equation:

$$R(V) = -2.9052V^3 + 92.145V^2 - 948.64V + 3492 \quad (7.1)$$

where:

R: response time, [s]

V: cruising speed, [knots]

The data for the derivation of this equation was calculated with SIMX5, as described in Appendix A. The following assumptions are made for calculating the response time of the vessel in as generic manner as possible (a similar approach will be followed in the early design stage):

- The hard to port (or starboard) command is given as the last resort to avoid the collision
- Surrounding restrictions are not considered (i.e. the channel is wide enough to allow for such manoeuvre)
- No wind or current is included in the model
- The manoeuvre is performed in deep water

The annual probability of collision for the tanker vessel is 0.134 or every 7.5 years. It should be mentioned that based on the risk analysis for ROPAX ships performed in (Konovessis, 2007), the annual probability of collision is 1.25×10^{-2} . The difference between the two results is attributed to the highly localised character of the case study presented here compared to the more general one, where the global fleet of ROPAX ships over 1,000 GRT, between 1994 and 2004, was considered.

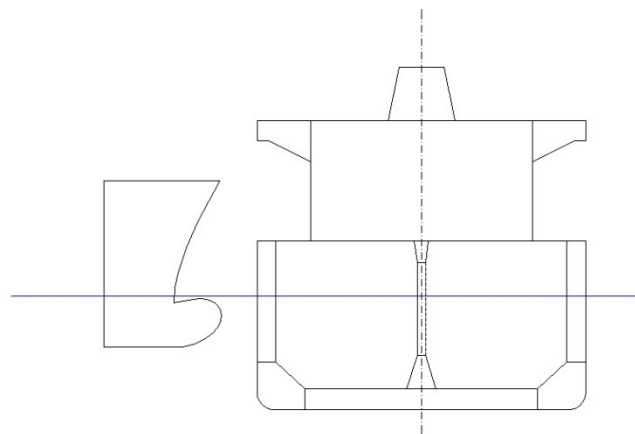


Figure 7.6: Relative position of the ROPAX and the tanker vessel for the case study

Probability of oil outflow

The next element of probability is whether a breach occurs and if it does, what is the most probable size of it. Additionally, because the target ship a double-hull tanker, it is necessary to check whether the penetration will be adequate to lead to oil outflow, i.e. exceed the 2.1 m double hull span of the ship.

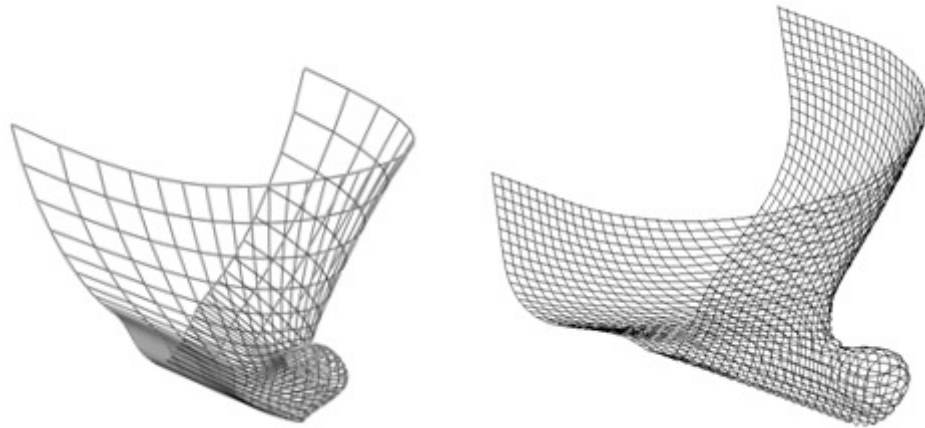


Figure 7.7: The Bezier surface representation (left) and the actual surface (right) of the ROPAX bow

As demonstrated in Figure 7.6, due to the relative size and operational draught of the two vessels, the bulb of the ROPAX is expected to cause the main damage to the side of the tanker. The Bezier surface (Appendix B) of the striking bow is presented in Figure 7.7. Despite the simplification of the geometrical representation, it is clear that the quality of the result can be improved by increasing the number of control points but this comes at a high computational price with little benefit to the current demonstration purposes.

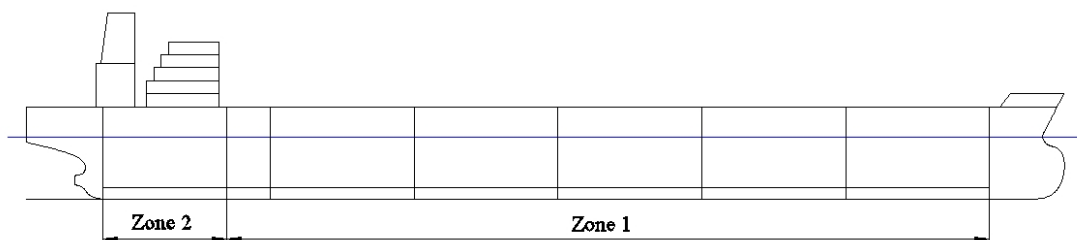


Figure 7.8: The two structural zones of the tanker vessel exposed to collision events

As was mentioned at the beginning of Section 7.2, the tanker under examination has a double hull, which extends from the engine room bulkhead up to the collision

bulkhead. The remaining area exposed to side collision is the area of the engine room. The scantlings in these two areas (called *zones* from this point onwards) are different due to different levels of stiffening. This directly translates into different response (energy absorption) in case of a collision incident. Modelling of the side shell for the calculations is therefore split in two zones as depicted in Figure 7.8. In this way, the variation in crashworthiness is captured and can be expressed in the end result of the calculations.

Besides, water ingress in the engine room or the cargo area leads to different consequences in the course of a risk analysis process. This is one extra reason why it is necessary to model different structural zones of the struck vessel. It should be stressed that only the sway added mass is taken into consideration in the calculations. The yaw added mass is not considered in this example. Finally, the following calculations are conducted with $c = -0.05$ for faster processing time. The plate rigidities of each zone are summarised in Table 7.5 with detailed calculations in Appendix D.

Finally, for the MC simulation that follows, it is assumed that the speed of the ROPAX vessel is normally distributed with mean 28.0 knots and standard deviation 2.0 knots. The reason for this discrepancy is related to the very stiff side shell of the tanker. Preliminary calculations showed that the ROPAX does not have enough kinetic energy to create serious structural damage at its normal operating speed. In order to demonstrate the method though, the alternative speed range was selected. The striking angle is varying between 0.0° (i.e. vertically on the side of the tanker) and $\pm 45.0^\circ$ with mean at 0.0° and standard deviation 15.0° . If the angle of impact becomes any larger than 45° the radii of curvature increase substantially and the whole phenomenon reduces to the contact of two approximately flat surfaces. This is a further assumption for this particular example and has no general application. The results are presented in Table 7.6.

	Zone 1	Zone 2
D	0.078	0.053
D_x	5.96×10^3	0.40×10^3
D_y	2.60×10^3	1.51×10^3

Table 7.5: Stiffness values for each zone in MNxm

	Zone 1	Zone 2
Probability of rupture	0.256	0.856
Breach size		
Mean	104.83 m ²	151.70 m ²
SD	28.10 m ²	29.66 m ²
Penetration		
Mean	10.00 m	14.36 m
SD	2.38 m	2.82 m
Penetration Potential		
Mean	1.21	0.85
SD	0.39	0.25

Table 7.6: Results for the first case study

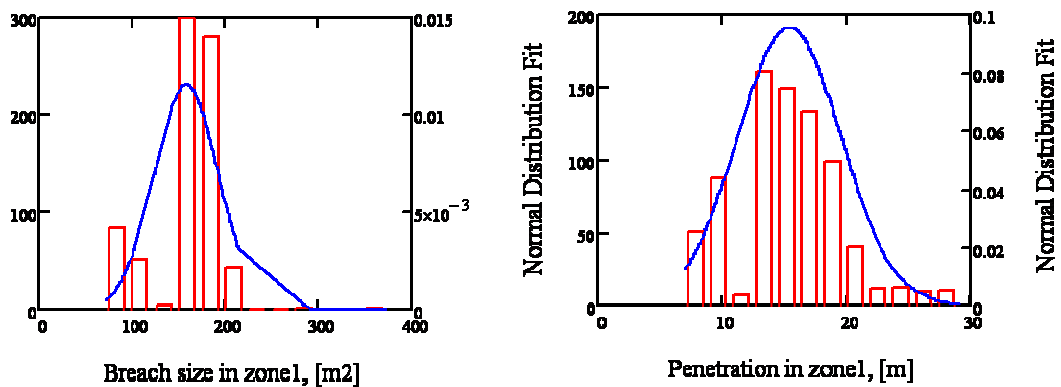


Figure 7.9: Histograms and probability density functions for the breach size in zone 1

Figure 7.9 and Figure 7.10 demonstrate the stiffer character of the side shell of the tanker vessel especially in the area of the double-hull arrangement. This is demonstrated by the narrow distribution of the breach size and the limited penetration. Contrary to this, the engine room area (zone 2) appears more vulnerable in the particular combination of speed and angles when the ROPAX vessel acts as the striking ship. The non-uniformity of the histograms of Figure 7.9 and Figure 7.10 is attributed to the narrow standard deviation of the striking ship speed (2.0 kn), which does not allow sampling from a wide range of speeds, in combination to the poor random number generator algorithm of the particular compiler used for the current version of CRASED.

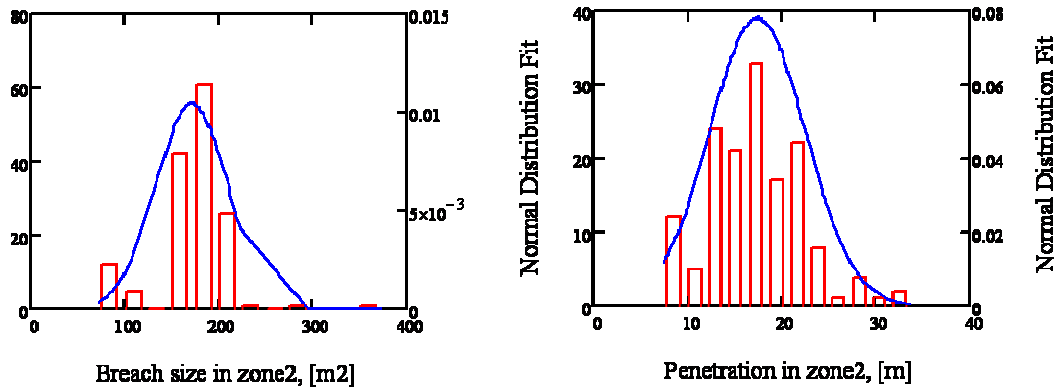


Figure 7.10: Histograms and probability density functions for penetration in zone 2

Figure 7.11 presents the Cumulative Distribution Function of the Normal fit for the penetration in zone 1. Given that the double-hull span is 2.1 m, it becomes evident that the chance of having an oil spill under the current scenario is almost certain.

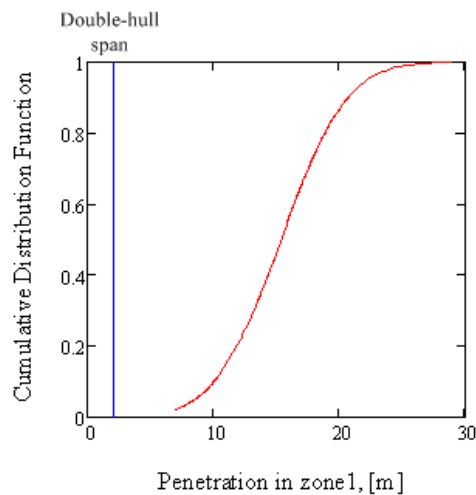


Figure 7.11: Oil outflow will occur in almost all collision cases in zone 1 as the penetration exceeds the double-hull span

7.5 Case study 2: collision of the tanker with the ROPAX

In this case study the roles between the two vessels are reversed. Such an accident is different from the first one not only in terms of striking geometries and shell structures but also in terms of the associated consequences further to the accident. This time environmental pollution is the least of concerns since the issue of survivability of the ROPAX vessel and the safe evacuation of a large number of passengers and crew has priority.

Parameter	Mean value	Standard deviation
Speed of tanker	14 knots	2 knots
Speed of surrounding traffic	14 knots	7 knots
Annual number of ship passages	109,500	10,000
Channel width	5 nm	0.5 nm

Table 7.7: The parameter details for the MC simulation scheme

Probability of ROPAX collision

The entropy of information in this case is calculated as it was described in Table 7.3 with the sole exemption that the traffic conditions are more familiar to the navigators of the ROPAX vessel, so human error probability is taken as 0.0168. The final value of entropy is 2.768. The parameters that will be simulated in the MC scheme are presented in Table 7.7.

This time, the annual probability of collision is 0.06 or one collision accident every 17 years.

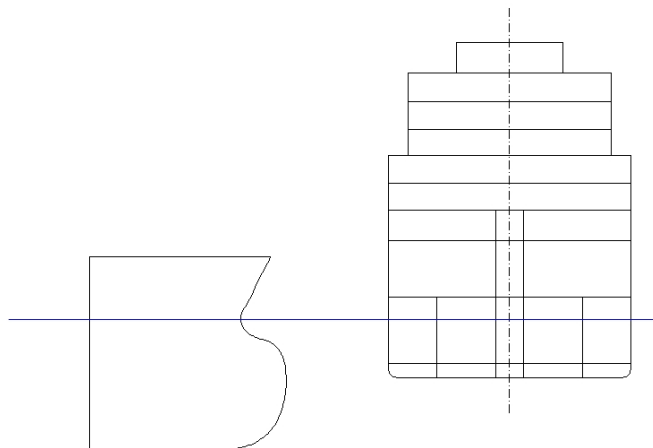


Figure 7.12: The tanker stem is primarily aiming at the garage deck area

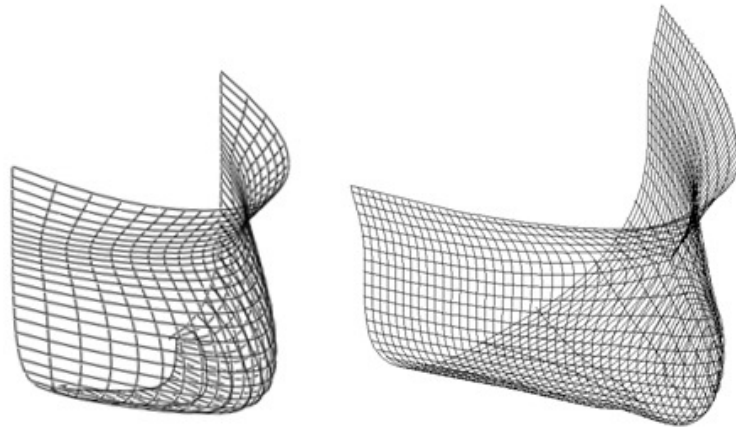


Figure 7.13: The Bezier surface representation (left) and the real bow (right)

Probability of water ingress

The relative flotation position of the two vessels at their operational draught creates a situation where the stem of the tanker is likely to create side shell failure of the ROPAX in the garage deck area (Figure 7.12).

The Bezier surface representation of the tanker stem is presented in Figure 7.13. The simplified geometry of its bow allows for better accuracy in the modelling.

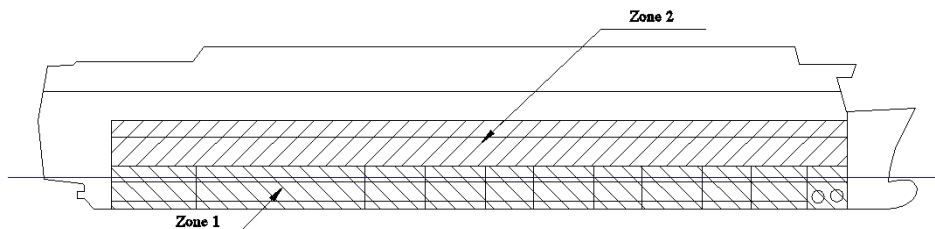


Figure 7.14: The two structural zones of the ROPAX vessel

Table 7.8 summarises the stiffness values for the two zones and Table 7.9 the results of the MC simulation considering a Normal distribution for the striking speed of the tanker with mean speed of 10 knots and standard deviation of 2 knots. The data for the striking angle remains the same.

	Zone 1	Zone 2
D	0.036	0.036
D_x	0.44×10^3	0.15×10^3
D_y	0.19×10^3	0.07×10^3

Table 7.8: Stiffness values for the two zones of the ROPAX vessel in MN×m

	Zone 1	Zone 2
Probability of rupture	0.969	0.996
Breach size		
Mean	37.85 m ²	31.14 m ²
SD	35.18 m ²	41.24 m ²
Penetration		
Mean	1.24 m	1.49 m
SD	0.26 m	0.31 m
Penetration Potential		
Mean	0.20	0.08
SD	0.24	0.11

Table 7.9: Results for the second case study

The final step is to define the properties of the side shell structure of the ROPAX. Like in the case of the tanker, this can be separated in two zones due to internal subdivision below the bulkhead deck and above it (Figure 7.14).

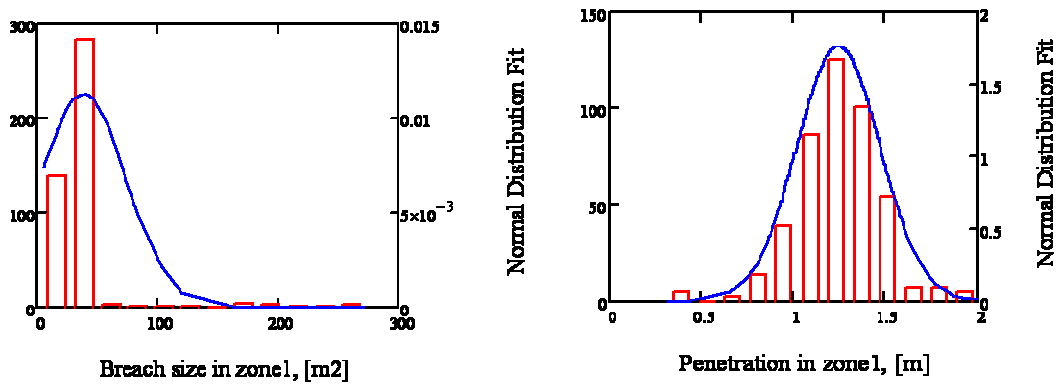


Figure 7.15: Histograms and Normal distribution fit for the breach size in zone 1

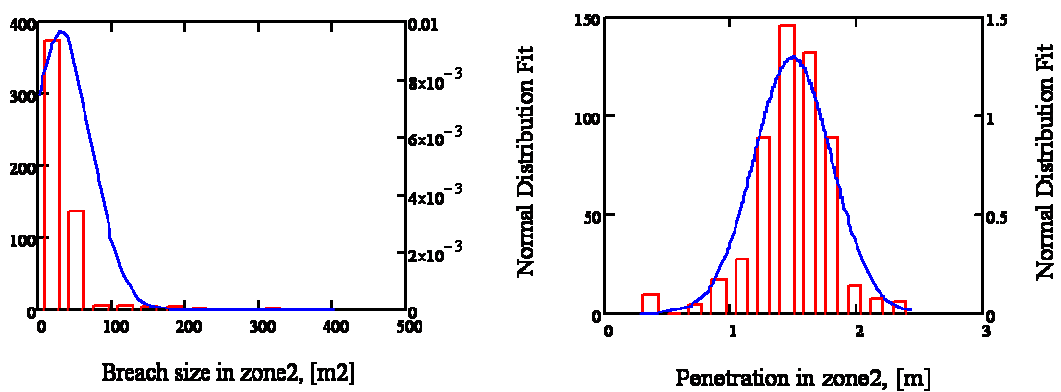


Figure 7.16: Histograms and Normal distribution fit for the penetration in zone 2

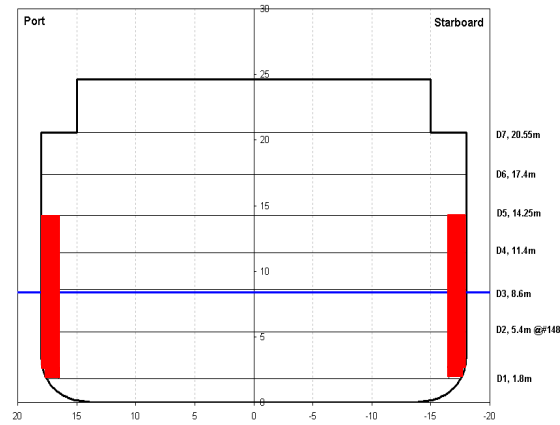


Figure 7.17: Crashworthiness improvement of the vessel, (Vassalos et al., 2006b)

Given the results of this study it becomes evident that there is a very high probability of flooding (Figure 7.15 and Figure 7.16) if the ROPAX vessel is struck by a tanker and alternative arrangements should be considered by the designer in order to improve either the crashworthiness characteristics of the side shell, the survivability potential or both. The case study with the tanker clearly demonstrates the benefits a “double hull” configuration can offer. As a result, arrangements like those analysed in (Vassalos et al, 2006b), Figure 7.17, and in (Pawlowski, 1999) appear very attractive and worth further elaboration as design solutions.

Additionally, the problem can be tackled from a more fundamental point of view by preventing the collision from happening in the first place. This can be achieved by improving the manoeuvrability of the tanker vessel, Figure 7.18, as it is argued in (Sodhal, 2002).



Figure 7.18: The double-rudder arrangement can improve the manoeuvrability of larger ships and reduce the chances of unwanted incidents, (www.concordia-maritime.se)

7.6 Case study 3: Crashworthiness of Y-sections panel

The third case study in this chapter is concerned with the rather more generic topic of assessing the crashworthiness capacity of flat panels with alternative stiffening arrangements. In this way, a comparison can be readily made among the variations of structural configuration of the side shell. In this particular case, only the crashworthiness capacity of the panel is examined but obviously in a more general design context other aspects will be considered as well (production cost, maintenance, etc.).

The idea of the comparative work presented here derives from (Naar et al., 2002) and (Graaf et al., 2004), and it is focusing on the crashworthiness assessment of flat steel panels with stiffeners of alternative configuration. Because of the unconventional arrangement this design alternative may be appealing to the designer but its assessment is extremely time-consuming and does not fit to the tight schedule of concept or preliminary design phase. As a result, it is discarded very early in the process. The methodology presented here can assist in this direction and allow for a wider search of the design space.

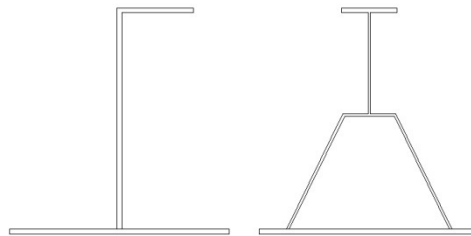


Figure 7.19: Schematic comparison between conventional and alternative stiffeners

Figure 7.19 presents the basic layout of the cross-sectional area of a stiffener that is assessed here. It is further assumed that only longitudinal stiffeners are modified from the conventional L-shape ones whereas the transverse stiffeners remain the same (i.e. the fabricated deep T-sections), as it is presented in Figure 7.20.

In particular, the size of the panels have dimensions 12 m \times 10 m and they are made of mild steel ($\sigma_y = 235$ MPa, $E = 2.09 \times 10^{11}$ MPa, $\nu = 0.3$). The plating thickness is 10 mm. The spacing of longitudinal stiffeners is 1.0 m. The transverse stiffeners are fabricated sections (T 500 \times 350 \times 12) at intervals of 4.0 m.

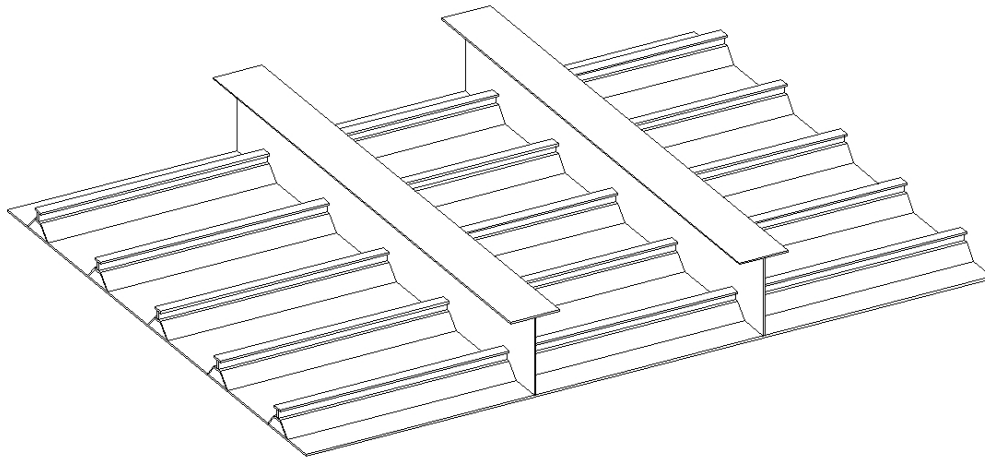


Figure 7.20: The panel that is assessed here has conventional deep frames in the transverse direction and alternative longitudinal stiffeners.

	wp1	1000 mm
	tp1	10 mm
	L1	400 mm
	B1	300 mm
	t1	18 mm

Table 7.10: Conventional L-shape stiffener particulars

	wp2	1000 mm
	tp2	10 mm
	t21	9 mm
	ϕ	45 deg.
	L21	350 mm
	B21	120 mm
	L22	350 mm
	t22	8 mm
	B22	120 mm
	t23	15 mm

Table 7.11: Alternative stiffener particulars

	Conventional panel	Alternative panel
D	0.019×10^6	
D_x	249.73×10^6	477.00×10^6
D_y	84.24×10^6	

Table 7.12: Stiffness values for each panel in Nxm

For both panels it is assumed that they are the exposed parts on the side shell of a ship engaged in a collision situation. Since this example case is very generic, it is further assumed that the striking body is a sphere with radius 3.0 m that weighs 5,000 tonnes and moves at speed of 12 knots. The diagram of Figure 7.21 presents the amount of strain energy that can be stored in each panel and clearly depicts that at the same energy level the alternative panel configuration can absorb a marginally higher (approximately 5.5%) amount of energy. This fact would be appealing to a designer and it would create the incentive for more thorough investigation. That is, a systematic variation of one of the geometrical parameters presented in Table 7.11 would reveal the strong points of the alternative stiffening and would eventually contribute to the decision-making process by providing solid evidence about the virtues of this innovative feature.

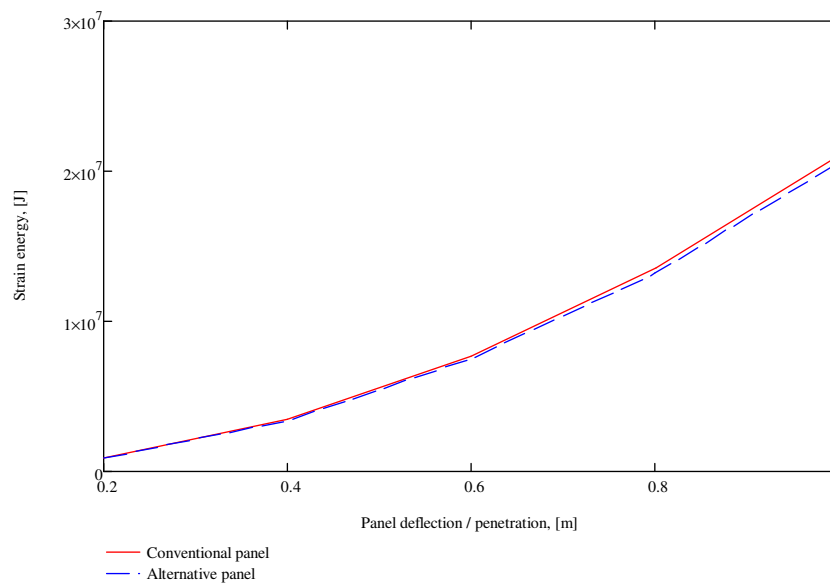


Figure 7.21: Comparison of strain energy absorption for the two panels

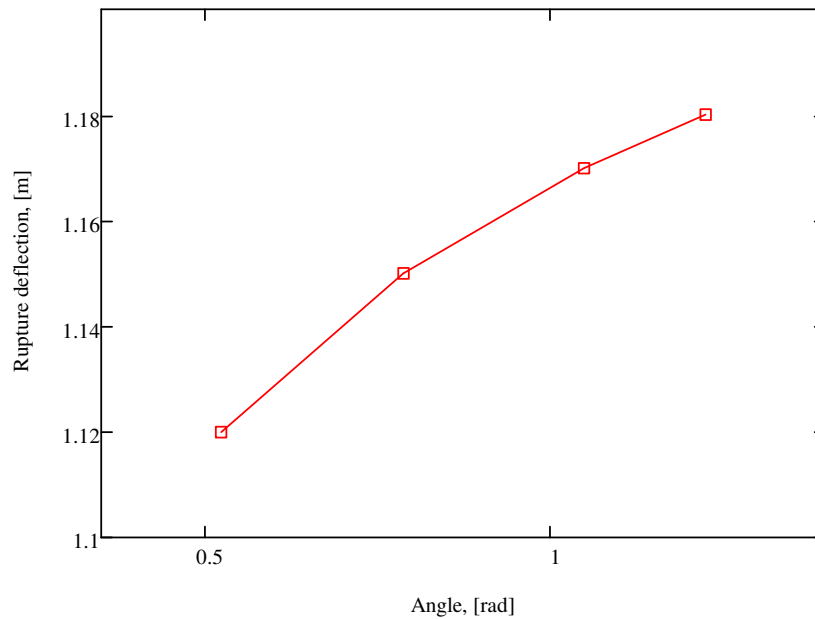


Figure 7.22: Variation of rupture deflection for various angles

In the example presented here, the element that is systematically varied is the angle φ and its effect on the magnitude of the stiffness along x-axis (D_x). As the angle increases, D_x becomes larger and the deflection where plate rupture occurs is increasing (Figure 7.22).

The arbitrary character of this numerical example does not intend to provide thorough insight on the benefits this alternative type of stiffening offers. It does however demonstrate how the methodology developed in this thesis can practically and effectively be used during the design process and provide the required answers quickly and cost-effectively.

7.7 Case study 4: Side shell configuration versus payload capacity

It was discussed in earlier chapters that part of the inability of modern designers to thoroughly explore the design space is the lack of appropriate parametric tools which allow the quantification of performance of various design virtues and therefore provide the means for more rational choices.

In terms of crashworthiness assessment, the structural configuration of the side shell provides the link to the watertightness of a ship and its payload capacity. The former

issue is straightforward in its approach: the side shell should be stiff enough to provide sufficient protection against a range of collision scenarios. Reinforcement of the side panels will evidently improve their crashworthiness which in turn will lead to smaller breach sizes. In this way, improvement to the survivability of the ship is evident.

However, improving the crashworthiness of the side structure will most probably entail increase in steel weight. This alternative directly implies that the deadweight of the ship should be reduced, assuming that the draught remains constant. To sacrifice payload capacity for improving survivability is a topic that requires more extensive analysis and it lies outside the scope of this study. Nevertheless, the issue whether there is any way to satisfy both aspects still remains.

This example demonstrates the implementation of the proposed methodology in the configuration of the side shell of a Ro-Ro passenger ship without reducing its payload capacity. The results should be treated with care as they only reflect part of reality as it is discussed next.

Problem setup

In order to investigate whether there are any side shell configurations that would not compromise the watertightness and at the same time improve the payload capacity of a Ro-Ro passenger ship, an optimisation routine with two objective functions is set up.

The first objective is the calculation of the crashworthiness of the side shell, which should not be ruptured for a series of collision scenarios. The second objective is the improvement of the payload capacity of a Ro-Ro ship. The particulars of the example ship for this study are presented in Table 7.1. Its deadweight is 2,400 tonnes. The parameters that are varied are related to the scantlings of the side shell (plating thickness, longitudinal and transverse stiffeners). The increase or decrease of the shell steel weight will cause the opposite effect to the deadweight. The stiffening offered by bulkheads and decks was not included in the process due to its dependency to other design aspects (e.g. loading capacity of decks).

A basic assumption for this example is that the striking ship is of similar size to the ship in the design process and it is travelling at 14.00 knots. This selection is based on the fact that it is less than the operational speed (collisions hardly ever occur at full speed) and it is higher than any speed in congested waters and busy waterways. Therefore it could represent the average speed of navigation of the striking ship.

Configurations	Plating thickness, [mm]	Longitudinal stiffeners		Transverse stiffeners		
		Section & dimensions, [mm]	Spacing, [mm]	Web, [mm]	Flange, [mm]	Spacing, [mm]
Nominal	10.00	L 250×100×10	375.00	600×10	250×20	4500.00
Best alternative	13.00	FB 250×13	450.00	550×15	-	6000.00

Table 7.13: The initial and the best alternative side shell scantlings

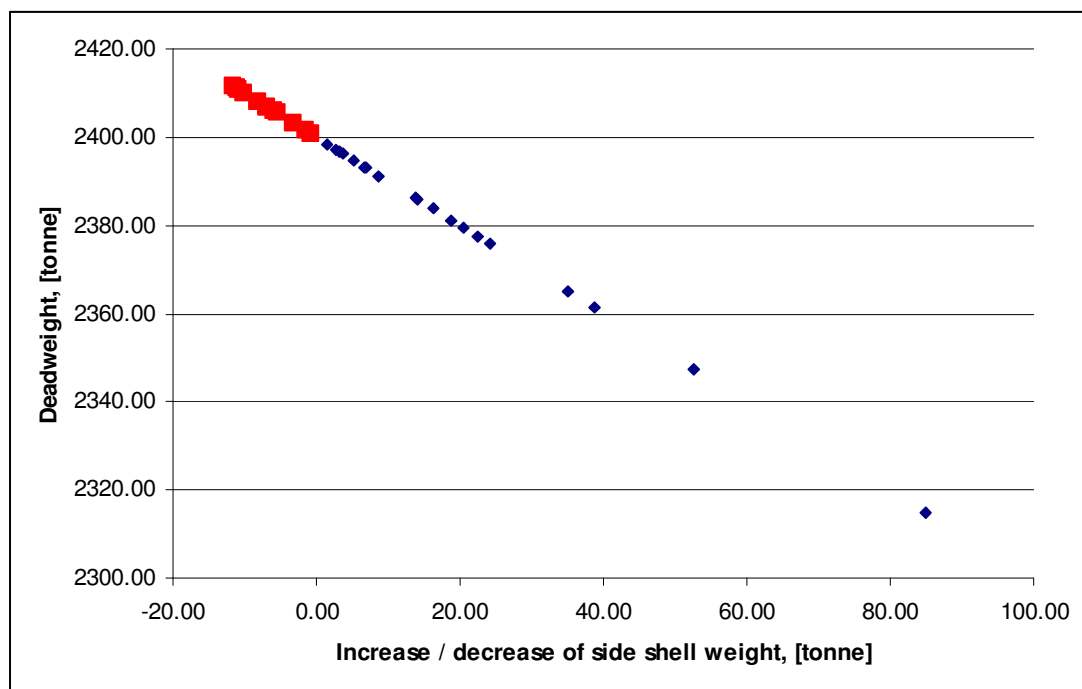


Figure 7.23: The red dots are the most promising alternatives for reduction of steel weight and increase of deadweight.

Results

The nominal and the best alternative configuration for the side shell are summarised in Table 7.13. The results of this short optimisation process are presented in Figure 7.23. The blue dots represent the configurations that offer additional crashworthiness

at the cost of reducing the deadweight capacity of the vessel. The red dots offer adequate protection against a set of collision scenarios and at the same time they improve the payload capacity. However, it should be stressed that the obtained configuration is not adequate as flat bars will buckle and trip in various loading conditions. This implies that additional objective functions should be deployed in order to account for these effects.

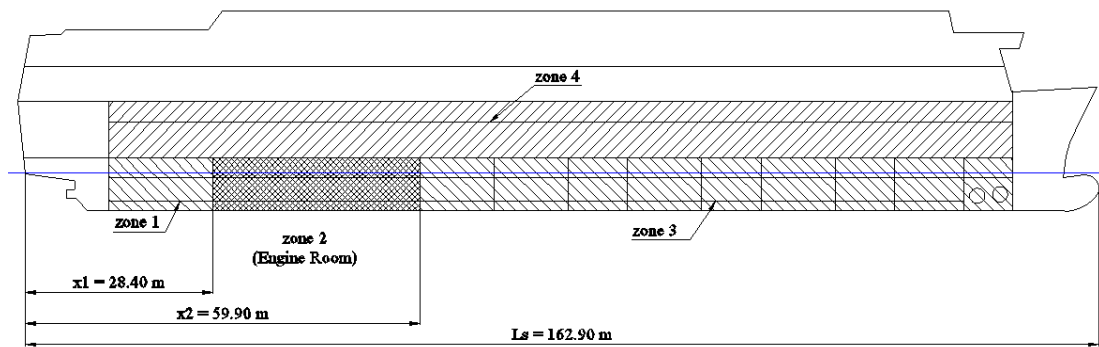


Figure 7.24: Since the compartment of interest is the engine room, the exposed area of the ROPAX ship is split in four zones

7.8 Case study 5: Comparative calculations

This final numerical application focuses on the comparison of the proposed methodology with (i) the derivation of the p-factor according to the probabilistic framework, and (ii) the methodology for flooding survivability analysis.

In the first case, the subject ship is the ROPAX vessel presented earlier in this chapter, and the area of operation is the Dover Strait as it was discussed for the first two case studies. An indicative calculation of the probability of water ingress will be performed for the engine room shown in Figure 7.24. The summary of the calculations is presented in Table 7.14.

It becomes evident that any variation of the parameters involved in the calculation of P_c and $P_{w/c}$ will affect their magnitude. That is, any variation in the traffic density or channel width for example will alter the probability of collision. Moreover, reinforcing the shell plating of the engine room (by increasing the values of D_x , D_y and D) will increase the stiffness and reduce the collision damage and this response will depend on the geometry of the striking bow. Contrary to this rationale, the

calculation of the p-factor according to SOLAS involves only the geometrical limits of the compartment under consideration.

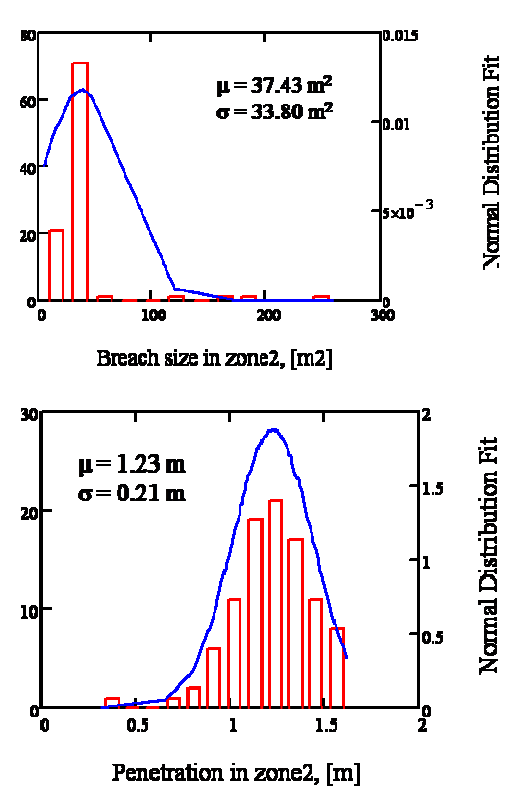
Probabilistic framework, (IMO, 2009a)		New methodology
P_c - Probability of collision		
Input	N/A	All input is presented in case study 2 (Section 7.5), with overall probability 0.06 / year.
Output	P _c = 1.0	Probability of experiencing a collision in the area of the engine room (zone 2): P _c = 0.1 × 0.06 / year = 6 × 10 ⁻³ / year
P_{w/c} – Probability of water ingress due to collision		
Input	<ul style="list-style-type: none"> ○ Ls = 162.90 m ○ x1= 28.40 m ○ x2 = 59.90 m ○ b = B/2 = 12.00m 	All input is presented in case study 2 (Section 7.5).
Output	1-compartment damage case, i.e. engine room (zone 2): P _{w/c} = 0.128	 <p style="text-align: center;">P_{w/c} = 0.960</p>
P_c × P_{w/c}	0.128	5.76 × 10 ⁻³ / year

Table 7.14

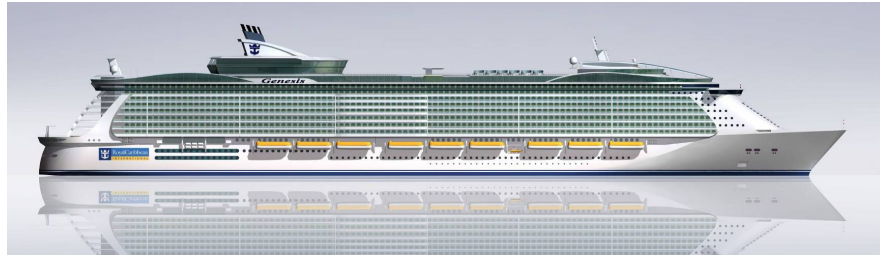


Figure 7.25: Project Genesis

Length	361 m
Breadth	47 m
Draught	9.15 m
Gross Tonnage	225,000
Air Draught	72 - 65 m
Number of Guests	5,400
Number of Crew	2,166
LSA Capacity	8,460

Table 7.15: The Project Genesis main particulars

In the second case, a similar comparison is performed for the Project Genesis (Figure 7.25), the largest cruise liner ever built. Its main particulars are summarised in Table 7.15. The risk of capsizing was calculated during the preliminary design stage of the ship, and the probability and consequence elements of it are expressed as (i) the frequency of flooding, and (ii) the number of fatalities following the flooding event, respectively, (Vassalos, 2009). The rest of the discussion is focusing on the former part only.

In the Project Genesis study, the frequency of flooding is based on statistical data presented in (IMO, 2009b) and it is taken equal to 1.48×10^{-3} per ship-year. This figure is comprised by the probability of collision and the probability of water ingress due to collision, and represents the average frequency for the exposed fleet to flooding hazard, irrespective of the individual operational profile of the ships comprising the fleet under consideration.

Item	Remarks	
Route, traffic density and operational speed	It is assumed that the ship will be deployed in the route Miami to Southampton. As such, the probability of collision in the proximity to either destination will be higher. For this example, the Southampton area will be considered with parameter as presented in Table 7.7.	
Response time	It is assumed that the simple model used for calculating the response time of the ROPAX ship is valid for Genesis as well.	
Exposed zone	The exposed side of the ship is comprised by a single zone between 0.0 and 316 m, as it is presented in Figure 7.26.	
D	0.040 MN×m	10% increase of the corresponding values for the zone 1 of the ROPAX is assumed.
D_x	0.485×10^3 MN×m	
D_v	0.210×10^3 MN×m	
P_c × P_{w/c}	$0.623 \text{ year}^{-1} \times 0.84 = 0.523 \text{ year}^{-1}$	

Table 7.16: Details of fictional scenario for the calculation of the frequency for flooding for Project Genesis

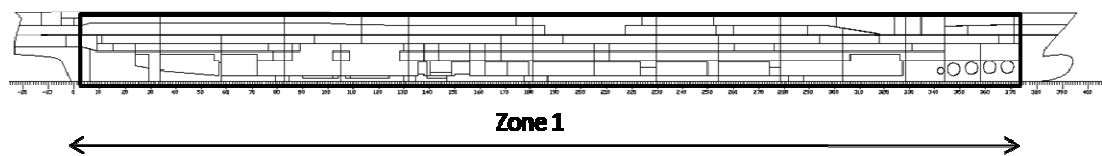


Figure 7.26: The exposed side to collision is comprised by a single zone for this numerical example

Based on the so far discussion, the operational scenario and governing design parameters presented in Table 7.16 will be used for highlighting a more rational way of accounting for the frequency of flooding in the calculations. A large majority of the information included is fictional and inappropriate for this type of vessel but it is used only for demonstration purposes. As a consequence, the frequency of flooding every 1.9 years has no meaningful interpretation.

7.9 Chapter summary

The five examples illustrated in this chapter demonstrate a number of interesting issues regarding the applicability of the proposed methodology. These are:

- unambiguous results with straightforward interpretation;
- direct and concrete input to the design process;

-
- feasibility and advantages in modelling the operational profile of a vessel in a probabilistic manner;
 - rational utilisation of the information entailed in the operational profile of the ship.

Concerning the first two case studies, the statistical data for oil tankers and passenger ships regarding collision accidents (Figure 1.2) is confirmed by the above results. The following two examples are presented with the sole purpose to show two important ways that the methodology can be implemented. As facilitation of innovative ideas in design has been one of the motivations behind this project from the beginning, it is demonstrated how the new methodology can help towards this objective. Investigation of alternative structural arrangements in the concept design phase is out of the question due to the amount of computational time that is required with FE analyses. Multi-objective optimisation schemes that can provide optimum configurations and compliance with design specification documents require parametric models in order to produce results within short time intervals. Both these objectives can be readily satisfied with the proposed methodology. The final numerical study highlights the rationale of the proposed methodology in comparison to the prescribed process in SOLAS 2009 and the existing flooding risk assessment methodology.

8 Discussion & conclusions

8.1 Introduction

The concepts developed and documented in this thesis should be perceived as high level improvements of the ship design process. They are summarised in this chapter and discussion follows on the work that is necessary to reduce the underlying assumptions of the two analytical models along with recommendations for further development. The chapter closes with an explicit list of conclusions in direct response of the objectives set in Chapter 1.

8.2 Summary of findings

Probability of collision

A new model that can accommodate the operational profile of the vessel during the design stage has been developed. It comprises two elements, each addressing virtues of different complexity and nature.

- *Ship domain* is the result of inherent design features of a ship that reflects its operational profile in terms of topology and traffic density. The geometrical shape of the domain is a circle. As long as its diameter is larger than the length of the vessel, no collision occurs.
- *Entropy of information* has the property of aggregating in single number qualitative and quantitative parameters that govern a hazardous event and provide a measure of the seriousness of the situation and how this can change in various circumstances.

All the information is blended in a single equation expressing the diameter of the domain and with a MC simulation scheme (with a typical 10,000 samples) the probability of collision is obtained. The results are compared with existing studies for collision risks and provide better approximation for navigation in confined waters.

Probability of water ingress due to collision

The dramatic event of collision between two bodies of substantial proportions is addressed, at the design level, by consideration of the energy exchange between them. That is, the available kinetic energy of the striking vessel is absorbed as impact (potential) energy from the side shell of the struck ship. The energy components are the potential energy of the stiffened panel and its membrane energy. The formulations are based on large deflections of the involved structural elements.

Geometrical compatibility between the geometry of the striking bow and the deformation / breach pattern of the struck ship is captured with calculation of the principle radii of curvature at the contact points of the striking bow (which is

assumed non-deformable) and they are used as input for the calculation of the progressive deformation of the struck panel. For the current stage of development, *Bezier surface* formulation has been used due to its simplicity and programming-friendly nature. Such inherently parametric definition of the striking bow allows for a more systematic variation of the geometry in a Monte Carlo simulation scheme. The struck panel deforms according to the pattern of a simple function called *Witch of Agnesi*, which takes into account the deflection / penetration and the stiffness of the struck surface, and the sharpness of the striking body. The approach is based on the notion of *deformation* rather than the *strain* due to its more direct meaning and applicability, and the uncertainty associated with failure strain.

The proposed approach has the fundamental advantage that the collision probability in certain areas of interest (e.g. the garage deck in the case of the ROPAX vessel) can be established very early in the design process. Thus, it is no longer necessary to *assume* a breach of an exact size on or below the waterline of a tanker, for example, in order to assess the oil outflow following a collision event. Instead, it is now possible to obtain the probability of striking the compartment of interest along with the probability density function of the breach size and penetration by direct consideration of the operational profile of the ship (in terms of size and type of ships of the surrounding traffic). The results compare favourably with statistical analyses of past accidents and open the way for further development and research.

The new methodology

The information obtained by these two models provides a solid foundation in a risk-based design context, where systematic risk analysis is integrated in the design development. Additionally, both models of P_c and $P_{w/c}$ can be included in multi-objective / multi-criteria optimisation design routines and allow much better exploration of the design space. In this approach, the claim that safety is another design objective, which can be achieved cost-effectively and efficiently, can be supported further.

Finally, the tools developed here can be deployed for risk analysis at a regulatory level and therefore provide the opportunity to migrate from an infertile set of rules based on conditional probability approach to a first-principles one. As such, the probabilistic damage stability regulations presented in SOLAS Chapter II-1 can be rationalised and, in turn, facilitate innovation and inherent safety of ships and marine industry in general.

8.3 Recommendations for future work

The above summary opens the way for further research and refinement of the proposed methodology. The following paragraphs set the pace of future developments and highlight the areas where more thorough investigation is needed.

Rupture energy

At the beginning of this research it was highly appreciated that for the purpose of design implementation it would be necessary to examine the crashworthiness of the structure in more macroscopic scale than FE analyses or more simplified approaches like (Hansen & Simonsen, 2001) or (Paik & Pedersen, 1996) can provide. Fine details of the structural configuration side shell are not known very early in the design process and these methods are heavily dependent on it.

A viable alternative appeared to be the energy balance of the striking and the struck ship and, in particular, the assessment of the energy exchange between the two of them following initial contact. Despite the generic nature of the approach there is one critical issue that has to be addressed. That is, the rupture point of the plating of the stiffened panel with various degrees of stiffening. There is no analytical model or study on this topic except of course the experiments on plain plates like those presented in (Jones & Birch, 2006) and eventually implemented here.

There is a compelling need to study the amount of energy a stiffened panel can absorb as a function of its material, its structural configuration and its maintenance levels. Without such a study, the results of the current design-oriented methodology or FE analyses will always be approximate and there will never be a real potential to

implement them reliably and uniformly during design, (Brown, 2002b). Additionally, the results of such studies should not only focus on configurations of conventional stiffened panels but they should expand in more advanced concepts like sandwich panels, (Paik et al., 1999b), (Kitamura, 1997), etc. In any case the effect of potential structural defects and corrosion should also be quantified.

Structural singularities and zonal modelling

One issue that has not been investigated in detail is related to the effect of structural singularities. That is, as long the stiffened panel has some uniform degree of stiffening then assessing its dynamic response represents only one dimension of the challenge. The second element that has to be addressed is the presence of one or more heavy stiffening members in the vicinity of the panel like a deck or a bulkhead. It is straightforward to qualitatively predict that the stiffness of the panel will increase in the specific area, but (i) the extent of the area and (ii) the exact contribution of the member to the capacity of the panel (i.e. deformation before rupture) are still unknown.

In the analysis for the tanker vessel, ignoring the effect of transverse bulkheads is justified by the very small area they occupy in comparison to the overall side shell area exposed to collision. This is obviously not the case for the ROPAX vessel where heavy subdivision is taken into account in the calculation of stiffness values for the shell panels.

Friction: an important part of the energy balance

Crashworthiness assessment of the side shell structure of a ship in case of collision with another ship has been based on the energy balance between the available kinetic energy and the absorbed strain energy by the struck structure. An important element of this balance is the friction between the surfaces of the striking bow and the ruptured shell of the struck ship. Quantification of the heat lost due to friction will allow for more precise determination of the strain energy for the sole reason that no matter how localised the impact is and the volume of material that actually absorbs

the impact energy, heat is dissipated in a larger area and the surrounding water. The fact that once the collision phenomenon initiates it will terminate only when all the kinetic energy transforms into heat and strain energy indicates that formulations from *irreversible thermodynamics* should be included in the study, (Chaboche, 2003). Finally, the presence of a heat source in the areas should be further investigated in terms of incurred fire as in the case of *Dona Paz* (Table 1.1).

Analytical representation of the striking and the struck surface

In the current work only the basic ideas of implementing a complicated geometry as the striking body is presented. However, the basic reason for such a choice is to set the foundation for a more rigorous treatment and integration of collision risk in ship design. Parametric surface definition would allow the variation of the bow geometry not only according to speed and displacement but also in terms of bow deformation. Having such a facility available would allow the designer to simulate a wider range of operational scenarios and appreciate the collision risks to a wider extent. Additionally, parametric surface definition can be used for the deformation of the struck ship, thus allowing for a more detailed assessment of the struck panel deformation and rupture.

Chaos theory application in design and operation

Finally, the main revelation of the work presented here is perhaps one of the most interesting and exciting ideas of modern science and mathematics: the application of chaos theory. It was discussed in the corresponding chapters that the three main characteristics of recursiveness, determinism and sensitivity to initial conditions play a definitive role in the probabilistic results and statistical analyses. Basic prerequisite for the search of chaotic behaviour is the availability of analytical non-linear deterministic models, (Stewart, 1997). This requirement matches very well with the risk-based design requirement for parametric models and the basic outcome of this research.

However, the challenging philosophy of the chaotic approach to problems like those treated here and the complexity of the mathematical analysis rendered the whole exercise rather infeasible. As a result, only a very first application in the area of probability of collision is presented here with the measure of entropy of information in a dynamically developed situation, which might end up to collision. The obvious benchmarking of the models and treatment of potential deficiencies are only trivial steps before the major outcome, which can shed new light in the way risk is treated today.

The following phase plots provide a glimpse of the potentials of a chaotic approach. This is a technique used for identification of areas where the state of a system is found most often or where it tends to converge. Figure 8.1 presents the variation of the ship domain diameter of the ROPAX vessel. The blue lines identify the length of the vessel. Similar information is presented in Figure 8.2 for the tanker. The density of the points appears to be inversely proportional to the statistical and calculated probability of collision for each ship. However, proper quantification of this fact and extraction of more useful information (e.g. the dominant size of the domain) are issues of further investigation.

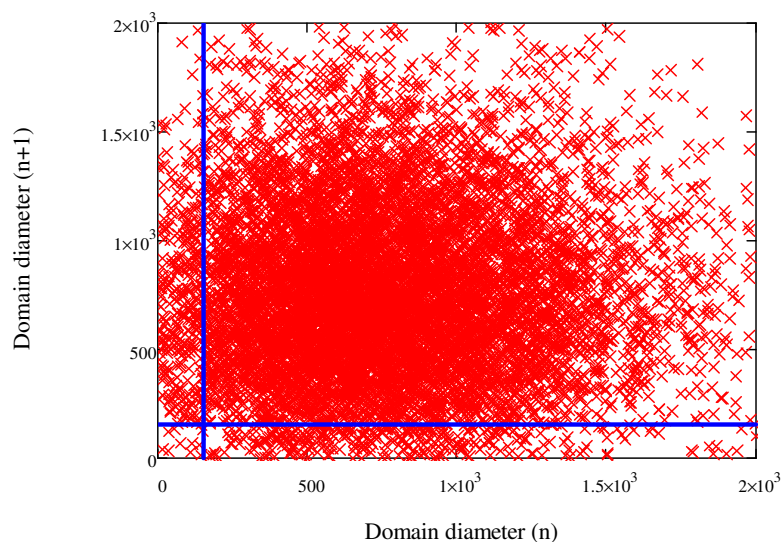


Figure 8.1: Ship domain variation for the ROPAX vessel

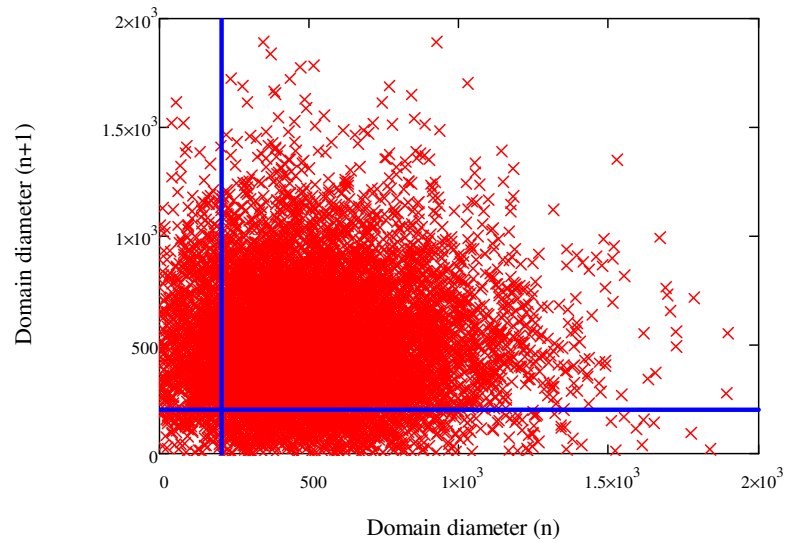


Figure 8.2: Ship domain variation for the tanker

8.4 Conclusions

Finally, the following conclusions can be drawn with respect to the methodology proposed in this thesis:

- The probability of a ship-ship collision in a particular waterway is based on the concept of ship domain and it is calculated with direct comparison of the domain diameter with the length of the ship under consideration.
- The crashworthiness of the side shell of the struck ship is assessed according to the energy balance between the initial kinetic energy of the striking ship and the potential of the struck panels to absorb this energy before plate tearing. Dissipation of the energy is considered in the form of friction and added mass inertia.
- The operational profile of the ship under consideration is heavily taken into account in the calculation of both elements of probability. The input to the calculations is related to the traffic density and the size, type and speed of surrounding ships.

- Both models comply with the requirement of risk-based design for availability of analytical parametric tools, in order to perform thorough search of the available design space.
- The combination of the proposed models can supersede the existing formulation of the p-factor in the probabilistic damage stability framework of SOLAS, Chapter II-1.

9 References

-
- (ABS, 2004), "Review and Analysis of Accident Databases: 1991-2002 Data", American Bureau of Shipping, Corporate Technology Division, Safety Assessment and Human Factors Department, March 2004
- (Ambramowicz, 2003), "Thin-walled structures as impact energy absorbers", Abramowicz, W., *Thin-Walled Structures* 41, pp. 91–107, 2003
- (Ambramowicz & Simonsen, 2003), "Effect of Fracture on Crushing of Ship Structures", Abramowicz, W., Simonsen, B. C., *Journal of Ship Research*, Vol. 47, No. 3, pp. 194–207, September 2003
- (Amrozowicz et al., 1997), "A Probabilistic Analysis of Tanker Groundings", Amrozowicz, M. D., Brown, A., Golay, M., 7th International Offshore and Polar Engineering Conference (ISOPE), Honolulu, Hawaii, May 1997
- (Applebaum, 1996), "Probability and information: An integrated approach", Applebaum, D., University of Cambridge, Press Syndicate, 1996
- (Barik & Mukhopadhyay, 2002), "A new stiffened plate element for the analysis of arbitrary plates", Barik, M., Mukhopadhyay, M., *Thin-Walled Structures* 40, pp. 625–639, 2002
- (Barker & McCafferty, 2005), "Accident database review of human element concerns: what do the results mean for classification", Barker, C. C., McCafferty, D. B., *Human Factors in Ship Design Safety and Operation*, Event organised by the Royal Institution of Naval Architects, London, UK, 23-24 February, 2005
- (Bergander et al., 1992), "Standard formulation of elastic-plastic deformation laws", Bergander, H., Kreibitz, R., Gerlach, J., Knauer, U., *Acta Mechanica*, 91, pp. 157-178, 1992
- (Berger, 1955), "A new approach to the analysis of large deflection of plates", Berger, H. M., *Journal of Applied Mechanics*, Vol. 22, pp. 465-472, December 1955
- (BMT, 2005), "Annual Report of Operations", The Salvage Association, 2005

-
- (Boniface & Bea, 1996), "Assessing the Risk of and Countermeasures for Human and Organisational Error", Boniface, D. E. and Bea, R. G., SNAME Transactions, Vol. 104, pp. 157-177, 1996
- (Brown & Amrozowicz, 1996), "Tanker Environmental Risk - Putting the Pieces Together", Brown, A., Amrozowicz, M., Joint SNAME/SNAJ Conference on Designs and Methodologies for Collision and Grounding Protection of Ships, San Francisco, 1996
- (Brown & Haugene, 1998), "Assessing the Impact of Management and Organizational Factors on the Risk of Tanker Grounding", 8th International Offshore and Polar Engineering Conference (ISOPE), May 1998
- (Brown et al., 2000), "Structural Design and Response in Collision and Grounding", Brown, A., Tikka, K., Daidola, J. C., Lützen, M., Choe, I. H., SNAME Transactions, 108, pp. 447-473, 2000
- (Brown et al., 2002), "Structural Design for Crashworthiness in Ship Collisions", Brown, A., Moon, W., Louie, J., SNAME Annual Meeting T&R 2002 and SNAME Transactions 110, pp. 499-512, 2002
- (Brown & Chen, 2002), "Probabilistic Method for Predicting Ship Collision Damage", Brown, A., Chen, D., Ocean Engineering International Journal, Vol. 6, No. 1, pp. 54-65, 2002
- (Brown, 2002a), "Collision scenarios and probabilistic collision damage", Brown, A. J., Marine Structures 15, pp. 335-364, 2002
- (Brown, 2002b), "Modelling structural damage in ship collisions", Brown, A. J., Ship Structure Committee (SSC), Report 422, 2002
- (Brown & Sajdak, 2004), "Predicting Probabilistic Collision Damage Extents for Tanker Oil Outflow Assessment and Regulation", Brown, A., Sajdak, J., SNAME Transactions, 2004
- (Bryant, 1991), "*The Human Element in Shipping Casualties*", Bryant, D.T., Report prepared for the Dept. of Transport, Marine Directorate, United Kingdom, 1991

-
- (Byklum & Amdahl, 2002), “A simplified method for elastic large deflection analysis of plates and stiffened panels due to local buckling”, Byklum, E., Amdahl, J., *Thin-Walled Structures*, 40, pp. 925–953, 2002
- (Cahill, 2002), “Collisions and their causes”, Cahill, Captain R. A., The Nautical Institute, 3rd Edition, 2002
- (Cengel & Boles, 2005), “Thermodynamics: An Engineering Approach”, Cengel, Y. A. and Boles, M. A., McGraw-Hill Higher Education, 5th edition, 2005
- (Chaboche, 2003), “Thermodynamics of local state: Overall aspects and micromechanics-based constitutive relations”, Chaboche, J. L., *Technische Mechanik*, Band 23, Heft 2-4, pp. 113–129, 2003
- (Chanda, 2003), “Static Responses of Elasto –plastic Nonuniform Plates of Arbitrary Shape”, Chanda, S., *Transactions of the 17th International Conference on Structural Mechanics in Reactor Technology (SMiRT 17) Prague, Czech Republic, 17 –22 August, 2003*
- (COLREG, 2003) “Convention on the International Regulations for Preventing Collisions at Sea”, International Maritime Organisation, Consolidated Edition 2003
- (Cox et al., 2005), “Modern topics and challenges in dynamic fracture (review)”, Cox, B. N., Gao, H., Gross, D. and Rittel, D. *Journal of Mechanics and Physics of Solids*, No. 53, pp. 565-596, 2005
- (Datubo et al., 2006), “Enabling a Powerful Marine and Offshore Decision-Support Solution through a Bayesian Network Technique”, Datubo, A. G. E., Wall, A., Saajedi, A. and Wang, J., *Risk Analysis*, Vol. 26, No. 3, pp. 695-721, 2006
- (DEXTREMEL, 2001), “Design for Structural Safety under Extreme Loads (DEXTREMEL) – Final Technical Report”, BE97-4375, 23 January, 2001
- (Dias & Pereira, 2004), “Optimisation methods for crashworthiness design using multi-body models”, Dias, J. P., Pereira, M. S., *Computers & Structures*, Vol. 82, No. 17-19, pp. 1371-1380, 2004

- (DNV Technica, 1996), "Safety Assessment of Passenger Ro-Ro Vessels", NW European project on Ro-Ro safety, Methodology report and appendices, DNV Technica, October 1996
- (Drawshi & Betten, 1992), "Axially symmetric deformations and stability of a geometrically non-linear circular plate subjected to multi-parametrical static loading", Drawshi, M., Betten, J., *Archive of Applied Mechanics* 62, pp. 455-462, 1992
- (Ellinas, 1995), "Mechanics of ship-jackup collisions", Ellinas, C. P., *Journal of Construction Steel Research*, 33, pp. 283-305, 1995
- (Endo et al., 2004), "Verification of the effectiveness of buffer bow structure through FEM simulation", Endo, H, Yamada, Y. and Kawano, H., *Proceedings of the 3rd International Conference on Collision and Grounding of Ships (ICCGS)*, Izu, Japan, 25-27 October, 2004
- (Fakuchi et al., 2006), "An elastic-plastic analysis of large deflection of thin shell structure using a delta-sequence function", Fukuchi, N., Okada, K., Sugita, N., *Thin-Walled Structures*, 44, pp. 91-101, 2006
- (Filipowicz, 2004), "Vessel traffic control problems", Filipowicz, W., *The Journal of Navigation*, vol. 57, pp. 15-24, 2004
- (Fujii et al., 1974), "Some factors affecting the frequency of accidents in marine traffic: I-The diameter of evasion for crossing encounters, II-The probability of stranding, III-The effect of darkness on the probability of collision and stranding, IV-Visual range and the degree of risk", Fujii, Y., Oshima, R., Yamanouchi, H., Mizuki, N., *The Journal of Navigation*, Vol. 27, No. 2, April 1974
- (Fung, 1965), "Foundations of Solid Mechanics", Y. C. Fung, Prentice – Hall, 1965
- (Gao et al., 2005), "A study on type II structures. Part I: a modified one-dimensional mass-spring model", Gao, Z. Y., Yu, T.X., Lu, G., *International Journal of Impact Engineering*, 3, pp. 895-910, 2005

-
- (GL, 2006), “GL Regulations for strengthening against collisions, Section 33”, Germanischer Lloyd, 2006
- (Goodwin, 1979), “Determination of ship domain size”, Goodwin, E.M., published in “Mathematical aspects of marine traffic” based on the proceedings of the Conference on Mathematical Aspects of Marine Traffic held at Chelsea College London in September, 1977, organized by the Institute of Mathematics and its Applications edited by S.H. Hollingdale, London Academic Press, 1979
- (Graaf et al., 2004), “Construction aspects of the Schelde Y-shape crashworthy hull structure”, Graaf, B., Broekhuijsen, J., Vredefeldt, A. and Ven, A., Proceedings of the 3rd International Conference on Collision and Grounding of Ships (ICCGS), Izu, Japan, 25-27 October, 2004
- (Graciano, 2003), “Ultimate resistance of longitudinally stiffened webs subjected to patch loading”, Graciano, C. A., Thin-Walled Structures 41, pp. 529–541, 2003
- (Guo et al., 2003), “Efficient modeling of panel-like structures in perforation simulations”, Guo, J., Shi, G., Wang, Y., Lu, C., Computers & Structures, Vol. 81, No. 1, pp. 1-8, 2003
- (Gupta & Ray, 1999), “Simply supported empty and filled thin-square tubular beams under central wedge loading”, Gupta, N. K., Ray, P., Thin-Walled Structures 34, pp. 261–278, 1999
- (Hallquist, 1998), “LS-DYNA Theoretical Manual”, Hallquist, J. O., Livermore Software Technology Corporation, May 1998
- (Hansen, 2000), “Bayesian Networks as a Decision Support Tool in Marine Applications”, Friis-Hansen, A., PhD Thesis, Department of Naval Architecture and Offshore Engineering, Technical University of Denmark, 2000
- (Hansen et al., 2004) “FSA of the navigational safety in Baltic west”, Hansen, P. F., Ravn, E. S., Hartman, J. P. and Sorensen, A., Proceedings of the 3rd International Conference on Collision and Grounding of Ships (ICCGS), Izu, Japan, 25-27 October, 2004

-
- (Hansen & Simonsen, 2001), “GRACAT: Software for Grounding and Collision Risk Analysis”, Hansen, P. F. and Simonsen, B. C., 2nd International Conference on Collision and Grounding (ICCGS), Copenhagen, Denmark, 1-3 July, 2001
- (HARDER, 2001a) “Collision Energy Distribution”, Technical University of Denmark, Report No.: 2-21-D-2000-01-1, Harmonisation of Rules and Design Rationale (HARDER), GRD1-1999-10721, 2001
- (HARDER, 2001b) “Damage Distributions”, Technical University of Denmark, Report No.: 2-22-D-2000-01-4, Harmonisation of Rules and Design Rationale (HARDER), GRD1-1999-10721, 2001
- (HARDER, 2003), “Final Technical Report”, Det Norske Veritas, Harmonisation of Rules and Design Rationale (HARDER), GRD1-1999-10721, 2003
- (Harrald et al., 1998), “ Using system simulation to model the impact of human error in a maritime system”, Harrald, J. R., Mazzuchi, T. A., Spahn, J., Van Dorp, R., Merrick, J., Shrestha, S. and Grabowski, M., Safety Science, Vol. 30, pp. 235-247, 1998
- (Hartog, 1952), “Advanced Strength of Materials”, J. P. Den Hartog, republished by Dover Publications in 1987, McGraw – Hill, 1952
- (Hausler et al., 2004), “Description of plastic anisotropy effects at large deformations - part II: the case of transverse isotropy”, Hausler, O., Schick, D., Tsakmakis, C., International Journal of Plasticity, 20, pp. 199-223, 2004
- (Heitzer, 1996), “Dynamic Interaction of a plate and an impactor”, Heitzer, J., Computers & Structures, Vol. 60, No. 5, pp. 837-848, 1996
- (Henley & Kumamoto, 1992), “Probabilistic Risk Assessment: Reliability, Engineering, Design and Analysis”, Henley, E. J. and Kumamoto, J., IEEE Press, 1992
- (Herbert Engineering, 2001), “Vertical extent of damage analysis”, Herbert Engineering Corp., HEC Report No-9933-2, Technical support to the

- “Harmonisation of Rules and Design Rationale – HARDER” project, February 2001
- (Hoppe, 2005), “Goal-Based Standards – A new approach to the international regulation of ship construction”, Hoppe, H., World Maritime University Journal of Maritime Affairs, Vol. 4, No. 2, 2005
- (Houtman et al., 2005), “Fatigue in the shipping industry”, Houtman, I., Miedema, M., Jettinghoff, K., Starren, A., Heinrich, J., Gort, J., Wulder, J. and Wubbolts, S., TNO Report 20834 / 11353, December 2005
- (HSE, 2000), “Collision resistance of ship-shaped structures to side impact”, MSL Engineering Ltd, Health and Safety Executive (HSE), OTO 053-2000
- (HSE, 2004), “Ship collision and capacity of brace members of fixed steel offshore platforms”, Visser Consultancy, Health and Safety Executive (HSE), Research Report 220, 2004
- (Huang et al., 2002), “Energy absorption in splitting square metal tubes”, Huang, X., Lu, G., Yu, T. X., Thin-Walled Structures 40, pp. 153–165, 2002
- (Hughes, 1995), “Ship Structural Design: A Rationally-Based, Computer-Aided Optimisation Approach”, Hughes, O. F., SNAME Publications 1995
- (Husky, 2000), “White Rose Oil Field development Application – Appendix D: Assessment of ship impact frequencies”, Husky Oil Operations Limited, July 2000
- (Iglesias et al., 2001), “Generating drop trajectories on parametric surfaces”, Iglesias, A., Puig-Pey, J., Gálvez, A., CAD/Graphics '01, Kunming, International Academic Publishers, 22-24 August, 2001
- (IMO, 1978), “International Convention of Standards of Training, Certification and Watchkeeping for Seafarers”, 1978; entry into force April 1984; last amended in July 1995 and entry into force in February 1997
- (IMO, 2002) “Guidelines for Formal Safety Assessment (FSA) for use in the IMO rule-making process”, MSC/Circ. 1023, April 2002

-
- (IMO, 2004) “Revised SOLAS Chapter II-1, Parts A, B and B-1”, International Maritime Organisation, Report to Maritime Safety Committee, SLF 47/17, 2004
- (IMO, 2006), “Adoption of amendments to the international convention of Safety of Life at Sea, 1974, as amended”, International Maritime Organisation, Resolution MSC.216(82), Annex 2, December 2006
- (IMO, 2009a), “Adoption of amendments to the international convention of Safety Of Life At Sea, 1974, as amended”, Resolution 216(82), Annex 2, 2009
- (IMO, 2009b), “FSA for Cruise Ships”, IMO MSC 85, Submitted by Denmark, May 2009
- (Jensen, 1996), “An Introduction to Bayesian Networks”, Jensen, F. V., Springer-Verlag New York Inc, 1996
- (Jensen & Nielsen, 2001), “Bayesian Networks and Decision Graphs”, Jensen, F. V. and Nielsen, T., Springer-Verlag New York Inc, 2001
- (Jones, 1979), “A literature survey on the collision and grounding protection of ships”, Jones, N., Ship Structure Committee, SSC-283, 1979
- (Jones, 1989), “Structural Impact”, Jones, N., Cambridge University Press, 1989
- (Jones & Shen, 1993), “Criteria for the inelastic rupture of ductile metal beams subjected to large dynamic loads”, Jones, N., Shen, W. Q., Structural Crashworthiness and Failure (Ch. 3), Edited by N. Jones and T. Wierzbicki, 1993
- (Jones, 1994), “Low velocity perforation of metal plates”, Jones, N., Shock and Impact on Structures, ed. Brebbia, C. A. and Sanchez-Galvez, V., Ch. 3, pp. 53-71, 1994
- (Jones, 1995), “Quasi-Static Analysis of Structural Impact Damage”, Jones, N., Journal of Constructional Steel Research 33, pp. 151-177, 1995

- (Jones, 1998), “Some recent developments and future trends in thin-walled sections for structural crashworthiness”, Jones, N., Technical Note in Thin-Walled Structures 32, pp. 231–233, 1998
- (Jones & Jones, 2002), “Inelastic failure of fully clamped beams and circular plates under impact loading”, Jones, N., Jones, C., Proceedings of the Institution of Mechanical Engineers, Part C: Journal of Mechanical Engineering Science, Vol. 216, No.2, pp. 133 – 149, 2002
- (Jones & Birch, 2006), “Low velocity perforation design of metal plates”, Jones, N. & Birch, R. S. , *Structures Under Shock and Impact IX*, WIT Transactions on the Built Environment, Vol. 87, pp.179-186
- (Kachanov, 1986), “Introduction to continuum damage mechanics”, Kachanov, L. M., Martinus Nijhoff Publishers, Dordrecht, 1986
- (Kaliszky & Logo, 2006), “Optimal design of elasto-plastic structures subjected to normal and extreme loading”, Kaliszky, S., Logo, J., Computers & Structures, Vol. 84, No. 28, pp. 1770-1779, 2006
- (Kao et al., 2007) “A fuzzy logic method for collision avoidance in Vessel Traffic Service”, Kao, S.L., Lee, K. T., Chang, K.Y. and Ko, M. D., The Journal of Navigation, Vol. 60, pp. 17-31, 2007
- (Kent, 2006), “Introduction to the IALA Risk Management Tool for Ports and Restricted Waterways”, Kent, P., IMO Sub-Committee on Safety of Navigation, www.iala-aism.org, 17 July, 2006
- (Khattab, 2007), “Brief Description of Manoeuvring Suite SIMX”, Khattab, O., Safety at Sea Ltd (www.safety-at-sea.co.uk), Internal Report, 2007
- (Kitamura, 1997), “Comparative study on collision resistance of side structure”, Kitamura, O., Marine Technology, Vol. 34, No. 4, pp. 293-308, 1997
- (Kitamura, 2001), “FEM approach to the simulation of collision and grounding damage”, Kitamura, O., 2nd International Conference on Collision and Grounding (ICCGS), Copenhagen, Denmark, 1-3 July, 2001

-
- (Komori, 1999), “Proposal for use of a void model for the simulation of ductile fracture behaviour”, Komori, K., *Acta Metallurgica*, 47, No. 10, pp. 3069-3077, 1999
- (Komori, 2005), “Ductile fracture criteria for simulating shear by node separation method”, Komori, K., *Theoretical and Applied Fracture Mechanics* 43, pp. 101–114, 2005
- (Konovessis & Vassalos, 2001), “ Integration of first-principle approaches to design for damage survivability”, Konovessis, D., Vassalos, D., 8th Practical Design of Ships and Other Floating Structures Conference (PRADS), Shanghai, China, 16-21 September, 2001
- (Konovessis, 2001), “A Risk-based Design Framework for Damage Survivability of Passenger Ro-Ro Vessels”, Konovessis, D., PhD Thesis, University of Strathclyde, 2001
- (Konovessis & Vassalos, 2003), “An implementation of a life-cycle risk-based design for safety methodology”, Konovessis, D., Vassalos, D., *Safety and Reliability Proceedings of the ESREL 2003 Conference*, Maastricht, The Netherlands, 15-18 June, 2003
- (Konovessis, 2007), “Risk analysis for ROPAX”, Konovessis, D., FP6 project SAFEDOR (IP-516278), Deliverable D4.2.2, February 2007
- (Konovessis et al., 2007), “Risk Analysis for RoPax Vessels”, Konovessis, D., Vassalos, D. and Mermiris, G., *International Symposium on Marine Safety, Security and Environmental Protection (SSE '07)*, Athens, Greece, 20-21 September, 2007
- (Krajcinovic, 1984), “Continuum Damage Mechanics”, Krajcinovic, D., *Applied Mechanics Reviews*, Vol. 37, No. 1, pp.1-6, 1984
- (Kriastiansen, 2005), “Maritime Transportation: Safety Management and Risk Analysis”, Kristianse, S., Elsevier Butterworth-Heinmann, 2005
- (Kuo, 1998) “Managing ship safety”, Kuo, C., LLP Professional Publishing, 1998

-
- (Langhaar, 1952), "Note on Energy of Bending of Plates", Langhaar, H. L., Journal of Applied Mechanics, Vol. 19, No. 2, June 1952
- (Le Sourme et al., 2003), "LS-DYNA Applications in shipbuilding", Le Sourme, H., Couty, N., Besnier, F., Krammerer, C., Legavre, H., 4th European LS-DYNA Users Conference, Ulm, Germany, 22-23 May, 2003
- (Leclere et al., 2004), "Rupture simulation of 3D elastoplastic structures under dynamic loading", Leclere, G., Neme, A., Cognard, Y. J., Berger, F., Computers & Structures, Vol. 82, pp. 2049-2059, 2004
- (Lehman & Yu, 1995), "Progressive flooding of bulbous bows", Lehman, E. and Yu, X., 6th International Symposium on Practical Design of Ships and Mobile Units (PRADS), September, 1995
- (Lehmann & Peschmann, 2002), "Energy absorption by the steel structure of ships in the event of collisions", Lehmann, E., Peschmann, J., Marine Structures 15, pp. 429–441, 2002
- (Lekhnitskii, 1968), "Anisotropic plates", Lekhnitskii, S. G., translated from the 2nd Russian edition by S. W. Tsai and T. Cheron, Gordon & Breach Science Publishers
- (Lellep & Torn, 2005), "Shear and bending response of a rigid-plastic beam subjected to impulsive loading", Lellep, J., Torn, K., International Journal of Impact Engineering 31, pp. 1081–1105, 2005
- (Lemaitre, 1984), "How to use damage mechanics", Lemaitre, J., Nuclear Engineering and Design, 80, pp. 233-245, 1984
- (Lemaitre, 1985), "A continuous damage mechanics model for ductile fracture", Lemaitre, J., Journal of Engineering Materials and Technology, Vol. 107, pp. 83-89, 1985
- (Liu & Wu, 2003), "The Human Element in Ship Collisions at Sea", Liu, Z., Wu, Z., Asia Navigation Conference, Kobe, Japan, 4 September, 2003

-
- (Liu & Wu, 2004), “A method for human reliability analysis in collision avoidance of ships”, Liu, Z., Wu, Z., Proceedings of the 3rd International Conference on Collision and Grounding of Ships (ICCGS), Izu, Japan, 25-27 October, 2004
- (Liua et al., 2005), “Structural intensity study of plates under low-velocity impact”, Liua, Z. S., Leeb, H. P., Lua, C., International Journal of Impact Engineering 31, pp. 957–975, 2005
- (Lutzen et al., 2000), “Rapid Prediction of Damage to Struck and Striking Vessels in a Collision Event”, Lützen, M., Simonsen, B. C., Pedersen, P. T., Ship structure Symposium, SNAME, 2000
- (Lutzen, 2001), “Ship Collision Damage”, Lutzen, M., PhD Thesis, Department of Naval Architecture and Offshore Engineering, Technical University of Denmark, 2001
- (Macduff, 1974), “The probability of vessel collisions”, Macduff, T., Ocean Industry, September 1974
- (MAIB, 2005), “Report of the investigation of the collision between Cepheus J and Ileksa in the Kattegat, 22 November 2004”, Marine Accident Investigation Branch (MAIB), www.maib.gov.uk, Report Number 12/2005, 2005
- (Majumder et al., 2005a) “Modelling and simulation of shipboard environment and operation”, Majumder, J., Vassalos, D., Guarin, L., Vassalos, G. C., 5th International EuroConference on Computer Applications and Information Technology in the Maritime Industries (COMPIT), Hamburg, Germany, 8-11 May, 2005
- (Majumder et al., 2005b) “Automated generation of shipboard environment model for simulation and design”, Majumder, J., Vassalos, D., Guarin, L., Vassalos, G. C., International Conference on Control Automation and Systems (ICCAS), Gyeong Gi, Korea, 2-5 June, 2005
- (McDermott et al., 1974), “Tanker structural analysis for minor collisions”, McDermott, J. F., Kline, R. G., Jones, E. L., Maniar, N. M., Chiang, W. P., SNAME Transactions, Vol. 82, pp. 382-407, 1974

-
- (Mermiris & Vassalos, 2007a), “A Generic Approach to Breach Size Assessment Following a Ship-Ship Collision Event”, Mermiris, G. and Vassalos, D., The Asialink-EAMARNET International Conference on Ship Design, Production and Operation, Harbin, China, pp. 38-43, 17-18 January, 2007
- (Mermiris et al., 2007b), “First-Principles Collision Analysis for Design”, Mermiris, G., Vassalos, D. and Konovessis, D., 1st International Conference on Marine Structures (MARSTRUCT 2007), pp. 217-223, Glasgow, UK, 12-14 March, 2007
- (Mermiris et al., 2007c), “A safety-driven framework for the navigation in restricted waterways”, Mermiris, G., Konovessis, D. and Vassalos, D., 2nd International Maritime – Port Technology and Development Conference (MTEC 2007), Singapore, 26-28 September, 2007
- (Micunovic, 1992), “Normality rule from plastic work extremals”, Micunovic, M. V., Material Science Forum Vol. 123-125 (1993) pp. 609-616 and in Proceedings of the 7th Symposium on Continuum Models of Discrete Systems, Paderborn, Germany, June 1992
- (Minorsky, 1959), “An analysis of ship collisions with reference to protection of nuclear power plants”, Minorsky, V. V., Journal of Ship Research, 1959
- (Moon, 1992), “Chaotic and Fractal Dynamics”, Moon, F. C., John Wiley & Sons Inc., 1992
- (Morino et al., 1971a), “An improved numerical calculation technique for large elastic-plastic transient deformations of thin shells - Part I: background and theoretical formulation”, Morino, L., Leech, J. W., Witmer, E. A., Journal of Applied Mechanics, pp. 423-428, June 1971
- (Morino et al., 1971b), “An improved numerical calculation technique for large elastic-plastic transient deformations of thin shells - Part II: evaluation and applications”, Morino, L., Leech, J. W., Witmer, E. A., Journal of Applied Mechanics, pp. 429-435, June 1971

- (Motora, 1960), "On the measurement of added mass and added moment of inertia of ships in steering motion", Motora, S., First Symposium on Ship Manoeuvrability, David Taylor Model Basin, Washington DC, pp. 241-273
- (Motora et al., 1971), "Equivalent added mass of ships in collisions", Motora, S., Fujino, M., Sugiura, M. and Sugita, M., Selected papers from the Journal of the Society of Naval Architects of Japan, No. 7, pp. 138-148, 1971
- (Naar et al., 2002) "Comparison of the crashworthiness of various bottom and side structures", Naar, H., Kujala, P., Simonsen, B. C., Ludolph, H., Marine Structures, Vol. 15, pp. 443-460, 2002
- (NORSOK, 1999), "NORSOK Standard – Actions and Action Effects (N-003)", NORSOK, February 1999
- (NORSOK, 2004), "NORSOK Standard – Design of Steel Structures (N-004)", NORSOK, October 2004
- (Oestvik, 2001) "A design for safety methodology", Oestvik, I., PhD Thesis, University of Strathclyde, 2001
- (Ohtsubo & Wang, 1996), "Strength of ships during collision and grounding", Ohtsubo, H., Wang, G., International Conference on Design Methodologies for Collision and Grounding Protection of Ships, San Francisco, California, August 22-23, 1996
- (Øresund, 2006), "Navigational safety in the sound between Denmark and Sweden (Øresund): Risk and Cost-benefit analysis", The Royal Danish Administration of Navigation and Hydrography, The Danish Maritime Authority, The Swedish Maritime Administration, [http://www.frv.dk/nyheder/indhold/R-568125-002-1\(Risk%20analysis\)MainReport.pdf](http://www.frv.dk/nyheder/indhold/R-568125-002-1(Risk%20analysis)MainReport.pdf), August 2006
- (Ozguç et al., 2005), "A comparative study on the structural integrity of single and double side skin bulk carriers under collision damage", Ozguç, O., Das, P. K., Barltrop, N., Marine Structures 18, pp. 511–547, 2005

-
- (Paik & Pedersen, 1996), "Modelling of internal mechanics of ship collisions", Paik, J. K. and Pedersen, P. T., *Marine Technology*, Vol. 34, No. 4, pp. 293-308, 1996
- (Paik & Wierzbicki, 1997), "A Benchmark Study on Crushing and Cutting of Plated Structures", Paik, J. K., Wierzbicki, T., *Journal of Ship Research*, Vol. 41, No. 2, pp. 147-160, 1997
- (Paik et al., 1999a), "On rational design of double hull tanker structures against collision", Paik, J. K., Chung, J. Y., Choe, I. H., Thayamballi, A. K., Pedersen, P. T., Wang, G., *SNAME Transactions*, Vol. 107, pp. 323-363, 1999
- (Paik et al., 1999b), "The strength characteristics of aluminium honeycomb sandwich panels", Paik, J. K., Thayamballi, A. G. and Kim, G. S., *Thin-walled Structures*, No. 35, pp. 205-231, 1999
- (Paik et al., 2004), "An Efficient and Accurate Finite Element Modelling Technique to Simulate Structural Crashworthiness in Collisions and Grounding", Paik, J. K., Thayamballi, A. K., Kang, H. Y., For publication in *Ships & Offshore Structures (SOS paper 0407, Submitted 17 November 2004)*
- (Paik & Seo, 2007), "A method for progressive structural crashworthiness analysis under collisions and grounding", Paik, J. K. and Seo, J. K., *Proceedings of the 1st International Conference on Marine Structures (MARSTRUCT 2007)*, pp. 241-248, Glasgow, UK, 12-14 March, 2007
- (Paté-Cornell & Regan, 1998), "Dynamic Risk Management Systems: Hybrid Architecture and Offshore Platform Illustration", Paté-Cornell, M. E. and Regan, J. P., *Risk Analysis*, Vol. 18, No. 4, 1998
- (Pawlowski, 1999), "Subdivision of RO/RO Ships for Enhanced Safety in the Damaged Condition", Pawlowski, M., *Marine Technology*, Vol. 36, No. 4, pp. 194-202, 1999
- (Pawlowski, 2005), "Probability of flooding a compartment (the p_i factor) – a critique and a proposal", Pawlowski, M., *Proceedings of Institute of*

-
- Mechanical Engineers, Vol. 219, Part M: J. Engineering for the Maritime Environment, 2005
- (Pedersen et al., 1993), "Ship Impacts: Bow Collisions", Pedersen, P. T., Valsgard, S., Olsen, D. and Spangenberg, S., International Journal of Impact Engineering, Vol. 13, No. 2, pp. 163-187, 1993
- (Pedersen & Zhang, 1998), "On impact mechanics in ship collisions", Pedersen, P. T. and Zhang, S., Marine Structures, No. 11, pp. 429-449, 1998
- (Pedersen & Zhang, 1999), "Collision analysis for MS Dextra", Pedersen, P. T. and Zhang, S., Paper No.2, SAFEREURORO Spring Meeting, Nantes, 1999
- (Pedersen & Zhang, 2000), "Absorbed energy in ship collisions and grounding: revising Minorsky's empirical method", Pedersen, P. T., Zhang, S., Journal of Ship Research, Vol. 44, No. 2, pp. 140-154, June 2000
- (Petersen, 1982), "Dynamics of ship collisions", Petersen, M. J., Ocean Engineering, Vol. 9, No. 4, pp. 295-329, 1982
- (Piegl & Tiller, 1997), "The NURBS book", Piegl, L. and Tiller, W., Springer, 2nd Edition, 1997
- (Puisa et al., 2009), "Design for safety with minimum life-cycle cost", Puisa, R., Vassalos, D. and Guarin, L., Proceedings of the 10th International Conference on Stability of Ships and Ocean Vehicles, St. Petersburg, Russia, 21st-26th June, 2009
- (Quek, 2003), "Surface parameterisation in volumetric images for curvature based feature classification", Quek, F. K. H., Yarger, R. W. I., Kirbas, C., IEEE Transactions on Systems, Man and Cybernetics—Part B: Cybernetics, Vol. 33, No. 5, October 2003
- (Ravn et al., 2006) "Modelling the causation factor for ship under power", Ravn, E., Hansen, P. F., Leva, C., Cernusco, A. and Lepsoe, A., FP6 project SAFEDOR (IP-516278), Deliverable D2.4.3, 2006

- (Rawson et al., 1998), "Assessing the Environmental Performance of Tankers in Accidental Grounding and Collision", Rawson, C., Crake, K., Brown, A., SNAME Transactions 106, pp. 41-58, 1998
- (Reason, 1990), "Human Error", Reason, J., Cambridge University Press, 1990
- (Reckling, 1983), "Mechanics of minor ship collisions", Reckling, K. A., International Journal of Impact Engineering, 1, pp. 281-299, 1983
- (Rigo et al., 2003), "Sensitivity analysis on ultimate strength of aluminium stiffened panels", Rigo, P., Sarghiuta, R., Estefen, S., Lehmann, E., Otelea, S. C., Pasqualino, I., Simonsen, B. C., Wan, Z., Yao, T., Marine Structures 16, pp. 437-468, 2003
- (Rothblum, 2000), "Human Error and Marine Safety", Rothblum, A., U.S. Coast Guard Research & Development Centre, Risk-based Decision Making Guidelines, Vol. 4 (<http://www.uscg.mil/hq/g-m/risk/e-guidelines/RBDMGuide.htm>), 2000
- (Ruan & Yu, 2005), "Collision between mass -spring systems", Ruan, H. H., Yu, T.X., International Journal of Impact Engineering, 31, pp. 267-288, 2005
- (Sajdak & Brown, 2004), "Modelling longitudinal damage in ship collision", Sajdak, J. A. W. and Brown, A. J., Ship Structure Committee, SSC-437, 2004
- (Samuelides, 1984), "Structural Dynamics and Rigid Body Response Coupling in Ship Collisions", Samuelides, E., PhD Thesis, University of Glasgow, 1984
- (Samuelides et al., 2008), "Scenarios for the assessment of the collision behaviour of ships", Samuelides, M. S., Tabri, K., Incecik, A. and Dimou, D., International Shipbuilding Progress, 55, pp. 145-162, 2008
- (Sastranegara et al., 2005), "Improvement of energy absorption of impacted column due to transverse impact", Sastranegara, A., Adachi, T., Yamaji, A., International Journal of Impact Engineering, 31, pp. 483-496, 2005
- (Servis & Samuelides, 1999), "Ship collision analysis using Finite Elements", Servis, D. P., Samuelides, M., Paper Number (x) SAFER EURORO Spring Meeting, Nantes, France, 28 April, 1999

-
- (Servis et al., 2002), “Implementation of Finite-Element Codes for the Simulation of Ship-Ship Collisions”, Servis, D., Samuelides, M., Louka, T., Voudouris, G., *Journal of Ship Research*, Vol. 46, No. 4, pp. 239–247, December 2002
- (Shachter, 1986), “Evaluating Influence Diagrams”, Shachter, R. D., *Operations Research* 34, No. 6, pp. 871-882, 1986
- (Shannon, 1948), “A Mathematical Theory of Communication”, Shannon, C. E., Reprinted with corrections from the *Bell System Technical Journal*, Vol. 27, pp. 379-423, pp. 623-656, July, October, 1948 (<http://cm.bell-labs.com/cm/ms/what/shannonday/shannon1948.pdf>)
- (Simonsen, 1997), “Mechanics of Ship Grounding”, Simonsen, B. C., PhD Thesis, Department of Naval Architecture and Offshore Engineering, Technical University of Denmark, 1997
- (Simonsen & Wierzbicki, 1997), “Plasticity, fracture and friction in steady-state plate cutting”, Simonsen, B. C., Wierzbicki, T., *International Journal of Impact Engineering*, Vol. 19, No. 8, pp.667-691, 1997
- (Simonsen & Ocakli, 1999), “Experiments and theory on deck and girder crushing”, Simonsen, B. C., Ocakli, H., *Thin-Walled Structures* 34, pp. 195–216, 1999
- (Simonsen & Lauridsen, 2000), “Energy absorption and ductile failure in metal sheets under lateral indentation by a sphere”, Simonsen, B. C. and Lauridsen, L. P., *International Journal of Impact Engineering*, Vol. 24, No. 10, pp. 1017-1039
- (Simonsen & Tornqvist, 2004), “Experimental and numerical modelling of ductile crack propagation in large-scale shell structures”, Simonsen, B. C., Tornqvist, R., *Marine Structures* 17, pp. 1–27, 2004
- (Sirkar et al., 1997), “A Framework for Assessing the Environmental Performance of Tankers in Accidental Groundings and Collisions”, Sirkar, J., Ameer, P., Brown, A., Goss, P., Michel, K., Willis, W., *SNAME Transactions* 105, pp. 253-295, 1997

-
- (Smith, 2007) "Chaos: A very short introduction", Smith, L., Oxford University Press, 2007
- (Skjong et al., 2005), "Risk Evaluation Criteria", Skjong, R., Vanem, E. and Endresen, O., FP6 project SAFEDOR (IP-516278), Deliverable D4.5.2, 2005
- (Sodhal, 2002), "Stena V-MAX: A total concept for safe oil transportation in confined waters", Sodhal, B., Maritime Technology, Vol. 39, No. 4, pp. 250-255, 2002
- (Spouge, 1996), "Safety Assessment of Passenger RoRo Vessels", Spouge, J., International Seminar on The Safety of Passenger Ro-Ro Vessels (presenting the results of the NorthWest European R&D Project), The Royal Institution of Naval Architects, London, 7 June, 1996
- (Squire, 2003), "The Hazards of Navigating the Dover Strait (Pas-de-Calais) Traffic Separation Scheme", Squire, D., Journal of Navigation, Vol. 56, pp. 195-210, 2003
- (Stewart, 1997), "Does God Play Dice? The new mathematics of chaos", Steart, I., Penguin Books, 1997
- (Struik, 1988), "Lectures on Classical Differential Geometry", Dirk J. Struik, 2nd Edition, Dover Publications, 1988
- (Swain & Guttmann, 1983), "Handbook of Human Reliability Analysis with Emphasis on Nuclear Power Plant Applications", Swain, A.D. and Guttman, H. E., NUREG / CR 1278, Albuquerque, N. M.: Sandia National Laboratories, 1983
- (Symonds, 1968), "Plastic shear deformation in dynamic load problems", Symonds, P. S., Engineering Plasticity Conference, Cambridge, pp. 647-664, March 1968
- (Teng & Wierzbicki, 2005), "Dynamic shear plugging of beams and plates with an advancing crack", Teng, X., Wierzbicki, T., International Journal of Impact Engineering 31, pp. 667-698, 2005

-
- (Thomson, 1955), "The formation of a conical crater in a thin plastic sheet", Thomson, W. T., *Journal of Applied Mechanics*, Vol. 22, pp. 175-176, June 1955
- (Timoshenko & Woinowski-Kreiger, 1964), "Theory of plates and shells", Timoshenko, S. P. & Woinowski-Kreiger, S., McGraw-Hill Publishing Co., 1964
- (Tornqvist, 2003), "Design of crashworthy ship structures", Tornqvist, R., PhD Thesis, Technical University of Denmark, 2003
- (Tsakmakis, 2004), "Description of plastic anisotropy effects at large deformations - part I: restrictions imposed by the second law and the postulate of Il'iusin", Tsakmakis, C., *International Journal of Plasticity*, 20, pp. 167-198, 2004
- (Vafai et al., 2003), "A modified approach to determine the energy dissipation capacity of the basic folding mechanism", Vafai, A., Shahbeyk, S., Kamalan, A., *Thin-Walled Structures* 41, pp. 835–848, 2003
- (Van Matter et al., 1979), "Critical evaluation of low energy ship collision damage theories and design methodologies: Evaluation and recommendations (Vol. I)", Van Matter, P. R., Giannotti, J. G., Jones, N. and Genalis, P., *Ship Structure Committee, SSC-284*, 1979
- (Vanem & Skjong, 2006), "Holistic and risk-based approach to collision damage stability of passenger ships", Vanem, E, Skjong, R., *Proceedings of the 9th International Conference on Stability of Ships and Ocean Vehicles (STAB2006)*, Sao Paulo, Brazil, 25-29 September, 2006
- (Vassalos, 2000), "Shaping Ship Safety: The Face of the Future", Vassalos, D., *Marine Technology*, Vol. 36, No. 2, pp. 61 – 76, 2000
- (Vassalos et al., 2000a), "Recent Developments and Application of a Formalised Design for Safety Methodology in an Integrated Environment", Vassalos, D., Oestvik, I., Konovessis, D., *SNAME Transactions*, Vol. 108, pp. 419-442, 2000
- (Vassalos et al., 2000b), "Design for Safety: Development and Application of a Formalised Methodology", Vassalos, D., Oestvik, I., Konovessis, D.,

-
- Proceedings of the 7th International Marine Design Conference (IMDC), Kyongju, Korea, pp. 151-165, 21-24 May, 2000
- (Vassalos et al., 2003), “A Risk-Based Framework on Ship Design for Safety”, Vassalos, D., Konovessis, D., Vassalos, G. C., Proceedings of the 8th International Marine Design Conference (IMDC), Athens, Greece, pp. 225-239, 5-8 May, 2003
- (Vassalos, 2004), “A risk-based approach to probabilistic damage stability”, Vassalos, D., Proceedings of the 7th International Ship Stability Workshop, Shanghai, November 2004
- (Vassalos et al., 2004), “Effectiveness of passenger evacuation performance for design, operation and training using first-principles simulation tools”, Vassalos, D., Guarin, L., Bole, M., Majumder, J., Vassalos, G. C., Kim, H., Escape, Evacuation and Recovery, Lloyds List Events, London, March 2004
- (Vassalos et al., 2005a), “Fundamental Concepts of Risk-Based Ship Design”, Vassalos, D., Konovessis, D., Guarin, L., Proceedings of the 11th International Congress of the International Maritime Association of the Mediterranean (IMAM), Lisbon, Portugal, 26-30 September, 2005
- (Vassalos et al., 2005b), “Passenger Ship Safety – Science Paving the Way”, Vassalos, D., Jasionowski, A., and Guarin, L., Proceedings of the 8th International Ship Stability Workshop, Istanbul, Turkey, October 2005
- (Vassalos et al., 2006a), “Risk-Based Ship Design Implementation – Riding the Learning Curve”, Vassalos, D., Guarin, L., Konovessis, D., Proceedings of the 9th International Marine Design Conference (IMDC), Ann Arbor, Michigan, US, May 2006
- (Vassalos et al., 2006b), “Design Implications of the New Harmonised Probabilistic Damage Stability Regulations”, Vassalos, D., York, A., Jasionowski, A., Kanerva, M. and Scott, A., Proceedings of the 9th International Conference on Stability of Ships and Ocean Vehicles (STAB 2006), Rio de Janeiro, Brazil, 25-29 September, 2006

- (Vassalos and Jasionowski, 2007), “SOLAS 2009 – Raising the alarm”, Vassalos, D. and Jasionowski, A., Proceedings of the 10th International Ship Stability Workshop, August 2007
- (Vassalos, 2007), “Safe Return to Port – A framework for passenger ship safety”, Vassalos, D., Proceedings of the 10th International Symposium on Practical Design of Ships and Other Floating Structures (PRADS '07), Houston, Texas, 2007
- (Vassalos, 2009), “Design for Safety”, Vassalos, D., chapter in the paper titled “State of the Art Report on Design for X”, Papanikolaou, A., Andersen, P., Kristensen, H. O., Levander, K., Riska, K., Singer, D., McKenney, T. A. and Vassalos, D., Proceedings of the International Marine Design Conference (IMDC) 2009, Trondheim, Norway, May 2009
- (Vlassak et al., 2003), “The indentation modulus of elastically anisotropic materials for indenters of arbitrary shape”, Vlassak, J. J., Ciavarella, M., Barber, J. R., Wang, X., Journal of the Mechanics and Physics of Solids, 51, pp.1701 – 172, 2003
- (Vose, 2000), “Risk Analysis: A Quantitative Guide”, Vose, D., John Wiley & Sons, Ltd, 2nd Edition, 2000
- (Vredeveldt, 2001a), “Crashworthiness as means to improve damage stability survivability”, Vredeveldt, A., Netherlands Organisation for Applied and Scientific Research (TNO), <http://crashcoaster.rtdproject.net/>, 2001
- (Vredeveldt, 2001b), “Two examples of applied scientific research in ship safety”, Vredeveldt, A., WEGEMT Annual Conference, October 2001
- (Vredeveldt, 2005), “Crashworthiness”, Vredeveldt, A., Training Course on Risk-Based Ship Design, Universities of Glasgow and Strathclyde, Glasgow, UK, 7-8 June, 2005
- (Wang, 1970), “Large plastic deformation of a circular sheet caused by punch stretching”, Wang, N. M., Journal of Applied Mechanics, pp. 431-440, June 1970

- (Wang et al., 2000), “Behaviour of a double hull in a variety of stranding or collision scenarios”, Wang, G., Arita, K., Liu, D., *Marine Structures* 13, pp. 147-187, 2000
- (Wang et al., 2003), “Consideration of Collision and Contact Damage Risks in FPSO Structural Designs”, Wang, G., Jiang, D. and Shin, Y., *Offshore Technology Conference (OTC)*, Houston, US, 5-8 May, 2003
- (Wang et al., 2005), “Dynamic plastic response of a circular plate based on unified strength theory”, Wang, Y. B., Yu, M. H., Xiao, Y., Li, L. S., *International Journal of Impact Engineering* 31, pp. 25–40, 2005
- (Weisstein, 1999a), “Elliptic Paraboloid”, Weisstein, E. W. from MathWorld – A Wolfram Web Resource, <http://mathworld.wolfram.com/EllipticParaboloid.html>, 1999
- (Weisstein, 1999b), “Paraboloid”, Weisstein, E. W. from MathWorld – A Wolfram Web Resource, <http://mathworld.wolfram.com/Paraboloid.html>, 1999
- (Weisstein, 2002), “Vieta’s Formulas”, Weisstein, E. W. from MathWorld – A Wolfram Web Resource, <http://mathworld.wolfram.com/VietasFormulas.html>, 2002
- (Weisstein, 2004), “Witch of Agnesi”, Weisstein, E. W. from MathWorld – A Wolfram Web Resource, <http://mathworld.wolfram.com/WitchofAgnesi.html>, 2004
- (Weisstein, 2005), “Buffon’s Needle Problem”, Weisstein, E. W. from MathWorld – A Wolfram Web Resource, <http://mathworld.wolfram.com/BuffonsNeedleProblem.html>, 2005
- (Wen & Jones, 1992), “Semi-empirical equations for the perforation of plates struck by a mass”, Wen, H. M., Jones, N., *Structures under Shock and Impact*, 2nd International Conference, Portsmouth, UK, pp. 114-132, 16-18 June, 1992
- (Wendel, 1960), “Die Wahrscheinlichkeit des Uberstehens von Verletzungen”, Wendel, K., *Schiffstechnik*, Vol. 7, No. 36, pp.47-61, 1960

- (Wendel, 1968), “Subdivision of Ships”, Wendel, K., Diamond Jubilee International Meeting – 75th Anniversary, SNAME, New York, paper No. 12, 1968
- (White & Molloy, 2003), “ Factors that determine the cost of oil spills”, White, I. C. and Molloy, F. C., International Oil Spill Conference (IOSC), Vancouver, Canada, 6-11 April, 2003 (www.itopf.com)
- (Wierzbicki & Driscoll, 1995), “Crushing damage of web girders under localised static loads”, Wierzbicki, T, Driscoll, J. C., Journal of Constructional Steel Research, 33, pp. 199-235, 1995
- (Williams, 1997) “Chaos Theory Tamed”, Williams, G. P., Joseph Henry Press, 1997
- (Wisniewski et al., 2001), “Dynamic FE simulation of damage in ships collision”, Wisniewski, K., Kolakowski, P., Rozmarynowski, B. and Gierlinski, J. T., 2nd International Conference on Collision and Grounding (ICCGS), Copenhagen, Denmark, 1-3 July, 2001
- (Wu et al., 2004), “Using numerical simulation to analyse ship collision”, Wu, F., Spong, R. Wang, G., 3rd International Conference on Collision and Grounding of Ships (ICCGS), Japan, 25-27 October, 2004
- (Yefimov et al., 2004), “A comparison of a statistical-mechanics based plasticity model with discrete dislocation plasticity calculations”, Yefimov, S., Groma, I., Giessena, E. van der, Journal of the Mechanics and Physics of Solids, 52, pp. 279 – 300, 2004
- (Zhang, 1999), “The Mechanics of Ship Collisions”, Zhang, S., PhD Thesis, Technical University of Denmark, 1999
- (Zhang et al., 2004), “Approved procedure concept for alternative arrangements”, Zhang, L., Egge, E. D. and Bruhns, H., Proceedings of the 3rd International Conference on Collision and Grounding of Ships (ICCGS), Izu, Japan, 25-27 October, 2004
- (Zhang & Vassalos, 2007), “Capsize probability of damaged Ro-Ro passenger ships”, Zhang, Y., Vassalos, D., International Conference on Ship Design, Production and Operation, Harbin, China, 17-18 January, 2007

-
- (Zheng et al., 2007), "Study on the side structure resistance to ship-ship collisions", Zheng, Y., Aksu, S., Vassalos, D. and Tuzcu, C., *Ships and Offshore Structures*, Vol. 2, No. 3, pp.273-293, 2007
- (Zhu, 1990), "Dynamic Inelastic Behaviour of Ship Plates in Collision", Zhu, L., PhD Thesis, University of Glasgow, 1990
- (Zhu & Cescotto, 1992), "A fully coupled elastoplastic damage modelling between two deformable bodies", Zhu, Y. Y., Cescotto, S., *Structures under Shock and Impact*, 2nd International Conference, Portsmouth, UK, pp. 114-132, 16-18 June, 1992

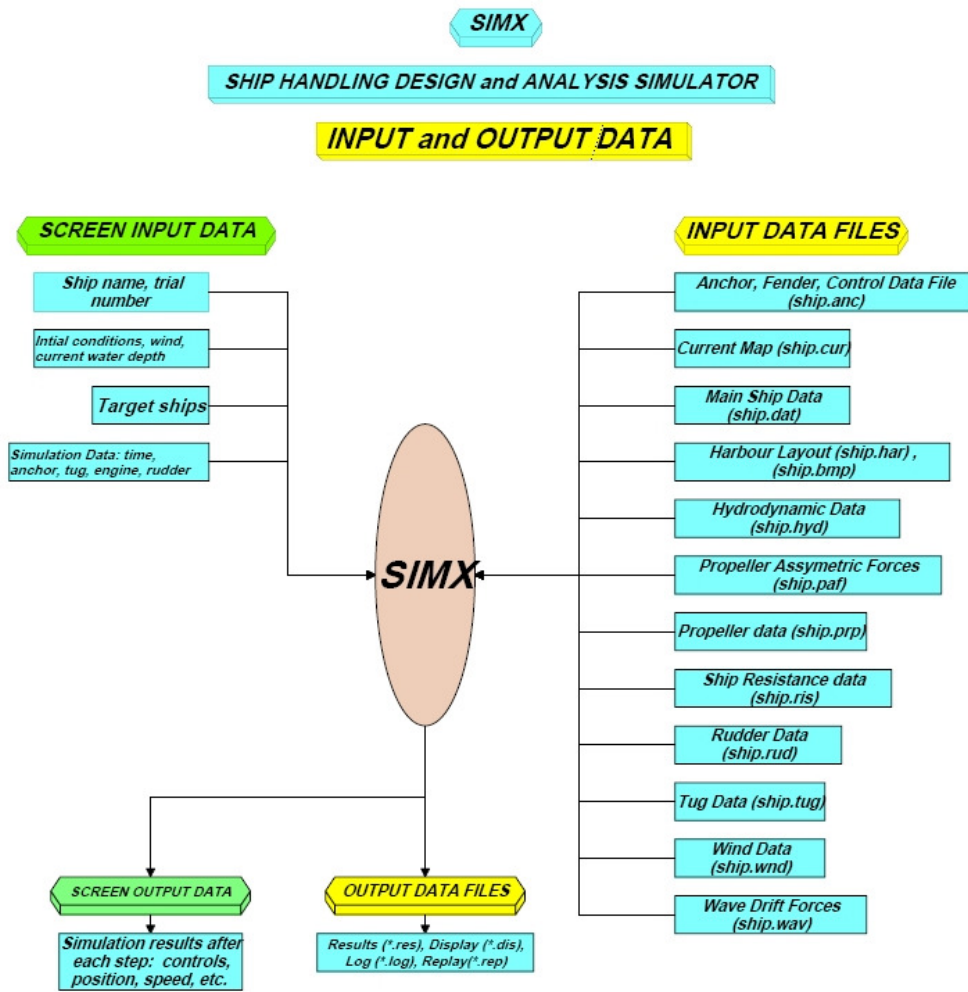
Appendix A: SIMX5

The Ship Handling Design and Analysis Simulator “SIMX” has been designed to provide an accurate simulation of ship handling of a given ship in a wide range of conditions such as low speed, confined water and different environmental conditions. SIMX is based upon extensive theoretical and experimental research work carried out by Dr Omar Khattab and other published work by many researchers. Full scale and model test data were used to validate and check the results of the model. SIMX encompasses more than 35 years of the author’s experience in research and development in the field of simulation of ship handling in different conditions.

SIMX simulates the ship handling performance for a given condition in a step by step approach. The operator manages the control devices such as rudder(s), propeller(s), thruster(s), tug(s), etc. and specifies the required time of control applications as the simulation progresses. SIMX will calculate the ship handling performance at the specified condition and displays the results on the screen. The displayed results show ship position on the chart and detailed information about the ship position, speed, acceleration, squat, current and wind data. The operator assesses the ship performance and decides on the next manoeuvre. The time interval between manoeuvres is determined by the ship operator.

SIMX is subject of continuous development to including up to date research and technological development in the field of ship handling simulation and data presentation. The program is in continuous use for simulation of ship handling, investigation of ship manoeuvring, IMO manoeuvring standards, manoeuvring booklet, port design, tug estimation, design of steering devices, re-construction of ship collisions, incidents of berth damage, groundings, and other casualties. The program allows in depth analyses of manoeuvres. The expertise of ship masters, harbour pilots, tug skippers, port authorities, port designers and casualty investigators are combined together to achieve a well-balanced solution taking into account a wide range of experience and expertise.

More thorough information about SIMX can be found in (Khattab, 2007) and <http://hydrosim.mysite.wanadoo-members.co.uk/>.



The functionality of SIMX in terms of input and output data

Appendix B: Surface representation

B.1 Introduction

The derivation of the principle radii of curvature of a surface is briefly presented here along with some applications of fundamental shapes towards the end of the chapter. The chapter is concluding with an introduction to Bezier surfaces for the purposes of striking body representation. More detailed elaboration on parametric surface definition can be found in (Struik, 1988). The basic source for the material related to Bezier surfaces comes from (Piegl & Tiller, 1997).

B.2 Surface definition

Assuming a right-handed coordinate system xyz , a surface is expressed in a parametric form of two independent real variables (say u and v) within a closed interval as follows (boldface representation indicates a vector):

$$\left\{ \begin{array}{l} \mathbf{x} = \mathbf{x}(u, v) \\ y = y(u, v) \\ z = z(u, v) \end{array} \right\} \text{ or } x_i = x_i(u, v) \text{ or } \mathbf{x} = \mathbf{x}(u, v) \quad (\text{B.1})$$

$$\forall u \in [u_1, u_2] \text{ and } v \in [v_1, v_2], \quad i = 1, 2 \text{ and } 3$$

Functions x_i should be continuous and differentiable within the given interval, at least up to order of $n-1$, and the n -th derivatives should exist. Then we can expand them using the Taylor series approach as follows:

$$\begin{aligned} x_i(u, v) = & x_i(u_0, v_0) + h \left(\frac{\partial x_i}{\partial u} \right)_0 + k \left(\frac{\partial x_i}{\partial v} \right)_0 + \frac{1}{2!} \left(h \frac{\partial}{\partial u} + k \frac{\partial}{\partial v} \right)_0^2 x_i + \dots \\ & + \frac{1}{(n-1)!} \left(h \frac{\partial}{\partial u} + k \frac{\partial}{\partial v} \right)_0^{n-1} x_i + \frac{1}{n!} \left(h \frac{\partial}{\partial u} + k \frac{\partial}{\partial v} \right)_0^n x_i(u_0 + \theta h, v_0 + \theta k), \theta \in (0, 1) \end{aligned}$$

The three – dimensional character of the surface is guaranteed if u and v enter the definition of it as independent variables. That is, the rank of matrix M (i.e. the size of its largest non-zero determinant) is 2:

$$M = \begin{bmatrix} \frac{\partial x}{\partial u} & \frac{\partial y}{\partial u} & \frac{\partial z}{\partial u} \\ \frac{\partial x}{\partial v} & \frac{\partial y}{\partial v} & \frac{\partial z}{\partial v} \end{bmatrix} = \begin{bmatrix} x_u & y_u & z_u \\ x_v & y_v & z_v \end{bmatrix}$$

Another useful way to define a surface is by using the notion of the *vector* as presented in (B.1) and write:

$$\mathbf{x} = \mathbf{x}(u, v) = x \mathbf{i} + y \mathbf{j} + z \mathbf{k}$$

The condition for avoiding discontinuities (singular points) on the surface could then be expressed as the cross product of two vectors:

$$\begin{aligned} \mathbf{x}_u \times \mathbf{x}_v &\neq 0 \\ \mathbf{x}_u &= \frac{\partial \mathbf{x}}{\partial u} \text{ and } \mathbf{x}_v = \frac{\partial \mathbf{x}}{\partial v} \end{aligned} \quad (\text{B.2})$$

Equation (B.2) can be interpreted geometrically when we keep one of the variables constant and vary the other within the interval of definition. For example, when we keep u constant, we create a family of curves for all the values of v since \mathbf{x} depends only on v . In the same manner we could keep v constant and vary u . In both cases we created a net of parametric curves which define the surface in the three dimensional space. The vector \mathbf{x}_u will be tangent to constant v – curves and the vector \mathbf{x}_v to the constant u – curves, as presented in Figure B.1. In this way the familiar curvilinear coordinates are defined.

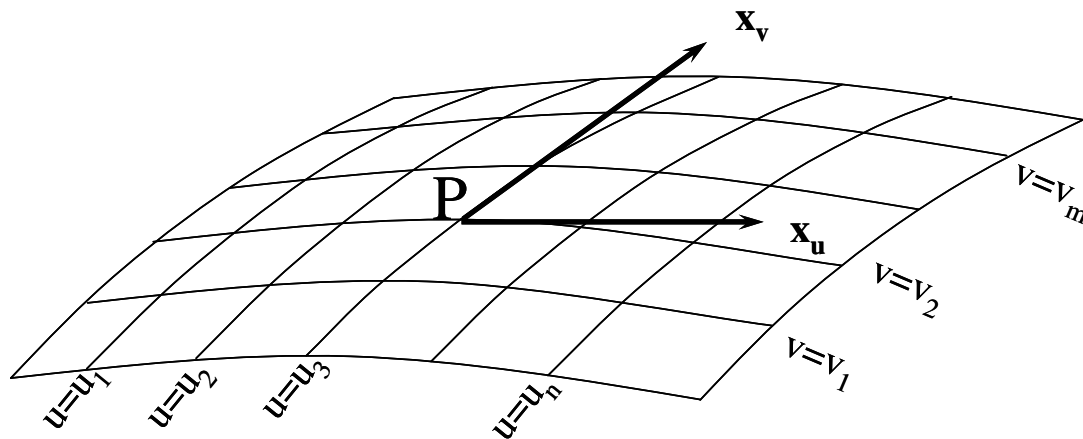


Figure B.1: Surface definition

B.3 Fundamental surface forms

Further to the basic definitions presented in the previous paragraph, the fundamental forms of a surface are briefly described in the following lines. These are the 1st and the 2nd Fundamental Form and their definition will directly lead to the evaluation of the curvature of a surface at a point.

B.3.1 1st Fundamental Form

Considering the way we recently defined a surface as a net of parametric curves, we could claim that a curve on this surface is determined by some function f of the independent variables u and v either in an explicit form of the type $f(u,v) = 0$ or implicitly in a parametric fashion:

$$u = u(t), v = v(t)$$

The second approach is not always possible for the functions we use.

If we adopt the convention to express the derivative with respect to t in the form of $(\dot{\cdot})$, then the vector $\dot{\mathbf{x}} = d\mathbf{x}/dt$ (tangent to the curve and therefore to the surface) at a point P of the surface is given by:

$$\dot{\mathbf{x}} = \frac{d\mathbf{x}}{dt} = \frac{d\mathbf{x}}{du} \frac{du}{dt} + \frac{d\mathbf{x}}{dv} \frac{dv}{dt} = \mathbf{x}_u \dot{u} + \mathbf{x}_v \dot{v} \quad (\text{B.3})$$

Equation (B.3) can be written in a differential form independent of the choice of parameter. That is,

$$d\mathbf{x} = \mathbf{x}_u du + \mathbf{x}_v dv \quad (\text{B.4})$$

The distance between point P and another point on the surface, say Q , can be obtained by :

$$ds^2 = \sum_{i=1}^3 dx_i dx_i = d\mathbf{x} \cdot d\mathbf{x} \quad (\text{B.5})$$

Combining (B.4) and (B.5) we derive the 1st Fundamental Form of a surface.

$$ds^2 = (\mathbf{x}_u du + \mathbf{x}_v dv) \cdot (\mathbf{x}_u du + \mathbf{x}_v dv) = Edu^2 + 2Fdudv + Gdv^2 \quad (\text{B.6})$$

$$\text{where } E = \mathbf{x}_u \cdot \mathbf{x}_u, F = \mathbf{x}_u \cdot \mathbf{x}_v \text{ and } G = \mathbf{x}_v \cdot \mathbf{x}_v$$

Its square root is equal to the modulus of the vector differential $|d\mathbf{x}|$ and it is called *element of arc*. As long as we study real surfaces, the first fundamental form is always positive definite: $Edu^2 + 2Fdudv + Gdv^2 > 0$ (unless of course $du = dv = 0$).

Quantities E , F and G can be used to express the angle of two tangent directions to the surface, say du/dv and $\delta u/\delta v$. Then, given that $d\mathbf{x} = \mathbf{x}_u du + \mathbf{x}_v dv$ and $\delta \mathbf{x} = \mathbf{x}_u \delta u + \mathbf{x}_v \delta v$, we can find the angle α from the definition of the dot product:

$$\cos \alpha = \frac{\mathbf{dx} \cdot \delta \mathbf{x}}{|\mathbf{dx}| |\delta \mathbf{x}|} = \frac{Edu\delta u + F(du\delta v + dv\delta u) + Gdv\delta v}{\sqrt{Edu^2 + 2Fdu\delta v + Gdv^2} \sqrt{E\delta u^2 + 2F\delta u\delta v + G\delta v^2}} \quad (\text{B.7})$$

When $\alpha = \pi/2$, we obtain the condition of *orthogonality* between two directions on the surface: $Edu\delta u + F(du\delta v + dv\delta u) + Gdv\delta v = 0$

The angle θ between the parametric lines is given by:

$$\cos \theta = \frac{Fdv\delta u}{\sqrt{Gdv^2} \sqrt{E\delta u^2}} = \frac{F}{\sqrt{EG}}$$

$$\sin \theta = \sqrt{1 - \cos^2 \theta} = \frac{\sqrt{EG - F^2}}{\sqrt{EG}}$$

From the last equation we see that if $F = 0$ then $\alpha = 90^\circ$ which means that the parametric curves are orthogonal. This is an important conclusion for the rest of the discussion and we will recall it later.

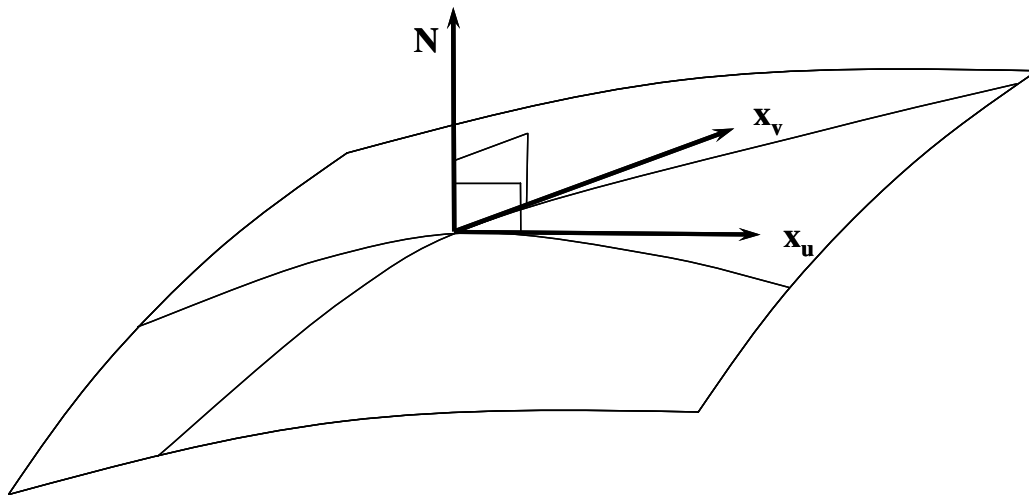


Figure B.2: The principal normal unit vectro

B.3.2 Principal Normal of a surface

All vectors $d\mathbf{x}/dt$ through P tangent to the surface satisfy (B.3) and therefore lie in the plane of the vectors \mathbf{x}_u and \mathbf{x}_v , for non-singular points (as expressed by (B.2)). This is the tangent plane at point P to the surface with equation $\mathbf{X} = \mathbf{x} + \lambda\mathbf{x}_u + \mu\mathbf{x}_v$ (λ and μ are real parameters). The derivatives are taken with respect to point P(x,y,z) and are considered real and continuous.

The surface normal is the line perpendicular to the tangent plane at a point. The unit vector \mathbf{N} in this direction is defined as:

$$\mathbf{N} = \frac{\mathbf{x}_u \times \mathbf{x}_v}{|\mathbf{x}_u| |\mathbf{x}_v|} = \frac{\mathbf{x}_u \times \mathbf{x}_v}{\sqrt{EG - F^2}} \quad (\text{B.8})$$

With some algebraic manipulations of (B.6) we can get:

$$ds^2 = \frac{1}{E} (Edu + Fdv)^2 + \frac{EG - F^2}{E} dv^2$$

Since ds^2 is always positive and $E = \mathbf{x}_u \cdot \mathbf{x}_u > 0$ we see that $EG - F^2$ is positive definite.

B.3.3 2nd Fundamental Form

The 2nd Fundamental Form of a surface is obtained by taking a curve C on it which passes through a point P and by considering the curvature vector of C at P . If \mathbf{t} is the unit tangent vector of C , the curvature vector \mathbf{k} will be equal to $d\mathbf{t}/ds$. If we decompose \mathbf{k} , we get $\mathbf{k} = \mathbf{k}_n + \mathbf{k}_g = d\mathbf{t}/ds$.

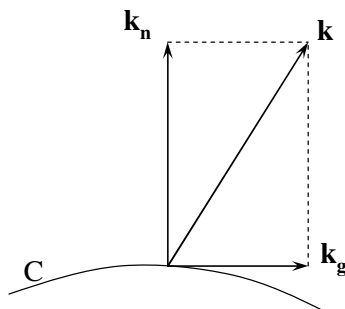


Figure B.3: Total curvature vector decomposed into its components

The vector \mathbf{k}_n is the normal curvature vector determined by C alone and can be expressed in terms of the unit vector \mathbf{N} : $\mathbf{k}_n = \kappa_n \mathbf{N}$, where the scalar κ_n is the normal curvature. Its sign depends on the sign of \mathbf{N} . \mathbf{k}_g is the tangential or geodesic curvature vector and it is of no immediate interest. By differentiating $\mathbf{N} \cdot \mathbf{t} = 0$ along the curve C we get:

$$\frac{d\mathbf{t}}{ds} \cdot \mathbf{N} = -\mathbf{t} \cdot \frac{d\mathbf{N}}{ds} = -\frac{d\mathbf{x}}{ds} \cdot \frac{d\mathbf{N}}{ds} \text{ or } \kappa_n \mathbf{N} \cdot \mathbf{N} = \kappa_n = -\frac{d\mathbf{x} \cdot d\mathbf{N}}{d\mathbf{x} \cdot d\mathbf{x}} \quad (\text{B.9})$$

Now, both \mathbf{N} and \mathbf{x} are functions of u and v , which in turn depend on C . The differentials of these two vectors are: $d\mathbf{N} = \mathbf{N}_u du + \mathbf{N}_v dv$ and $d\mathbf{x} = \mathbf{x}_u du + \mathbf{x}_v dv$. Substituting them in (B.9) we get the following expression for κ_n :

$$\kappa_n = -\frac{(\mathbf{x}_u \cdot \mathbf{N}_u)du^2 + (\mathbf{x}_u \cdot \mathbf{N}_v + \mathbf{x}_v \cdot \mathbf{N}_u)dudv + (\mathbf{x}_v \cdot \mathbf{N}_v)dv^2}{Edu^2 + 2Fdudv + Gdv^2} \quad (\text{B.10})$$

$$\text{or } \kappa_n = \frac{edu^2 + 2fdudv + gdv^2}{Edu^2 + 2Fdudv + Gdv^2}$$

where $e = -\mathbf{x}_u \cdot \mathbf{N}_u$, $2f = -(\mathbf{x}_u \cdot \mathbf{N}_v + \mathbf{x}_v \cdot \mathbf{N}_u)$, $g = -\mathbf{x}_v \cdot \mathbf{N}_v$ are functions of u and v and depend on second derivatives of \mathbf{x} with respect to u and v (due to the presence of the vector \mathbf{N} – see Equation (B.8)). For this reason e , f and g can be further expressed as:

$$E = \mathbf{x}_{uu} \cdot \mathbf{N}, \quad f = \mathbf{x}_{uv} \cdot \mathbf{N} \quad \text{and} \quad g = \mathbf{x}_{vv} \cdot \mathbf{N}$$

On the other hand, factors E , F and G depend on the first derivatives of u and v . Using (B.8) for \mathbf{N} we can get the following expressions which allow for the computation of e , f and g once the equation of the surface is provided.

$$\mathbf{e} = \mathbf{x}_{uu} \cdot \mathbf{N} = \mathbf{x}_{uu} \cdot \frac{\mathbf{x}_u \times \mathbf{x}_v}{\sqrt{EG - F^2}} = \frac{\mathbf{x}_{uu} \mathbf{x}_u \mathbf{x}_v}{\sqrt{EG - F^2}} = \frac{\begin{vmatrix} x_{uu} & y_{uu} & z_{uu} \\ x_u & y_u & z_u \\ x_v & y_v & z_v \end{vmatrix}}{\sqrt{EG - F^2}}$$

$$\text{and similarly, } f = \frac{\mathbf{x}_{uv} \mathbf{x}_u \mathbf{x}_v}{\sqrt{EG - F^2}} \quad \text{and} \quad g = \frac{\mathbf{x}_{vv} \mathbf{x}_u \mathbf{x}_v}{\sqrt{EG - F^2}}$$

In (B.9) and (B.10), we see that the right-hand side depends only on u , v and dv/du . The coefficients e , f , g , E , F and G are constants at point P and therefore κ_n is fully determined at P by the direction dv/du . All curves through P , tangent to the same direction, have the same normal curvature vector (assuming that the sense of \mathbf{N} is the same for all of them).

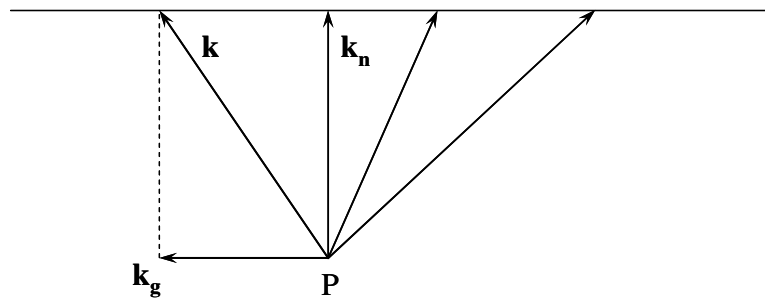


Figure B.4: Same normal curvature vector irrespective of direction

B.3.4 Principal curvatures

The normal curvature in the direction du/dv is given by (B.10) which is reproduced here slightly modified and assigning $\lambda = dv/du$:

$$\kappa_n = \frac{e du^2 + 2f du dv + g dv^2}{E du^2 + 2F du dv + G dv^2} = \frac{e + 2f\lambda + g\lambda^2}{E + 2F\lambda + G\lambda^2} = \kappa(\lambda) \quad (\text{B.11})$$

The extreme values of κ can be found if $d\kappa/d\lambda = 0$. That is,

$$(E + 2F\lambda + G\lambda^2)(f + g\lambda) - (e + 2f\lambda + g\lambda^2)(F + G\lambda) = 0$$

Since

$$E + 2F\lambda + G\lambda^2 = (E + F\lambda) + \lambda(F + G\lambda)$$

$$e + 2f\lambda + g\lambda^2 = (e + f\lambda) + \lambda(f + g\lambda)$$

we can manipulate (B.11) into the form

$$\kappa = \frac{f + g\lambda}{F + G\lambda} = \frac{e + f\lambda}{E + F\lambda}$$

Therefore, κ can simultaneously satisfy the following two equations

$$(E\kappa - e) + (F\kappa - f)\lambda = 0$$

$$(F\kappa - f) + (G\kappa - g)\lambda = 0$$

By eliminating κ we obtain a quadratic equation with respect to λ with real roots:

$$(Fg-Gf)\lambda^2 + (Eg-Ge)\lambda + (Ef-Fe) = 0$$

The last equation determines the two directions in which κ obtains its extreme values (unless the 2nd Fundamental Form is zero or proportional to the 1st). The two values must be one minimum and one maximum and the directions in which they occur are called *directions of principle curvature* or *curvature directions*. Making use of Vieta's formulas, (Weisstein, 2002), λ_1 and λ_2 will satisfy

$$\begin{aligned} & G\lambda_1\lambda_2 + F(\lambda_1 + \lambda_2) + E \\ &= -\frac{1}{gF - Gf} [G(eF - Ef) - F(eG - Eg) - E(gF - Gf)] = 0 \end{aligned}$$

we see that the curvature directions are *orthogonal*.

In order to obtain the values of curvature, we observe that:

$$\left\{ \begin{array}{l} (E\kappa - e) + (F\kappa - f)\lambda = 0 \\ (F\kappa - f) + (G\kappa - g)\lambda = 0 \end{array} \right\} \text{ or } \begin{vmatrix} E\kappa - e & F\kappa - f \\ F\kappa - f & G\kappa - g \end{vmatrix} = 0 \quad (\text{B.12})$$

This is a quadratic equation with roots κ_1 and κ_2 which admittedly is quite complicated as is depicted in the following examples. The alternative approach is to apply the Vieta's formulas once more:

$$\begin{aligned} M &= \frac{1}{2}(\kappa_1 + \kappa_2) = \frac{Eg - 2fF + eG}{2(EG - F^2)} \text{ mean curvature} \\ K &= \kappa_1\kappa_2 = \frac{eg - f^2}{EG - F^2} \text{ Gaussian or total curvature} \end{aligned} \quad (\text{B.13})$$

Considering that the radius of curvature is the inverse of the curvature, (B.13) can be modified into the more convenient form of:

$$M = \frac{1}{2} \left(\frac{1}{r_1} + \frac{1}{r_2} \right) \text{ and } K = \frac{1}{r_1} \frac{1}{r_2} \quad (\text{B.14})$$

B.4 Fundamental surfaces

The above theoretical results are useful in the study of some fundamental surfaces. Despite their theoretical interest, they can be used in idealised situations for studying the response of stiffened panels in various situations. That is, they can be used in elementary optimisation of a stiffened panel during design, assessment of different alternatives or even for theoretical modelling of lab experiments and result processing.

B.4.1 Sphere

The parametric equations of a sphere of radius r are following. Figure B.5 is presenting a section of it. The angles θ and φ correspond to the independent variables u and v respectively.

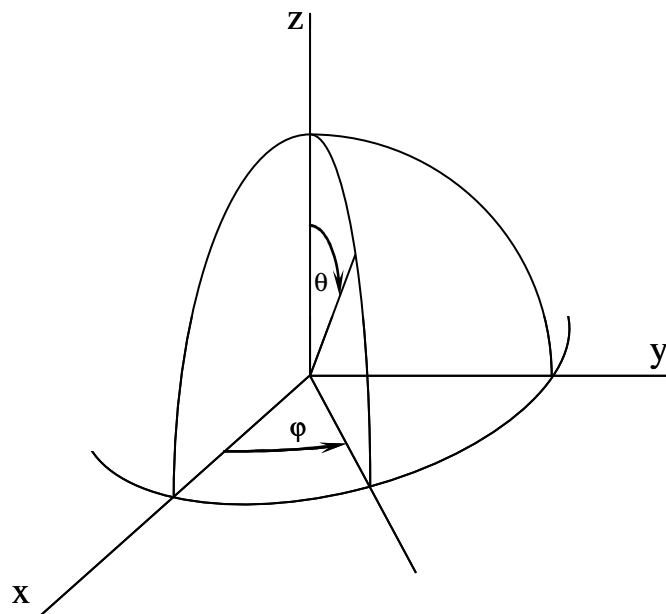


Figure B.5

$$\left. \begin{aligned} x(\theta, \varphi) &= r \sin(\theta) \cos(\varphi) \\ y(\theta, \varphi) &= r \sin(\theta) \sin(\varphi) \\ z(\theta, \varphi) &= r \cos(\theta) \end{aligned} \right\} \quad \forall \theta, \varphi \in [0, 2\pi) \quad (\text{B.15})$$

The first derivatives of the parametric equations are the elements of the matrix M with rank equal to r :

$$\text{rank}(M) = \text{rank} \begin{bmatrix} r \cos(\theta) \cos(\varphi) & r \cos(\theta) \sin(\varphi) & -r \sin(\theta) \\ -r \sin(\theta) \sin(\varphi) & r \sin(\theta) \cos(\varphi) & 0 \end{bmatrix} = 2$$

The coefficients of the 1st fundamental form (E , F and G), the principal normal vector \mathbf{N} and the coefficients of the 2nd fundamental form are following.

$$E = r^2, F = 0, G = r^2 \sin^2(\theta)$$

$$\mathbf{N} = \begin{bmatrix} \sin(\theta) \cos(\varphi) \\ \sin(\theta) \sin(\varphi) \\ \cos(\theta) \end{bmatrix} \quad (\text{B.16})$$

$$e = -r, f = 0, g = -r \sin^2(\theta)$$

Equation (B.14) will give:

$$M = -\frac{1}{r} \text{ and } K = \frac{1}{r^2} \quad (\text{B.17})$$

B.4.2 Elliptic Paraboloid

This is a quadratic surface with an elliptical cross section, (Weisstein, 1999a). The elliptic Paraboloid has height h , semi-major axis a and semi-minor axis b and it is specified parametrically by:

$$\left. \begin{array}{l} x(u, v) = a\sqrt{u} \cos(v) \\ y(u, v) = b\sqrt{u} \sin(v) \\ z(u, v) = u \end{array} \right\} \quad \forall v \in [0, 2\pi) \text{ and } u \in [0, h] \quad (\text{B.18})$$

The coefficients of the 1st and the 2nd surface fundamental forms along with the principal normal unit vector would be:

$$E = \frac{1}{4u} (a^2 \cos^2(v) + b^2 \sin^2(v) + 4u)$$

$$F = -\frac{a^2 - b^2}{2} \cos(v) \sin(v)$$

$$G = u(a^2 \sin^2(v) + b^2 \cos^2(v))$$

$$N = \begin{bmatrix} -b\sqrt{u} \cos(v) \\ -a\sqrt{u} \sin(v) \\ \frac{ab}{2} \end{bmatrix} \quad (\text{B.19})$$

$$e = \frac{ab}{2u\sqrt{4u(a^2 \sin^2(v) + b^2 \cos^2(v)) + (ab)^2}}$$

$$f = 0$$

$$g = \frac{2abu}{\sqrt{4u(a^2 \sin^2(v) + b^2 \cos^2(v)) + (ab)^2}}$$

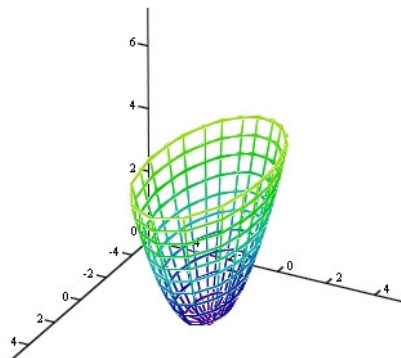


Figure B.6: Elliptic Paraboloid

By using the above results, the mean and the Gaussian curvature are readily obtained. Also, the usefulness of Vieta's formulas is obvious in this case where application of Equations (B.13) and (B.14) creates a lot of algebra manipulations.

B.4.3 Paraboloid

In the case where the semi-major and the semi-minor axes are equal, the elliptic Paraboloid becomes a Paraboloid like the one presented in Figure B.7.

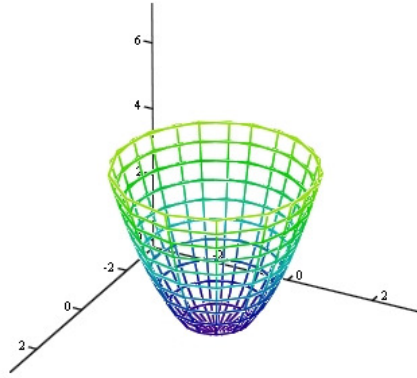


Figure B.7: Paraboloid, (Weissten, 1999b)

The parametric equations in this case are the same as for the elliptic paraboloid, only this time $a = b$. The coefficients of the surface fundamental forms are significantly simplified and they become:

$$E = \frac{a^2}{4u} + 1$$

$$F = 0$$

$$G = a^2 u$$

$$\mathbf{N} = \begin{bmatrix} -a\sqrt{u} \cos(v) \\ -a\sqrt{u} \sin(v) \\ \frac{a^2}{2} \end{bmatrix} \quad (\text{B.20})$$

$$e = \frac{a}{2u\sqrt{a^2 + 4u}}$$

$$f = 0$$

$$g = \frac{2au}{\sqrt{a^2 + 4u}}$$

Finally, the Vieta's formulas in this case will give:

$$M = \frac{a^2 + 2u}{a(a^2 + 4u)^{3/2}} \quad \text{and} \quad K = \frac{4}{(a^2 + 4u)^2} \quad (\text{B.21})$$

B.4.4 Witch of Agnesi

The final surface which we will examine in this study is the one with the unusual name of “Witch of Agnesi” function due to Maria Agnesi who studied it in 1748, (Weisstein, 2004). Its parametric form is given by Equation (B.22) and the space graph in Figure B.8.

$$\begin{aligned} x(u, v) &= u \\ y(u, v) &= v \\ z(u, v, h) &= \frac{h}{\left[1 + \left(\frac{u}{a}\right)^2 + \left(\frac{v}{b}\right)^2\right]^{3/2}} \end{aligned} \quad (\text{B.22})$$

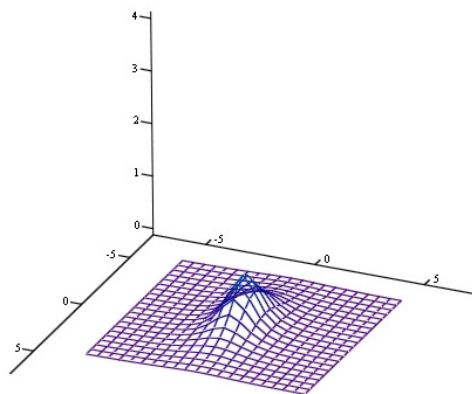


Figure B.8: Witch of Agnesi surface

Parameters a and b represent once more the semi-major and the semi-minor axes of the surface whereas h is the height above the $z = 0$ plane. This function is extensively used in meteorology in the prediction of wind flow around mountain – like shapes⁷. In the context of the current study it provides a very useful tool for the description of the way in which an initially flat panel deforms under the action of an external body like a sphere or a paraboloid of some kind.

B.5 Bezier surfaces

To allow for more flexibility and accuracy in the definition of the striking body, the Bezier surfaces are used. These mathematical abstractions are based on *Bernstein's*

⁷ For example: http://mesonh.aero.obs-mip.fr/mesonh/dir_doc/book1_14dec2001/node13.html

polynomials and a set of control points, the so called *control polygon*. n-th degree Bernstein's polynomial for a two-dimensional curve is:

$$B_{i,n}(u) = \frac{n!}{i!(n-i)!} u^i (1-u)^{n-i}, \quad u \in [0,1] \quad (\text{B.23})$$

A generalisation of (B.23) for the case of a three-dimensional parametrical surface definition with independent variables u and v (both taking values in $[0,1]$) is the set of equations (B.24). The vectors P_x , P_y and P_z are forming the control polygon of the surface. As the main part of the definition (with respect to u and v) remains the same, the surface is manipulated by alterations of the control polygon.

$$\begin{aligned} x(u, v) &= \sum_{i=0}^n \sum_{j=0}^m \left[\frac{n!}{i!(n-i)!} u^i (1-u)^{n-i} \right] \left[\frac{m!}{j!(m-j)!} v^j (1-v)^{m-j} \right] \mathbf{P}_{x_{i,j}} \\ y(u, v) &= \sum_{i=0}^n \sum_{j=0}^m \left[\frac{n!}{i!(n-i)!} u^i (1-u)^{n-i} \right] \left[\frac{m!}{j!(m-j)!} v^j (1-v)^{m-j} \right] \mathbf{P}_{y_{i,j}} \\ z(u, v) &= \sum_{i=0}^n \sum_{j=0}^m \left[\frac{n!}{i!(n-i)!} u^i (1-u)^{n-i} \right] \left[\frac{m!}{j!(m-j)!} v^j (1-v)^{m-j} \right] \mathbf{P}_{z_{i,j}} \end{aligned} \quad (\text{B.24})$$

For example, the bows of the tanker and the ROPAX vessels presented in the case studies of Chapter 7 were derived based on 9th degree polynomials. This arrangement allowed for enough flexibility of the definition surface yet not very lengthy 1st and 2nd derivatives for the needs of the calculations.

(0,1)	0.0	(0,2)	0.0	(0,3)	0.0	(0,4)	0.0	(0,5)	0.0
	1.5		4.5		8.0		12.0		9.0
	25.0		5.0		5.0		0.0		0.0
(1,1)	0.5	(1,2)	0.5	(1,3)	0.5	(1,4)	0.5	(1,5)	0.5
	1.5		4.5		5.0		14.0		18.5
	58.2		48.0		42.0		25.0		0.0
(2,1)	3.0	(2,2)	3.0	(2,3)	3.0	(2,4)	3.0	(2,5)	3.0
	1.5		4.5		5.0		14.0		18.5
	69.0		63.0		55.0		25.0		0.0
(3,1)	8.3	(3,2)	8.3	(3,3)	8.3	(3,4)	8.3	(3,5)	8.3
	1.5		4.5		5.0		14.0		18.5
	55.0		50.0		45.0		25.0		0.0
(4,1)	11.0	(4,2)	11.0	(4,3)	11.0	(4,4)	11.0	(4,5)	11.0

	1.5		4.5		8.0		14.0		18.5
	48.0		50.0		46.0		25.0		0.0
(5,1)	12.0	(5,2)	12.0	(5,3)	12.0	(5,4)	12.0	(5,5)	12.0
	1.5		4.5		8.0		14.0		18.5
	40.0		28.0		25.0		15.0		0.0
(6,1)	12.3	(6,2)	12.3	(6,3)	12.3	(6,4)	12.3	(6,5)	12.3
	1.6		4.9		8.0		14.0		18.5
	40		28.0		25.0		15.0		0.0
(7,1)	12.5	(7,2)	12.5	(7,3)	12.5	(7,4)	12.5	(7,5)	12.5
	1.6		4.9		8.0		14.0		18.5
	40.0		28.0		25.0		15.0		0.0
(8,1)	16.1	(8,2)	16.1	(8,3)	16.1	(8,4)	16.1	(8,5)	16.1
	1.6		4.9		11.1		16.0		18.5
	50.0		43.0		39.0		34		0.0
(9,1)	18.0	(9,2)	18.0	(9,3)	18.0	(9,4)	18.0	(9,5)	18.0
	1.62		4.9		10.0		14.0		18.5
	55.0		48.0		44.0		39.0		0.0

Table B.1 is presenting the control polygon points of the ROPAX in the conventional coordinate axes system for ships (i.e. x-axis along the length of the vessel, y-axis along its breadth and z-axis along the depth of its hull). That is, the numbers presented are corresponding to z, y and x coordinates of each point. Only half the surface is presented due to symmetry.

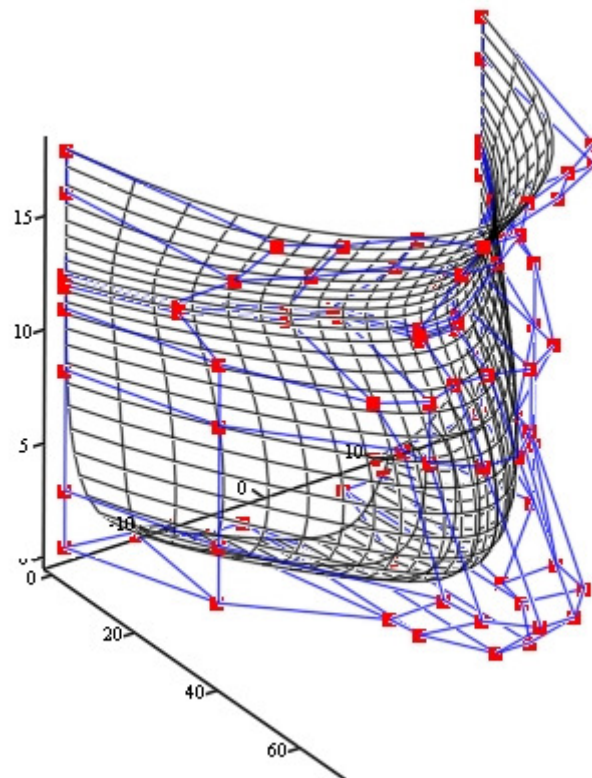
Point id	[z,y,x]	Point id	[z,y,x]	Point id	[z,y,x]	Point id	[z,y,x]	Point id	[z,y,x]
(0,1)	0.0	(0,2)	0.0	(0,3)	0.0	(0,4)	0.0	(0,5)	0.0
	1.5		4.5		8.0		12.0		9.0
	25.0		5.0		5.0		0.0		0.0
(1,1)	0.5	(1,2)	0.5	(1,3)	0.5	(1,4)	0.5	(1,5)	0.5
	1.5		4.5		5.0		14.0		18.5
	58.2		48.0		42.0		25.0		0.0
(2,1)	3.0	(2,2)	3.0	(2,3)	3.0	(2,4)	3.0	(2,5)	3.0
	1.5		4.5		5.0		14.0		18.5
	69.0		63.0		55.0		25.0		0.0
(3,1)	8.3	(3,2)	8.3	(3,3)	8.3	(3,4)	8.3	(3,5)	8.3
	1.5		4.5		5.0		14.0		18.5
	55.0		50.0		45.0		25.0		0.0
(4,1)	11.0	(4,2)	11.0	(4,3)	11.0	(4,4)	11.0	(4,5)	11.0
	1.5		4.5		8.0		14.0		18.5
	48.0		50.0		46.0		25.0		0.0
(5,1)	12.0	(5,2)	12.0	(5,3)	12.0	(5,4)	12.0	(5,5)	12.0
	1.5		4.5		8.0		14.0		18.5
	40.0		28.0		25.0		15.0		0.0
(6,1)	12.3	(6,2)	12.3	(6,3)	12.3	(6,4)	12.3	(6,5)	12.3
	1.6		4.9		8.0		14.0		18.5
	40		28.0		25.0		15.0		0.0
(7,1)	12.5	(7,2)	12.5	(7,3)	12.5	(7,4)	12.5	(7,5)	12.5
	1.6		4.9		8.0		14.0		18.5
	40.0		28.0		25.0		15.0		0.0
(8,1)	16.1	(8,2)	16.1	(8,3)	16.1	(8,4)	16.1	(8,5)	16.1
	1.6		4.9		11.1		16.0		18.5
	50.0		43.0		39.0		34		0.0
(9,1)	18.0	(9,2)	18.0	(9,3)	18.0	(9,4)	18.0	(9,5)	18.0
	1.62		4.9		10.0		14.0		18.5
	55.0		48.0		44.0		39.0		0.0

Table B.1: The control polygon for the bulb of the tanker vessel

The final element of geometry deployed in the analysis is the turn of bow by certain degrees (ϕ), which represents the striking angle. In this case, the conventional transformation scheme of plane coordinate is used (rotation around z-axis).

$$z'(u, v) = z(u, v) \cos(\phi) + y(u, v) \sin(\phi)$$

$$y'(u, v) = z(u, v) \sin(\phi) - y(u, v) \cos(\phi)$$

**Figure B.9: The bulb of the tanker vessel with the control polygon**

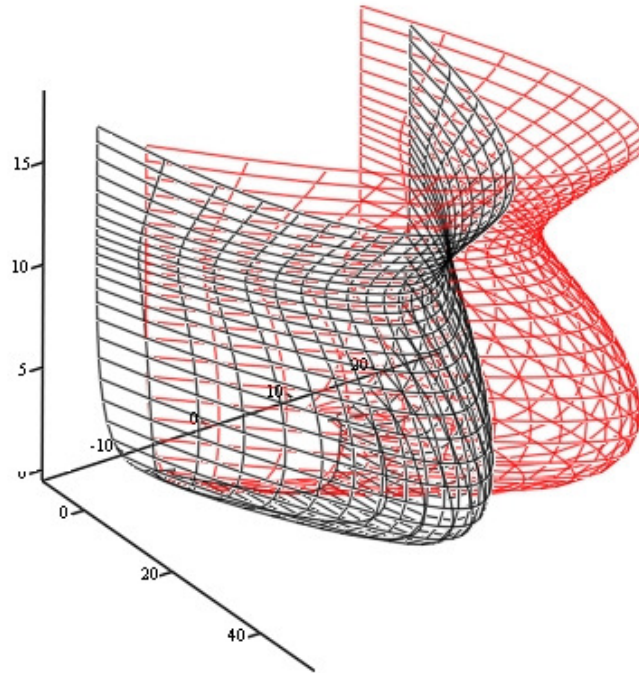
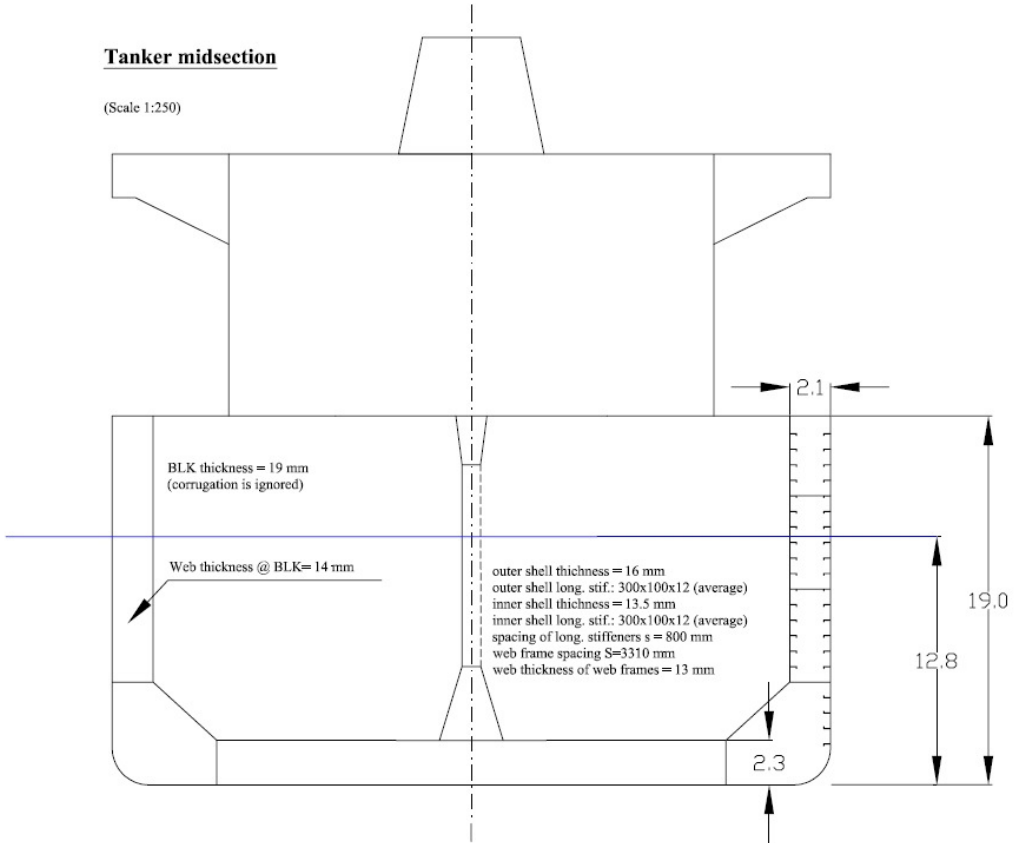
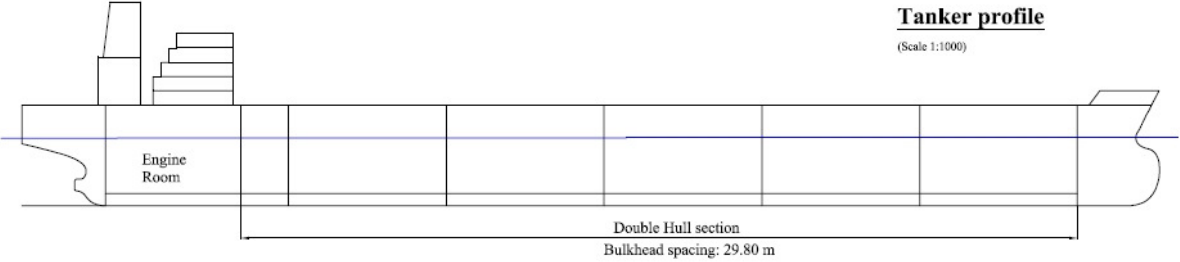


Figure B.10: Turn of the bulb by 25°

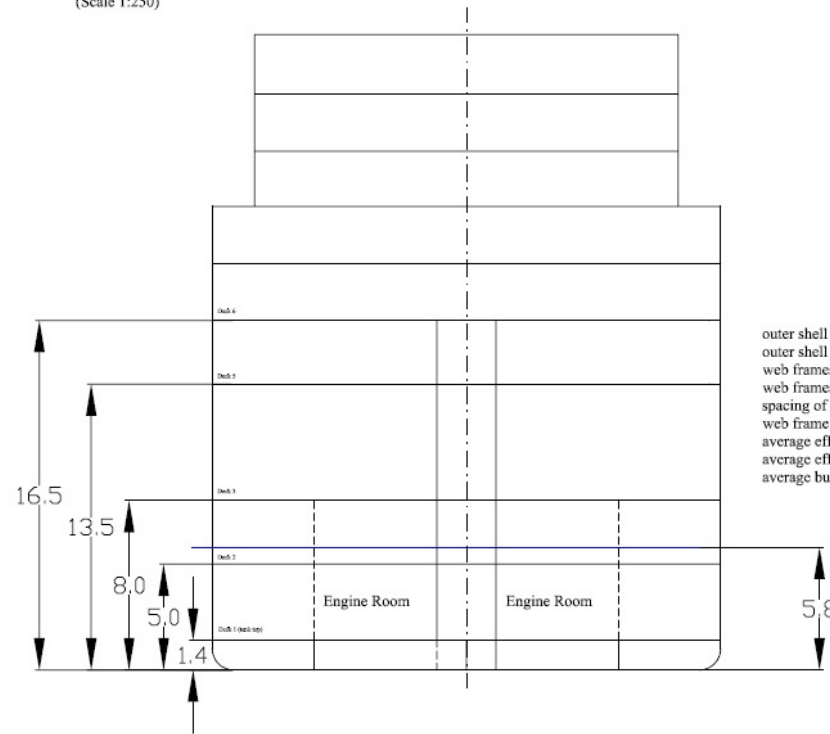
Appendix C: Vessel drawings





ROPAX midsection

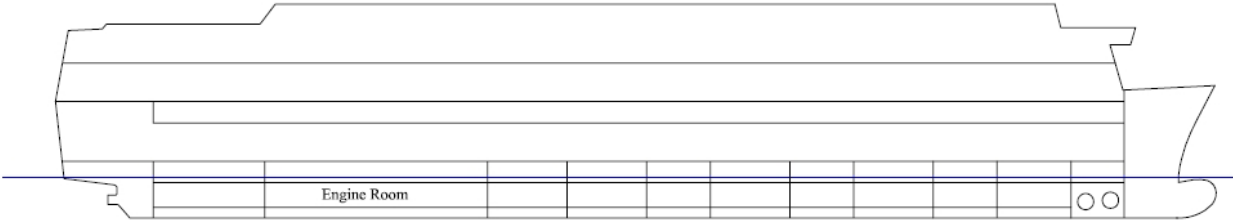
(Scale 1:250)



outer shell thickness = 10 mm
 outer shell long. stif.: 250x100x10 (no long. stif. above Deck 3)
 web frames 600x10 (web), 250x20 (flange) (up to Deck 3)
 web frames 500x9 (web), 200x20 (flange) (above Deck 3)
 spacing of long. stiffeners $s = 375$ mm
 web frame spacing $S = 4500$ mm
 average effective thickness of decks 1, 2 & 3: 10 mm
 average effective thickness of decks 5 & 6: 7.6 mm
 average bulkhead thickness below Deck 3: 6.5 mm

ROPAX profile

(Scale 1: 750)



Appendix D: Calculation of side shell stiffness values D , D_x and D_y

$$\begin{aligned} \underline{\underline{\text{MPa}}} &:= 10^6 \text{ Pa} & \underline{\underline{\text{MN}}} &:= 10^6 \text{ N} & \nu &:= 0.3 & E &:= 2.09 \cdot 10^{11} \frac{\text{N}}{\text{m}^2} & \underline{\underline{\text{G}}} &:= \frac{E}{2(1 + \nu)} & G &= 8.038 \times 10^4 \cdot \text{MPa} \end{aligned}$$

ROPAX

Number of zones: 2

Zone 1: Expanding from tank top up to deck 3 (at 8.0 m, total = 8-1.5 = 6.5 m)

$$t_{\text{shell}} := 10 \text{ mm} \quad \text{long. stif.: } 250 \times 100 \times 10$$

$$\underline{\underline{l}} := 250 \text{ mm} \quad b := 100 \text{ mm} \quad t := 10 \text{ mm} \quad \underline{\underline{s}} := 375 \text{ mm}$$

$$A_{\text{stifL}} := l \cdot t + (b - t)t \quad A_{\text{stifL}} = 3.4 \times 10^{-3} \text{ m}^2$$

$$c_{\text{gstif}} := \frac{l \cdot \frac{1}{2} + (b - t)t \cdot \left(1 - \frac{t}{2}\right)}{A_{\text{stifL}}} \quad c_{\text{gstif}} = 0.157 \text{ m} \quad I_{\text{cgstif}} := \frac{t \cdot l^3}{12} + l \cdot t \cdot \left(\frac{1}{2} - c_{\text{gstif}}\right)^2 + \frac{(b - t)t^3}{12} + (b - t)t \cdot (1 - t - c_{\text{gstif}})^2$$

$$I_x := I_{\text{cgstif}} + A_{\text{stifL}} \cdot \left(c_{\text{gstif}} + \frac{t_{\text{shell}}}{2}\right)^2 \quad I_x = 1.108 \times 10^{-4} \text{ m}^4 \quad I_{\text{cgstif}} = 2.179 \times 10^{-5} \text{ m}^4$$

trans. stif.

- web: 600 x 10

- flange: 250 x 20

$$\underline{\underline{l}} := 600 \text{ mm} \quad t_1 := 10 \text{ mm} \quad \underline{\underline{b}} := 250 \text{ mm} \quad t_b := 20 \text{ mm} \quad A_{\text{stifT}} := l \cdot t_1 + b \cdot t_b$$

$$\underline{\underline{S}} := 4.5 \text{ m}$$

$$\underline{\underline{\text{cgstif}}} := \frac{l \cdot t_1 \cdot \frac{1}{2} + b \cdot t_b \cdot \left(\frac{t_b}{2} + 1\right)}{A_{\text{stifT}}} \quad \text{cgstif} = 0.441 \text{ m}$$

$$I_{cgstif} := \frac{t_l \cdot l^3}{12} + l \cdot t_l \cdot \left(\frac{l}{2} - c_{gstif}\right)^2 + \frac{b \cdot t_b^3}{12} + b \cdot t_b \cdot \left(\frac{t_b}{2} + l - c_{gstif}\right)^2 \quad I_{cgstif} = 4.423 \times 10^{-4} \text{ m}^4$$

$$I_y := I_{cgstif} + A_{stif} T \cdot \left(c_{gstif} + \frac{t_{shell}}{2}\right)^2 \quad I_y = 2.629 \times 10^{-3} \text{ m}^4$$

$$t_{blk} := 6.5 \text{ mm (on average)}$$

(twice the web of stif. frames is considered for the blk effective plating)

$$\text{span}_{blk} := \frac{15.8 + 31.5 + 11.3 \cdot 4 + 9 \cdot 3 + 10.5 + 7.5}{12} \text{ m} \quad \text{span}_{blk} = 11.458 \text{ m}$$

$$I_{blk} := \frac{(2 \cdot 0.60 \text{ m})^3 \cdot t_{blk}}{12} + (2 \cdot 0.60 \text{ m} \cdot t_{blk}) \cdot \left[\frac{(2 \cdot 0.60 \text{ m})}{2}\right]^2 \quad I_{blk} = 3.744 \times 10^{-3} \text{ m}^4$$

3 decks are included: tank top + deck 2 + deck, the thickness of which is smeared as follows (half breadth is considered in the calculations and the whole length of the zone, i.e. $146.9 - 9.6 = 137.3 \text{ m}$)

$$t_{ttsm} := 10 \cdot \text{mm} + \left(160 \cdot 8 \cdot \text{mm}^2\right) \cdot \frac{\frac{2 \cdot 0.60 \text{ m}}{700 \text{ mm}} - 1}{2 \cdot 0.60 \text{ m}} \quad t_{deck2sm} := 6 \text{ mm} + \left(140 \cdot 8 \text{ mm}^2\right) \cdot \frac{\frac{2 \cdot 0.60 \text{ m}}{700 \text{ mm}} - 1}{2 \cdot 0.60 \text{ m}}$$

$$t_{deck3sm} := 11 \text{ mm} + [250 \cdot 9 + (90 - 9) \cdot 9] \text{ mm}^2 \cdot \frac{\frac{2 \cdot 0.60 \text{ m}}{700 \text{ mm}} - 1}{2 \cdot 0.60 \text{ m}} \quad \text{(smeared thickness for the three decks)}$$

$$\text{Average thickness:} \quad t_{deck} := \frac{t_{ttsm} + t_{deck2sm} + t_{deck3sm}}{3} \quad t_{deck} = 10.067 \cdot \text{mm}$$

Average span of the three decks: $\text{span}_{\text{deck}} := \frac{3.5 + 3}{2} \text{m}$ $\text{span}_{\text{deck}} = 3.25 \text{m}$

$$I_{\text{deck}} := \frac{(2 \cdot 0.60 \text{m})^3 \cdot t_{\text{deck}}}{12} + 2 \cdot 0.60 \text{m} \cdot t_{\text{deck}} \cdot \left(\frac{2 \cdot 0.60 \text{m}}{2} \right)^2 \quad I_{\text{deck}} = 5.799 \times 10^{-3} \text{m}^4$$

$$D1 := \frac{E \cdot t_{\text{shell}}^3}{12 \cdot (1 - \nu)^2} \quad D1 = 3.554 \times 10^4 \cdot \text{N} \cdot \text{m} \quad D1_x := D1 + E \cdot \frac{I_x}{s} + E \cdot \frac{I_{\text{deck}}}{\text{span}_{\text{deck}}} \quad D1_x = 4.347 \times 10^8 \cdot \text{N} \cdot \text{m}$$

$$D1_y := D1 + E \cdot \frac{I_y}{S} + E \cdot \frac{I_{\text{blk}}}{\text{span}_{\text{blk}}} \quad D1_y = 1.904 \times 10^8 \cdot \text{N} \cdot \text{m} \quad (\text{plate} + \text{longitudinals} + \text{smeared decks})$$

(plate + transverses + bulkheads)

Smeared thickness for the calculation of rupture energy according to N. Jones' experiments:

$$t_{\text{smear1}} := t_{\text{shell}} + A_{\text{stifL}} \cdot \frac{\frac{6.5 \text{m}}{s} - 1}{6.5 \text{m}} + A_{\text{stifT}} \cdot \frac{\frac{(146.9 - 9.6) \text{m}}{S} - 1}{(146.9 - 9.6) \text{m}} \quad t_{\text{smear1}} = 20.908 \cdot \text{mm}$$

Zone 2: Expanding from deck 3 to deck 6 (at 16.5.0 m, total = 16.5-8 = 8.5 m)

$$t_{\text{shell}} := 10 \text{mm} \quad \text{no longitudinal stiffeners in this zone}$$

Transverse stiffeners are **not** the same in this area:

trans. stif.
 - web: 500 x 9
 - flange: 200 x 20

$$l_w := 500\text{mm} \quad t_w := 9\text{mm} \quad b_f := 200\text{mm} \quad t_b := 20\text{mm} \quad A_{stif} := l_w + b_f \cdot t_b$$

$$S_y := 4.5\text{m} \quad c_{gstif} := \frac{l_w \cdot \frac{1}{2} + b_f \cdot t_b \cdot \left(\frac{t_b}{2} + 1\right)}{A_{stif}} \quad c_{gstif} = 0.372\text{m}$$

$$I_{cgstif} := \frac{t_w \cdot l_w^3}{12} + l_w \cdot t_w \cdot \left(\frac{1}{2} - c_{gstif}\right)^2 + \frac{b_f \cdot t_b^3}{12} + b_f \cdot t_b \cdot \left(\frac{t_b}{2} + 1 - c_{gstif}\right)^2 \quad I_{cgstif} = 2.37 \times 10^{-4} \text{m}^4$$

$$I_y := I_{cgstif} + A_{stif} \cdot \left(c_{gstif} + \frac{t_{shell}}{2}\right)^2 \quad I_y = 1.447 \times 10^{-3} \text{m}^4$$

No bulkheads in this zone

Decks in this zone: $t_{deck3sm} = 12.773 \cdot \text{mm}$ $t_{deck5sm} := 7\text{mm} + \left(160 \cdot 8\text{mm}^2\right) \cdot \frac{\frac{2 \cdot 0.5\text{m}}{660\text{mm}} - 1}{2 \cdot 0.5\text{m}}$

$$t_{deck6sm} := 7\text{mm} + \left(140 \cdot 8\text{mm}^2\right) \cdot \frac{\frac{2 \cdot 0.5\text{m}}{660\text{mm}} - 1}{2 \cdot 0.5\text{m}}$$

$$t_{deck} := \frac{t_{deck3sm} + t_{deck5sm} + t_{deck6sm}}{3} \quad t_{deck} = 9.337 \cdot \text{mm} \quad (\text{it is necessary to include deck 3 again for consistency, i.e. deck 3 does not only provide stiffness in zone 1 but also in zone 2})$$

Average span of the three decks: $span_{deck} := \frac{5.4 + 3.1}{2} \text{m} \quad span_{deck} = 4.25 \text{m}$

$$I_{\text{deck}} := \frac{(2 \cdot 0.5 \text{ m})^3 \cdot t_{\text{deck}}}{12} + 2 \cdot 0.5 \text{ m} \cdot t_{\text{deck}} \cdot \left(\frac{2 \cdot 0.5 \text{ m}}{2} \right)^2 \quad I_{\text{deck}} = 3.112 \times 10^{-3} \text{ m}^4$$

$$D2 := \frac{E \cdot t_{\text{shell}}^3}{12 \cdot (1 - \nu)^2} \quad D2 = 3.554 \times 10^4 \cdot \text{N} \cdot \text{m} \quad D2_x := D2 + E \cdot \frac{I_{\text{deck}}}{\text{span}_{\text{deck}}} \quad D2_x = 1.531 \times 10^8 \cdot \text{N} \cdot \text{m} \quad (\text{plate} + \text{decks})$$

$$D2_y := D2 + E \cdot \frac{I_y}{S} \quad D2_y = 6.726 \times 10^7 \cdot \text{N} \cdot \text{m} \\ (\text{plate} + \text{transverses})$$

Smearred thickness for the calculation of rupture energy according to N. Jones' experiments:

$$t_{\text{smear2}} := t_{\text{shell}} + A_{\text{stif}} \cdot \frac{\frac{(146.9 - 9.6) \text{ m}}{S} - 1}{(146.9 - 9.6) \text{ m}} \quad t_{\text{smear2}} = 11.827 \cdot \text{mm}$$

$$L1 := 146.9 \text{ m} - 9.6 \text{ m} \quad B1 := 8 \text{ m} - 1.5 \text{ m}$$

$$L2 := L1 \quad B2 := 16.5 \text{ m} - 8 \text{ m}$$

Summary:

Zone 1

$$L_{\text{low}} := 9.6\text{m}$$

$$L_{\text{hi}} := 146.9\text{m}$$

$$B_{\text{low}} := 1.5\text{m}$$

$$B_{\text{hi}} := 8\text{m}$$

$$E = 2.09 \times 10^5 \cdot \text{MPa}$$

$$G = 8.038 \times 10^4 \cdot \text{MPa}$$

$$D1 = 0.036 \cdot \text{MN} \cdot \text{m}$$

$$D1_x = 434.668 \cdot \text{MN} \cdot \text{m}$$

$$D1_y = 190.449 \cdot \text{MN} \cdot \text{m}$$

$$ts1 := 0.01\text{m}$$

$$t_{\text{smear1}} = 0.021\text{m}$$

Zone 2

$$L_{\text{low}} := 9.6\text{m}$$

$$L_{\text{hi}} := 146.9\text{m}$$

$$B_{\text{low}} := 8\text{m}$$

$$B_{\text{hi}} := 16.5\text{m}$$

$$E = 2.09 \times 10^5 \cdot \text{MPa}$$

$$G = 8.038 \times 10^4 \cdot \text{MPa}$$

$$D2 = 0.036 \cdot \text{MN} \cdot \text{m}$$

$$D2_x = 153.081 \cdot \text{MN} \cdot \text{m}$$

$$D2_y = 67.259 \cdot \text{MN} \cdot \text{m}$$

$$ts2 := 0.01\text{m}$$

$$t_{\text{smear2}} = 0.012\text{m}$$

$$\begin{aligned} \underline{\underline{MPa}} &:= 10^6 \text{ Pa} & \underline{\underline{MN}} &:= 10^6 \text{ N} & \nu &:= 0.3 & E &:= 2.09 \cdot 10^{11} \frac{\text{N}}{\text{m}^2} & \underline{\underline{G}} &:= \frac{E}{2(1 + \nu)} & G &= 8.038 \times 10^4 \cdot \text{MPa} \end{aligned}$$

Calculation of D factors for tanker: there are two structural zones from tank top up to main deck with total span 16.70 m

$$\underline{\underline{H}} := 16.7 \text{ m}$$

Zone 1: Pump room up to collision bulkhead (double hull area)

Zone limits along the length of the ship: $L_{\min} := 36.0 \text{ m}$ $L_{\max} := 193.9 \text{ m}$

Outer shell plate thickness: $t_{\text{out1}} := 16 \text{ mm}$ Inner shell plate thickness: $t_{\text{in}} := 13.5 \text{ mm}$

Longitudinal stiffener spacing: $\underline{\underline{s}} := 800 \text{ mm}$

Outer and inner shell have the same longitudinal stiffeners: 300 x 100 x 12

Web frames spacing: $\underline{\underline{S}} := 3.31 \text{ m}$ Plate thickness for web frames: $t_{\text{web}} := 13 \text{ mm}$

Stringer spacing: $s_{\text{str}} := 4.8 \text{ m}$ Stringer plating thickness: $t_{\text{str}} := 10.5 \text{ mm}$

Double hull span: $\text{dbspan} := 2.1 \text{ m}$

- Calculation of outer shell longitudinal stiffeners' 2nd moment of area with respect to outer shell:

$$l_w := 300\text{mm} \quad b := 100\text{mm} \quad t := 12\text{mm}$$

Cross sectional area of longitudinal stiffeners:

$$A_{\text{stif}} := l \cdot t + (b - t)t$$

$$A_{\text{stif}} = 4.656 \times 10^{-3} \text{ m}^2$$

Vertical centroid of stiffener (along its web):

$$c_{g_{\text{stif}}} := \frac{l \cdot t \cdot \frac{1}{2} + (b - t)t \cdot \left(1 - \frac{t}{2}\right)}{A_{\text{stif}}}$$

$$c_{g_{\text{stif}}} = 0.183 \text{ m}$$

2nd moment of area of stiffener about its centroid:

$$I_{c_{g_{\text{stif}}}} := \frac{t \cdot l^3}{12} + l \cdot t \cdot \left(\frac{1}{2} - c_{g_{\text{stif}}}\right)^2 + \frac{(b - t)t^3}{12} + (b - t)t \cdot (1 - t - c_{g_{\text{stif}}})^2$$

$$I_{c_{g_{\text{stif}}}} = 4.257 \times 10^{-5} \text{ m}^4$$

2nd moment of area of stiffener about NA of outer shell plating:

$$I_x := I_{c_{g_{\text{stif}}}} + A_{\text{stif}} \cdot \left(c_{g_{\text{stif}}} + \frac{t_{\text{out1}}}{2}\right)^2$$

$$I_x = 2.118 \times 10^{-4} \text{ m}^4$$

- Calculation of 2nd moment of area of web frame plating with respect to outer shell:

2nd moment of area of plating of web frame about NA of outer shell plating:

$$I_y := \frac{t_{\text{web}} \cdot \text{dbspan}^3}{12} + t_{\text{web}} \cdot \text{dbspan} \cdot \left(\frac{\text{dbspan}}{2} + \frac{t_{\text{out1}}}{2}\right)^2$$

$$I_y = 0.041 \text{ m}^4$$

- Calculation of inner shell longitudinal stiffeners' 2nd moment of area with respect to outer shell:

2nd moment of area of stiffener about NA of outer shell plating:

$$I_{x_in} := I_{cgstif} + A_{stif} \cdot (dbspan - cg_{stif})^2$$

$$I_{x_in} = 0.017 \text{ m}^4$$

- Calculation of stringers' 2nd moment of area with respect to outer shell:

2nd moment of area of stringer about NA of outer shell plating:

$$I_{str} := \frac{t_{str} \cdot dbspan^3}{12} + t_{str} \cdot dbspan \cdot \left(\frac{dbspan}{2} + \frac{t_{out1}}{2} \right)^2$$

$$I_{str} = 0.033 \text{ m}^4$$

- Calculation of smeared thickness of outer shell for the rupture energy criterion (paragraph 5.4.2)

Inner shell smeared thickness:

$$t_{in_sm} := t_{in} + A_{stif} \cdot \frac{\frac{H}{s} - 1}{H}$$

$$t_{in_sm} = 19.041 \cdot \text{mm}$$

Overall smeared thickness:

$$t_{smear1} := t_{out1} + A_{stif} \cdot \frac{\frac{H}{s} - 1}{H} + t_{in_sm} + (t_{web} \cdot dbspan) \cdot \frac{\frac{L_{max} - L_{min}}{S} - 1}{L_{max} - L_{min}}$$

$$t_{smear1} = 48.657 \cdot \text{mm}$$

- Calculation of plate rigidities for Zone 1:

Outer shell rigidity:

$$D1 := \frac{E \cdot t_{out1}^3}{12 \cdot (1 - \nu^2)}$$

$$D1 = 0.078 \cdot \text{MN} \cdot \text{m}$$

Inner shell rigidity:
$$D_{in_shell} := \frac{E \cdot t_{in}^3}{12 \cdot (1 - \nu^2)}$$
 $D_{in_shell} = 0.047 \cdot \text{MN} \cdot \text{m}$

Rigidity along x-axis:
$$D1_x := D1 + E \cdot \left(\frac{I_x}{s} + \frac{I_{x_in}}{s} + \frac{I_{str}}{s_{str}} \right) + D_{in_shell}$$
 $D1_x = 5.966 \times 10^3 \cdot \text{MN} \cdot \text{m}$

Rigidity along y-axis:
$$D1_y := D1 + E \cdot \frac{I_y}{S}$$
 $D1_y = 2.563 \times 10^3 \cdot \text{MN} \cdot \text{m}$

Zone 2: Engine room (single hull area)

Zone limits along the length of the ship: $L_{min} := 10.4\text{m}$ $L_{max} := 36.0\text{m}$

Outer shell plate thickness: $t_{out2} := 14\text{mm}$

Side shell longitudinal stiffeners: 200 x 90 x 9 Stiffener spacing: $s := 700\text{mm}$

Side shell stringers: 800 x 11 (web), 200 x 15 (flange) Stringer spacing: $s_{str} := 2.1\text{m}$

$h_{wstr} := 800\text{mm}$ $t_{wstr} := 11\text{mm}$ $h_{fstr} := 200\text{mm}$ $t_{fstr} := 15\text{mm}$

Web frames spacing: $S := 800\text{mm}$ Web frame dimensions

- Web $h_w := 925\text{mm}$ $t_w := 11\text{mm}$
- Flange $h_f := 190\text{mm}$ $t_f := 17\text{mm}$

- Calculation of web frames' 2nd moment of area with respect to outer shell:

Total web frame area:

$$A_{\text{stif}} := h_w \cdot t_w + h_f \cdot t_f$$

$$A_{\text{stif}} = 0.013 \text{ m}^2$$

Vertical centroid of stiffener
(along its web):

$$c_{\text{gstif}} := \frac{(h_w \cdot t_w) \cdot \frac{h_w}{2} + h_f \cdot t_f \cdot h_w}{A_{\text{stif}}}$$

$$c_{\text{gstif}} = 573.942 \cdot \text{mm}$$

2nd moment of area of web
frame with respect to its
centroid:

$$I_{\text{cgstif}} := \frac{t_w \cdot h_w^3}{12} + (h_w \cdot t_w) \cdot \left(\frac{h_w}{2} - c_{\text{gstif}} \right)^2 + \frac{h_f \cdot t_f^3}{12} + (h_f \cdot t_f) \cdot (h_w - c_{\text{gstif}})^2$$

$$I_{\text{cgstif}} = 1.25 \times 10^{-3} \text{ m}^4$$

2nd moment of area of web frame
about NA of outer shell plating:

$$I_{\text{yy}} := I_{\text{cgstif}} + A_{\text{stif}} \cdot \left(c_{\text{gstif}} + \frac{t_{\text{out}2}}{2} \right)^2$$

$$I_y = 5.774 \times 10^{-3} \text{ m}^4$$

- Calculation of stringers' 2nd moment of area with respect to outer shell:

Total web frame area:

$$A_{\text{str}} := h_{\text{wstr}} \cdot t_{\text{wstr}} + h_{\text{fstr}} \cdot t_{\text{fstr}}$$

$$A_{\text{str}} = 0.012 \text{ m}^2$$

Vertical centroid of stiffener
(along its web):

$$c_{\text{gstr}} := \frac{(h_{\text{wstr}} \cdot t_{\text{wstr}}) \cdot \frac{h_{\text{wstr}}}{2} + h_{\text{fstr}} \cdot t_{\text{fstr}} \cdot h_{\text{wstr}}}{A_{\text{str}}}$$

$$c_{\text{gstr}} = 501.695 \cdot \text{mm}$$

2nd moment of area of web frame with respect to its centroid:

$$I_{cgstr} := \frac{t_{wstr} \cdot h_{wstr}^3}{12} + (h_{wstr} \cdot t_{wstr}) \cdot \left(\frac{h_{wstr}}{2} - c_{gstr} \right)^2 + \frac{h_{fstr} \cdot t_{fstr}^3}{12} + (h_{fstr} \cdot t_{fstr}) \cdot (h_{wstr} - c_{gstr})^2$$

$$I_{cgstr} = 8.274 \times 10^{-4} \text{ m}^4$$

2nd moment of area of web frame about NA of outer shell plating:

$$I_{str} := I_{cgstr} + A_{str} \cdot \left(c_{gstr} + \frac{t_{out2}}{2} \right)^2$$

$$I_{str} = 3.881 \times 10^{-3} \text{ m}^4$$

- Calculation of outer shell longitudinal stiffeners' 2nd moment of area with respect to outer shell:

$$l := 200 \text{ mm} \quad b := 90 \text{ mm} \quad t := 9 \text{ mm}$$

Cross sectional area of longitudinal stiffeners:

$$A_{stifl} := l \cdot t + (b - t) \cdot t$$

$$A_{stifl} = 2.529 \times 10^{-3} \text{ m}^2$$

Vertical centroid of stiffener (along its web):

$$c_{gstif} := \frac{l \cdot \frac{1}{2} + (b - t) \cdot t \cdot \left(1 - \frac{t}{2} \right)}{A_{stifl}}$$

$$c_{gstif} = 0.128 \text{ m}$$

2nd moment of area of stiffener about its centroid:

$$I_{cgstif} := \frac{t \cdot l^3}{12} + l \cdot t \cdot \left(\frac{1}{2} - c_{gstif} \right)^2 + \frac{(b - t) \cdot t^3}{12} + (b - t) \cdot t \cdot (1 - t - c_{gstif})^2$$

$$I_{cgstif} = 1.031 \times 10^{-5} \text{ m}^4$$

2nd moment of area of stiffener about NA of outer shell plating:

$$I_{xx} := I_{cgstif} + A_{stifl} \cdot \left(c_{gstif} + \frac{t_{out1}}{2} \right)^2$$

$$I_x = 5.676 \times 10^{-5} \text{ m}^4$$

- Calculation of smeared thickness of outer shell for the rupture energy criterion (paragraph 5.4.2)

Overall smeared thickness:

$$t_{smear2} := t_{out2} + A_{stif} \cdot \frac{\frac{L_{max} - L_{min}}{S} - 1}{L_{max} - L_{min}} + A_{stifl} \cdot \frac{\frac{L_{max} - L_{min}}{s} - 1}{L_{max} - L_{min}} + A_{str} \cdot \frac{\frac{L_{max} - L_{min}}{s_{str}} - 1}{L_{max} - L_{min}}$$

$$t_{smear2} = 38.905 \cdot \text{mm}$$

- Calculation of plate rigidities for Zone 2:

Outer shell rigidity:

$$D2 := \frac{E \cdot t_{out2}^3}{12 \cdot (1 - \nu^2)}$$

$$D2 = 0.053 \cdot \text{MN} \cdot \text{m}$$

Rigidity along x-axis:

$$D2_x := D2 + E \cdot \left(\frac{I_x}{s} + \frac{I_{str}}{s_{str}} \right)$$

$$D2_x = 403.236 \cdot \text{MN} \cdot \text{m}$$

Rigidity along y-axis:

$$D2_y := D2 + E \cdot \frac{I_y}{S}$$

$$D2_y = 1.509 \times 10^3 \cdot \text{MN} \cdot \text{m}$$

Summary:**Zone 1**

$$D1 = 0.078 \cdot \text{MN} \cdot \text{m}$$

$$D1_x = 5.966 \times 10^3 \cdot \text{MN} \cdot \text{m}$$

$$D1_y = 2.563 \times 10^3 \cdot \text{MN} \cdot \text{m}$$

$$t_{\text{out1}} = 0.016 \text{ m}$$

$$t_{\text{smear1}} = 0.049 \text{ m}$$

Zone 2

$$D2 = 0.053 \cdot \text{MN} \cdot \text{m}$$

$$D2_x = 403.236 \cdot \text{MN} \cdot \text{m}$$

$$D2_y = 1.509 \times 10^3 \cdot \text{MN} \cdot \text{m}$$

$$t_{\text{out2}} = 0.014 \text{ m}$$

$$t_{\text{smear2}} = 0.039 \text{ m}$$